

LOUGHBOROUGH
UNIVERSITY OF TECHNOLOGY
LIBRARY

AUTHOR

QAZI, S

COPY NO.

067238/01

VOL NO.

CLASS MARK

ARCHIVES
COPY

FOR REFERENCE ONLY

MULTICHANNEL BIOMEDICAL TELEMETRY SYSTEM

USING DELTA MODULATION

BY

SALAHUDDIN QAZI

A Doctoral thesis

Submitted in partial fulfilment of the requirements for the award of the degree of Doctor of Philosophy of the University of Technology, Loughborough.

November, 1974

Supervisor: Mr. D.W. Hoare,
Department of Electronic and Electrical Engineering.

© by Salahuddin Qazi 1974.

Loughborough University of Technology Library	
Date	May 76
Class	
Acc. No.	067238/01

To my Mother

To AFTAB
and
my friends

ACKNOWLEDGEMENTS

The author would like to thank his supervisor, Mr. D.W. Hoare, and Dr. J.M. Ivison and Mr. R. Steele for their guidance and useful discussions.

Thanks are also due to the University of Technology, Loughborough, for sponsoring the project.

Finally my thanks go to Mrs. S.M. Peach who very patiently carried out the typing of this thesis.

SYNOPSIS

Telemetry of biomedical data from unrestrained subjects requires a system to be compact, reliable and efficient.

A survey of the existing multichannel biomedical telemetry showed that most of the systems employ analogue or uncoded (digital) techniques of encoding biomedical signals. These techniques are less reliable, employ wider bandwidth and are difficult to implement compared to the coded (digital) techniques of modulation.

A theoretical study of the coded techniques of modulation for encoding biomedical signals showed that pulse code modulation, though more efficient, calls for extensive circuitry and makes it expensive and difficult to implement. Delta modulation and delta sigma modulation were found to be simpler, easier to implement and efficient.

Further theoretical studies and computer simulations were carried out and it was found that delta modulation system is more suitable than delta sigma modulation system.

A simulated baseband telemetry system using delta modulation was investigated and analysed using various signal processing techniques.

A four channel biomedical telemetry system was designed and constructed using a radio link.

For a short range when radio telemetry is not necessary, a single wire time division multiplexed system was designed and constructed.

Due to the interdisciplinary nature of the project, various associated topics were discussed in detail and relevant references are given.

LIST OF PRINCIPAL SYMBOLSChapter 2

- E = Potential across the membrane and the two concentrations of the ions
 T = Absolute temperature in degree Kelvin
 R = Gas constant
 n = Valence of ion
 f = Frequency response of the amplifier

Chapter 3

- f_s = Clock frequency (sampling frequency)
 T_s = $\frac{1}{f_s}$ clock period or sampling interval
 f_c = $\frac{1}{2\pi RC}$ (characteristic frequency of RC network)
 T_c = RC (time constant of RC integrator)
 f_m = Frequency of input signal
 f_o = Bandwidth of input signal or the low pass filter
 N_q = Quantization noise
 S = Mean signal power
 A = Amplitude of input sinewave
 V = Amplitude of digital pulses
 d = Step size
 K = Numerical factor associated with quantization noise
 V_m = Maximum amplitude of input sinewave to be accommodated
 V_{min} = Minimum signal which can be coded
 ω_m = $2\pi f_m$ angular frequency (input sinewave)

Chapter 5

- ω_m = Angular frequency of modulating signal
 ω_c = Angular frequency of carrier
 f_c = Carrier frequency
 β = Modulation Index

TABLE OF CONTENTS

	<u>Page</u>
ACKNOWLEDGEMENTS	(i)
SYNOPSIS	(ii)
LIST OF PRINCIPAL SYMBOLS	(iii)
CHAPTER 1 Introduction	
1.0 Review of Biomedical Telemetry	1
1.1 Purpose and structure of the project	10
CHAPTER 2 Biomedical signals and their acquisition	
2.0 Introduction	12
2.1 Biomedical signals	12
2.2 Transducers	14
2.3 Electrodes	15
2.3.1 Electrode theory	15
2.3.2 Equivalent circuit of electrodes	16
2.3.3 Problems of electrodes	16
2.3.4 Motion artefact	18
2.3.5 Half cell potential	19
2.3.6 Polarisation	19
2.3.7 Types of bioelectric electrodes and requirements	20
2.3.8 Surface electrodes	21
2.4 Amplification of biomedical signals	24
2.5 Design techniques	26
2.5.1 Method of achieving high input impedance	29
2.6 Biological amplifier	29
2.6.1 Practical circuit for ECG amplifier	31
CHAPTER 3 Digital techniques of modulation	
3.0 Introduction	33
3.1 Digital modulation of analogue signals	33
3.1.1 Linear or uncoded pulse modulation	34
3.1.2 Coded pulse modulation	36
3.1.3 Delta modulation	36
3.1.4 Delta sigma modulation	37

	<u>Page</u>
3.2 Comparison of coded and uncoded modulation, system	37
3.2.1 Comparison of PCM and delta modulation system (delta sigma and delta modulation)	38
3.2.2 Comparison of PCM and delta modulation	38
3.2.3 Comparison of delta sigma modulator and modified delta modulator	40
3.3 Delta modulation system	42
3.3.1 Delta modulator	43
3.4 Delta sigma modulation system	45
3.4.1 Delta sigma modulator	46
3.5 Theory of delta modulator	48
3.5.1 Overload characteristic and noise	48
3.5.2 Quantization noise	51
3.5.3 Determination of K	56
3.5.4 Signal to noise ratio	57
3.5.5 Threshold of coding	58
3.5.6 Dynamic range	58
3.5.7 Limitation of delta modulation	59
3.6 Theory of delta-sigma modulation	60
3.6.1 Quantization noise of delta-sigma modulation	60
3.6.2 Signal to noise ratio	63
3.6.3 Overload for delta-sigma modulation	64
3.6.4 Dynamic range	65
3.6.5 Companded delta modulation	65
3.7 Multiplexing of digital signals	67
3.7.1 Time division multiplexing	67
3.7.2 Frequency division multiplexing	69
3.8 Pulse generation and synchronisation	71
3.9 Bandwidth of T.D.M. signals	73
CHAPTER 4 Computer simulation and signal processing	74
4.0 Introduction	74
4.1 Simulation	75

	<u>Page</u>	
4.1.1	Input signal	77
4.1.2	Simulation of the ECG waveform	78
4.1.3	Simulation of the encoder	81
4.1.4	Simulation of the decoder	85
4.1.5	Digital filters	85
	1. Recursive filters	86
	2. Non-recursive filters	86
4.1.6	Methods of design	87
4.1.7	Advantages of sampling method	89
4.1.8	Simulation of the practical low pass filter	91
	1. Principle	91
	2. Design	92
4.2	Waveform preservation study of the delta modulator and delta sigma modulator	97
4.2.1	Delta modulator	104
4.2.2	Delta sigma modulator	104
4.3	Further analysis	112
4.3.1	Pattern of output pulses	113
4.3.2	Frequency domain analysis	118
4.3.3	Cepstral analysis	118
4.4	Addition of random noise	125
4.5	Discussion	129
4.5.1	Nature of delta sigma modulator	129
4.5.2	Filtering action (decoding)	130
4.6	Time-variant delta modulator	131
4.6.1	Methods of investigation	131
4.6.2	Nature of the delta modulator noise	133
4.7	Experimental arrangement for simulation	134
4.7.1	Noise generator	135
4.7.2	Delta modulator and decoder	137
4.8	Results	137
4.9	Discussion	140
4.10	Effects of errors (digital) on the output of the delta modulation	149
4.11	Theory	149
4.12	Results and discussion	158

	<u>Page</u>
CHAPTER 5 Transmitting and receiving systems	166
5.0 Introduction	166
5.1 Radio link	166
5.2 Radio transmission system	167
5.2.1 Narrow band frequency modulation	168
5.2.2 Digital modulation	170
5.2.3 Choice of modulation method	171
5.3 Frequency modulation transmitters (radio link)	172
5.3.1 Indirect frequency modulation	173
5.3.2 Narrow-band frequency modulation using crystal controlled oscillator	176
5.4 Line links	177
5.4.1 Wire link	178
5.5 Telephone link	178
5.6 Tape recorder	179
5.7 Photocoupler	180
5.8 Acoustic or ultrasonic link	180
5.9 The receiver system	181
5.10 Radio receiver	181
5.10.1 Phase lock loop	182
5.11 Antenna	184
5.11.1 Effect of human body on the performance of antenna	184
5.11.2 Problems of biomedical telemetry antennae	189
5.11.3 Receiving antenna	192
CHAPTER 6 Practical system	193
6.0 Introduction	193
6.1 Design of the system	193
6.2 Transmitting system	197
6.2.1 Electrodes and signal conditioners	197
6.2.2 Encoders (Modulators)	197
6.2.3 Clock	200
Practical circuit	200
6.2.4 Multiplexing unit	202
Practical circuit	203
6.2.5 Combining unit	203
Practical circuit	204

	<u>Page</u>
6.3 Modulator and Radio frequency transmitter	204
6.3.1 Radio frequency oscillator	207
Practical circuit	207
6.3.2 Coupling and matching of the antenna	210
6.4 Receiving system	213
6.4.1 FM receiver (RF/IF Unit) and waveshaping unit	213
Practical circuit	216
6.4.2 Synchronisation and demultiplexing	217
6.4.3 Clock	217
6.4.4 Synchronisation circuitry	219
6.4.5 Demultiplexer	221
6.4.6 Decoder	223
6.4.7 Low pass filter	223
6.5 Single wire time division multiplexing system	225
6.6 Practical system	229
6.6.1 Clock and control circuitry	229
6.6.2 Control circuitry on the transmitting end	231
6.6.3 Transmitting circuitry	231
6.6.4 Receiving circuitry	232
6.7 Performance and characteristics of the system	238
6.7.1 Bandwidth of the system	238
6.7.2 Noise	241
6.7.3 Power consumption	246
6.7.4 DC input-output characteristics and drift	249
6.7.5 Size, weight and range of transmission	252
6.8 Discussion and conclusion	253
CHAPTER 7 Conclusions	254
REFERENCES	256
APPENDIX A	269
APPENDIX B	271
APPENDIX C	275
APPENDIX D	285
APPENDIX E	286
APPENDIX F	287
APPENDIX G	289
APPENDIX H	290
APPENDIX I	306
APPENDIX J	310

CHAPTER I

INTRODUCTION

I. Review of Biomedical Telemetry

The transmission and reception of information in the form of electrical signals has been a common practice by engineers and scientists for a long time. However, the transmission of physiological data has only recently become a common technique, especially with the progress in space technology and hospital automation. The purpose of transmitting physiological data in these cases is the preservation of life and the furtherance of investigations into life functions.

Johnston¹ suggested that there are two somewhat related reasons for sending physiological data, one is for a normal life in an abnormal environment such as a pilot or astronaut tied to his craft by an umbilical cord while the other is an abnormal life in a normal environment such as a patient in the hospital intensive care unit tied to his bed.

Similar reasons apply to extra terrestrial investigators and the ambulatory outpatients who can be linked to their monitors via a radio link. Most of the work done to preserve the life of high risk aircraft pilots and astronauts has led to the design of electronic equipment and instrumentation which can be used for hospital intensive care units and ambulatory patients.

Literally, telemetry is the science of making measurements at a distance. The subject of this thesis is Biomedical Telemetry, which is a technique for obtaining physiological information from the body of unrestrained living organisms at a remote recording or data processing station. The means of transmitting the information from the point of generation to the point of reception may be by the direct connection of wires or cables, or by wireless linkage using radio, ultrasonics, and optics. Radio linkage is most commonly used

In order to reduce the constraint caused by the instrumentation on the subject.

In the case of a direct connection the term 'line telemetry' is used when the subject and station are in different localities. Very short connections, for example in patient monitoring, are not to be included in the field of telemetry as such. In the case of a radio link the transmitter can be implanted or surface mounted. In the first case the transmitter might be implanted totally within the body of the organism.

Einthoven², the founder of practical electrocardiography, used biomedical telemetry for the first time in 1903 by transmitting human electrocardiograms (ECG) from a hospital to his laboratory many miles away. He only used the wires of the Leiden Telephone Company, instead of the whole system and connected a patient having immersion electrodes to a remote galvanometer. Since the existing wires were unsatisfactory due to noise, Einthoven had to install specially designed and insulated conductors. The installation was an example of simple 'hard wire telemetry'.

Barker³ in 1910 used hard wire and not telephone telemetry to connect various wards of a hospital to a heart station. He found, like Einthoven, that induced current on the hard wire causes major problems.

Barker and Brown in 1910 transmitted heart sound for a hundred miles over the telephone and called the system a Telephone Stethoscope⁴. Barker conducted these experiments only for teaching or clinical purposes. The telephone system was used occasionally for medical purposes until 1949 when more progress in this field took place.

Ray and Bickford⁵ (1963) described the use of a telephone link in the Mayo Clinic, Rochester, for connecting the patient monitoring

system to an averaging instrument to process the electroencephalogram (EEG). Stander et al⁶ (1963) and Levine et al⁷ (1966) also used telephone lines for transmitting foetal ECG's and integrated electromyograms (EMG) respectively. Berson et al⁸ (1965) described a typical example of on-line processing by connecting the clinic to a big computer.

Similar work was carried out at the Royal College of Surgeons, London, and the first system was demonstrated by Hill⁹ (1966), whereby test signals were transmitted by telephone to the college from one or more hospitals.

The Institute of Medical Physics TNO, Utrecht, made a 16-channel telephone link for transmitting and recording EEG signals from the local hospital to the Institute. (Kamp¹⁰ 1963)

Although the radio transmission of analogue signals has been known since 1884 (Prescott¹¹) its use to transmit physiological data was used for the first time in 1921 by the U.S. Army signal corp, when they developed a radiotelemetry system for the transmission of heart sounds from ships without an onboard physician to medical facilities on shore (Winters¹² (1921)). Since this use, biomedical radiotelemetry was dormant until 1946 (Caceres¹³ (1965)).

In 1948 Frequency Modulation (FM) was used to transmit ECG by Breaksell and Parker¹⁴ in England, and they developed the first modern working system for transmitting ECG.

Holter and Gengerelli¹⁵ in 1949 studied the radio electrocardiogram of moving subjects by strapping a small portable transmitter on their backs. Holter¹⁶ (1957) later on developed more elaborate radio telemetry systems and was responsible for the development of miniature equipment in this field. The subject carried a small transmitter in his coat pocket and the ECG or EEG was recorded on a

tape recorder in a nearby briefcase.

Holter¹⁷ (1961) eventually eliminated the radio link, so that the patient carried the tape recorder on his body and the ECG was recorded directly.

Winsor¹⁸ and Bellet¹⁹ in 1961 independently used a tiny FM transmitter for telemetering ECG during exercise.

Radio-telemetry is successfully used to monitor the foetal heart which provides a useful tool for clinician and research scientists. It was introduced by Hess²⁰ (1960) after obtaining a successful record of detailed pattern of foetal heart activity during labour and gestation (Hon & Hess 1957, 1960; Lacomme et al 1957, Larks²¹ 1961).

A different development in biomedical radio-telemetry is the transmission of biomedical data such as pressure, pH or temperature from inside the intestines commonly known as an "Endoradiosonde" technique.

Mackay et al²² (1957) and Farrar et al⁴³ (1957) were the first to investigate this by making the subject swallow a radio transmitter and monitoring the data outside the body.

Another direction where biomedical radio-telemetry was developed is in space. Radio-telemetry has become increasingly important to the investigator studying the effect of flight on the body or monitoring the physiology of the pilot or astronaut.

Barr²³ in 1954 pointed out the fact that a large percentage of military plane accidents are due to pilot failure and developed a system for monitoring five physiological parameters.

Kousnetzov²⁴ in 1958 first reported the results from space. All the early studies have used standard method of transmission using FM. Biomedical telemetry from subjects underwater to stations on the surface is becoming an important and common technique. Baldwin²⁵ (1965) and Anderson²⁶ (1970) reported more effective use of sound or ultrasonics to transmit physiological data in these situations.

For most biomedical experiments, and monitoring, simultaneous recordings of several signals is often an essential requirement. For example voltage differences, obtained from the scalp or from inside the brain, are always synchronously recorded from different sites. Similarly in vectorcardiography three analogue signals are used and phonocardiography requires two signals (a sound channel and an ECG channel used for timing). When the number of channels is more than one or two, the use of several single-channel units is not efficient and is often difficult to operate. A multichannel (multiplex), telemetry system is the logical solution and as a result a number of multichannel systems have been devised.

Hoare and Ivison²⁷ (1960) developed a multichannel system using FM-AM, the transmitter being crystal controlled.

Kamp and Storm Van Leeuwen²⁸ (1961) described a two channel EEG radiotelemetry system which has been the basis for development work by others (Hambrecht²⁹ et al (1963)) who used pulse width modulation (PWM) instead of frequency modulation.

Marko and McLennan³⁰ (1963) devised a seven channel transmitting system for EEG having a range of 300 feet using PWM.

Murray, Marko, Kissen and McGuire³¹ (1967) developed a miniaturized time division multiplex pulse duration (PPM)-FM system.

Robrock and Ko³² (1967) developed a six channel telemetry system using a tunnel diode subcarrier oscillator operating from a constant current using FM-FM.

Fischer, Peled, and Yerushalmi³³ (1967) developed a multichannel radiotelemetry system for handling biological data using FM-FM continuous wave.

Rokushima³⁴ (1969) designed a multichannel PWM-FM radiotelemetry system for EEG.

Skutt, Fell and Kertzer³⁵ (1970) developed a multichannel telemetry system for use in exercise physiology. It is a four channel radiotelemetry system using PDM-FM. It has about 100 metres range and weighs 100 gm.

Weller and Manson³⁶ in 1971 developed a low cost three channel system using AM and FM compatible with the British Medical and Biological Telemetry Regulations³⁷. They discussed the practical methods of obtaining maximum transfer of data within the allowed bandwidth and concluded that narrow band frequency modulation can be used to operate several multi-channel transmitters simultaneously in the restricted bandwidth of 200 KHZ.

Zerzawy and Bachmann³⁸ in 1971 developed a four channel programmable long time biomedical radiotelemetry system using FM-FM. Each channel of the device is programmable for ECG, blood pressure, respiration curve, temperature and phonocardiogram. The system transmits D.C. signals with less than 1% drift per hour for an operating time up to 24 hours.

Ijsenbrandt, Kimmich, and Van Den Akker³⁹ in 1971 developed a personal biomedical telemetry system capable of transmitting one to seven D.C. channels compatible with telemetry regulations of many European countries. It uses PDM-FM and is time division multiplexed.

Skutt, Fell and Hagstrom⁴⁰ in 1971 developed a four channel frequency division multiplexing system having a range of 200 metres. The data in this system is transmitted slowly and in digital form using an ultrasonic link.

With a relatively small history of multichannel telemetry there are a number of systems developed. However the requirements for a good biotelemetry system are more than mere communication from the subject to the observer.

For the requirement of a good system the following problems must be considered in addition to the usual concern with signal and noise level, bandwidth, and dynamic range⁴¹.

1. Size and weight. A conveniently small size and low weight to attach it on the surface without any strain.
2. Low power consumption and long life.
3. Stability, reliability and ease of handling.
4. Suitable transmission range and ability to transmit multichannel data.
5. Correct frequency band allocated for transmitting biomedical data, (reference 37 Appendix A).

Multichannel systems based on analogue techniques of encoding biomedical signals suffer from various inherent inefficiencies and do not fulfill all the requirements of a good system mentioned before.

However, digital techniques of encoding the signals are simpler, more reliable, easier to multiplex and make a system compact due to the facility of using microcircuits. In addition they have less cross channel modulation and have lower⁴² sensitivity to temperature and battery voltage (due to the use of two states instead of analogue circuits). These advantages of encoding analogue signals make a system more desirable and efficient.

There are two classes of digital techniques of modulation.

The first is linear or uncoded modulation which includes pulse amplitude modulation (PAM), PPM, PDM, or PWM.

Some research workers^{42,31} have shown that PDM is best suited for compact multichannel biomedical telemetry systems. These systems are insensitive to carrier frequency shifts and have high noise immunity. Comparable analogue systems FM-FM with low power consumption and high baseline stability are complicated and costly and can be troubled by

interference between different measurement channels.

Pulse position modulation has also been tried for biomedical telemetry systems but noise causes synchronisation difficulties and loss of information transmitted.

The other class of digital modulation is the coded modulation which includes PCM and delta modulation. This class of modulation is better than linear modulation because of its superior immunity from the effects of channel noise, higher signal to noise ratio and bandwidth reduction.

The bandwidth required for each of these multiplexing systems is quite different. According to Nicholas and Rauch⁴⁴ the following bandwidths are needed for different multiplexing systems having ten channels, signal cut-off frequency of 100 Hz and signal to noise ratio of 100.

Pulse Code Modulation-FM	18 kHz
Pulse Duration Modulation-FM	92 kHz
FM-FM	140 kHz
Pulse Position Modulation	400 kHz

Another consideration is that of size and weight. A very rough calculation based on the number of transistors needed shows that Pulse Code Modulation-FM requires about three times more components than Pulse Duration Modulation-FM or FM-FM and it also uses more power. Although Pulse Code Modulation-FM is better in bandwidth, signal to noise ratio, and other aspects, it is bigger in size and consumes more power due to its complicated circuitry. Delta modulation is a simpler digital technique for encoding and decoding analogue signals than PCM (Chapter 3). It has all the advantages of digital modulation mentioned above including PCM, but has a wider bandwidth than PCM.

A narrow band frequency modulation used to transmit multi-channel digital data can reduce the bandwidth.

The simplicity of delta modulation and other advantages mentioned above makes it a suitable form of modulation to use it in a multichannel personal biomedical telemetry system.

1.1 Purpose and Structure of the Project

The multichannel biomedical telemetry systems reviewed in the previous section do not fulfil all the requirements of a good system (mentioned in the last section). To meet these requirements a system based on delta modulation was investigated, designed and developed. In order to transmit the multichannel encoded data reliably and with a smaller bandwidth, narrow band frequency modulation was investigated and employed for the radio link.

A single wire time division multiplexed system was also designed and developed for a short range transmission.

The investigation included simulation of the system on the computer. In addition further analysis and study of the system for the suitability of biomedical signals was performed. This involves the use of various signal processing techniques for the biomedical signals.

To present the project in a logical sequence, the thesis is divided into seven chapters. Each chapter is further divided into sections. The relevance of each chapter to the thesis is discussed below.

The first chapter introduces the subject of the thesis, tracing the historical background of biomedical telemetry and various systems in existence. Requirements for a suitable system are then discussed.

The second chapter deals with the origin and nature of biomedical signals, techniques of acquiring and amplifying these signals.

The third chapter discusses and compares various digital techniques of encoding biomedical signals and discusses their suitability. The suitable technique considered and its theory is described in detail.

The fourth chapter is on the computer simulation of a biomedical telemetry system based on delta modulation and delta sigma modulation. The systems are studied for waveform preservation and long time monitoring of these modulation systems for ECG waveforms.

The effect of error pulses at the digital output of the delta modulator is studied on the decoded ECG waveform.

The fifth chapter describes the transmitting and receiving system with various transmitting links. It also discusses a suitable technique for transmitting the biomedical data via a radio link. The effects of human body on the transmitting antenna is discussed in detail.

The sixth chapter describes the design, development and construction of a multichannel system using a radio link and a coaxial cable. Their performances and characteristics are given.

The last chapter gives the conclusions and suggestions for further work.

CHAPTER 2

BIOMEDICAL SIGNALS AND THEIR ACQUISITION

2. Introduction

Biomedical signals to be telemetered originate from the body itself at a cellular level. The signals are detected or acquired by appropriate devices and amplified by suitable techniques. However, it is important to know the nature and characteristics of the biomedical signals prior to their acquisition or amplification.

Certain systems in the living body produce bioelectric potentials in order to carry out various functions. These potentials can be monitored and carry useful information about the functions of the living system. The bioelectric potentials originate due to the ionic voltages produced as a result of the electrochemical activity of certain special types of cell. The idea of electricity being generated in the body goes back as far as 1786 when the Italian professor of anatomy, Luigi Galvani, reported to have found electricity in the muscle of a frog's leg, (Cromwell et al⁴⁵).

Several other scientists after that discovered electrical activity in various animals and in human beings. The human electrocardiogram was discovered by Waller⁴⁶ in 1887 (Caceres¹³ 1964). The first practical application was made in 1903 by a Dutch physician, William Einthoven, who measured the human electrocardiogram using a string galvanometer.

2.1 Biomedical Signals (47,45)

Although the biopotentials originate at the cellular level, the measurement is related to a specific physiological sub-system such as the signals due to the bioelectric potentials associated with nerve conduction, brain activity, muscle activity, heartbeat, and so on. Thus the electrocardiogram (ECG) is a recording of electrical activity of the heart, the electroencephalogram (EEG) of voltages in the brain, the electromyogram (EMG) of the muscles,

the electro-oculogram (EOG) of the eye, and electro-retinogram (ERG) of the response of the retina to light.

The most important body signals with their amplitudes and frequency spectra are given below:

Electrocardiogram (ECG)	0.5-5mV	0.1-100 Hz
Electroencephalogram (EEG)	5-100 μ V	0.1-100 Hz
Electromyogram (EMG)	50-5000 μ V	1-5000 Hz
Respiratory Ventilation		0-10 Hz
Temperature		0-1 Hz
Mean blood pressure		0-1 Hz

Other physiological parameters which change very slowly under most conditions are blood pH, pH in the digestive tract, pO_2 in blood and in expired air. Various sounds such as with phonocardiography are also of interest but these are difficult to pick up, especially from moving subjects.

With the exception of the EMG and heart sounds all physiological signals have a frequency spectrum below 100 Hz (though there has been some discussion of small ECG components of up to 200 Hz). Although measurement of individual action potentials can be made in some types of cells, these measurements are difficult because of the difficulty, the precise placement of an electrode inside a cell, presents. The common form of a measured biopotential is the combined effect of a large number of action potentials as they appear at the surface of a body or at one or more electrodes inserted into a muscle, nerve, or some part of the brain.

The exact method by which these potentials reach the surface of the body is not known. However, a number of theories have been advanced that seem to explain most of the observed phenomena fairly well, though none exactly fit the situation. For example the

biopotentials from the heart as they appear at the surface of the body, according to one theory, are a summation of the potentials developed by the electric fields set up by the ionic currents which generate the individual action potentials.

This theory, although plausible, does not explain a number of the characteristics indicated by the observed surface patterns. An approximation is obtained by assuming that the surface pattern is a function of the summation of the first derivatives of all the individual action potentials instead of the potentials themselves. Part of the difficulty arises from the many assumptions that must be made for the ionic current and the electric field pattern throughout the body, as the validity of some of the assumptions is questionable.

2.2 Transducers

In order to acquire biological signals from the human body a device capable of converting one form of energy or signal to another is required. Such a device is called a transducer and in the man-instrument system it is used to produce an electric signal that is the analogue of the physiological phenomenon being measured. The transducer may measure temperature, pressure, flow, or any other variable that can be found in the human body, by converting it to an electrical signal.

Transducers may be classified according to the type of input energy to which they are sensitive. The broad categories under such a classification include :

- (a) Mechanical
- (b) Temperature
- (c) Magnetic
- (d) Electrical
- (e) Radiation

In biomedical electronics and instrumentation all types of classification are utilized to some degree.

2.3 Electrodes

Despite the variety of transducers used to measure different physiological phenomena, the most common device used to acquire signals such as the ECG, EMG and EEG is an electrode. It is a device (transducer) used for measuring a bioelectric potential by converting ionic potentials and currents into electric potentials and currents. As a result an electrode used as the bioelectric transducer consists of two electrodes which measure the ionic potential difference between their respective points of application.

The electrodes come in many shapes, sizes and materials. The following theory applies to all electrodes, including biochemical electrodes used to measure pH, pO_2 and pCO_2 of the blood.

2.3.1 Electrode Theory (50)

The interface of metallic ions in a solution with their associated metals results in an electric potential and is called the electrode potential. The generation of this potential is the result of the difference in diffusion rate of ions into and out of the metal. An equilibrium is produced by the formation of a layer of charge at the interface. The charge in reality is a double layer with the layer nearest the metal being of one polarity and the layer next to the solution being of opposite polarity. Other materials, such as non-metals like hydrogen, also have electrode potentials when interfaced with their associated ions in solution. The determination of the absolute electrode potential of a single electrode for the measurement of the potential across the electrode and its ionic solution would require the placing of another metallic interface in the solution. Therefore all electrode potentials are given as relative

values and must be stated in terms of some reference. By international agreement, normal hydrogen was chosen as the reference standard. An electrode potential of zero volts is arbitrarily assigned to it.

Another source of an electrode potential is the unequal exchange of ions across a membrane which is semi-permeable to a given ion, when the membrane separates liquid solutions with different concentrations of that ion. This potential across the membrane is given by the equation called the Nernst equation:-

$$E = (-RT/nF) \ln(c_1 f_1 / c_2 f_2) \quad n = \text{valence of ion}$$

where T = Absolute temperature in degrees Kelvin, F = the Faraday constant

R = the gas constant (8.315×10^7 ergs per mole per degree Kelvin)

$C_1, C_2,$ = the two concentrations of the ions and f_1, f_2 = the respective activity coefficients of the ions on the two sides of the membrane.

2.3.2 Equivalent Circuit of Electrodes (50)

All the three types of biopotential electrodes mentioned in section 2.3.7. have a metal-electrolyte interface. The potential in each case is developed across the interface, proportional to the exchange of ions between the metal and the electrolytes of the body. The double layer of charge at the interface acts as a capacitor. Hence, the equivalent circuit of a biopotential electrode in contact with the body consists of a voltage connected in series with a resistance-capacitance network. The equivalent circuit is shown in figure 2.1.

2.3.3 Problems of Electrodes (51)

Certain chemical and physical disturbances in the measurement of a physiological signal using electrodes as transducers affect the stability of the interface between the electrodes and skin. This gives rise to extra and spurious voltages, sometimes comparable with the biological signals being measured.

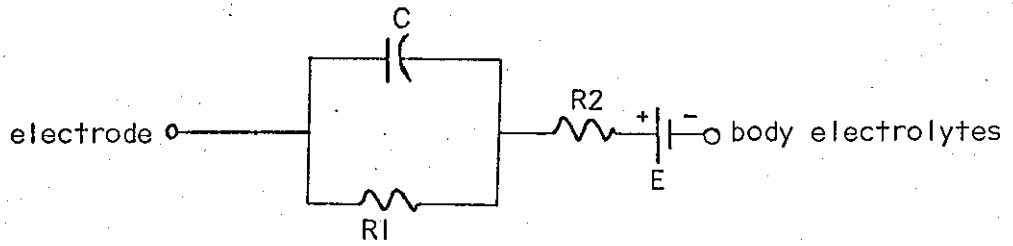


Figure 2.1(a)

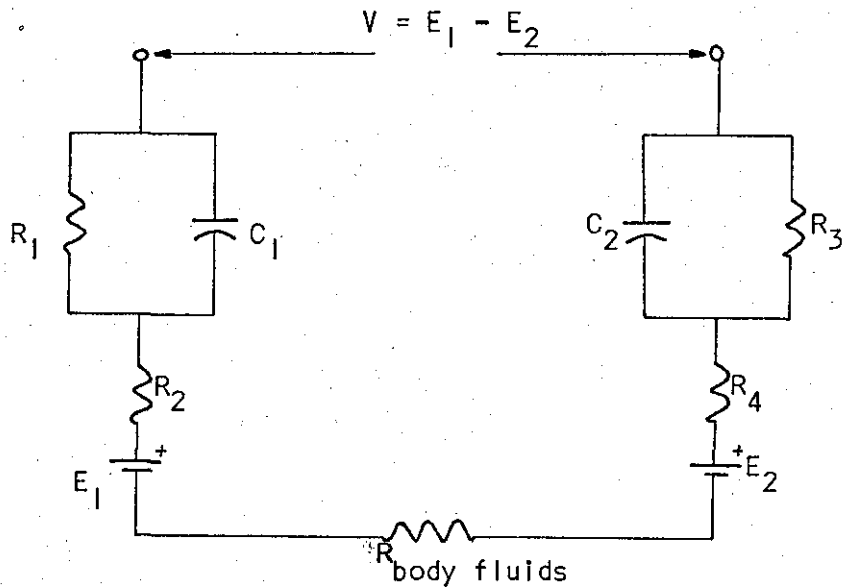


Figure 2.1(b)

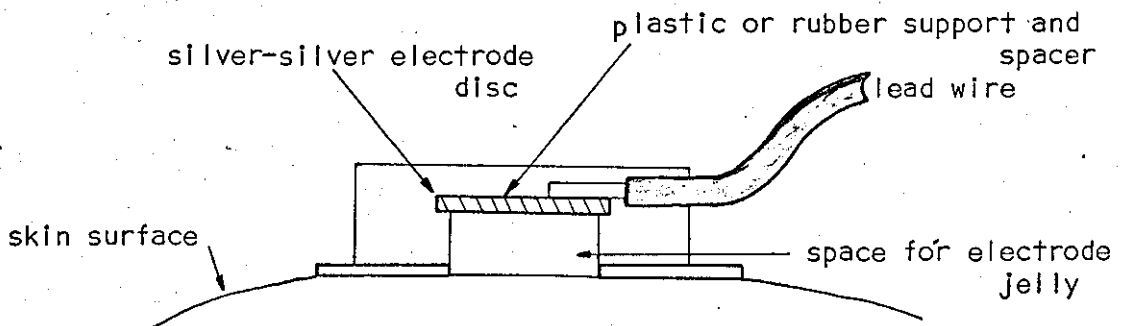


Figure 2.2.

Figure 2.1(a) Equivalent circuit of biopotential electrode interface.

Figure 2.1(b) Measurement of biopotential with two electrodes - equivalent circuit.

Figure 2.2 Floating type skin surface electrode.

In the use of various electrodes for measuring physiological phenomena, it is always a metal, usually silver, or a metal and its salt, (for example silver and silver chloride), which makes electrical contact with the body fluids.

The skin is composed in part of a dead corneal layer. A second layer of cells is actively producing more cells which are gradually dying and becoming a horny layer called the Epidermis. The layer below this is a soft connected tissue containing blood vessels and is called the Dermis. The impedance of the skin is often thought to be due to the dead layer of tissues. Most of the impedance really occurs in the deeper layer of cells and represents a liquid junction with an accompanying liquid junction potential.

This junction potential contributes to the bioelectric potential in the skin. One way to minimise and stabilise the liquid junction potential is to penetrate through the horny layer with a pin, not deep enough to draw blood.

2.3.4 Motion Artefact (51)

Motion of the skin with the surface electrode on it generates motion artefacts if the insulating skin surface is left intact. Artefacts in this context refer to any component of a signal that are extraneous to the variable represented by the signal and are produced by sudden changes in potential because interfaces are being disturbed. But the skin has many other apertures, such as sweat glands that also represent pathways. Hence, it is an example of a biological liquid junction where a liquid junction potential develops. Electrode jelly often contains quartz or glass granules which, when rubbed into the skin, break the horny layer and minimize and stabilise the junction potential. Electrode creams accomplish this result by the biochemical irritation of a very high chloride concentration.

2.3.5 Half Cell Potential (51)

With surface electrodes, a conducting paste or gel is applied between the electrode and skin to reduce the impedance.

The electrode-gel tissue combination forms an electrochemical half cell battery that produces a potential difference between the electrode and the tissue usually smaller than a volt but sometimes as large as three volts.

The electrode potential is a logarithmic function of the concentration of metal ions in the gel as described by the Nernst equation, in Section 2.3.1.

The silver electrode used in the body in this case has no silver ions in the electrolyte. This electrode, as a result, does not reach a stable known potential and the voltage wanders and drifts. The electrode potential is obtained by the formation of silver oxide on the surface. To avoid this, silver oxide can be deposited on the entire electrode surface, or a pressed silver chloride pellet can be used as an electrode. This makes it an artificially non-polarised electrode. The silver chloride is only slightly soluble and remains in equilibrium with its saturated solution thereby controlling and stabilising the silver ion concentration. The activity of the chloride determines the silver ion concentration which in turn determines the half cell potential. As a result the use of silver chloride makes the potential dependent on the chloride present in the body which is predictable and reaches a stable known value.

2.3.6 Polarisation (52)

In a human body there are no majority carriers of any metals which can be used for electrodes. If the metals used for electrodes do not have their ions as majority carriers the system is polarisable.

When a potential is applied to such a system certain ions build up and there is a variable interface that acts like a dielectric and charges up like a capacitor or a battery. The electrode potential and impedance change as a result of the direct current passing through the metal electrolyte interface. This electrochemical problem associated with electrodes is called polarisation.

2.3.7 Types of Bioelectric Electrodes and requirements (50,53)

These can be classified into one of the following types:

1. Surface Electrode. Electrode used to measure ECG, EEG, and EMG potential from the surface of the skin.
2. Micro-electrodes. These are used to measure bioelectric potentials near or within a single cell.
3. Needle electrodes. These are used to penetrate the skin to record EEG potentials from a local region of brain or EMG potentials from a specific group of muscles.

Surface electrodes being widely used in present biomedical telemetry systems are discussed here.

The requirements in respect of the electrochemical category of disturbance for the surface electrodes are the following :-

- (i) The method of applying the electrode should be as simple as possible.
- (ii) It should be possible to record continuously for a long time.
- (iii) Very few or no artefacts should occur in the recording of ECG during intensive movement by the subject.
- (iv) The surface electrodes should be watertight in such a way that over the surface of the skin no short circuiting is caused by heavy perspiration, or when the subject is under water.

2.3.8 Surface Electrodes (50,53)

The electrodes used to record biopotentials from the surface of the body occur in many different sizes and forms. It is usual to use larger electrodes for sensing ECG signals because the localisation of measurement is not important while the smaller electrodes are used mainly for EEG and EMG measurement.

The earliest electrode used by Einthoven was an immersion electrode. This was simply a bucket of saline solution into which the subject placed his hands and feet and used one bucket for each extremity.

Surface electrodes are of two types:

1. The direct contact electrode
2. The fluid or floating electrode

The first type includes the plate electrode and the metallized gauze electrode.

The plate electrode was first introduced in 1917 where the electrode was separated from the subject's skin by cotton or felt pads soaked in a concentrated saline solution. The soaked pads were later replaced by a conductive jelly or paste and the metal was in contact with the skin. This plate electrode is still in use. Another old type of direct contact electrode still in use is the suction-cup type in which only the rim makes contact with the skin.

One of the difficulties in using the plate electrode and the suction-cup electrode is the possibility of electrode slippage or movement. Even the slightest movement changes the thickness of the thin film of electrolyte between the metal and the skin which causes changes in the electrode potential and impedance. These potential changes in many cases are so severe that they completely disrupt the bioelectric potential which the electrode attempts to measure.

Metallized gauze electrodes reduce this movement artefact by limiting the electrode movement and reducing the interface impedance. These electrodes are made of metallized nylon and fixed with adhesive tape. Although better than plate electrodes they are not completely insensitive to movement.

The second type of surface electrodes include the flexible cup electrode and a newly developed rigid cup electrode.

The principle of this type of electrode is to practically eliminate movement artefact by avoiding any direct contact of the metal with the skin. The only conductive path between metal and skin is the electrolyte paste or jelly which forms an electrolyte bridge. It is shown in figure 2.2. These electrodes are generally attached to the skin by means of two-sided adhesive rings which stick to both the plastic surface of the electrode and the skin.

The flexible cup electrode consists of a plate and a gauze or thread fixed in a rubber housing, which is glued to the skin.

A newly developed rigid cup electrode is made of a silver plate fastened in a rigid housing. A linen gauze is attached to the housing which is glued to the skin after jelly has been poured into the cup under the gauze. This electrode overcomes the problems encountered in other types.

Various types of disposable electrodes have been introduced in recent years to eliminate the usual requirement for cleaning and care after use. In general these electrodes are of the floating (fluid) type and primarily intended for ECG monitoring but can also be used for EEG and EMG.

Special types of surface electrodes have been developed for other applications:

- (i) The wick electrode. It consists of a metal contact that interfaces with a soft wick filled with the electrolyte. This electrode is used in situations where the pressure or weight of a standard surface electrode cannot be tolerated, such as in measuring potentials from the surface of the eye or from an internal organ.
- (ii) Ear clip electrode. It was developed for use as a reference electrode for EEG measurement and can actually be clipped to the ear.
- (iii) Scalp electrode. It is usually a small disc about 7 mm in diameter or a small solder pellet that is placed on the cleaned scalp through electrolyte paste.
- (iv) Spray-on Electrodes. Conventional disc electrodes often present difficulty in obtaining good ECGs under conditions of perspiration and considerable movement. A new technique for applying electrodes, originally developed for instrumenting ⁴⁹ NASA test pilots, was recently evaluated on children. The technique consists of spraying a conductive mixture over the end of electrocardiograph wires and on to the skin. A solvent in the mixture evaporates quickly leaving a thin flexible layer of conductive material which firmly holds the lead wire in contact with the skin, (Bendersky⁴⁸).

AMPLIFICATION OF BIOMEDICAL SIGNALS

2.4 Introduction (52)

Most of the biomedical signals acquired by the transducers (electrodes) are often of a low amplitude and may be accompanied by interference. In order to bring these signals into a suitable form some sort of conditioning is required. The requirement for conditioning which includes amplification depends upon the type of transducers (electrode) used and the characteristics of the signal.

Signal characteristics, given in section 2.1, determine such requirements as gain, bandwidth and noise (referred to the input). The transducer (electrode in this case) characteristics determine the required input impedance, common-mode rejection and the maximum ejection current (current which flows in the source due to connection of amplifiers). Linearity, distortion and gain stability are also requirements in some applications. The impedance of electrodes is usually very high, sometimes as high as 10^{12} ohms in the case of microelectrodes. Such electrodes must be used with amplifiers having at least a 10^{15} ohms input impedance and feedback to cancel the electrode capacitance.

An equivalent circuit is given in figure 2.3 representing the subject, the electrode, skin interface and the amplifier input. The subject model can be considered to consist of parallel RC elements representing skin resistance, the deep tissue resistance, and skin capacitance. The approximate value of skin resistance can vary from hundreds of ohms for abraded skin to a megohm for dry skin. The value of deep tissue resistance lies in the range of a few hundred ohms. It is a direct function of the resistivity of blood and tissue and is proportional to the geometry and length of path between electrodes. The value of skin capacitance, the total equivalent capacitance from the electrode to the deep tissues, depends on the electrode surface area.

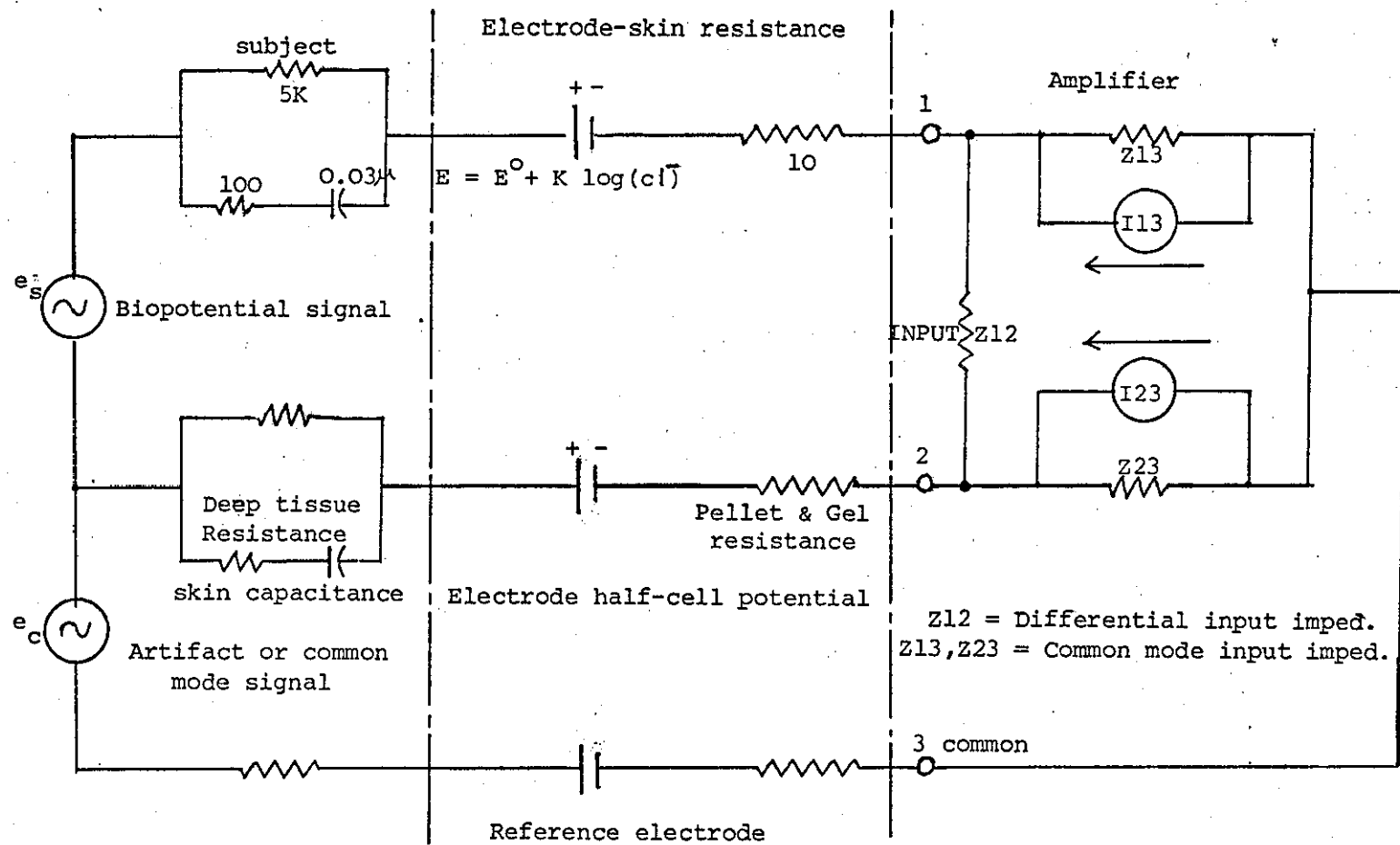


Figure 2.3 Equivalent Circuit showing interactions caused by the biopotential source - the subject and the electrode interface and amplifier characteristics for measuring a typical biopotential. The values shown are approximate since deep-tissue and skin resistance can vary widely.

In the case of a silver-silver chloride, the equivalent circuit shown in figure 2.3 consists of the electrode pellet and gel resistances⁵² and the electrode half-cell potentials. The electrode resistance is small enough to be ignored since measurement of the bioelectric potential requires two electrodes, the voltage measured is really the difference between the instantaneous potential of two electrodes.

The common-mode voltage source shown represents misleading signals and noise, including power line interference. Such voltages are not always completely common mode and show up as differential signals at the output.

2.5 Design Techniques

The design of biological amplifier should provide for the faithful amplification of bioelectric signals from the subject by means of an electrode with the characteristics given above. The amplification of these signals by a single ended amplifier can show up the interfering signals at the output. The most serious of these are 50 Hz potentials which are inevitably present in typical surroundings and are coupled into the amplifier input circuit through the fairly high and variable source resistance. Interference currents flowing round the input loop of the amplifier can develop input voltages to the amplifier which disrupt the desired signal.

To alleviate the interference problem it is necessary to use a differential amplifier shown in figure 2.4. The bioelectric signals are applied between the inverting and non-inverting inputs of the amplifier. If the impedance of each input terminal to earth is sufficiently high, the interference voltage is not able to inject a significant signal into the input loop. The amplifier, in addition

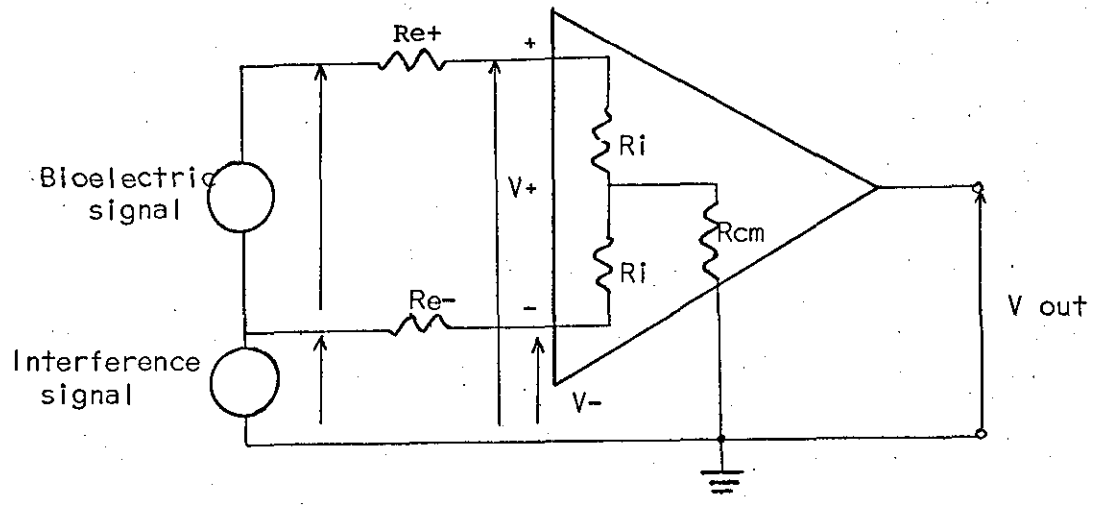


Figure 2.4 Differential Amplifier

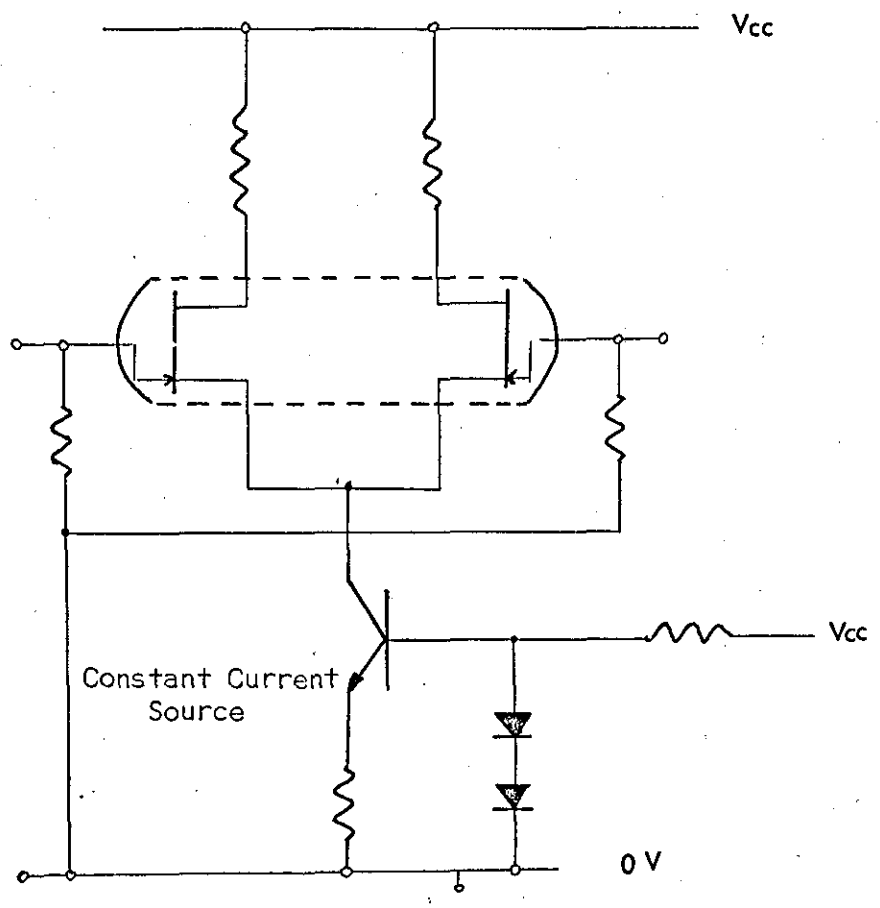


Figure 2.5 Input Stage (using FET's) of the Biological Amplifier with Constant Current Source.

to having a high impedance at both input terminals, must also be capable of discriminating against the interference voltage which appears at both input terminals simultaneously. The ratio of the output voltage to a common voltage applied to the inputs is termed the common mode gain, while the ratio of the output voltage to a differential input voltage is termed the differential gain. The ratio of the differential gain to the common-mode gain is called the common-mode rejection ratio (CMRR). A high value of common-mode rejection ratio enables the amplifier to distinguish between differential input signals and common-mode input signals.

The electrode impedances form a voltage divider with the impedance of the differential amplifier. If the electrode impedances are not identical, the interference signals at the two inputs of differential amplifiers may be different, and the desired degree of cancellation does not take place. Because the electrode impedances can never be made exactly equal, the high common-mode rejection ratio of a differential amplifier can only be realized if the amplifier has an input impedance much higher than the impedance of the electrodes to which it is connected. The input impedance as indicated in figure 2.4 may not be the same for the differential signal as it is for the common-mode signal. The use of a differential amplifier also requires a third connection for the reference or earth input. Hence an amplifier required to amplify bioelectric potential using electrodes ought to be a differential amplifier having the following characteristics:

1. High gain
2. High Input Impedance
3. High common-mode rejection ratio

2.5.1 Method of achieving high input impedance (54,55)

There are various ways of achieving a high amplifier input impedance. In the past the use of electrometer valves has provided the high impedance for the input stages of biological amplifiers.

The conventional bipolar transistors (D.W. Hill and R.S. Khandpur) are inherently current amplifying devices with a low input impedance and a high gain. As a result conventional transistors for ECG amplifier input stages are more complex than valve input stages for a cascade arrangement which gives high input impedance. The factors which limit the low frequency input impedance are the shunt impedances presented by the emitter circuits, the base bias resistors and the collector loads which are all in parallel across the input. There are new transistors with a high gain at a low collector current which can give a high input impedance.

Towers (1968), reviewed a number of methods for attaining high values of input impedance with bipolar transistors, such as the use of emitter followers, Darlington pairs, bootstrapping the input circuit and the use of complementary transistors in the input stages.

The semiconductor counterpart of the vacuum electrometer valve is the field effect transistor (FET). Dual field effect transistors encapsulated in a single can, and carefully chosen with regard to gate current, are better than electrometer tubes.

2.6 Biological Amplifier

The logical choice for a suitable biological amplifier is a differential amplifier using a FET as an input stage followed by a high gain amplifier. There are available at present a matched pair of FET's

and a linear amplifier in the same chip. The only disadvantage it has is the large D.C. offset voltage.

The pair of FET's forming the input stage of the amplifier is shown in figure 2.5. The pair of FET's is computer matched from the same wafer to obtain the best practical results and thermal performances are improved by mounting the FET's on an alumina substrate. To help compensate for thermal drift, the quiescent point of the differential pair is set such that both the gate-to-source voltage and the drain current of each FET are independent of temperature.

For higher values of CMRR the common mode source resistance is replaced by a compensating constant current source. This current source is a transistor whose output impedance is very high (about 100k ohms). The constant current source is shown in figure 2.5. It uses a transistor for constant current and two silicon diodes to compensate for any temperature drift in the base emitter voltage of the transistor. Any change in the base emitter voltage will be followed by a similar change in the forward voltage of the diodes. Hence the compensation for the temperature is achieved and the current remains constant in the transistor.

Although the input is differential the biological amplifier has a single ended output. The gain of this differential amplifier is not very high, hence a high gain is required in the following stage to obtain an appropriate signal for digital encoding.

As very high gain amplifiers are available in an integrated circuit mounted on a single chip, the choice of this amplifier will depend upon the power consumption and relative high open loop gain.

2.6.1 Practical circuit for ECG amplifier

The complete biological amplifier is shown in figure 2.6. The input stage is a differential amplifier using a silicon junction field effect transistor TIS68. The pinch off voltage V_p is -2.28 volts and the drain current I_{DSS} at gate source voltage $V_{GS} = 0$ is 5.05 mA. The operating gate-to-source voltage is -1.83 volts. The next stage from the field effect transistor is a high gain amplifier. The microcircuit amplifier used is a TEXAS μ A741, it is a low power device and uses a ± 5 volt supply. The amplifier has a low pass response achieved by using a RC network across the amplifier.

The frequency response of the amplifier extends from DC (direct coupled) to 100 Hz at the 3db point.

$$f = 1/2\pi RC$$

$$R = 1\text{Mohm}$$

A practical method of reducing the effects of the high common mode signal due to the A.C. environment is to connect the earth lead of the amplifier to the right leg of a subject. This reduces the amplitude of interfering signals and the common-mode rejection ratio of the amplifier is increased.

The following figures are achieved with the amplifier.

Input impedance	= 1 megohm
Output impedance	= 200 ohms
Differential voltage gain	= 600
Common-mode rejection ratio	= 70 db
Frequency response	= 0.1 Hz to 100 Hz (3 db point)

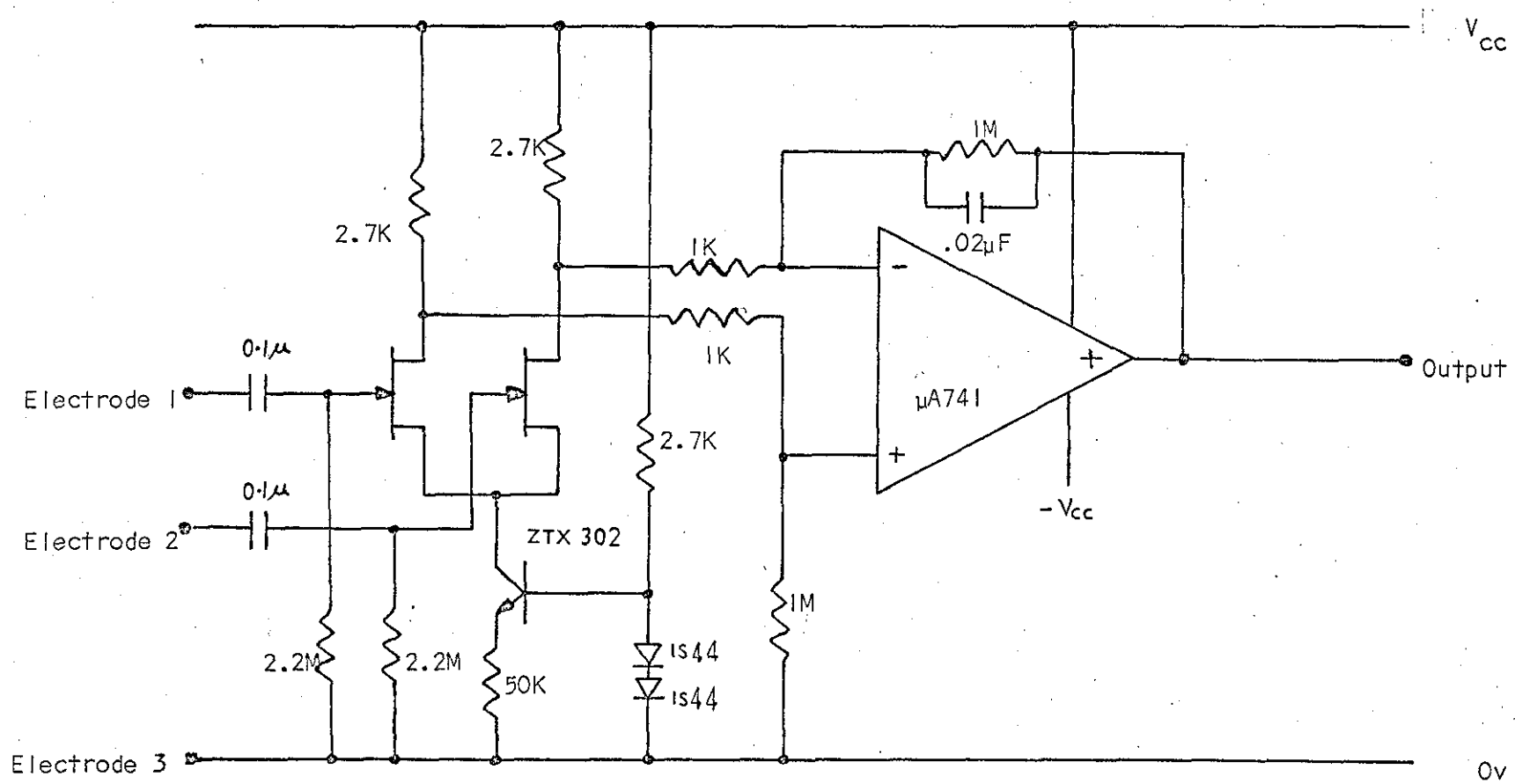


Figure 2.6 ECG Amplifier

CHAPTER 3

DIGITAL TECHNIQUES OF MODULATION

3. Introduction

In biomedical telemetry systems the signals obtained from the physiological transducers are properly amplified and transmitted via a suitable link. Most of the signals obtained are analogue in nature. For an efficient transmission the signals obtained are processed or modulated in some manner prior to actual transmission. The modulation and transmission of signals can be accomplished by digital or analogue techniques. Analogue techniques of modulating and transmitting the signals suffer from various inherent inefficiencies while the digital technique offers many advantages in the modern day technology. The following are some of the advantages for the digital technique of modulating and transmitting the signals⁵⁶.

1. The ability of digital signals to be coded such as to minimise the effects of noise and interference.
2. The relative simplicity of digital circuit design and the application of integrated circuit techniques to digital circuitry.
3. The widespread use of computers and digital processing techniques for handling all kinds of digital data.

3.1 Digital Modulation of Analogue Signals

In the digital transmission of signals the analogue signal is converted into discrete samples or pulses at fixed intervals. The samples can be further digitized (quantized) and encoded in the binary form. The modulation whereby the pulse parameters are modulated to contain the sampled values for transmission is called a pulse modulation system. In these systems a periodic sequence of pulses constitutes the carrier. There are two classes of pulse modulation.

1. Uncoded or linear modulation.
2. Coded pulse modulation.

The pulse modulation is derived basically from the sampling theorem. This states that if a bandlimited analogue signal is sampled at a rate at least twice the highest frequency (Nyquist rate) component of the signal, the information content of the signal is retained by the discrete set of instantaneous amplitude values resulting from sampling, and the original information can be recovered by a suitable demodulation process.

3.1.1 Linear or Uncoded Pulse Modulation

Linear pulse modulation is based on the sampling theory and it utilizes the properties of the pulse train which is modulated. These are the amplitude, width, and the phase or time of occurrence of the pulses. In some systems it may be desirable to modulate more than one of these variables simultaneously. The different types of pulse modulation are shown in figure 3.1.

A modulation whereby modulating signals vary the pulse amplitude is called pulse amplitude modulation (PAM).

In pulse width modulation (PWM) either the rise or fall of the pulse or both may be advanced and retarded to make the width proportional to the modulating signal. If the fall is modulated, the rises being regularly spaced in coincidence with the sampling time, the form of modulation is also known as pulse duration modulation (PDM).

In pulse position modulation (PPM) the width and the amplitude of the pulses are unaltered but the time of occurrence of the pulses effectively advances and retards in accordance with the modulating signal.

Pulse position modulation and pulse duration modulation systems require substantially more bandwidth than equivalent PAM systems for they depend on the accurate location of the pulse edges. This

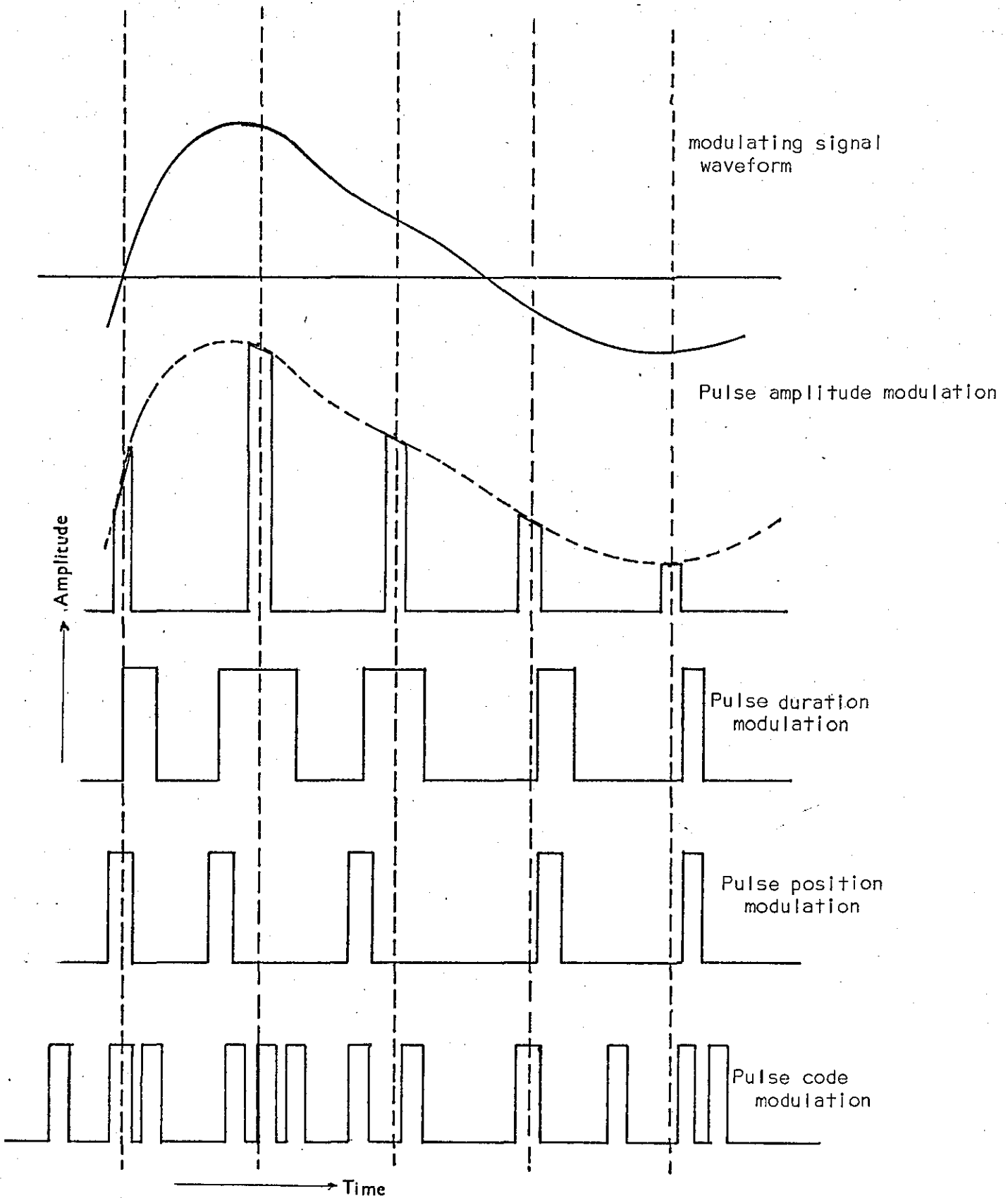


Figure 3.1 Methods of Pulse Modulation

increased bandwidth in the case of PPM leads to an improved signal-to-noise ratio, although the improvement is not as efficient as in the case of PCM. There is no signal-to-noise ratio improvement in PAM.

3.1.2 Coded Pulse Modulation

Pulse code modulation, delta modulation and delta sigma modulation make up the other class of coded pulse modulation. The feature common to these modulation processes lies in the choice of the pulse parameter to be modulated which is the presence (or absence) of a pulse. This parameter is a two state variable. Coded modulation is obtained by utilizing this feature together with a coding of the magnitude of the quantum level.

In pulse code modulation, the analogue signal is sampled and the amplitude range of the sampled data is divided into a finite number of discrete levels. The amplitude of a given pulse is referred to the nearest level and a digital code is generated. For example, in a binary system⁵⁷, 31 amplitude levels (or quanta) are uniquely specified by a 5-digit code, since $2^5 - 1 = 31$.

3.1.3 Delta Modulation

In delta modulation, instead of transmitting the instantaneous amplitude as in PCM, the derivative of the input is transmitted. The range of signal amplitude is divided into a similar number of quantum levels as in the PCM system. However, at each sampling instant, the presence or absence of only one transmitted pulse contains the intelligence.

Delta modulation is essentially a feed back system in which the analogue input signal is regenerated by integrating the digitally encoded signal and comparing with the analogue input. The difference

of the two signals decides the polarity of the output pulse which is chosen to reduce the error between the two waveforms.

3.1.4 Delta Sigma Modulation

If an integrator is included in the input circuit (forward path) of the delta modulation system, the system is called Delta Sigma modulation. In this system it is the instantaneous amplitude of the input signal, (like PCM), which is transmitted and not the rate of change (derivative) of the input signal. Delta sigma modulation uses a single digit code.

3.2 Comparison of Coded and Uncoded Modulation System

The binary or coded modulation, though complicated in the case of PCM, is more reliable and offers better noise immunity. As the information is carried by the binary pulses, the signal is represented either by the absence or presence of a pulse or by its polarity. The receiver function is to recognise the presence or absence of a pulse or polarity and then decode it into the original quantised form to reconstruct the signal. The pulse shape or its exact amplitude is not significant as in the case of the original signal or a PAM signal. By transmitting binary pulses of high enough amplitude, correct detection of the pulse in the presence of noise with as low an error rate (or possibility of mistakes) as required is possible.

Delta modulation and delta sigma modulation being coded systems offer all the advantages mentioned above and are more attractive to use because of their simplicity in circuitry which also makes them less expensive.

3.2.1 Comparison of PCM and Delta Modulation System (Delta Sigma & Delta Mod.)

Although all the modulation systems belong to the coded group the main difference⁽⁵⁷⁾ between the PCM and other modulation systems is that the former is n-digit code modulation while the other two employ only single digit codes. In PCM and Delta Sigma modulators, the instantaneous amplitude of the signal is transmitted while in Delta modulation it is the rate of change of signal amplitude which is communicated.

The basic principle of the PCM system requires near analogue-to-digital conversion because of its periodic transmission of absolute measurement of quantised levels. Thus it requires voltage comparators which retain a high degree of precision over the complete range of amplitudes of the input signal, and complex high speed gating circuitry to affect the analogue to digital coding. This aspect of PCM systems calls for extensive and specialised circuitry. The delta modulator and Delta sigma modulator offer considerable advantages in this regard.

3.2.2 Comparison of PCM and Delta Modulation (57,58)

For a sine wave input the delta modulator satisfies the limiting condition of non-overloading and PCM has a peak-to-peak amplitude occupying the full quantized amplitude range. In fact this comparison has been carried out on a number of occasions and usually a plot of signal-to-noise ratio against clock rate shows that the delta modulator is superior to PCM, when the latter uses a code group of five or less.

However, Betts⁽⁵⁷⁾ has reported that PCM for speech signals occupying a 30 db mean level range and using a 7-digit code is superior to the delta modulator. Although delta modulation is unsuitable in this application it has possible applications in other fields such as

telemetry for which the required dynamic range may not be so large or the permissible signal-to-quantizing ratio may be less than 26 dB.

The quantization noise in PCM is ⁽⁹⁵⁾

$$N_q^2 = \frac{\mu^2}{12}$$

where μ is the spacing between two adjacent quantization levels. If there are L levels, then a sinusoid having an amplitude $\frac{\mu L}{2}$ is the largest signal which the system can accommodate without causing overloading. The power in this sinusoid is $\frac{\mu^2 L^2}{8}$, resulting in a signal-to-noise ratio of

$$\frac{S^2}{N_q^2} = \frac{3}{2} \times L^2 = \frac{3}{2} \times 2^{2n} \quad (3.1)$$

where n is the number of coded pulses per quantized sample.

If the threshold signal is defined to be $\frac{\mu}{2}$ then the amplitude range is

$$A = \frac{\frac{\mu L}{2}}{\frac{\mu}{2}} = L = 2^n$$

and

$$\frac{S^2}{N_q^2} = \frac{3}{2} A^2 \text{ or } A = \sqrt{\frac{2}{3}} \left(\frac{S}{N_q}\right) \quad (3.2)$$

Similarly with delta modulation the amplitude range is given by

$$\frac{f_s}{\pi(f_c^2 + f_m^2)^{\frac{1}{2}}} \quad \text{from equation 3.20.} \quad (3.3)$$

The signal-to-noise ratio for a sinewave which just overloads the system can be derived from section 3.5.4

$$\frac{S^2}{N_q^2} = \frac{3}{8\pi^2} \frac{f_s^3}{(f_c^2 + f_m^2)f_o} \quad f_s = \text{clock frequency} \quad (3.4)$$

$$\frac{3}{8\pi^2} \approx \frac{1}{25}$$

$$f_c = \frac{1}{2\pi RC}$$

f_m = Input signal frequency

f_o = Bandwidth of low pass filter in the delta modulator decoder (or bandwidth of input signal)

Hence from equation 3.3 and 3.4

$$A = \frac{5}{\pi} \sqrt{\frac{f_o}{f_s}} \left(\frac{S}{N_q}\right) \quad (3.5)$$

Equations 3.2 and 3.5 show that the amplitude range of PCM is independent of the frequency of the input signal where as in delta modulation it depends on the bandwidth of the input signal. Since the

biomedical signals contain predominantly lower frequencies, the amplitude range is largest at these frequencies as shown in equation 3.5

3.2.3 Comparison of Delta Sigma Modulator and Modified Delta Modulator

As the decoder for a Delta Modulator consists of an integrator with a long time constant and a low pass filter, any transmission disturbances such as noise result in accumulating error due to the integrator time constant upon the demodulated signal. This makes it inadequate for signals containing DC levels.

But if the integrator of the conventional delta modulator mentioned above is replaced by a passive RC integrator, the integrator memory is reduced due to the discharge path. This simplifies the pulse generating circuitry at the expense of bandwidth. Such a system is called Modified Delta Modulation⁽⁵⁹⁾ and is capable of transmitting signals with a DC level. At any DC signal level, a specific number of pulses per second is required to hold the integrator voltage at that level. A signal with a DC level can also be transmitted by using delta sigma modulation because it integrates the signal before it enters the modulator. The output pulses are generated carrying the information corresponding to the amplitude of the input signal.

The signal-to-quantisation noise ratio of the Delta Modulation is shown to be

$$(S/N_q)^2 = \frac{3}{8\pi^2} \frac{f_s^3}{f_o f_m^2} \quad (3.6)$$

from equation 3.16 Section 3.5.4

while for Delta Sigma Modulation it is given by

$$(S/N_q)^2 = \frac{9}{8\pi^2} \left(\frac{f_s}{f_o}\right)^3 \quad (3.7)$$

from equation 3.25 Section 3.6.2

These equations show that the sampling pulse frequency has the same relationship with the S/N ratio in both the systems but in Delta-Sigma modulation, the signal frequency has no relationship with the signal to noise ratio.

Delta-sigma modulation is useful when the energy distribution in the spectrum of the input signal is flat. In the case of biomedical signals to be telemetered these lie in the range 0 to 100 Hz with the maximum amplitude at lower frequencies and a smaller amplitude at higher frequencies. The modified delta modulator whose signal handling capacity falls at higher frequencies (shown in Section 3.5.1) is well suited for the transmission of such signals.

A comparison between the $(S/N_q)^2$ ratios of the delta modulator and delta sigma modulator is obtained by dividing equation 3.6 by 3.7

$$\frac{(S/N_q)^2 \text{ delta sigma mod.}}{(S/N_q)^2 \text{ delta modulator}} (\phi)^2 = 3 \frac{f_m^2}{f_o^2}$$

$$\therefore \phi = 1.7 \frac{f_m}{f_o} \quad (3.8)$$

That is for a filter bandwidth $f_o = 100$ Hz, for ϕ to be less than unity, the input signal frequency (f_m) must be less than 60 Hz.

As the significant spectrum for the signals considered lie below this figure, the signal-to-noise ratio for delta modulation should be superior.

As the decoder for a delta sigma modulator is simply a low pass filter, the filter needed to recover the analogue signal is more critical and difficult to design. In certain conditions shown later, the decoded signal is often accompanied with transients and periodic noise.

Delta modulation, on the other hand, uses an integrator in the decoder and the low pass filter required to remove higher frequency components due to sampling is less critical and easier to design.

3.3 Delta Modulation System

Due to the advantages and simplicity of the delta modulator mentioned in the last section it was decided to use and investigate it for the coding of biomedical signals in the biomedical telemetry system along with the delta sigma modulator for comparison.

Delta modulation which is a member of a family of pulse modulation systems was first described by a French patent in 1946⁽⁶⁰⁾. It was then developed into the field of delta modulation systems by F. De Jager in 1952⁽⁶¹⁾. The Philips Company and the Bell telephone laboratories also worked on the differential pulse code or predictive system in the early fifties.

The differential pulse code or predictive system is based primarily on an invention by Cutler⁶³ and De Jager, who used one or two integrators to perform the predictive function. This invention is based on the transmission of the quantised difference between successive sample values rather than the samples themselves. When the quantiser has only two values, the system reduces to its simplest form and is referred to as Delta modulation. The coder makes an estimate or prediction of the signal value based on the previously transmitted signal and transmitted binary pulses carry the message information corresponding to the slope of the analogue signal. The decoder on the receiving end simply integrates the pulses to obtain the original waveform.

3.3.1 Delta modulator (59)

A block diagram of a conventional delta modulator is given in figure 3.2. The clock pulses either pass through or are inverted by the pulse generator depending on the waveform at the gating input 'b'. The output pulse train 'd' is integrated to form a stepped waveform. This stepped waveform can be viewed as a quantised or incremental representation of an analogue input signal. At each clock pulse interval a comparison is made between the analogue input signal 'a' and the quantised signal 'e'. The comparison is effectively between the present value of the analogue input signal and its value approximately one clock pulse earlier.

If the present analogue input voltage is greater than the delayed quantised output signal, the pulse generator is triggered by a positive step waveform and a positive output pulse appears at 'd'. If the present analogue input voltage is less than the stepped signal at 'e', a negative step triggers the pulse generator and a negative pulse appears at output 'd'. In this manner the output pulse waveform is continually compared with the analogue input signal and is modified as the input changes.

The basic approach outlined above gives rise to a variety of delta modulation systems which have been derived and studied. Various methods of integration can result in significant differences in the system characteristics. The basic system described by de Jager assumes integrators with long time constants in relation to the lowest signal frequency. Such a system using such long term (long time constant) integrators will be called conventional delta modulation. When the period of integration approaches or becomes less than the period of the lowest frequency signal the system characteristics change

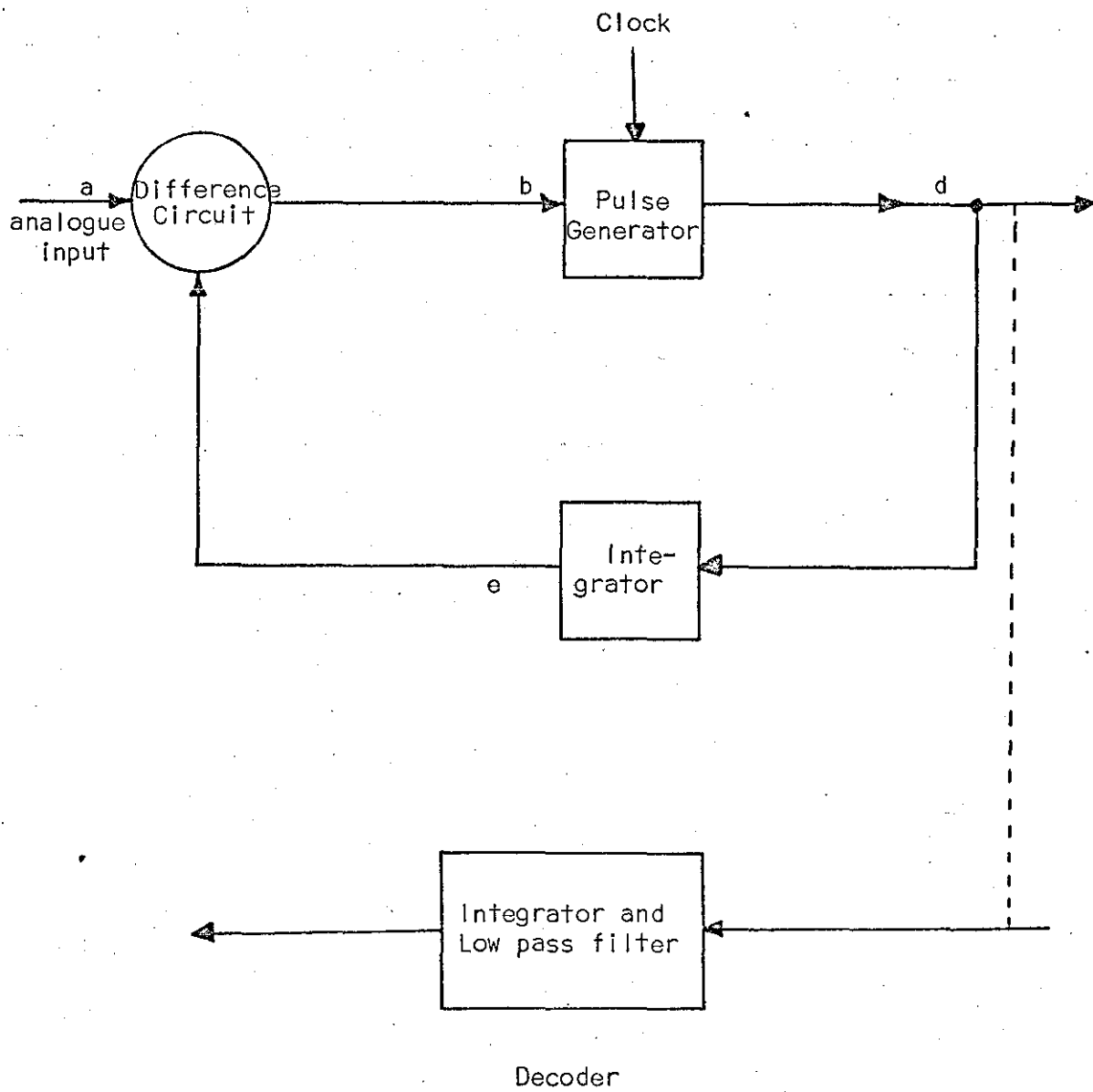


Figure 3.2 A Block Diagram of the Conventional Delta Modulator

significantly. This type of modulation has been called Limited-Integration Delta modulation. As the integration period decreases in relation to the inverse of the lowest signal frequency, the case of pulse rate modulation is approached.

It is not necessary to supply both pulse polarities to the integrator. The effect of one pulse polarity can be achieved by intentionally making the integrator memory short by use of an RC passive integrator with a discharge resistor. This simplifies the pulse-generating circuitry at the expense of bandwidth required to transmit a particular signal. At any given d.c. signal level, a specific number of pulses per second are required just to hold the integrator voltage at that level. This type of process is called the 'Modified delta-modulation system'. This principle of delta modulation is used in the practical system described later.

When signals with d.c. components must be handled, as is the case in the biomedical signals, the modified delta system is by far the simplest.

3.4 Delta-Sigma Modulation System

A conventional delta modulator suffers from a cumulative error due to transmission disturbances for signals with d.c. components. This takes place due to differentiation and subsequent integration inherent in the delta modulator. This incapability to handle d.c. components in the input signal presents a serious disadvantage for signals whose frequency spectra extend down to d.c.

A system that overcomes this difficulty was described by Inose, Yasuuda and Murakami⁽⁶⁴⁾ in 1962 and is called Delta-Sigma modulation.

The integrator in delta-sigma modulation is included in the input circuit or in the forward loop while the input signal and feedback pulse trains are subtracted from each other ahead of the integrator. As the input signal is integrated before it enters the pulse modulator so the output pulses generated carry the information corresponding to the amplitude of the input signal. The realisation of this principle makes a delta-sigma modulator free from cumulative error and is also useful for the transmission of signals containing a d.c. component.

3.4.1 Delta-Sigma Modulator

The block diagram of a delta sigma modulator is shown in figure 3.3. It is a closed loop system consisting of a sampling pulse generator, a pulse modulator (or a quantiser), an integrator and a difference circuit. The output digital pulses are fed back to the input and subtracted from the analogue input signal. The difference is integrated and enters the pulse modulator. The pulse modulator compares the amplitude of the integrated difference signal with a predetermined reference level. The pulse generator gives out a pulse depending on the polarity of the input signal to the pulse modulator. If the signal is positive the pulse generator will give out a pulse while if the input is negative, the pulse generator will be inhibited to give no pulse output or give a pulse of opposite polarity to the one obtained for the positive signal. The pulse generator rate or sampling frequency is much higher than the analogue input signal.

Demodulation in a delta-sigma modulator is carried out by passing the output pulses through a low-pass filter. Since the signal is integrated before it enters the modulator, no integrator is required on the decoding end. Therefore no accumulative error due to transmission disturbances results in the demodulated signal.

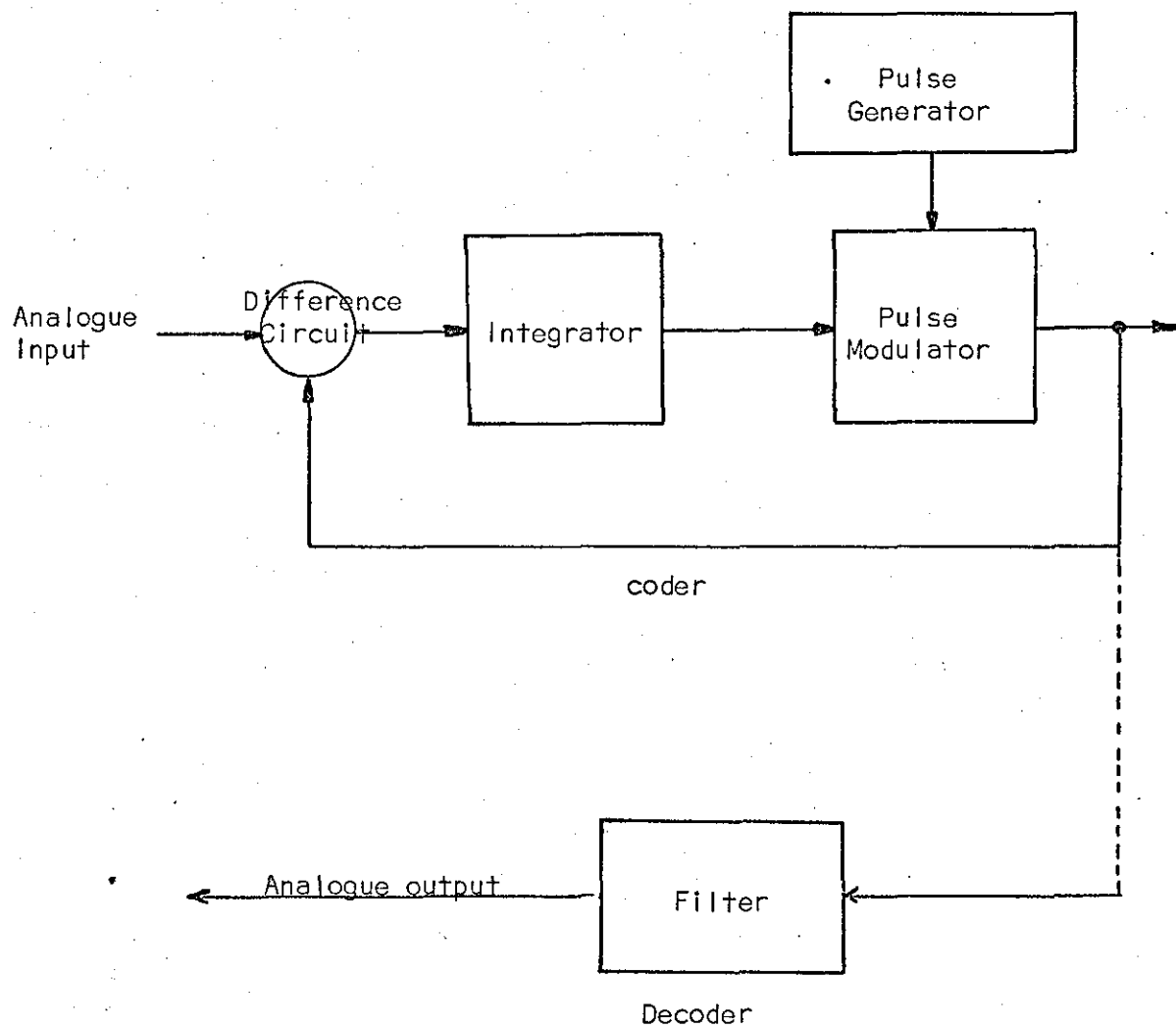


Figure 3.3 Block Diagram of the Delta Sigma Modulator.

3.5 Theory of Delta Modulator

The principle of the delta modulator is described in section 3.3.1. A theoretical analysis and characteristics are given here to study its performance in detail. This analysis and characteristics are for a practical delta modulator with a single integrator consisting of an RC combination so that the integration of a constant input results in an output which follows an exponential curve. The binary digits fed to the integrator use full width pulses of levels $+v$ and $-v$ volts. The clock rate is f_s per second, hence the rate of information sent over the digital transmission link is f_s bits per second and the duration of each digit is $\frac{1}{f_s} = T_s$ seconds.

The decoder at the receiver consists of an RC integrator followed by a low pass filter. The time constant of the RC combination used in the feedback path of the coder is equal to that of the RC combination in the forward path of the decoder. Let us call this time constant $RC = T_c$.

Hence the characteristic frequency (f_c) of the RC = $\frac{1}{2\pi T_c}$

It is assumed that the input signal is bandlimited to f_b as the highest frequency, the lower frequency being zero. The bandwidth of the input signal is f_o , hence the bandwidth of the low pass filter in the decoder is also f_o .

3.5.1 Overload Characteristic and Noise (65)

Consider the waveform when a binary input is applied. Whenever the input voltage to this network is $+v$ (the binary 1 condition, say), the voltage on the capacitor moves from the point at which it happens to be, along an exponential curve of time constant $RC = T_c$ tending toward the $+v$ level. Similarly, when the input is $-v$ (the binary 0 condition) it moves along a similar exponential curve toward the $-v$ level. This is shown in figure 3.4 as AB and CD

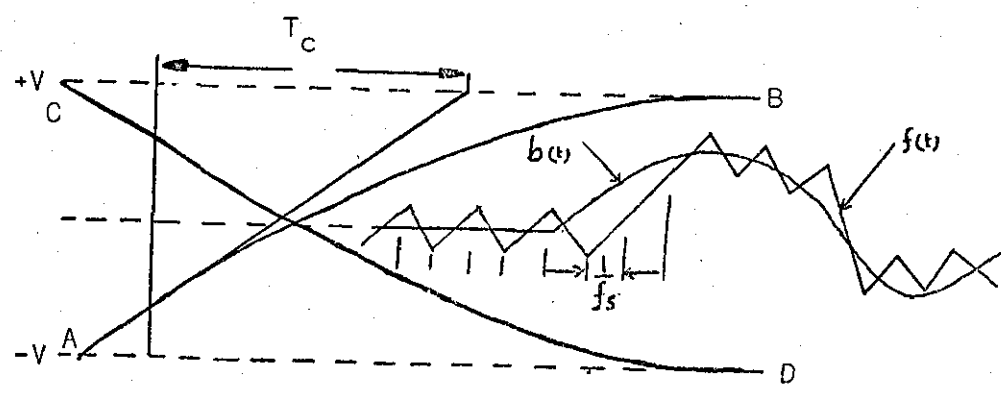


Figure 3.4

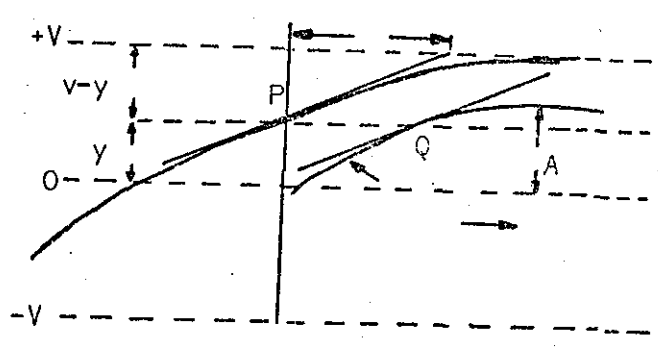


Figure 3.5

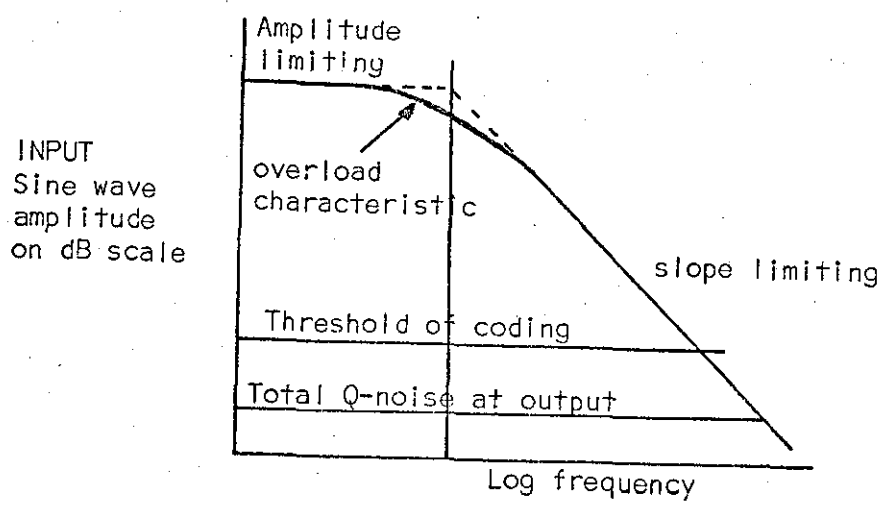


Figure 3.6

- Figure 3.4 Analogue input $b(t)$ and output of local integrator $f(t)$ employing an RC Integrator
- Figure 3.5 Conditions of equal slope.
- Figure 3.6 Delta Modulator Characteristics.

Let the input signal be a sine wave of amplitude A and angular frequency ω . As long as the slope of the input signal does not exceed too greatly the slope of the exponential curve at the amplitude common to both, the coder can produce at the integrator output for comparison with the input signal, a waveform which tracks the latter reasonably well. However, if either the amplitude or frequency or both of the input signal is raised, its slope may at times considerably exceed that of the exponential curve which determines the maximum rate at which the integrator output can move. The coder therefore cannot track the input signal and increased distortion will result in the code-decode process.

The Overload condition of the delta modulator is defined as the situation where the slope of the signal is equal to the slope of the exponential at some particular amplitude, but at all other amplitudes the slope of the signal is less than that of the exponential.

Consider the case of a point P on the exponential curve tending to V with time constant T_c , and a point Q on the sine wave $A \sin \omega_m t$. Both P and Q are at the same amplitude Y , where Y is less than A . This is shown in figure 3.5. The slope of the exponential at amplitude Y is $\frac{V-Y}{T_c}$.

The slope of the sine wave at amplitude Y is $\omega_m \sqrt{A^2 - Y^2}$

The difference between the slopes of the exponential and sine wave is

$$D = \frac{V-Y}{T_c} - \omega_m \sqrt{A^2 - Y^2} \quad (3.9)$$

Regarding D as a function of Y , it has a minimum at

$$Y = \frac{A}{\sqrt{1 + \omega_m^2 T_c^2}} \quad (3.10)$$

The value of D at minimum condition is given by

$$D_{\min} = \frac{V - A\sqrt{1 + \omega_m^2 T_c^2}}{T_c} \quad (3.11)$$

Overload condition is characterised by $D_{\min} = 0$

$$A = \frac{V}{\sqrt{1 + \omega_m^2 T_c^2}}$$

The relationship between A and ω_m gives the overload characteristics. The characteristics are plotted in figure 3.6 and it is noted that the slope is identical to the amplitude frequency characteristics of an RC network.

The curve falls off at 6 db per octave with increasing frequency which corresponds to the slope limiting condition. At the low frequency end the curve is flat and overloading is by virtue of an amplitude limitation. The overload characteristic is 3 db down at the frequency f_c . Increasing the clock frequency should help to accommodate higher frequencies or larger signals which is equivalent to increasing the quantisation level.

In practice it is desirable to work as closely as possible to the overload condition in order to keep the signal-to-noise ratio as high as possible.

3.5.2 Quantisation Noise

Quantisation noise is defined as the error or difference between the final decoded signal and the input signal. The comparison is made which accounts for the relative delay and amplitude change of the wanted part of the signal.

The spectrum of noise is defined as shown in the figure 3.7

$$\begin{aligned} \text{by } Q(j\omega) &= B(j\omega) - G(j\omega) \\ E(j\omega) &= B(j\omega) - F(j\omega) \\ &= B(j\omega) - L(j\omega) H(j\omega) \end{aligned}$$

$$E(j\omega) A(j\omega) = B(j\omega) - L(j\omega) H(j\omega) A(j\omega)$$

assuming $A(j\omega)$ is flat over the spectrum of $B(j\omega)$.

$$\therefore E(j\omega) A(j\omega) = B(j\omega) - G(j\omega)$$

and the noise spectrum $Q(j\omega)$ is given by

$$Q(j\omega) = E(j\omega) A(j\omega) \quad (3.12)$$

The calculations of $Q(j\omega)$ present a complex problem because of the difficulty in determining $E(j\omega)$. Even with a single sine-wave input the resulting output pulse train $L(t)$ is random and consequently $E(j\omega)$ is the Fourier transform of a non-deterministic function.

However it may be recognised that quantisation noise is related to the central delta step⁽⁶⁵⁾ which is the change in integrator output voltage during one clock pulse period when the mean voltage at the integrator output is zero. It is shown in figure 3.8 and can be related with other parameters.

$$d = \frac{V}{T_c f_s} = \frac{2\pi v f_c}{f_s} \quad (3.13)$$

When the input to the coder is zero, the coder is said to be idling producing a digital pattern 10101010 at its output. For zero input the error waveform $e(t)$, i.e. the quantisation noise before filtering and the integrator output is triangular. The triangular wave at the output of the integrator has peaks at $\pm \frac{d}{2}$ and the mean square difference between this and the input is $\frac{d^2}{12}$.
Hence the total error energy = $\frac{d^2}{12}$

This power will be contained in a line spectrum at multiples of f_s .

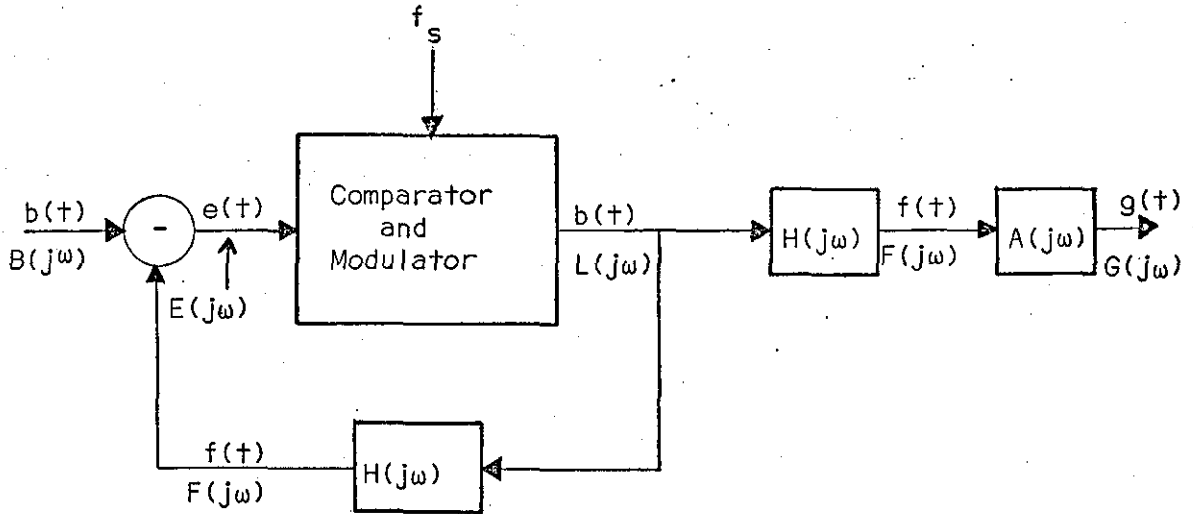


Figure 3.7 Quantization noise in Basic Delta Modulation

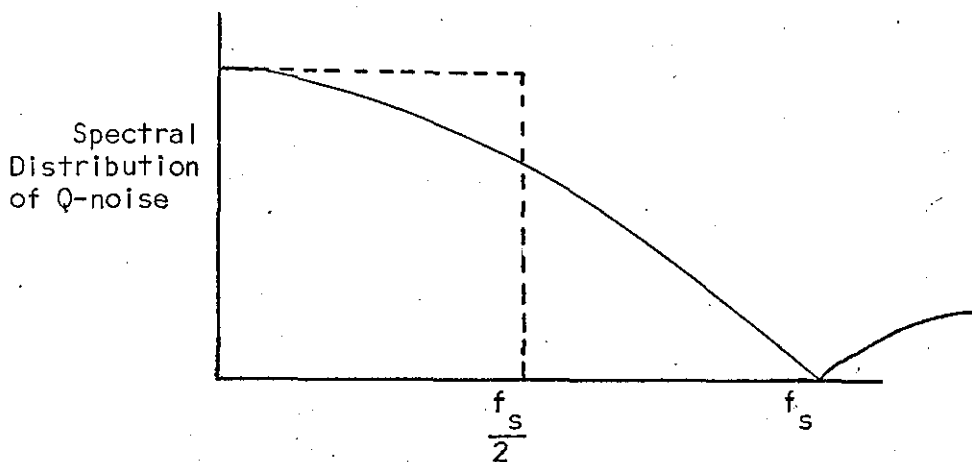


Figure 3.9 Assumed Frequency Distribution of Quantization Noise Energy.

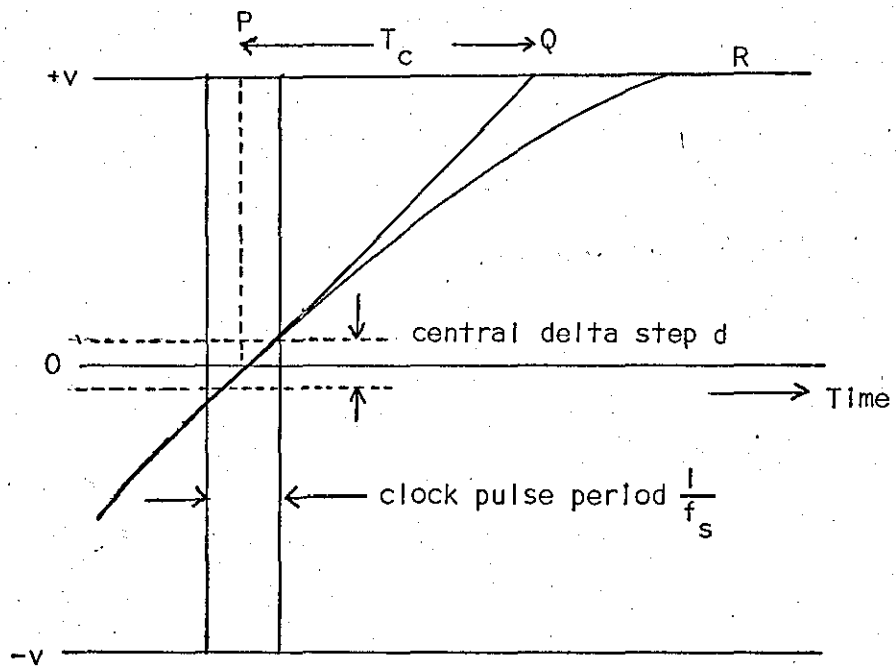


Figure 3.8 Derivation of central delta step

Johnson⁽⁶⁵⁾ simulated exponential delta modulation on a digital computer and found the mean square error averaged over 100 cycles of the input sine wave by comparing the integrator output with the analogue input signal.

In order to find the amount of quantisation noise in the final output Johnson assumed that due to its random nature and fundamental periodicity f_s the spectral distribution of the total error has the form $(\sin x/x)^2$ with its first null at f_s . This is shown in figure 3.9. In $(\sin x/x)^2$ distribution the total energy is equal to the energy which would result if the spectral density at the origin were held constant over a frequency band $f_s/2$ in width. Johnson also assumed that the highest frequency of the input signal is sufficiently small compared to f_s so that the quantisation noise spectrum will be essentially flat throughout the range of the final output filter. Thus he obtained quantisation noise energy appearing at the final output in the computer program by multiplying the total mean square error by $2 \frac{f_o}{f_s}$.

Hence the quantisation noise appearing at the decoder output can be expressed as

$$N_q^2 = \frac{2 K d^2 f_o}{f_s} \quad (3.14)$$

Where K is a numerical factor to be determined, substituting for d from equation. 3.13.

Total mean square quantisation noise at decoder output

$$N_q^2 = \frac{8\pi^2 K v^2 f_c^2 f_o}{f_s^3}$$

The above expression shows that

1. Quantisation noise is proportional to the bandwidth of the input signal or the receiver low pass filter and will increase at a rate of 3 db per octave with increase of f_o .
2. It is directly proportional to the square of f_c (characteristic frequency of RC combination) and will increase at a rate of 6 db/octave with an increase of f_c .
3. It is inversely proportional to the cube of the clock frequency (f_s) and will decrease at a rate of 9 db/octave with an increase of clock rate.

3.5.3 Determination of K

Jager was the first to calculate S/N_q for a sine wave input at overload and determined the value of K equal to approximately 1/6. Abate⁽⁶⁶⁾ and O'Neal⁽⁶⁷⁾ followed Jager and gave results which agreed with him. Johnson's⁽⁶⁵⁾ computer simulation, however, indicated that for signals just above the threshold of coding the value of K is approximately 1/6 and it remains constant at this value over a range of input amplitudes until the slope overload condition is approached. On increasing the signal amplitude further, K for the total mean square error at the output increases and reaches a value of approximately 1/3 at the overload point which is the point of maximum signal to noise ratio. This increase in the value of K aligns with O'Neal⁽⁶⁷⁾ distinction between granular quantisation noise and slope overload quantisation noise. It is as if the basic granular quantisation noise has been supplemented by further noise, due to the onset of the slope overload condition.

3.5.4 Signal-to-Noise Ratio(65)

The mean square value for the amplitude of the overloading sine wave is given as

$$S^2 = \frac{V^2}{(2(1 + \omega_{m,c}^2))}$$

For a pure slope overload condition it reduces to

$$\frac{V^2}{(2\omega_{m,c}^2)} = \frac{V^2}{2} \left(\frac{f_c}{f_m}\right)^2$$

because $f_m \gg f_c$

and $\omega_{m,c}^2 \gg 1$

$$\omega_m = 2\pi f_m$$

where f_m is the frequency of input sine wave.

The mean square signal-to-mean square noise ratio at slope overload, from the above relation and equation 3.15 for $K = \frac{1}{6}$ is

$$(S/N_q)^2 = (3\beta\pi^2) \left(\frac{f_s^3}{(f_o f_m^2)}\right) \quad (3.16)$$

This shows that the signal-to-noise ratio

- (i) Improves at the rate of 9 db/octave with an increase of clock rate.
- (ii) Improves at the rate of 3 db/octave with a decrease in the bandwidth of receiver low pass filter
- (iii) Improves at the rate of 6 db/octave with a decrease in signal frequency.

3.5.5 Threshold of Coding

When there is no input to the delta modulator, the output digital pattern is called the idling pattern.

When the amplitude of the input signal is less than $d/2$, where d is the central step size, the idling pattern will not be disturbed and no coding will take place. This situation arises where $A = d/2$ is called the threshold of coding.

At the threshold of coding the mean square signal level for sine waves = $A^2/2 = d^2/8$, substituting the value of d from equation

3.13. The mean square value of signal level at threshold

$$S^2 = \frac{\pi^2 V^2 f_c^2}{(2f_s^2)} \quad (3.17)$$

The mean square value of quantisation noise is

$$N_q^2 = \frac{4\pi^2 V^2 f_o f_c^2}{(3f_s^3)} \quad (3.18)$$

At threshold,

$$(S/N_q)^2 = \frac{3f_s}{(8f_o)} \quad (3.19)$$

This shows that at threshold the S/N ratio is dependent on the ratio clock rate to signal bandwidth.

3.5.6 Dynamic Range

It is the amplitude range of the input sinusoid which the system can accommodate.

The maximum amplitude of the sine wave input consistent with the condition of overloading is given by

$$V_{\max} = \frac{V}{(1 + \omega_m^2 T_c^2)^{1/2}}$$

The maximum peak amplitude below which the input fails to excite the modulator occurs when the peak to peak amplitude of the signal is smaller than the central step size d .

$$V_{\min} = d/2 = \frac{\pi V f_c}{f_s}$$

Hence
$$V_{\min} = \frac{\pi f_c}{f_s} V_{\max} (1 + \omega_m^2 T_c^2)^{1/2}$$

Therefore

$$\left(\frac{V_{\max}}{V_{\min}} \right) = \frac{f_s}{\pi (f_c^2 + f_m^2)^{1/2}} \quad (3.20)$$

The ratio $\frac{V_{\max}}{V_{\min}}$ expressed in db, is the dynamic input range of the system.

3.5.7 Limitation of Delta Modulation

There are certain aspects of delta modulator which can contribute to an error or noise in the system.

The first is overload which is due to the frequency dependent network (integrator) in the feedback loop of the delta modulator. It occurs whenever the input signal changes too rapidly for the output of the local integrator to follow it. At the overload condition the signal handling capacity falls by 6 db per octave with an increase of input signal frequency. In general, biomedical signals do not have a large high frequency content so that the delta modulation is capable of handling them.

The second is the quantisation error which is inherent in a system based on a quantisation process. As the signal in this process is recovered from the quantised samples of the original analogue

signal, it can never be exactly the same as the original signal. As a result an error is produced. Quantisation noise increases with the bandwidth of the filter in the receiver and the quantisation level, and decreases as the clock frequency is increased. Hence by choosing suitable values for the above mentioned parameters quantisation noise is not a serious problem for biomedical signals.

3.6 Theory of Delta-Sigma Modulation

The principle of delta sigma modulation is described in Section 3.3.2. A delta sigma modulator can be regarded as being obtained from the single integration delta modulator by placing the RC network (integrator) in the input to the coder with the same time constant as that of the RC network in the coder feedback path. As a result the RC network in the decoder is omitted. Omission of the integrator at the decoder produces a system having the flat transfer characteristic shown in figure 3.10. This modifies the characteristics of the delta sigma modulator as shown in the following sections.

3.6.1 Quantisation Noise of Delta-Sigma Modulation

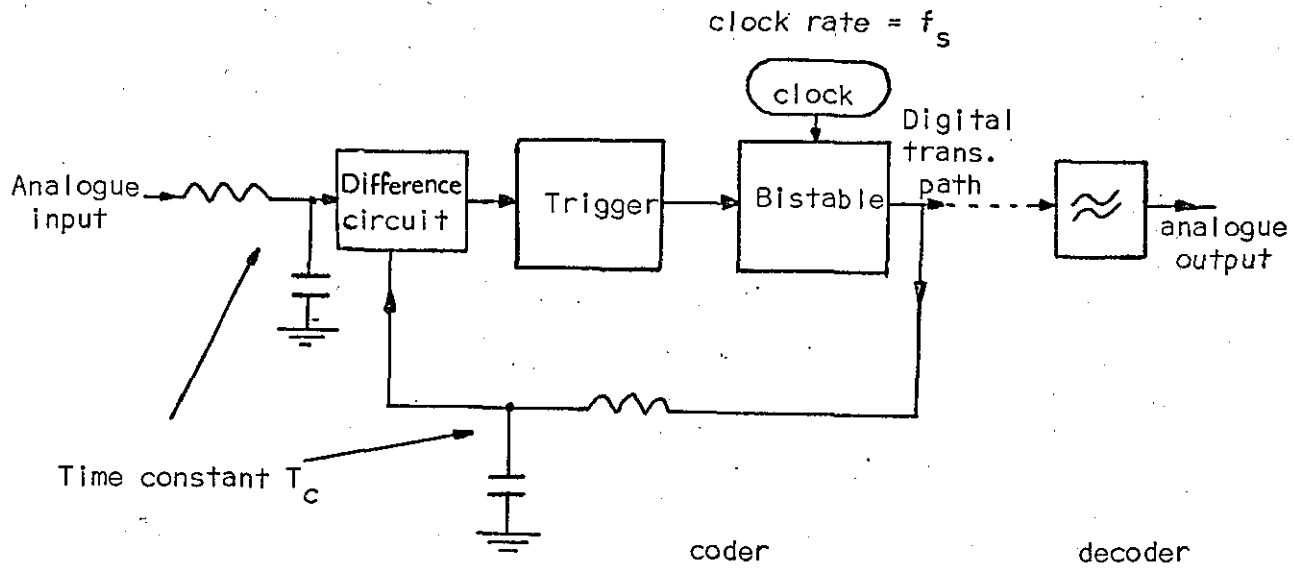
The quantisation noise for delta sigma modulation is calculated in a similar manner to that of delta modulation but the absence of the RC network will modify the expression. If $H(j\omega)$ is the transfer function of the RC network

$$H(j\omega) = \frac{1}{(1 + j\omega CR)}$$

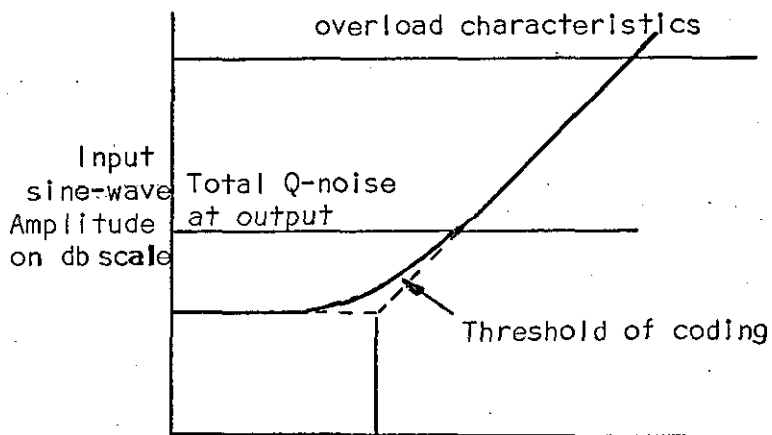
and $f_c = \frac{1}{(2\pi CR)}$

$$\omega = 2\pi f$$

or $\left| \frac{1}{H(j\omega)} \right|^2 = \frac{(f_c^2 + f^2)}{f_c^2}$ (3.21)



(a) Block Diagram of Delta-Sigma Modulator Coder.



(b) Display of Delta Sigma Characteristics.

Figure 3.10

The above expression is multiplied with the energy density of the quantisation noise ($2Kd^2/f_s$) to give the quantisation noise at the input of the decoder, assuming that the decoder consists of a perfect low pass filter of bandwidth equal to the bandwidth of output signal f_o .

The quantisation noise at the output of the decoder is given by

$$N_q^2 = \frac{2Kd^2}{f_s} \int_0^{f_o} \frac{(f_c^2 + f^2)}{f_c^2} df$$

$$= \frac{2Kd^2}{f_s f_c^2} \left[f_o f_c^2 + \frac{f_o^3}{3} \right]$$

Putting $d = \frac{2\pi V f_c}{f_s}$ from (3.13) and $K = 1/6$

Total quantisation noise at the decoder is

$$N_q^2 = \frac{4\pi^2 V^2}{3f_s^3} (f_o f_c^2 + f_o^3/3) \quad (3.22)$$

It is noted that quantisation noise is reduced by making f_c as small as possible, i.e. the time constant T of the RC network as large as possible.

If $f_o \gg f_c$

$$N_q^2 = \frac{(4\pi^2 V^2)}{9} (f_o/f_s)^3 \quad (3.23)$$

Quantisation noise in delta sigma modulation depends on the following

- (i) It is directly proportional to the cube of the bandwidth of the low pass filter in the decoder and increases by 9 db per octave with increase of this

frequency.

- (ii) It is inversely proportional to the cube of the sampling frequency and reduces by 9 db per octave with increase of this frequency.
- (iii) It is independent of the input signal frequency unlike delta modulation.

3.6.2 Signal-to-Noise Ratio

The mean signal power at the output of the low pass filter of a delta sigma modulator is approximately equal to the signal power at the comparator input

$$S^2 = \frac{V_m^2}{\{2(1 + \omega_m^2 T_c^2)\}}$$

Therefore the signal power at the output of a delta sigma modulator receiver is

$$\begin{aligned} \frac{V_m^2}{\{2(1 + \omega_m^2 T_c^2)\}} |H^{-1}(j\omega_m)|^2 &= \frac{V_m^2}{(1 + \omega_m^2 T_c^2)} (1 + \omega_m^2 T_c^2) \\ &= \frac{V_m^2}{2} = \frac{V^2}{2} \end{aligned}$$

Hence the mean square output power corresponding to the limit of non-overloading at the input is $V^2/2$.

The mean square signal-to-noise (quantisation) ratio is

$$(S/N_q)^2 \approx \frac{9}{8\pi^2} \left(\frac{f_s}{f_o}\right)^3 \quad f_c \ll f_o \quad (3.25)$$

3.6.3 Overload for Delta-Sigma Modulation

In order to find the maximum amplitude of a sine wave input consistent with the condition of non overloading, the slope of the output from the first RC integrator is

$$\begin{aligned} \frac{dV}{dt} &= \frac{\omega_m V_m \cos \omega_m t}{(1 + \omega_m^2 T^2)^{\frac{1}{2}}} \\ &= \frac{\omega_m \{V_m^2 - V^2(1 + \omega_m^2 T^2)\}^{\frac{1}{2}}}{(1 + \omega_m^2 T^2)^{\frac{1}{2}}} \end{aligned} \quad (3.26)$$

The difference D between the slope and the slope of the output from the feedback RC integrator is

$$D = (V-v)/T = \frac{\omega_m \{V_m^2 - V^2(1 + \omega_m^2 T^2)\}^{\frac{1}{2}}}{(1 + \omega_m^2 T^2)^{\frac{1}{2}}} \quad (3.27)$$

This must be greater than or at the limit equal to zero to avoid overloading. The zero limit is found by differentiating D with respect to v and equating to zero, which gives

$$V = \frac{V_m}{(1 + \omega_m^2 T^2)}$$

Substituting the value of D=0 and v from equation 3.27 gives the non-overloading condition

$$V_m = V_{\max} = V \quad (3.28)$$

This shows that the overload condition does not depend on the slope or frequency of the input signal but depends on the amplitude of the input waveform.

3.6.4 Dynamic Range

The maximum input consistent with non overloading is

$$V_{\max} = V$$

The minimum input corresponding to the threshold of coding is

$$B(t) = V_{\min} \sin \omega_m t$$

The peak output from the first RC network is .

$$\frac{V_{\min}}{(1 + \omega_m^2 T^2)^{\frac{1}{2}}} = \frac{d}{2} = \frac{(\pi V f_c)}{f_s}$$

Therefore

$$\frac{V_{\max}}{V_{\min}} = \frac{f_s}{\pi(f_c^2 + f_m^2)^{\frac{1}{2}}} \quad (3.29)$$

This is identical to ΔM .

3.6.5 Companded Delta Modulation

Since in delta modulation and delta sigma modulation quantization noise is independent of the signal level, a limited dynamic range in excess of 26 db is obtained. The quantization noise, in these cases, is set by the quantization step size. The modulation technique which employs a local decoder to modify the step size in accordance with the level of the input signal is called companding.

There are basically two methods of achieving this. The first⁽⁶²⁾ is to obtain a control signal whose magnitude is proportional to the mean level of the analogue input. The control signal is then used to amplitude modulate the digital sequence fed to the integrator in the feed back circuit. The second method⁽⁷⁰⁾ is similar except that the control signal is derived entirely from the digital output of the encoder. Although companding improves the dynamic range, it makes the system more complicated and its features are more attractive for speech transmission.

There are further variations of delta modulation⁽⁷¹⁾ and also improvements of the mentioned techniques for the transmission of television and video signals.

3.7 Multiplexing of Digital Signals (68)

It is often desirable to transmit a number of independent channels (also a requirement for the biomedical telemetry system as mentioned in Chapter 1) through a media. This is achieved by multiplexing the various channels which means that more than one channel (or function) can be transmitted simultaneously over one path without much loss of identity of each function.

There are two common ways of multiplexing which may be used for digital signals.

1. Time division multiplexing (TDM)
2. Frequency division multiplexing (FDM)

3.7.1 Time Division Multiplexing

This is a technique for transmitting several messages on one path by dividing the time domain into slots, one slot for each message. It was first used in the Bandot system of multiplex telegraphing in 1874⁽⁶⁹⁾. Later the invention of the electric wave filter and the thermionic valve made frequency division multiplexing practicable and carrier transmission became the standard method both for multi-channel telephony and telegraphy. The development of pulse techniques led to some revival of interest in T.D.M. before the last war and the use of U.H.F. pulse transmission for radar during the war led to the development of practical T.D.M. radio links.

The elementary TDM system is shown in figure 3.11. It consists of a transmission path at each end of which is connected a rotary switch. The separate input signals all bandlimited in W are connected to the transmission path and consequently are separated in time only by the rotary switch. Identical rotary switches are used in synchronisation so that sending and receiving apparatus of each

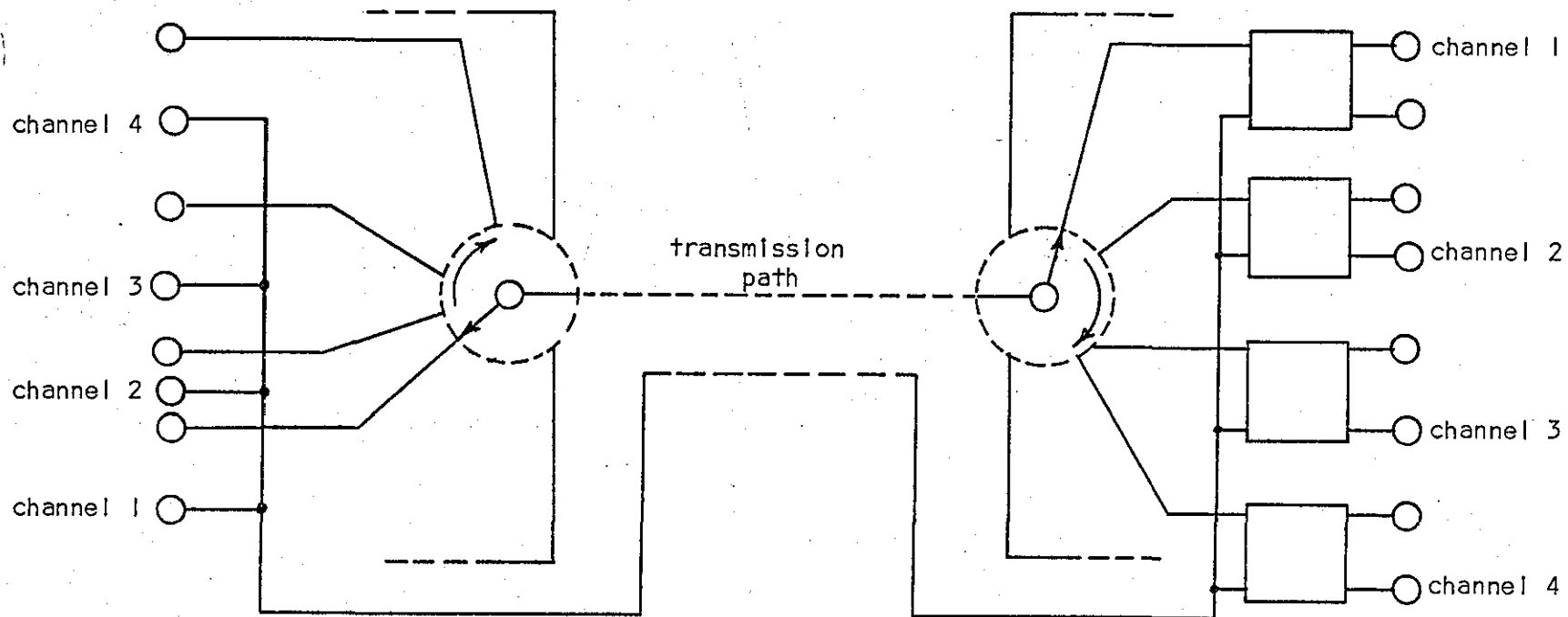


Figure 3.11 Time Division Multiplexing System

channel are connected together for their allotted time interval and disconnected throughout the remainder of each revolution of the switch.

3.7.2 Frequency Division Multiplexing

In frequency division multiplexing a number of independent channels can be accommodated in a communication system by sharing the allocated bandwidth. The essentials of any FDM system are shown in figure 3.12.

This method of multiplexing does not apply to the pulse modulated systems. The individual data channels are modulated by sub-carriers. The modulated channels are passed through band pass filters for each channel to be arranged to occupy adjacent frequency bands. For the final transmission the modulated signals are summed and the composite complex signal modulates a group carrier. The output of this modulator is suitably amplified and transmitted by line, radio link, etc., to the receiver.

Both TDM and FDM accomplish the same goals though the means are different. Indeed they can be visualised as dual techniques, in TDM the signals are separate in time domain but jumbled together in frequency, whereas in FDM the signals are separate in the frequency domain but jumbled together in time. From a theoretical point of view both are the same, but from a practical point TDM is superior in two ways.

First TDM instrumentation is simpler and is easy to implement, whereas FDM requires sub-carrier modulation, band pass filter and demodulation for each modulation signal. Second, TDM is immune to the usual sources of crosstalk from neighbouring channels, also to

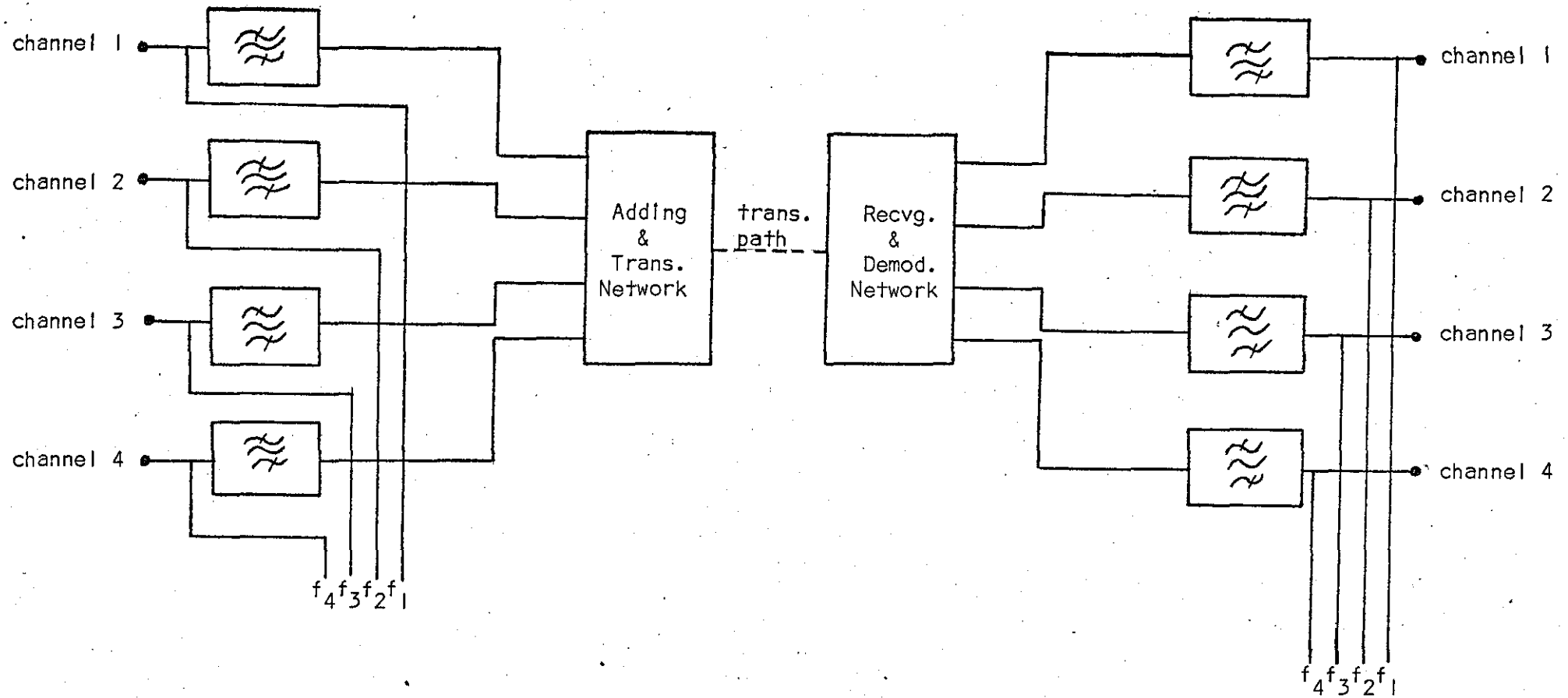


Figure 3.12 Frequency Division Multiplexing System

imperfect channel filtering and cross modulation due to non-linearities. There is no cross talk in TDM if pulses are completely isolated and non-overlapping, since message separation is achieved by de-commutation or gating in time, rather than by filtering. Actual pulse shapes, having decaying tails, do tend to overlap. This crosstalk can be effectively reduced by providing guard times between pulses, which is analogous to the guard bands of FDM. The other use of guard time is that the gates in the receiver are not ideal but require a finite time to open and close. Separation of channels requires opening the gate for a channel after the gate for the preceding channel has closed, and closing the gate before the beginning of gating action in the following channel.

Due to these advantages TDM is used in the present system.

3.8 Pulse Generation and Synchronisation

With any form of pulse modulation the sampling of each information channel is controlled by some master sequencing technique. This may be thought of as a sort of Electronic Commutator. One form is the ring counter of bistable (one shot) or multivibrator (flip flop) circuits, as shown in figure 3.13. In order to make it possible to generate pulses at precisely regular intervals, each pulse generator is arranged to operate only when it receives simultaneous triggering pulses from the preceding generator and from a master pulse source (i.e. the on state advances one step around the ring for every control pulse). If there are n number of channels to be multiplexed (sequenced) including the synchronisation pulse and f_s is the channel pulse repetition frequency, the clock repetition is equal to nf_s .

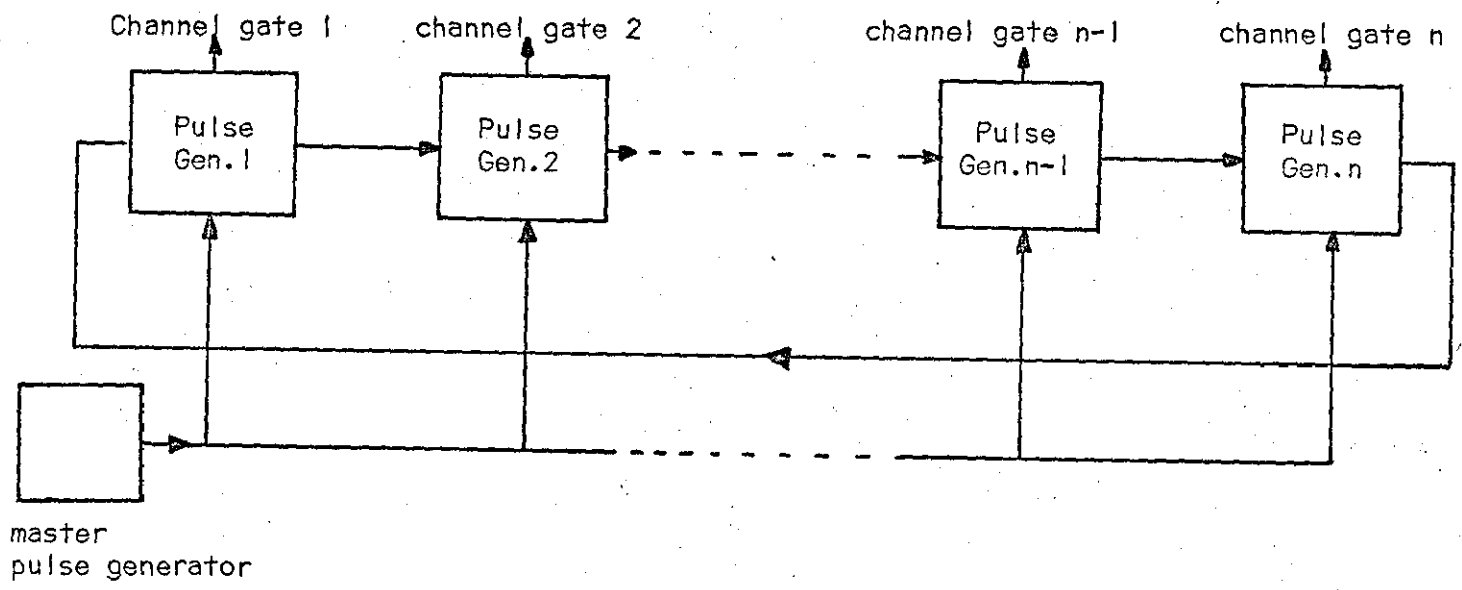


Figure 3.13 Ring Counter

After modulation, the actual multiplexing of the several pulse trains is accomplished by adding them linearly. A simple gate circuit (NOR or OR) can be used for the combining or adding purpose.

Before the channels can be demultiplexed in the receiver, the synchronisation pulse must be recognised. The synchronisation pulse must be sufficiently distinctive so that the receiver (decoder) never responds to an information pulse by mistake.

This is done by having one channel in the system allotted to a distinctive signal, a marker pulse, etc., so that this synchronisation pulse can be used to control the synchronisation circuit at the receiving terminal whose function is to open and close channel gates in proper sequence. In a simple way the synchronisation can be achieved by transmitting (or adding) an unmodulated pulse of the same duration as a channel on each cycle of the ring counter. The channels carrying information (modulated channels) will be sufficiently distinctive from the synchronisation.

3.9 Bandwidth of TDM Signals

Considering the TDM signal as a series of periodic sample points from different messages, then from the inverse sampling theorem, these points can be completely described by a continuous waveform $y(t)$, having no relation with the original message except that it passes through the correct sample values at the corresponding sample time.

As the points are spaced in time by $1/nf_s$, $y(t)$ can be bandlimited in $B = nf_s/2$.

If baseband reception (filtering) is employed and the sampling frequency is close to the Nyquist rate, ($f_s = 2W$), and the carrier modulation is SSB, the bandwidth for TDM transmission becomes

$$\begin{aligned} B &= nf_s/2 \\ &= nW. \end{aligned}$$

CHAPTER 4

COMPUTER SIMULATION AND SIGNAL PROCESSING

4. Introduction

The nature of the delta modulation system described in the last chapter enables it to be simulated on a computer. This simulation makes investigation of the system and real time processing of the biomedical signals possible.

A system based on delta modulation and delta sigma modulation was simulated, investigated and is reported in this chapter.

Physiological events and processes take place in the time domain, hence in the study of physiological processes like the ECG a time amplitude waveform is often required for certain diagnosis. An ECG waveform was simulated on the computer, and a waveform preservation study was performed on the simulated delta modulator and the delta sigma modulator. In addition these simulations made it possible to study the effects of various system parameters on these modulation systems.

In biomedical telemetry the physiological signals like the ECG are often monitored for a long time. The need may arise in the coronary unit when the patient is recovering from a heart surgery or in the field where the state of the heart of an athlete is to be continuously monitored. During the long time monitoring the ECG waveform may change due to the state of the heart, and also the ECG may be accompanied by noise and interfering signals.

The continuous recording of long time monitoring on a recorder or visual display devices presents some problems for clinicians and research workers who are interested in the long time

history of the state of the heart. Pen recorders use too much paper and ordinary visual devices can only display a few signals at a time. A long time monitoring of ECG was performed on the computer by building a histogram for the required time. The histogram can be displayed on special oscilloscopes or recorders, and enables study of the time-variant effect of delta modulation, obtained by the addition of noise (low pass band limited and wide band). The effect of noise was also studied on the waveform preservation capability of the delta modulator.

4.1 Simulation

A base band telemetry system (encoding and decoding) for physiological signals (ECG in the present case) was simulated. All the signal processing and analyses necessary for the study and investigation was simulated and performed on the computer. The telemetry system shown in figure 4.1 is based on Delta modulation and Delta sigma modulation. The simulation has the following features.

1. Simulated ECG waveform as an input.
2. Delta modulator as an encoder.
3. Delta sigma modulator as an encoder.
4. Decoder for delta modulator.
5. Decoder for delta sigma modulator.

The signal processing and simulations involved the following:

1. A digital filter was used in the decoders of delta modulation systems. It was also used in the low pass band limiting of the signals whenever required.
2. Waveform preservation was studied by obtaining the time-amplitude waveform on the graph plotter of the computer.

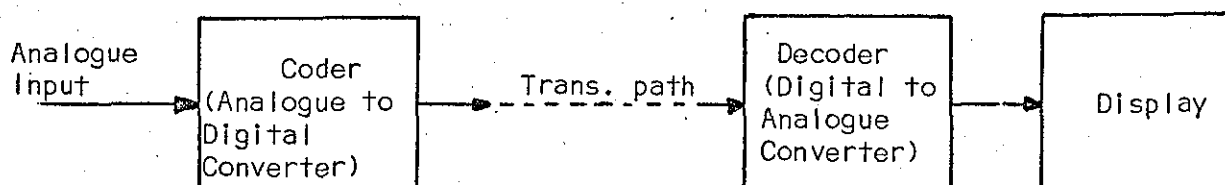


Figure 4.1 Basic Telemetry System.

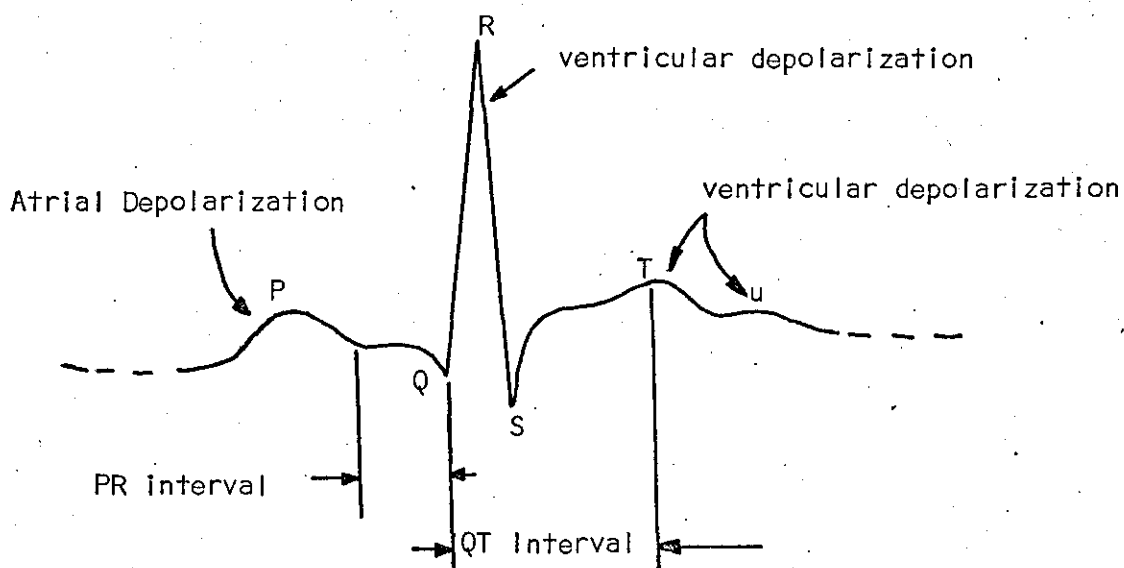


Figure 4.2(a) Electrocardiogram Waveform.

3. Spectral analysis was carried out on various waveforms to obtain the energy distribution in the frequency domain at various frequency components. This was obtained by using the discrete fourier transform.
4. Cepstral analysis was performed to observe any periodic components of higher frequency noise. This was obtained by using the direct and inverse fourier transform of the signals.
5. Pseudo random noise was used to make the ECG waveform change for each cycle which enabled the study to be made of the time-variant effect of the delta modulator.
6. The histograms were used to compress the large amount of data gained over a long period of time from monitoring the ECG signals.

4.1.1 Input Signal

The ECG is one of the most important and widely monitored physiological signals. The time and amplitude relation of the waveform is shown in figure 4.2a.

The whole waveform as shown is a combination of P, Q, R, S, T and occasionally U during each heart cycle⁽⁵²⁾. The P wave is a small, low voltage deflection produced due to the depolarisation of the atria as blood is pumped from the chamber into the ventricles. The P wave is followed by an interval of rest called the PR interval, marking the passage of the electrical impulses from atria to ventricles. The QRS complex which is a big deflection is caused due to the depolarisation of the ventricles and the pumping of blood into the aorta. A component of QRS indicates that the atria

has been repolarised and is ready for the next heart beat. The T wave marks the ventricular recovery. The U wave sometimes follows the T wave.

The following are the time-amplitude relations:

P wave	Amplitude (millivolts)	Duration (milliseconds)
P wave	0.1	90
PR interval		
Q	0.03	
R	0.98	
S	0.01	
QRS		83
T	0.29	
QT interval		397

The American Heart Association specifies a minimum frequency response of 0.1 Hz to 50 Hz for the systems used to process the ECG signals. Although the frequency content of the ECG is assumed to lie between these limits, there has been some discussion of small components up to 200 Hz. The amplitude of various frequency components are shown by the spectrum of an ECG as given in figure 4.2b.

It is seen from the spectrum that the main energy components of a normal ECG lie below 20 Hz, and the higher frequency components over 50 Hz are practically negligible.

4.1.2 Simulation of the ECG Waveform

Although the ECG waveform described earlier has the time-amplitude relation shown in the figure 4.2a, it nevertheless varies considerably from subject to subject. Hence an approximately typical

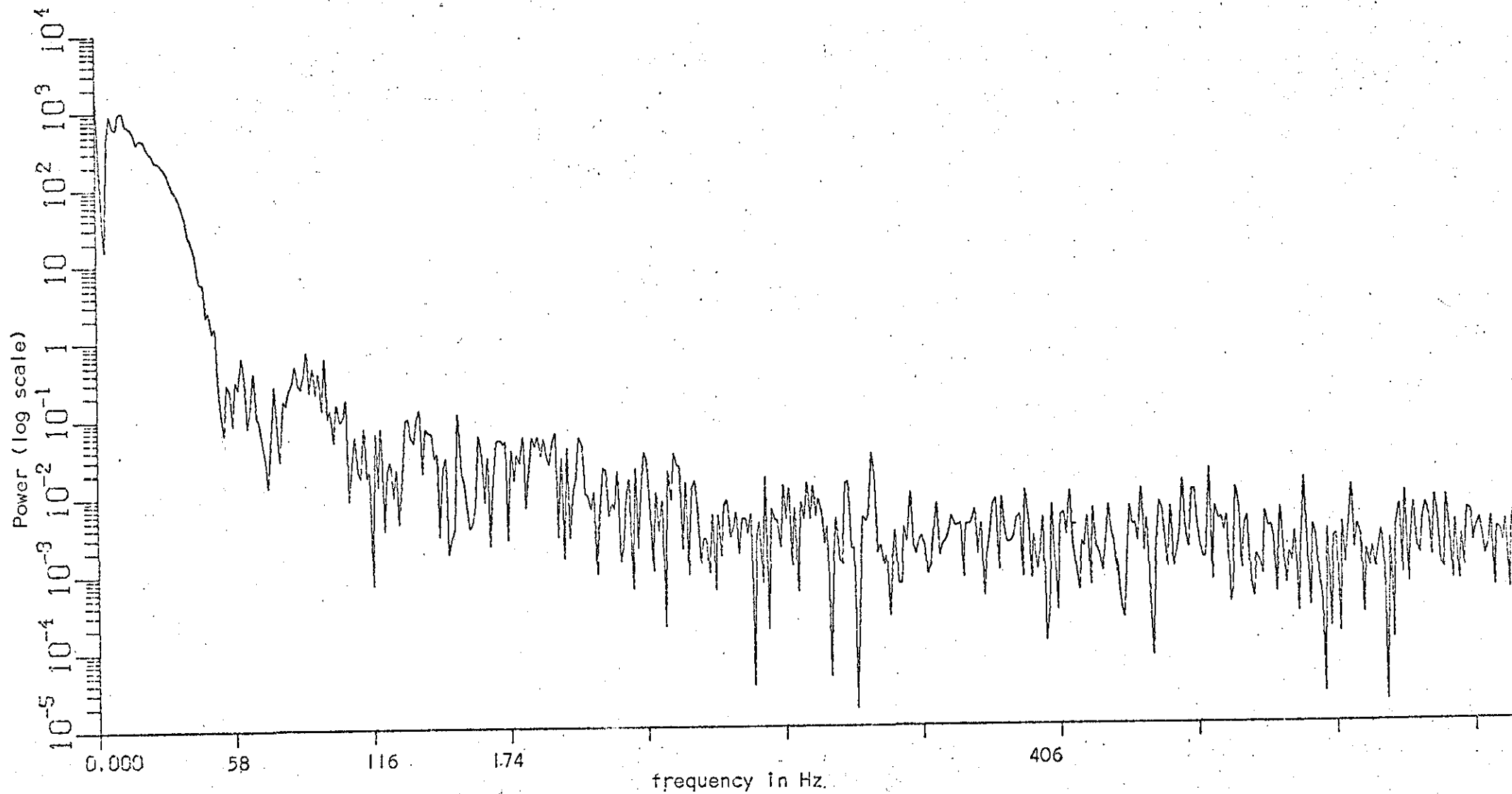


Figure 4.2(b) Spectrum of a Typical ECG

waveform obtained from a normal heart is simulated.

P and T segments of the ECG waveform were treated as rectified or half sine waves. The QRS complex is a triangular wave or two ramps of opposite slope.

The complete waveform was obtained by generating the above segments separately and then adding them. The total number of samples chosen to generate the whole ECG waveform was 851 which corresponds to the sampling frequency of the highest component present in the ECG waveform. The normal ECG waveform lasts for about 800 milliseconds with the highest frequency component of about 50 Hz. In delta modulation the sampling frequency was chosen about 20 times⁽⁵⁷⁾ the frequency of the signal to be encoded.

$$\begin{aligned} 800 \text{ ms} &= 851 \text{ samples} \\ \text{frequency} &= 851 \cdot 10^3 / 800 \\ &\approx 1 \text{ kHz} \end{aligned}$$

The amplitudes of all segments of the ECG waveform were normalised, the highest amplitude being that of QRS and taken as 1 (one) in the simulation.

The P waveform was obtained by generating a half sine wave rising to an amplitude of 0.2 in 200 samples. There were 26 samples of zero amplitude before the P segment started.

The equation of a half sine wave in the time domain is given by

$$f(t) = A \sin(\pi t / T)$$

where T is the period of the half sine wave. In discrete form the equation can be written as

$$f(n) = A \sin((n-k)/N)$$

where

$$n = k+1, k+2, \dots, N$$

$$A = \text{amplitude of the sinewave}$$

$$N = \text{total number of samples in the half sine wave}$$

and

$$k = \text{the number of samples before the P segment starts}$$

The QRS complex followed the P segment and was preceded by 48 samples of zero amplitude and consisted of ramps forming a nearly triangular waveform. The first triangular waveform was in the negative direction rising to an amplitude of 0.1 in 20 samples. The second triangular waveform started immediately after the negative triangular waveform and increased to a normalised amplitude of 1.0 in 200 samples. This was again followed by a small negative ramp rising to an amplitude of 0.1 in 30 samples. The triangular waveforms were simulated by generating two ramps of opposite slope. The equation of a ramp may be written as:

$$y(t) = m(n-k)/N$$

In the discrete form the equation is given by

$$y(n) = m(n-k)/N$$

where N is the total number of samples required to generate a ramp

$$n = 1, 2, 3, \dots, N$$

and k is the number of samples after which the ramp starts. The QRS complex was followed by 73 samples of zero amplitude and the T segment. The T segment rose to an amplitude of 0.4 in 300 samples which was simulated by generating a half sine wave.

The complete ECG waveform is given as the sum of all the segments generated and in this case consisted of 851 samples, shown in fig.4.8.

4.1.3 Simulation of the Encoder

The encoder was used to convert the analogue physiological signal into a coded form. It was based on delta modulation and delta sigma modulation. The simulation consisted of the following and is

also shown in figure 4.3.

1. Difference circuit
2. Quantiser
3. Integrator

1. Difference Circuit

The analogue input signal was simulated by a number of discrete samples corresponding to the sampling rate of the delta modulator.

In the delta modulator every sample of the analogue input signal was compared with the delayed sample of the integrated sample and the difference quantised.

In the delta sigma modulator the difference between the present sample of the analogue signal and the digital output was integrated. The difference circuit was simulated by simply taking the difference of the two sample values.

2. Quantiser

The quantiser gives out binary pulses of polarity depending upon its input. In the delta modulator it was simulated by testing the output of the difference circuit to observe whether it was greater than, equal to or less than zero. If the output of the difference circuit was greater than zero, a positive pulse (logical one) was generated from the quantiser. For the output to be equal to zero or less than zero a negative pulse (logical zero) was generated. In the delta sigma modulator the output of integrator was quantised.

3. Integrator

Because the integrator in the delta modulator is situated in the feedback loop, the output of the quantiser was integrated and compared with the input. In the delta sigma modulator the integrator

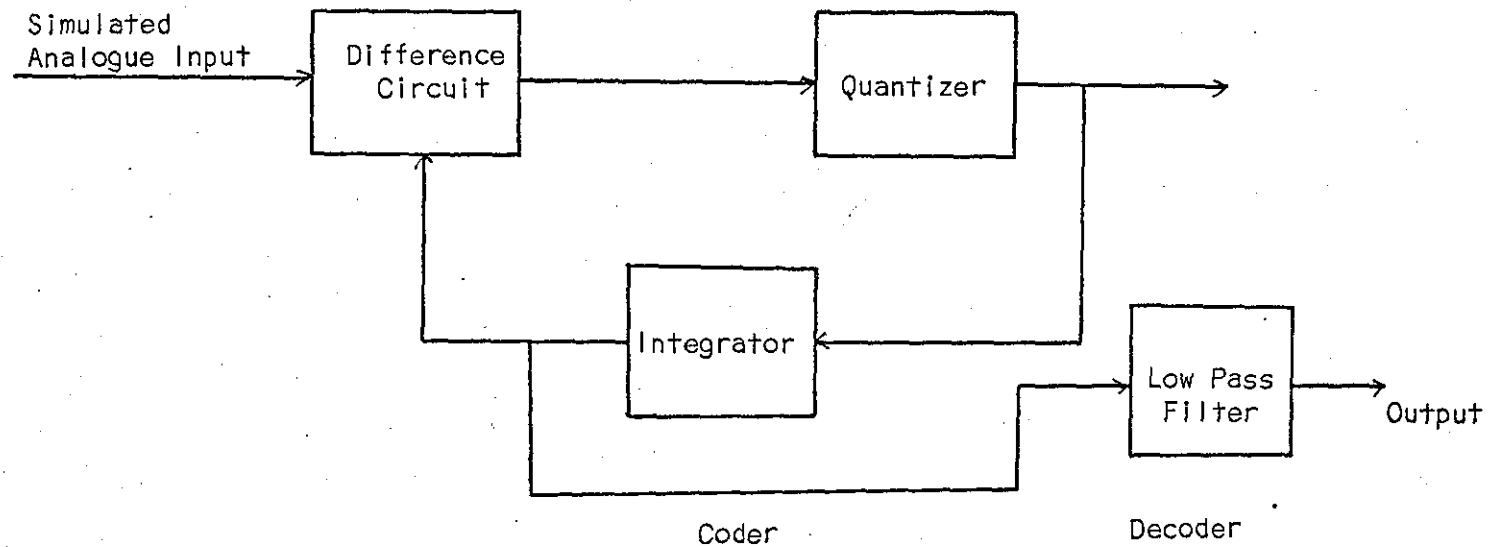


Figure 4.3(a)

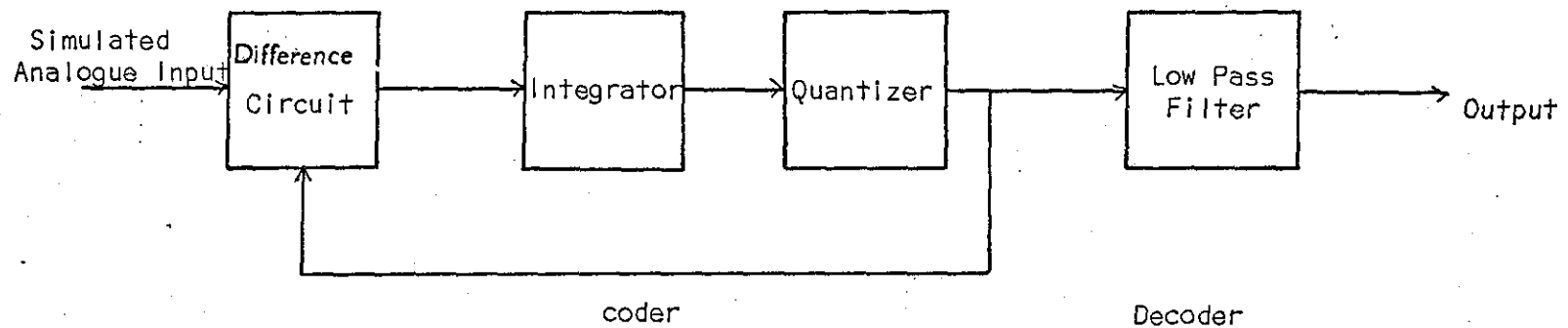


Figure 4.3(b)

Figure 4.3 (a) Block diagram for the simulation of the delta modulator.

Figure 4.3 (b) Block diagram for the simulation of the delta sigma modulator.

is situated in the forward path and it is the output of the difference circuit which is integrated.

In practical systems the RC integrator used has some leakage and has a time constant. The step voltage of the integrator is related to the time constant and defined as the change in integrator output voltage during one clock pulse when the mean voltage at the integrator output is zero.

Step voltage is given by

$$d = V / (T_c f_s)$$

where $T_c = RC$, $f_s =$ clock frequency

It is chosen according to the frequency and the amplitude of the signal to be encoded.

In the simulated ECG waveform the highest amplitude was 1.0 and 100 samples were taken to reach that amplitude value. The step voltage chosen, therefore, must be greater than 0.01 to track the highest amplitude (QRS complex) properly and it was chosen to be 0.02.

The Integrator in the delta modulator was simulated in discrete form and is shown mathematically in the Appendix B.

The Integrator was simulated in the delta modulator as follows:

$$A(I) = s * A(I-1) \pm \text{step voltage}$$

where $s =$ leakage

that is, the present output of the integrator was obtained by taking the previous output, multiplying it by the leakage s (which is slightly less than one) and adding or subtracting the step voltage. The step voltage was added when the output of the quantiser (which is the input to the integrator) was positive, and subtracted when it was negative.

4.1.4 Simulation of the Decoder

The Decoder in the digital modulation system converts the digitally encoded signal into the original analogue form. In the delta modulator, the decoder is an integrator of the same characteristics as the encoder. This is followed by a low pass filter to eliminate higher frequencies due to the sampling process. In the delta sigma modulator the encoder is simply a low pass filter.

For simulation the same integrator was used for the decoder of the delta modulator as was used in the encoder. A digital low pass filter was designed and simulated for the decoder of the delta sigma modulator and to filter the higher frequency components in the decoder of the delta modulator. The same filter was used in the signal processing required in the investigation of the system.

4.1.5 Digital Filters ^(72,73)

The requirement of the filter used in the decoder of the simulated modulation systems is to eliminate higher frequencies. As a result a low pass digital filter was designed and simulated by the frequency sampling technique ⁽⁷⁴⁾ in the frequency domain.

A digital filter is defined as a device which accepts a sequence of numbers as its input and operates on them to produce another sequence of numbers as its output. Due to the discrete nature of input and output used in this filter the z-transform can be used for its transfer function which is a polynomial in the variable z^{-1} . A digital computer can be easily programmed to implement a digital filter with greater simplicity and economy compared to analogue techniques. The inaccuracies of the digital computer which are due to rounding errors in the computer can be made as small as required.

There are two types of digital filters.

1. Recursive filters
2. Non-recursive filters

1. Recursive Filters

A recursive filter is formed on the principle of a closed loop whereby the current filter output is obtained explicitly in terms of past output as well as past and present inputs. There are some situations with biomedical signals⁽⁷³⁾ where recursive filters are not suitable. One such situation is in the study of ECG waveforms where height and time of a pulse are of interest. It is important to minimise the waveform distortion produced by a filter. The non-linear phase characteristics of recursive filter result in unacceptable modification of the waveform in such circumstances. Only special classes are phase linear. The design of a recursive filter is more sophisticated and it can be unstable. Impulse responses of these filters are infinite geometric (exponential) sequences or sums of these. The recursive filter is often more efficient, in the sense of frequency selectivity for a given complexity.

2. Non-Recursive Filters

A non-recursive filter is implemented without using any feedback, hence the current filter output is obtained explicitly in terms of only past and present inputs. It does not use the previous outputs to generate the current output. A non-recursive filter can be easily made phase linear and hence produces the minimum modification of the signal waveform (ECG, for example) compatible with a given gain characteristics. The design of a non-recursive filter is very simple.

For time-domain specifications, responses and co-efficients are related linearly and hence linear programming can be used. It is always stable and its impulse response is of finite duration so that particular input samples produce no effect at all on the output after a particular clock period. This removes the effect of spurious inputs and transients after a known length of time.

The impulse response can be arbitrarily long to achieve the required resolution, hence it involves more computer memory and is expensive in computation. The use of the Fast Fourier Transform algorithm in implementing a non-recursive digital filter can reduce the amount of computation and computing time considerably. Theory of non-recursive filters is given in Appendix C.

4.1.6 Methods of Design

Due to the advantages and simplicity of non-recursive filters, it was decided to design and simulate a non-recursive filter for the decoder in the delta modulation system. A filter with zero phase shift was used so as to avoid time displacement of low frequency components or to get the same time shift introduced by the filter at all frequencies in the pass band.

It is known that the filter when used as a decoder for the delta sigma modulator has ideally zero attenuation in the pass band and infinite attenuation outside it. As the input signal envisaged could have dc components, the filter had to be a low pass filter whose characteristics were a close approximation to the ideal filter. However this filter has an impulse response $h(t)$ of the $\sin(x)/x$ type which covers the time range from minus infinity to plus infinity.

A non-recursive digital filter has a finite duration impulse response and contains no poles (only zeros) in the z-plane. The problem is that of finding suitable approximations to various idealised filter transfer functions which may be magnitude or phase or both of the idealised filter. The commonly used approach for approximating the frequency domain filter characteristics is based on approximating the infinite impulse response of the ideal filter by the finite duration impulse response of the non-recursive realization. This means that truncating the infinite impulse response to get the finite response has to be performed. This gives rise to overshoot and ripples in the frequency response called the Gibbs phenomenon. The overshoot in the vicinity of discontinuity (at the point of truncation) does not diminish even if the response is increased in duration. Instead the severity of discontinuity can be reduced by a time-limited window function. Hence multiplying the ideal impulse response with a time window corresponds to smoothing the spectrum.

Kaiser⁽⁷⁵⁾ introduced these windows which are very close to optimum. This method gives an improvement in reducing the sidelobes at the expense of increased transition bandwidth.

Martin⁽⁷⁶⁾ designed non-recursive filters from a frequency response specification and specified initial values of the frequency response at selected frequencies, leaving unspecified values of the frequency response in preselected transition bands. He then used a minimisation procedure to solve for final values of the frequency response at equally spaced frequencies. From the ideal frequency response he minimised for both in-band and out of band frequencies. He obtained useful results for small value of N (number of impulse

response samples) for the case of lowpass filters and for a wideband differentiator.

Gold and Jordan⁽⁷⁷⁾ introduced a somewhat different approach to the approximation problem for non-recursive digital filters by specifying the frequency response at exactly equispaced frequencies. If the number of frequency samples are assumed to be equal to the number of samples in the impulse response, the continuous frequency response is exactly determined. The impulse response corresponding to the frequency sampled filter is now no longer truncated but aliased. This aliasing makes it different from the time window technique. The results of both the techniques are given in figures 4.4 and 4.5.

Gold and Jordan obtained results for a few low pass filters by using semi-automatic technique for computer optimisation. Recently Rabiner, Gold and McGonegal described the design and optimisation for more general cases and described them in more detail. The procedure adopted is more efficient and fully automated. This makes it possible to generate design data for a variety of low pass filters, bandpass filters and wideband differentiator.

4.1.7 Advantages of Sampling Method

1. When the design of a filter is required to approximate to a given ideal shape in the frequency domain with sufficiently long impulse response (more than 30 samples), then the sampling method is used. The impulse response is not required and high speed convolution using the fast fourier transform can be used for the synthesis, since the design results can be applied directly to get the synthesis.

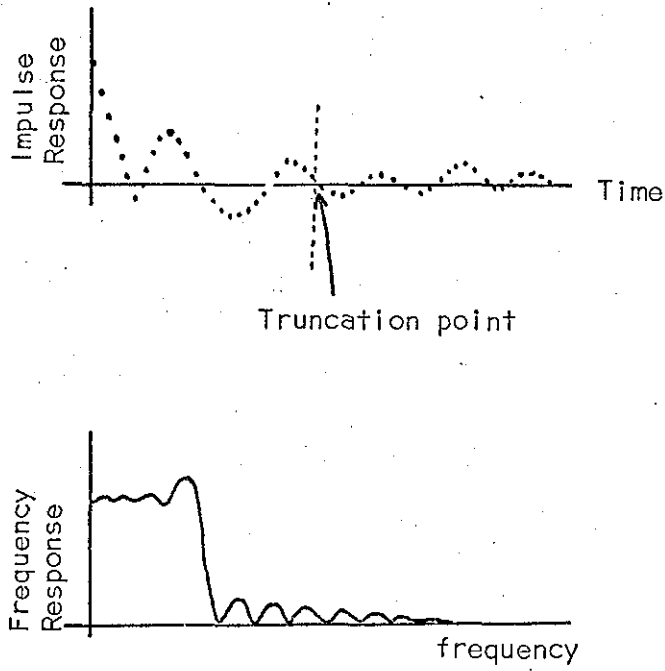


Figure 4.4. Diagrams showing the effects of truncating the impulse response on the frequency response.

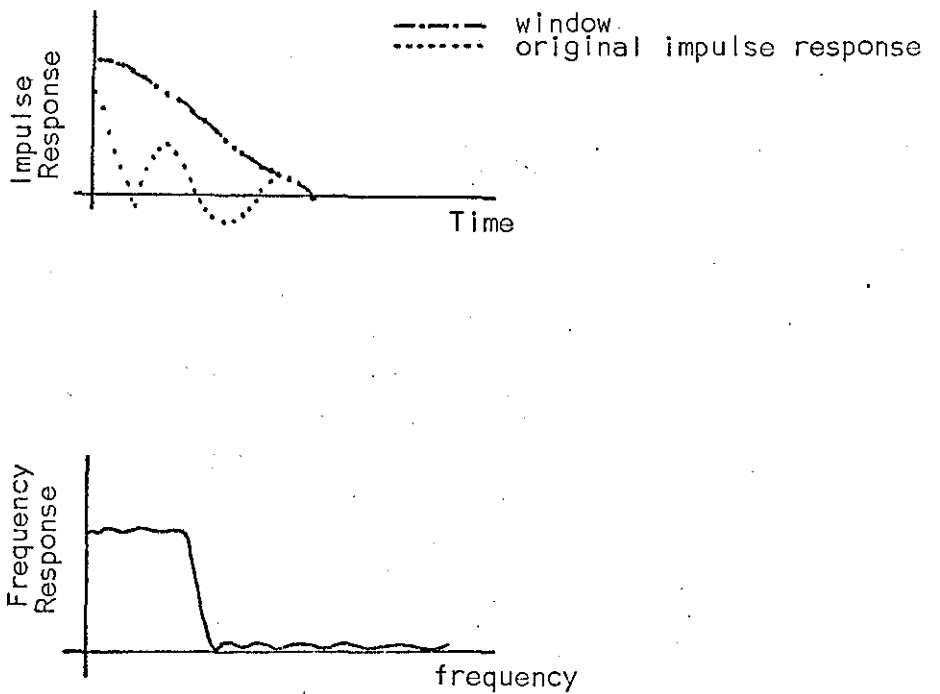


Figure 4.5. Diagrams showing the reduction of overshoot in the frequency by windowing the truncated impulse response

2. The sampling technique can be easily used to get an optimum filter on the computer. In a sampling technique once the transition bandwidth is chosen, the best filter in a practical sense can be obtained.

4.1.8 Simulation of the Practical Lowpass Filter

1. Principle

The lowpass filter was synthesised by direct convolution (Appendix D) and can be written as

$$y(n) = \sum_{n=0}^{m-1} h(n) x(n-m)$$

$h(n)$ is the impulse response of the filter

$x(n)$ is the input sequence of the signal to be filtered, and,

$y(n)$ is the output.

The limit in the above expression implies that $h(n)$ is of duration n , so that $h(m) = 0$ for $m \geq n$.

The simulation is based on the approximation of the frequency response of an ideal filter by placing frequency samples in the z -plane and choosing the remaining frequency samples to satisfy the optimization criteria⁽⁷⁴⁾. Having decided the shape of the frequency response $H(j\omega)$ for a required filter, the impulse response $h(n)$ was computed by means of the FFT algorithm and is given by

$$h(n) = \frac{1}{N} \sum_{k=0}^{N-1} H_k e^{j2kn/N}$$

$k = 0, 1, 2, \dots, N-1$ for each value of $n = 0, 1, \dots, N-1$, where N = total number of samples, and,

H_k = Discrete values of frequency samples.

The computer subroutine $N \log N$ for discrete fast Fourier transform is given in Appendix E.

2. Design

In the low pass digital filter the samples in the pass band were equated to one and in the stop band equal to zero. The number of samples in the transition band ($2M$) were varied until the maximum sidelobe was at a minimum. Symmetry considerations reduce the number of independent transition samples to M . Minimax search is a procedure which searches for the minimum value of the maximum sidelobe to converge and is a function of transition coefficients T_1, T_2, \dots . Using the search technique⁽⁷⁴⁾, the optimum values of minimax for the transition coefficients of the bandwidth used, stop band and transition band were designed and calculated.

The simulated digital filter was employed for band limiting the input signal, for acting as the final filter in the delta modulator decoder, and for acting as the complete decoder in the case of the delta sigma modulator.

The delta modulator and the delta sigma modulator simulated had the following parameters. Maximum frequency of the signal to be coded is 50 Hz and the clock frequency was 1.0 K bits (Chapter 4, section 4.1.1). The low pass filter required in the decoder of the above systems should therefore have a cut-off frequency of 50 Hz.

The total number of samples selected in the frequency response of the simulated filter were 64, as the cut-off frequency of low pass digital non-recursive filter under discussion depends on the number of samples in the pass band and the sampling rate.

Two filters were simulated and tried for the decoder. In the first filter the number of samples selected in the pass band were three.

Since the cut-off frequency of the filter was taken as the frequency range up to the 3 db point, and the first sample in the transition band is at the 3 db point, the cut-off frequency was computed as follows:

$$\text{Frequency spacing } (\Delta f) = \frac{1 \times 10^3}{64} = \frac{1}{NT}$$

where N = total number of samples in the frequency response of the filter, and,

T = the sampling time. Then,

$$\text{Cut-off frequency} = \frac{4}{64} \times 10^3 = 62.5 \text{ Hz}$$

Hence the filter with cut-off frequency 62.5 Hz was simulated as shown below.

1. Equated three samples in the pass band to one.
2. Found the value of minimax for the transition band for N when N is even and symmetrical about N/2.
3. Equated the remaining samples in the stop band to zero.

Due to symmetry of the response the samples were repeated to obtain the full response. These values were taken as the coefficients of the fast fourier transform and an inverse fourier transform was taken by using the computer to obtain the impulse response in the time domain. The values of the coefficients were arranged to obtain a response as shown in figure 4.6a. The values of frequency response are given in Table 1.

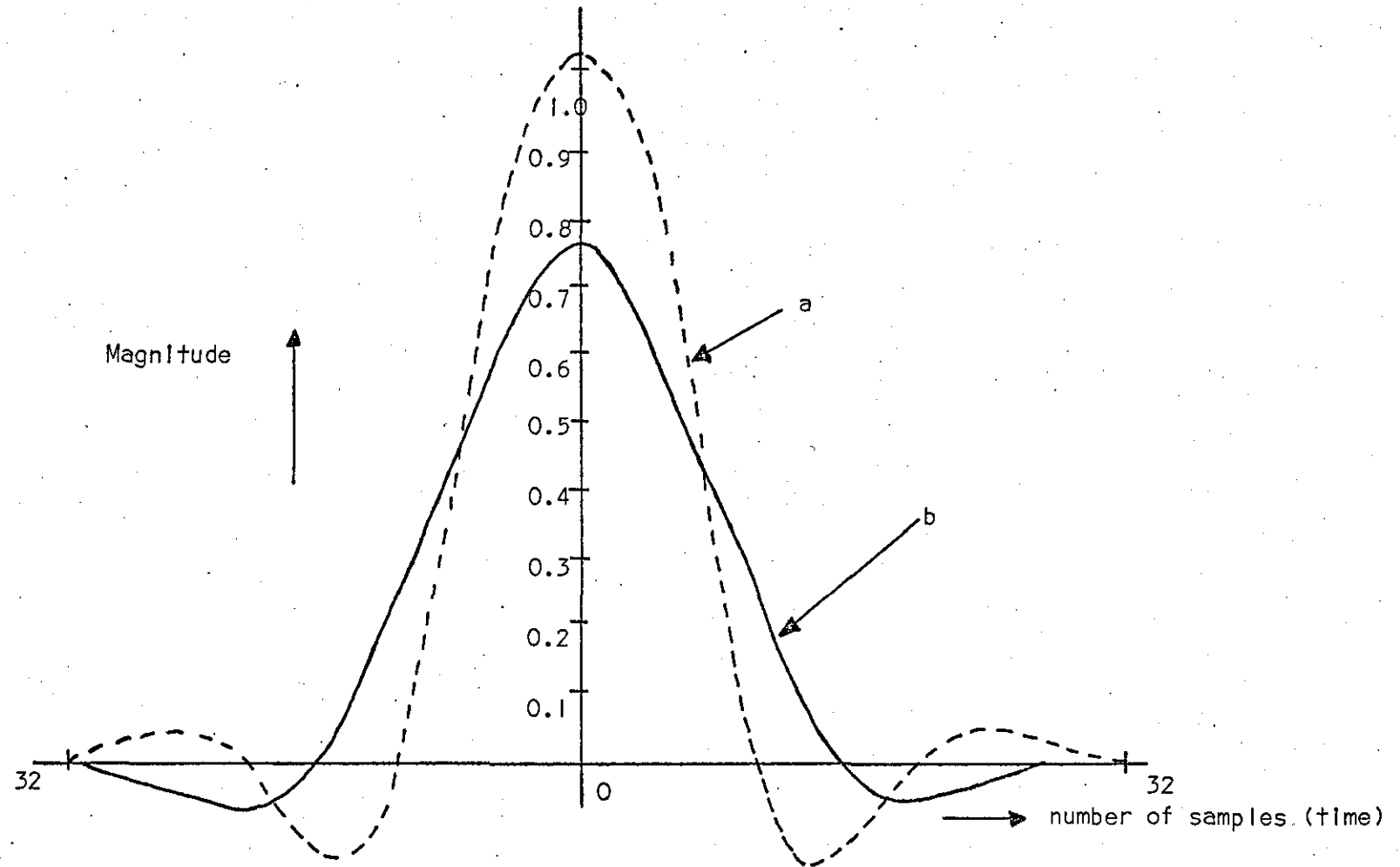


Figure 4.6 (a) Impulse response of the filter with cut off frequency = 62.5 Hz
 (b) Impulse response of the filter with cut off frequency = 47 Hz

Table 1. Weighting Coefficients for Low Pass Filter

First filter with cut-off frequency = 62.5 Hz

Total number of frequency samples (N) = 64

No. of samples in the pass band (BW) = 3

No. of transient coefficients = 3

In order to obtain the impulse response the following procedure was adopted :-

1. Equated $(2BW-1) = 5$ number of samples to 1
2. Used the values of transition coefficients as computed by Rabiner et al⁽⁷⁴⁾ (for type -1 data N even).
3. Applied discrete fourier transform to the above data as arranged in the following:

$H_0 = H_1 = H_2 = H_{62} = H_{63} = 1.0$	
$H_3 = H_{61} = 0.72204262$	
$H_4 = H_{60} = 0.24519492$	Transition
$H_5 = H_{59} = 0.02438354$	Coefficients
$H_6 \text{ --- } H_{58} = 0.0$	

The filtering action is obtained by convolving the impulse response with the desired signal to be filtered. In order to achieve this the values of the impulse response obtained were arranged as follows (making the imaginary values zero).

Table 1. (Continued)

1.	$-.6250 \times 10^{-3}$	33.	0.1069
2.	$-.5350 \times 10^{-3}$	34.	0.1046
3.	$-.2695 \times 10^{-3}$	35.	0.9810×10^{-1}
4.	0.1572×10^{-3}	36.	0.8784×10^{-1}
5.	0.7188×10^{-3}	37.	0.7473×10^{-1}
6.	0.1374×10^{-2}	38.	0.5982×10^{-1}
7.	0.2062×10^{-2}	39.	0.4427×10^{-1}
8.	0.2701×10^{-2}	40.	0.2919×10^{-1}
9.	0.3188×10^{-2}	41.	0.1556×10^{-1}
10.	0.3403×10^{-2}	42.	0.4106×10^{-2}
11.	0.3218×10^{-2}	43.	$-.4724 \times 10^{-2}$
12.	0.2514×10^{-2}	44.	$-.1077 \times 10^{-1}$
13.	0.1201×10^{-2}	45.	$-.1415 \times 10^{-1}$
14.	$-.7504 \times 10^{-3}$	46.	$-.1518 \times 10^{-1}$
15.	$-.3290 \times 10^{-2}$	47.	$-.1436 \times 10^{-1}$
16.	$-.6258 \times 10^{-2}$	48.	$-.1224 \times 10^{-1}$
17.	$-.9375 \times 10^{-2}$	49.	$-.9375 \times 10^{-2}$
18.	$-.1224 \times 10^{-1}$	50.	$-.6258 \times 10^{-2}$
19.	$-.1436 \times 10^{-1}$	51.	$-.3290 \times 10^{-2}$
20.	$-.1518 \times 10^{-1}$	52.	$-.7504 \times 10^{-3}$
21.	$-.1415 \times 10^{-1}$	53.	0.1201×10^{-2}
22.	$-.1077 \times 10^{-1}$	54.	0.2514×10^{-2}
23.	$-.4724 \times 10^{-2}$	55.	0.3218×10^{-2}
24.	0.4106×10^{-2}	56.	0.3403×10^{-2}
25.	0.1556×10^{-1}	57.	0.3188×10^{-2}
26.	0.2919×10^{-1}	58.	0.2701×10^{-2}
27.	0.4427×10^{-1}	59.	0.2062×10^{-2}
28.	0.5982×10^{-1}	60.	0.1374×10^{-2}
29.	0.7473×10^{-1}	61.	0.7188×10^{-3}
30.	0.8784×10^{-1}	62.	0.1572×10^{-3}
31.	0.9810×10^{-1}	63.	$-.2695 \times 10^{-3}$
32.	0.1046	64.	$-.5350 \times 10^{-3}$

The final filtering action was achieved by convolving the input sequence with the impulse response obtained.

For the second filter with the cut-off frequency less than ≈ 50 Hz, the number of samples were reduced in the pass band to two.

$$\text{Cut-off frequency} = \frac{3}{64} \times 10^3 = 46.8 \text{ Hz.}$$

This filter was realised on the computer in the same way as in the first case. The values of frequency response are given in table 2 and the shape is given in figure 4.7. The values of impulse response and shape in the time domain are given in Table 2 and figure 4.6b.

The simulated filter was used successfully to decode signals in the delta sigma modulator and to eliminate higher frequencies in the decoded output of delta modulator. The low pass filter with cut-off frequency 62.5 Hz when used as a decoder in a delta sigma modulator was accompanied by some noise and ripple like components in the decoded analogue signal as shown in figure 4.8. Reducing the cut-off frequency of the filter reduced this noise considerably. This is illustrated in figure 4.9 and explained in Section 4.3.

To observe the action of filtering, a wide band noise (Gaussian) of certain variance was added to the ECG signal. The resultant signal was used as an input to the filter and is shown in figure 4.10. The output from the filter is shown in figure 4.11.

4.2 Waveform Preservation Study of the Delta Modulator and the Delta Sigma Modulator

Since waveform preservation, as mentioned before, is an important criterion for certain ECG diagnosis, it becomes an essential requirement for the system used for the telemetering of biomedical data. A system

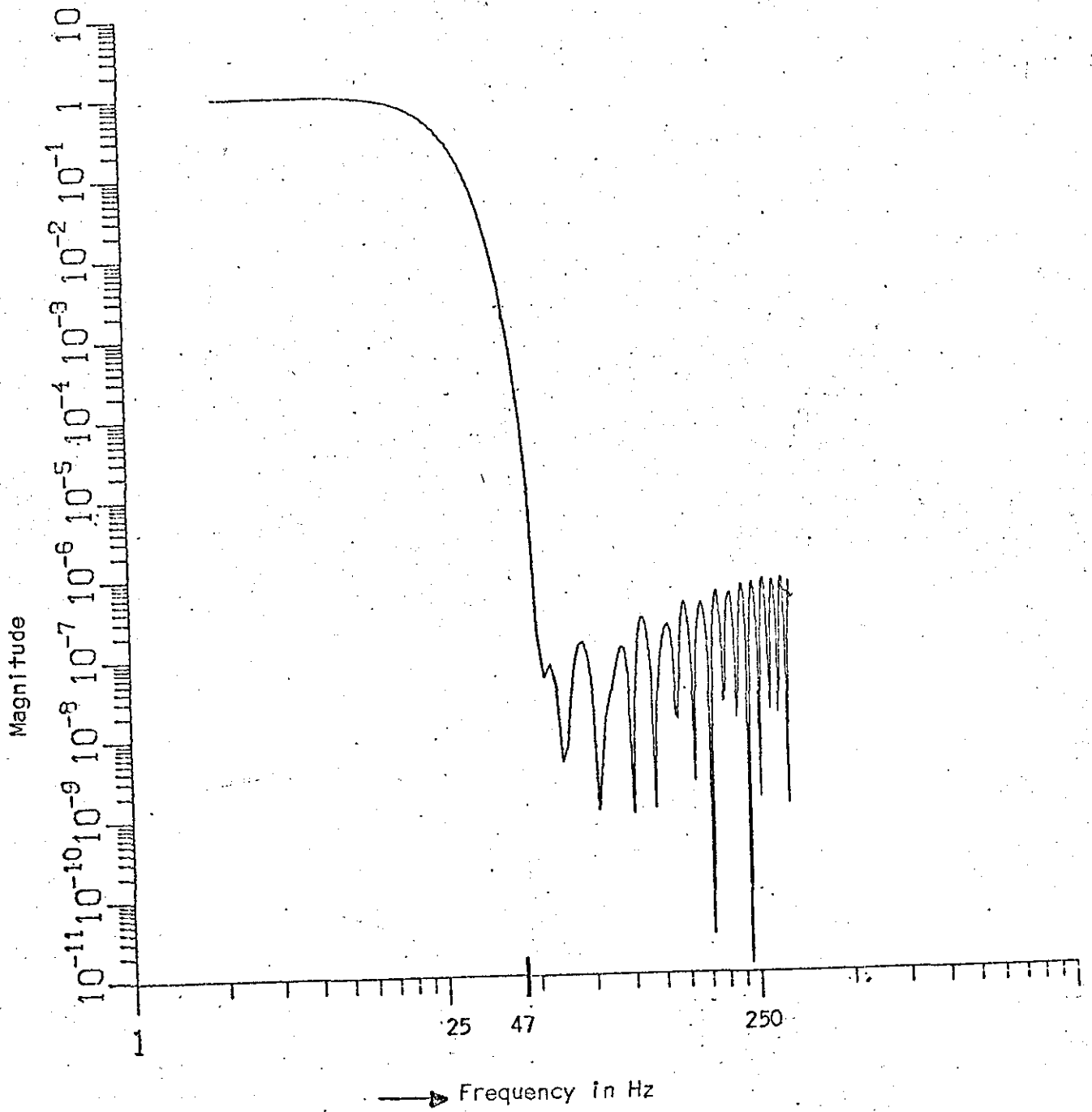


Figure 4.7. Interpolated frequency response of practical filters
(See Table 2.)

Table 2. Weighting Coefficients for Low Pass Filter

Second filter with cut-off frequency = 47 Hz

Total number of frequency samples (N) = 64

Number of samples in the pass band = 2

Number of transition coefficients = 3

The impulse response was obtained by taking the discrete fourier transform (as in Table 1) of the data as arranged in the following :-

$$H_0 = H_1 = H_{63} = 1.00$$

$$H_2 = H_{62} = 0.7051$$

$$H_3 = H_{61} = 0.2263$$

$$H_4 = H_{60} = 0.02057$$

$$H_5 = H_{59} = 0.0$$

The values of impulse response were arranged as in the following to be convolved with the signal to be filtered.

Table 2. (Continued)

1.	$-.9481 \times 10^{-4}$	33.	0.7297×10^{-1}
2.	$-.2004 \times 10^{-3}$	34.	0.6858×10^{-1}
3.	$-.3730 \times 10^{-3}$	35.	0.6278×10^{-1}
4.	$-.6332 \times 10^{-3}$	36.	0.5587×10^{-1}
5.	$-.1001 \times 10^{-2}$	37.	0.4821×10^{-1}
6.	$-.1493 \times 10^{-2}$	38.	0.4015×10^{-1}
7.	$-.2113 \times 10^{-2}$	39.	0.3208×10^{-1}
8.	$-.2854 \times 10^{-2}$	40.	0.2432×10^{-1}
9.	$-.3686 \times 10^{-2}$	41.	0.1716×10^{-1}
10.	$-.4554 \times 10^{-2}$	42.	0.1083×10^{-1}
11.	$-.5379 \times 10^{-2}$	43.	0.5469×10^{-2}
12.	$-.6053 \times 10^{-2}$	44.	0.1154×10^{-2}
13.	$-.6444 \times 10^{-2}$	45.	$-.2110 \times 10^{-2}$
14.	$-.6401 \times 10^{-2}$	46.	$-.4382 \times 10^{-2}$
15.	$-.5766 \times 10^{-2}$	47.	$-.5766 \times 10^{-2}$
16.	$-.4382 \times 10^{-2}$	48.	$-.6401 \times 10^{-2}$
17.	$-.2110 \times 10^{-2}$	49.	$-.6444 \times 10^{-2}$
18.	0.1154×10^{-2}	50.	$-.6053 \times 10^{-2}$
19.	0.5469×10^{-2}	51.	$-.5379 \times 10^{-2}$
20.	0.1083×10^{-1}	52.	$-.4554 \times 10^{-2}$
21.	0.1716×10^{-1}	53.	$-.3686 \times 10^{-2}$
22.	0.2432×10^{-1}	54.	$-.2854 \times 10^{-2}$
23.	0.3208×10^{-1}	55.	$-.2113 \times 10^{-2}$
24.	0.4015×10^{-1}	56.	$-.1493 \times 10^{-2}$
25.	0.4821×10^{-1}	57.	$-.1001 \times 10^{-2}$
26.	0.5587×10^{-1}	58.	$-.6332 \times 10^{-3}$
27.	0.6278×10^{-1}	59.	$-.3730 \times 10^{-3}$
28.	0.6858×10^{-1}	60.	$-.2004 \times 10^{-3}$
29.	0.7297×10^{-1}	61.	$-.9481 \times 10^{-4}$
30.	0.7570×10^{-1}	62.	$-.3908 \times 10^{-4}$
31.	0.7663×10^{-1}	63.	$-.2182 \times 10^{-4}$
32.	0.7570×10^{-1}	64.	$-.3908 \times 10^{-4}$

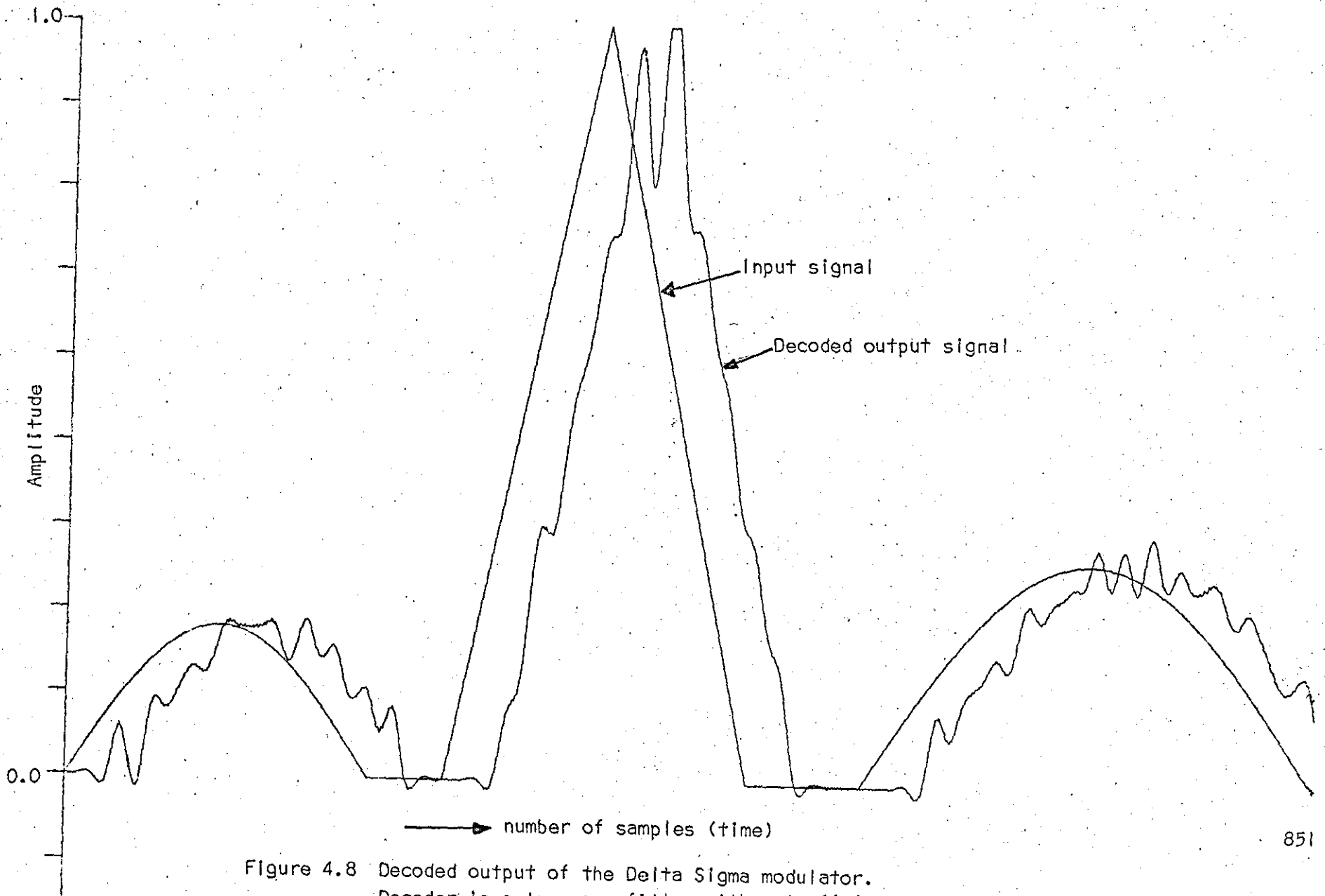


Figure 4.8 Decoded output of the Delta Sigma modulator.
 Decoder is a low pass filter with cut off frequency = 62.5 Hz

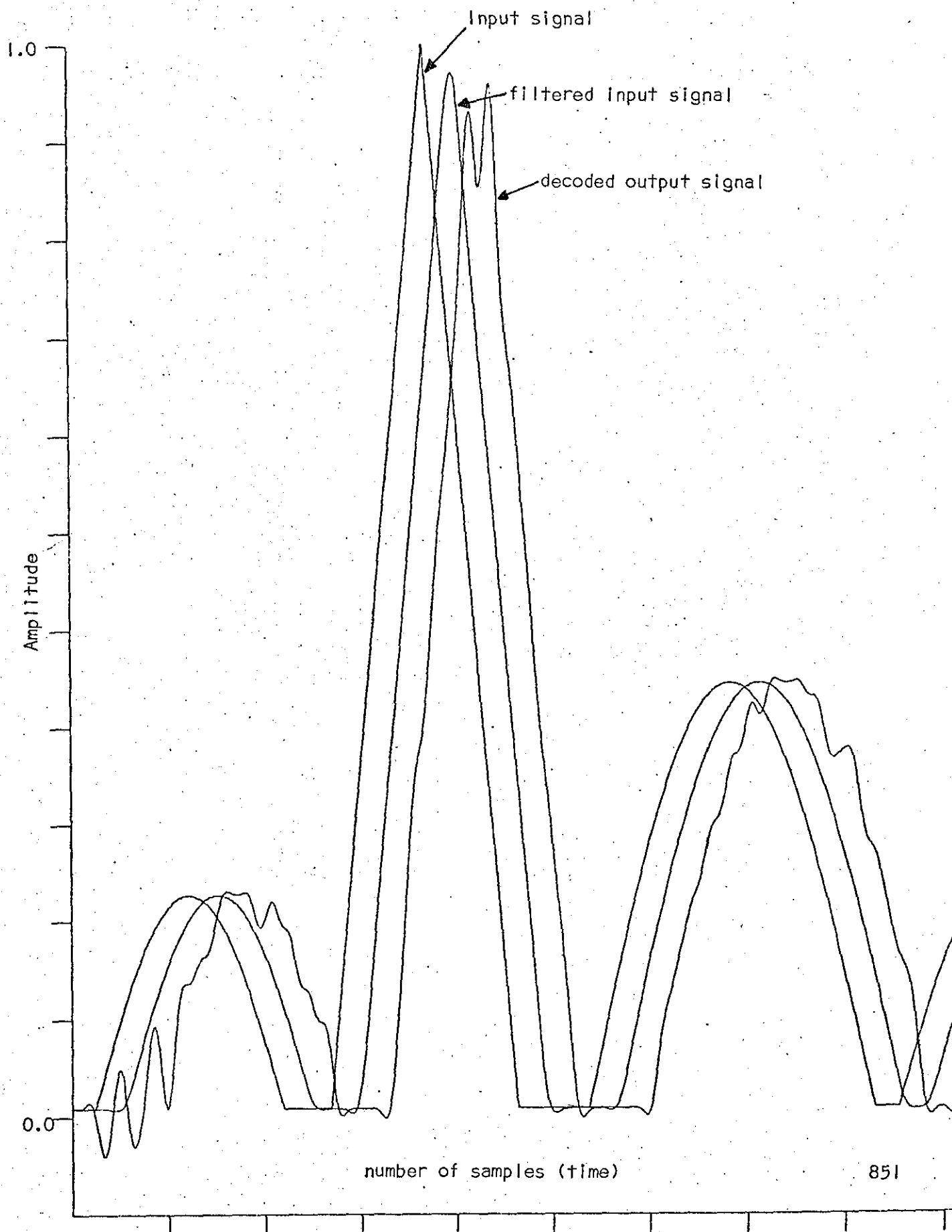


Figure 4.9 Decoded output of the Delta Sigma modulator when decoder is a low pass filter with cut off frequency = 47 Hz

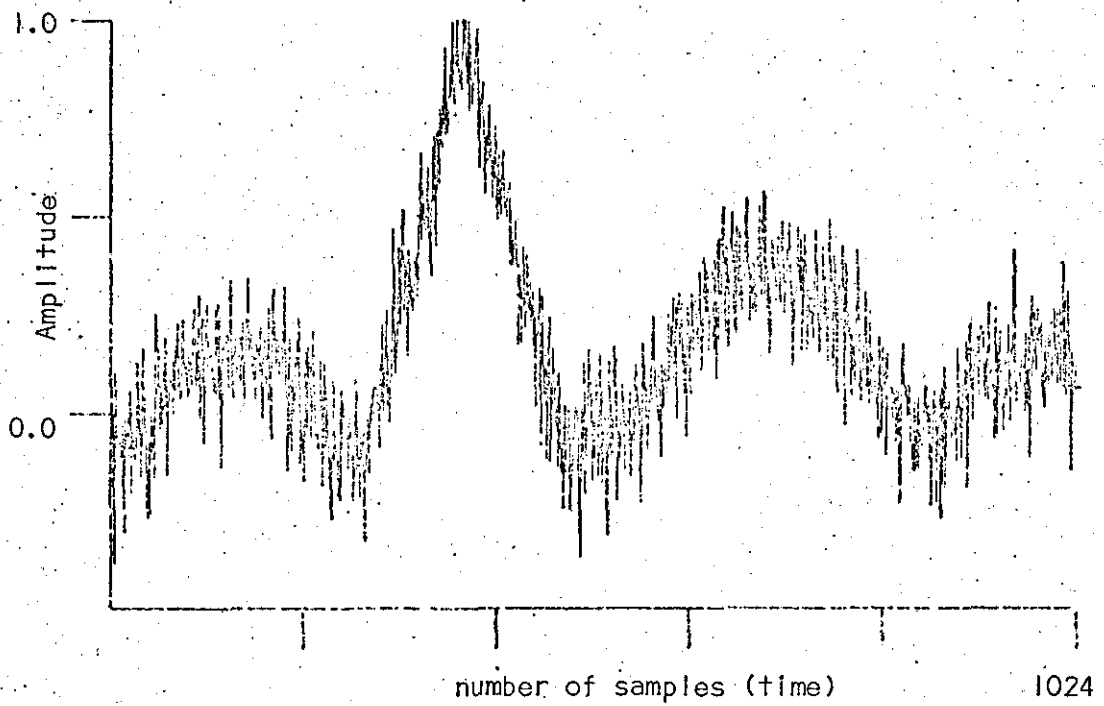


Figure 4.10 Input ECG waveforms with added Gaussian noise.

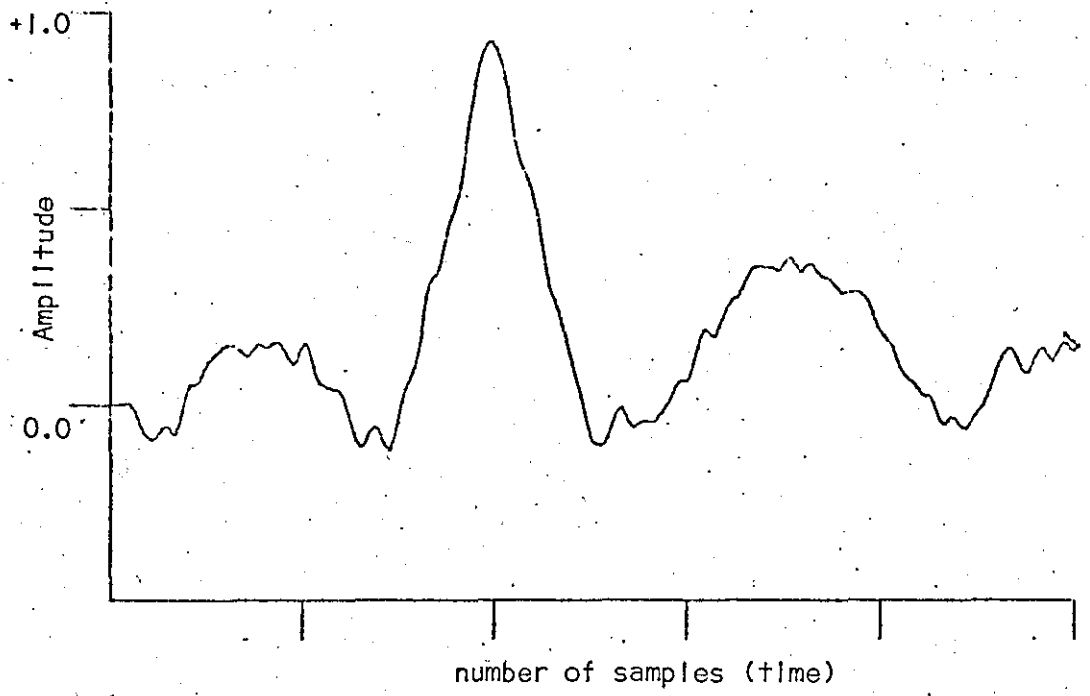


Figure 4.11 Noisy Signal (fig.4.10) filtered with low pass filter of cut off frequency 47 Hz.

based on the delta modulator and delta sigma modulator was investigated for the waveform preservation of an ECG waveform.

The simulated ECG waveform used as an input was filtered by a low pass filter to eliminate the higher frequencies at the sharp corners.

The delta modulator and the delta sigma modulator are described in the last section and were used as follows:

4.2.1 Delta Modulator

A suitable step voltage as given in section 4.1.3 was chosen so that all the segments of the ECG waveform were properly tracked without overloading the system. Assuming there were no transmission errors, the coded signals were decoded using the local integrator and the final analogue signal (time-amplitude waveform) was obtained by filtering the output of the integrator with a low pass filter.

The simulated input ECG waveform and the decoded ECG waveform are shown in figures 4.12 and 4.13.

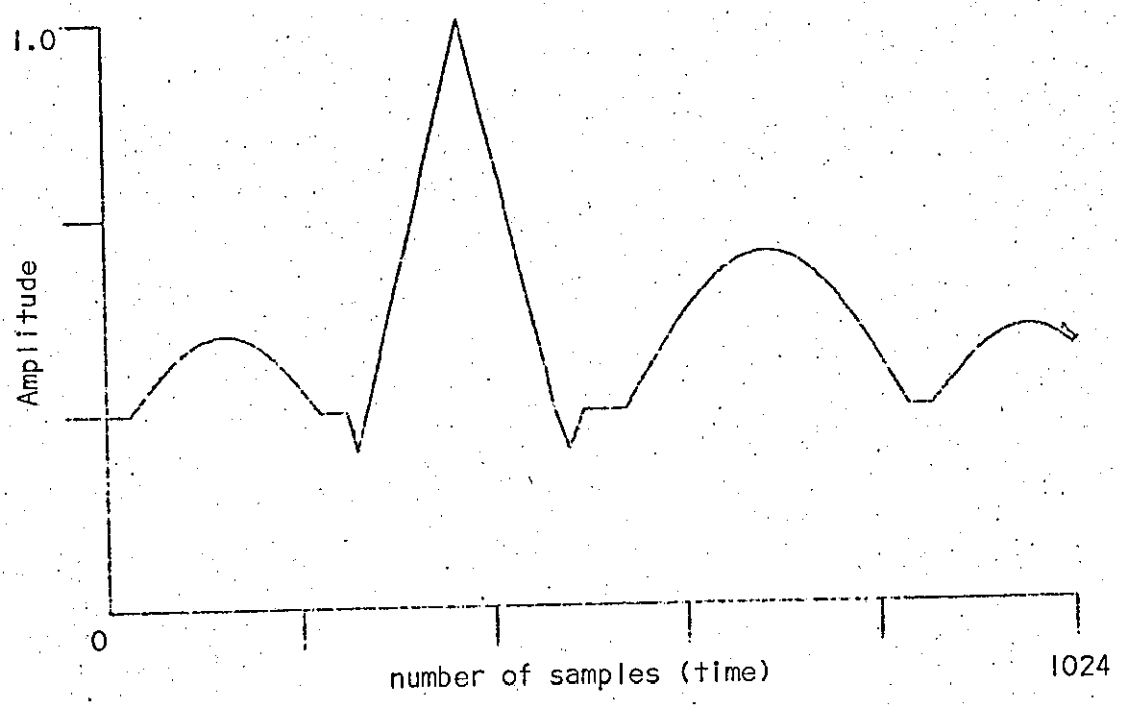
The error waveform and output of the local integrator are shown in figures 4.13 and 4.14 with and without leakage.

4.2.2 Delta Sigma Modulator

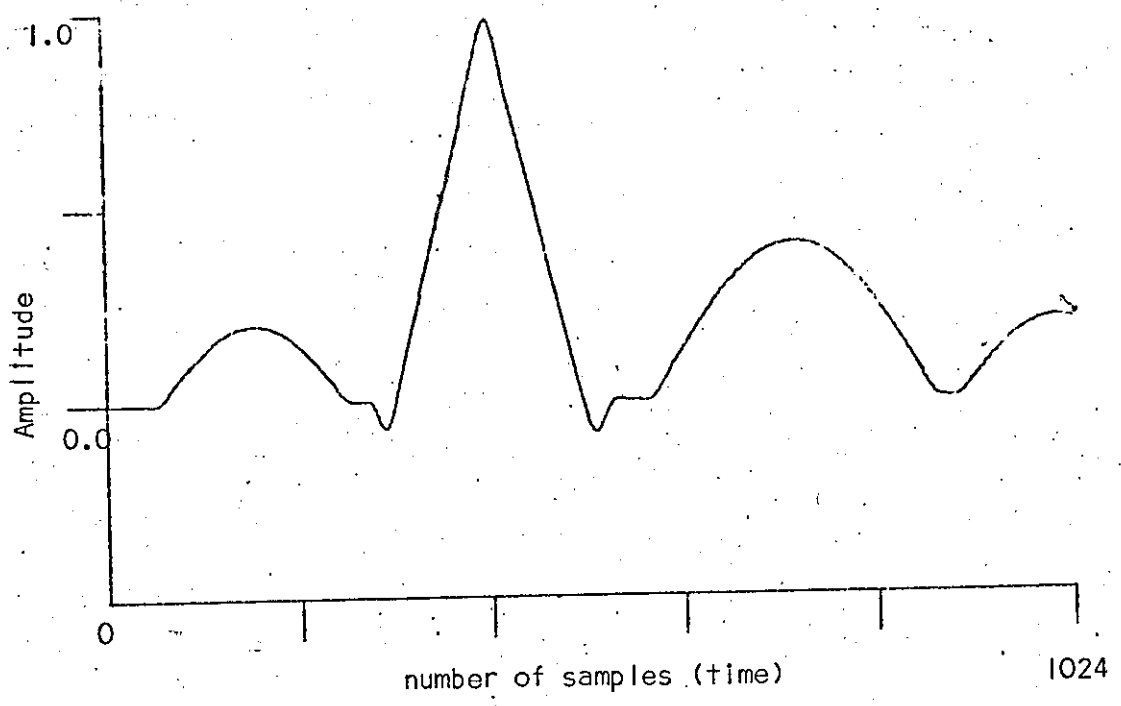
Since the integrator is situated in the forward loop of the delta sigma modulator, a suitable value of leakage was chosen. The digital output of the delta sigma modulator was decoded by a low pass filter to obtain the output signal in analogue form.

The value of leakage introduced is related to $T = CR$ as shown in the following.

A capacitor (C) with a leakage (a resistor) R is shown in figure 4.15.

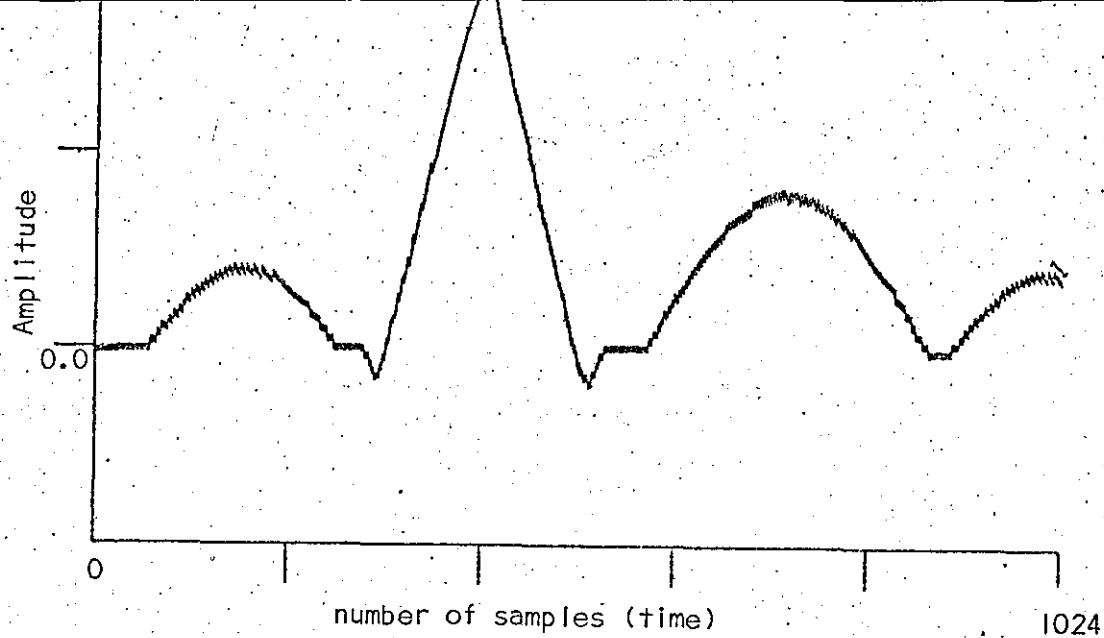


(a) Simulated ECG waveform

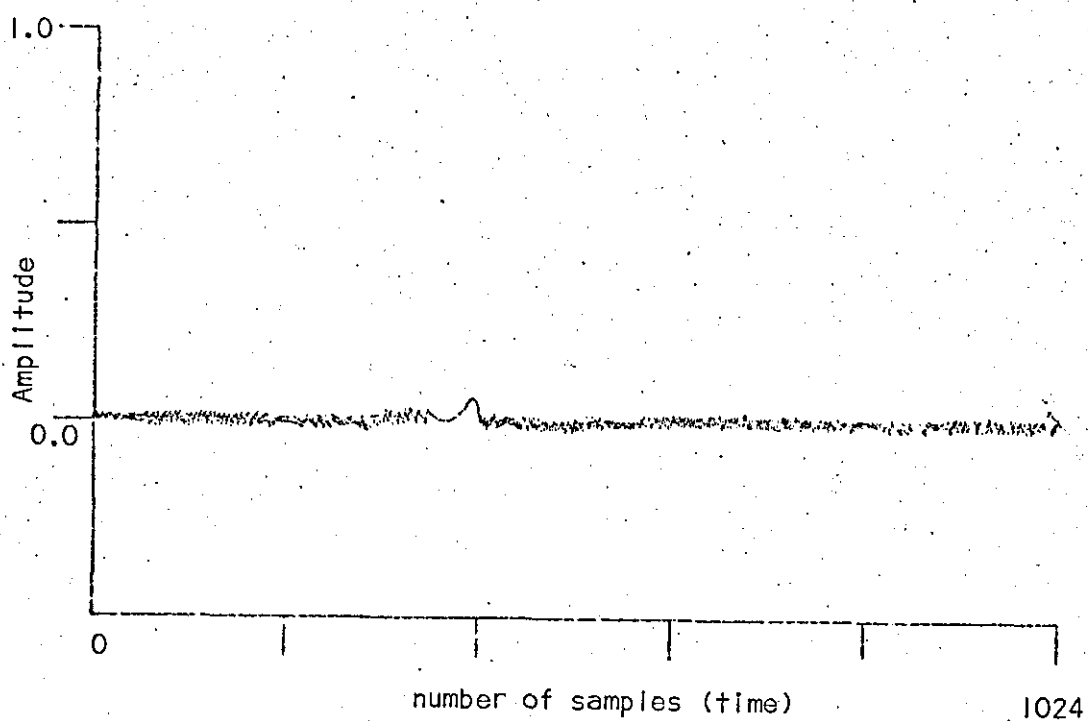


(b) Low pass band limited or filtered ECG waveform as an input to the delta modulator.

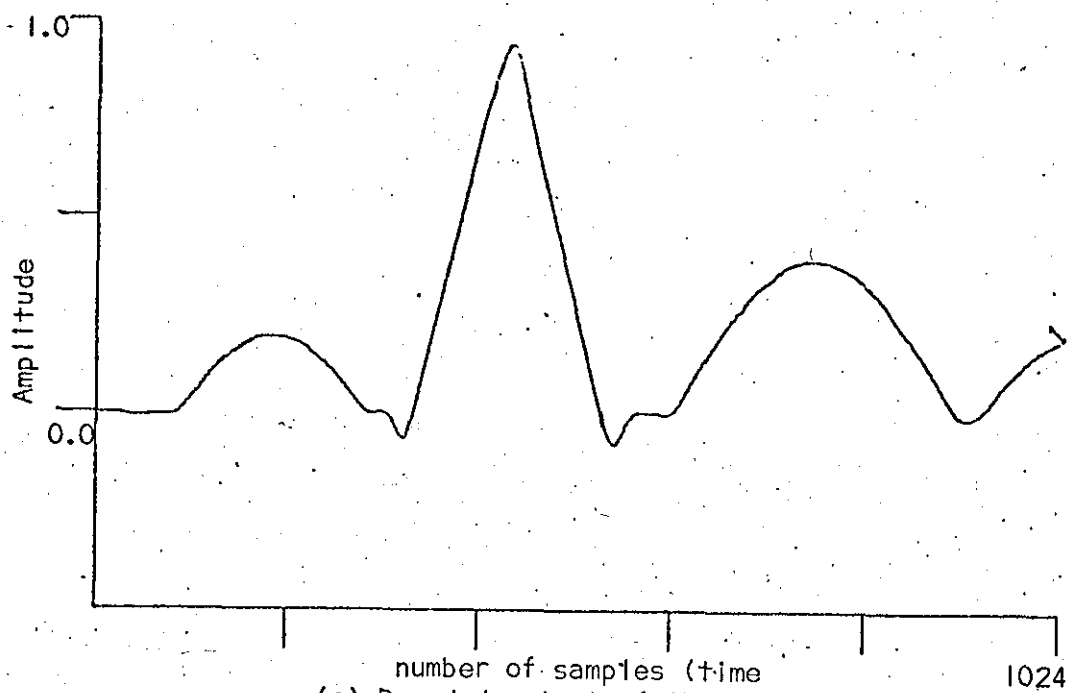
Figure 4.12



(a) Output of the local integrator with leakage $S = 0.985$



(b) Error waveform.



(c) Decoded output of the Delta modulator.

Figure 4.13.

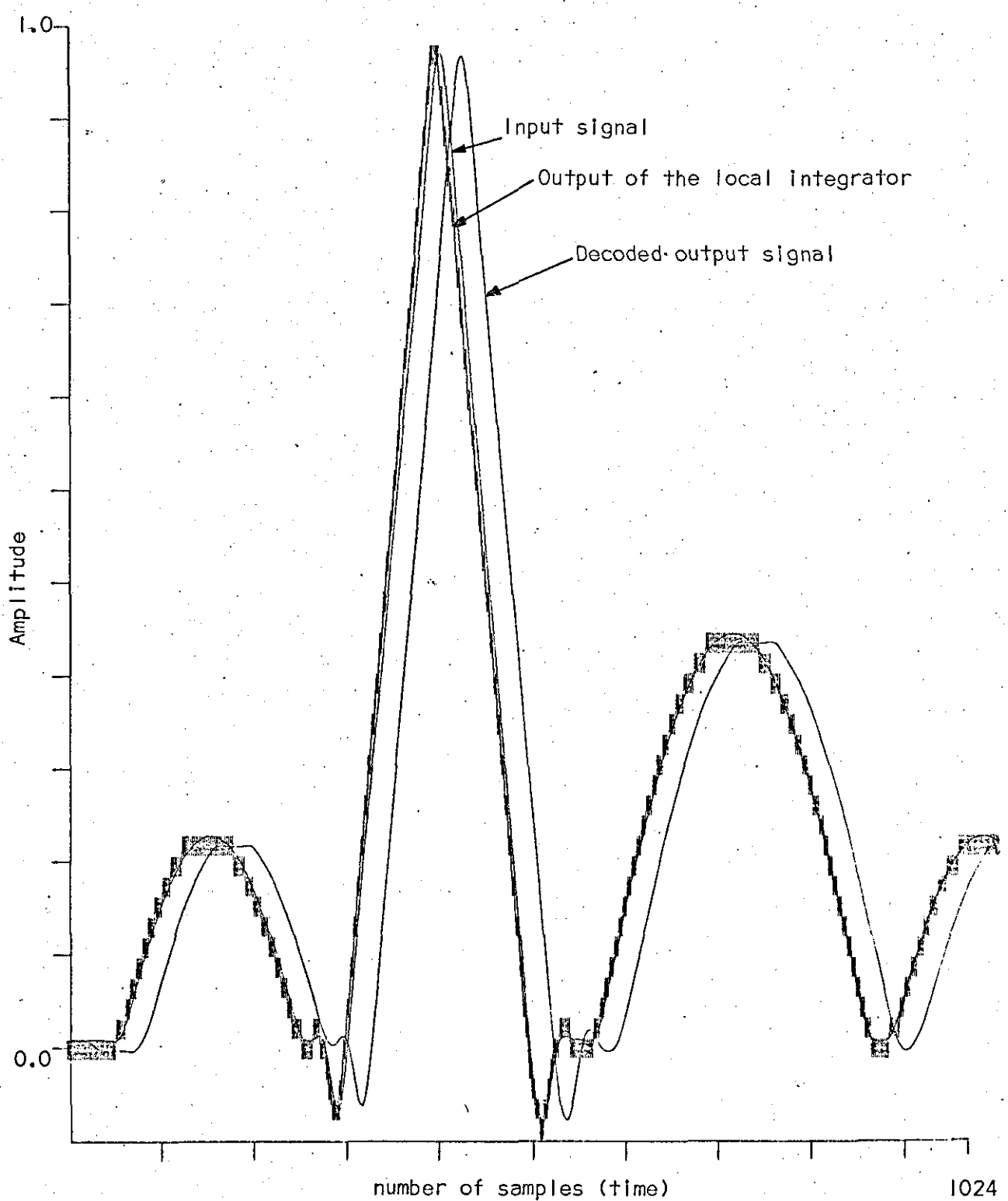
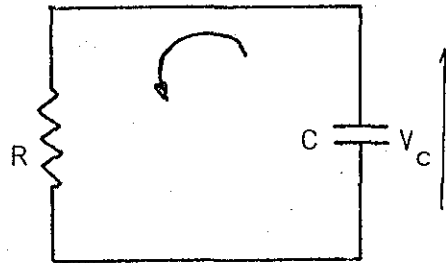
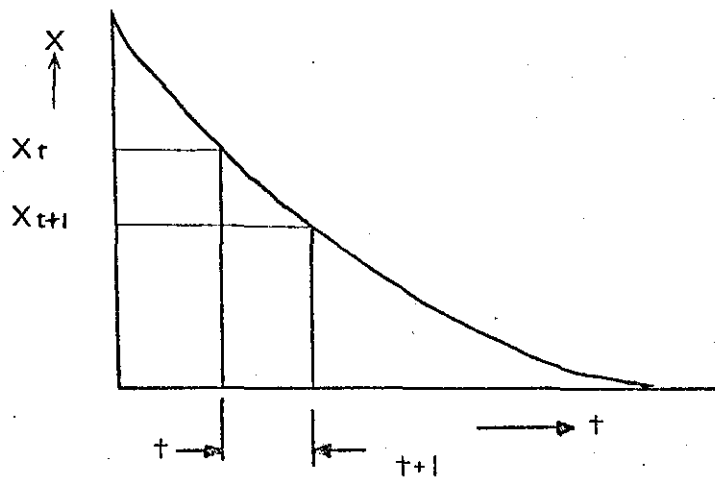


Figure 4.14 ECG waveform coded and decoded by the delta modulator with no leakage in the integrator.



(a) A Leaky Capacitor



(b) Discharge of a Capacitor

Figure 4.15

The current i in this circuit is given by

$$i = c \frac{dV_c}{dt}$$

V_c = voltage across the capacitor

As
$$i = \frac{V_c}{R}$$

Therefore

$$dV_c = \frac{dt}{CR} V_c$$

For discrete form, the discharge of a capacitor at two instants X_t and X_{t+1} in a time T is shown in figure 4.15. T is the time taken for one sample of the discrete simulated ECG waveform.

$$X_t - X_{t+1} = \frac{T}{CR} X_t$$

$$\frac{T}{CR} = 1 - \frac{X_{t+1}}{X_t} = \frac{X_t - X_{t+1}}{X_t}$$

$$CR = T \frac{X_t}{X_t - X_{t+1}}$$

For perfect integrator there is no leakage hence $X_t = X_{t+1}$.

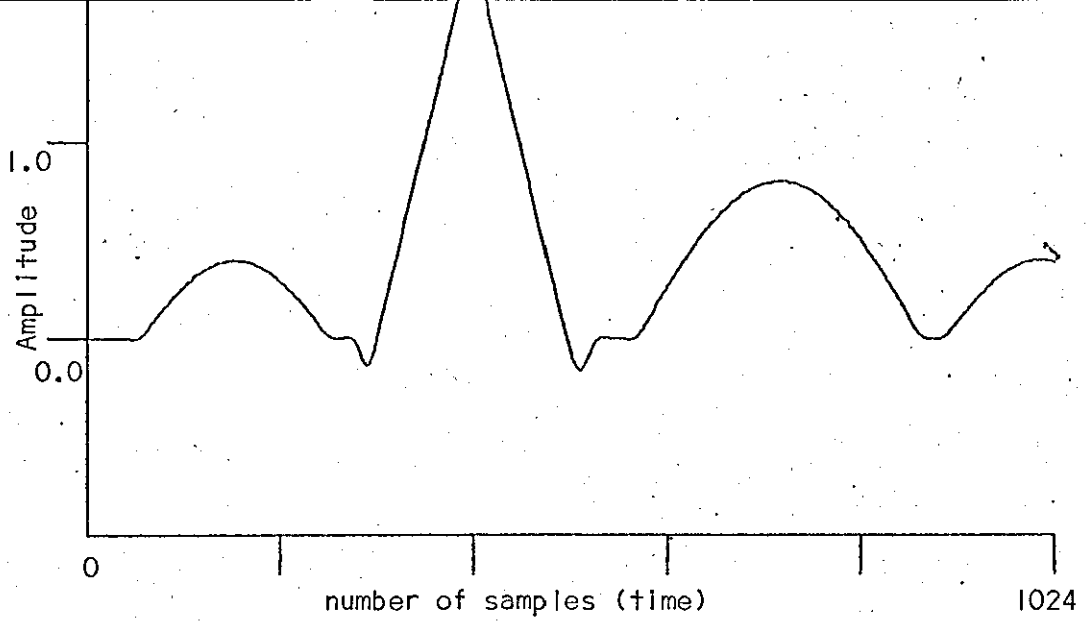
Therefore $CR = \infty$

for a leaky integrator if X_t is assumed to equal 1, X_{t+1} is not equal to 1, but is taken as the value of the chosen leakage.

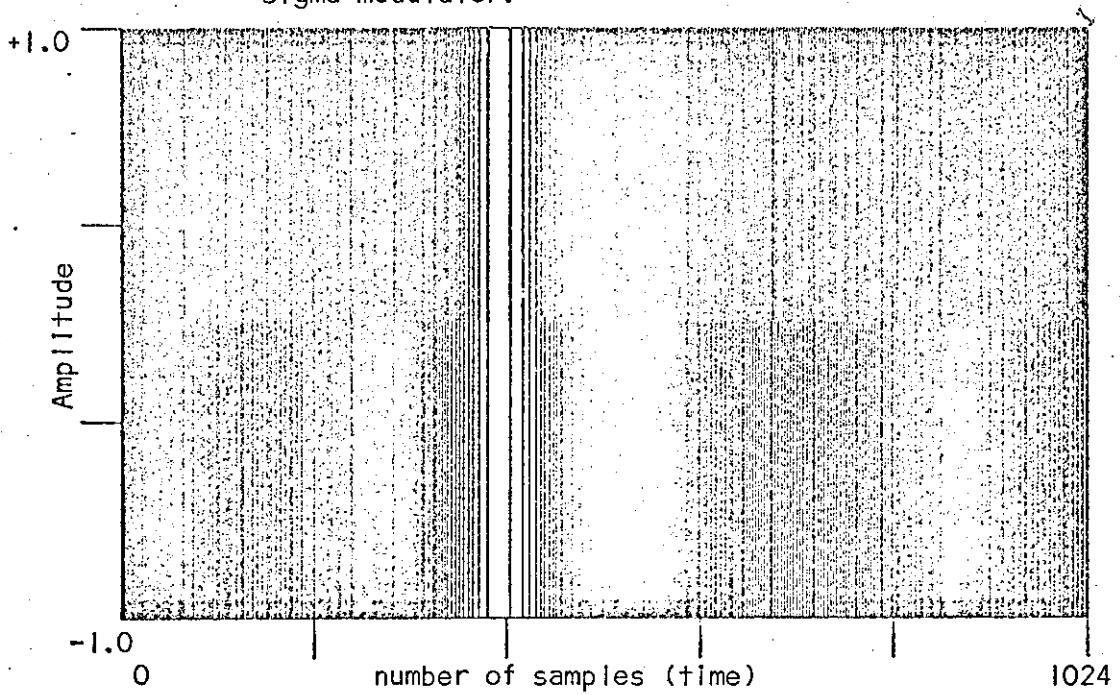
If the value of leakage is $S = 0.985$ as described in Section then

$$CR = \frac{800 \times 10^{-3}}{850} \frac{1}{1 - 0.985} = \frac{8}{8.5 \times 10^3} \frac{1}{.015}$$

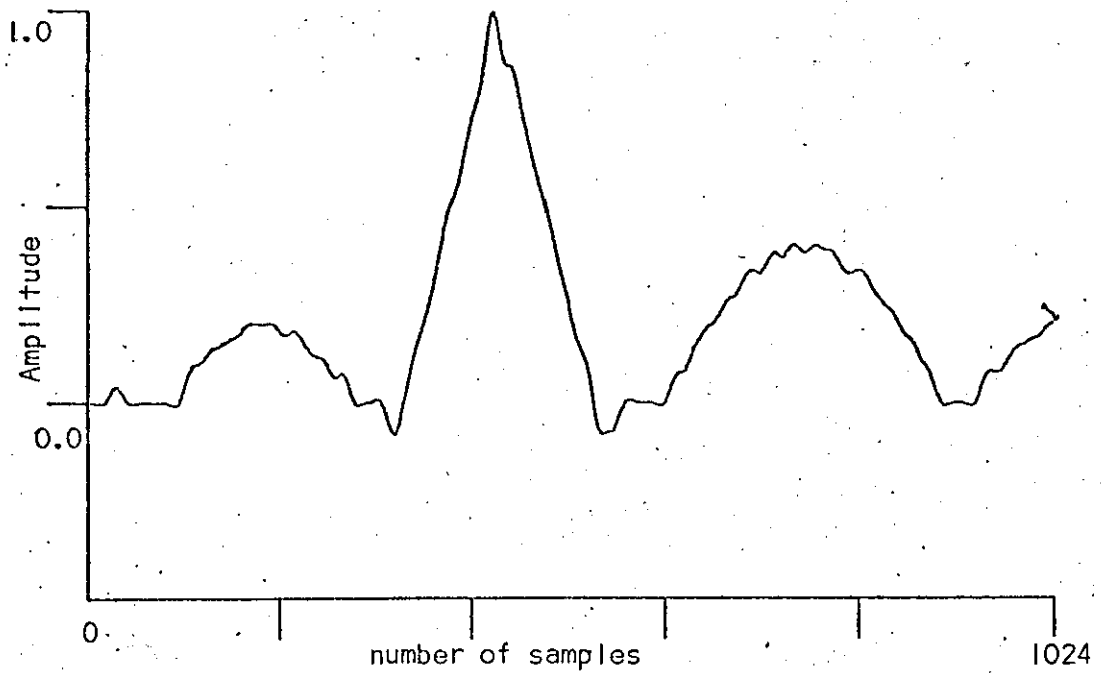
$$CR = 0.06 = T_c$$



(a) Filtered ECG waveform as an input to the delta sigma modulator.



(b) Digital output of the delta sigma modulator



(c) Decoded output of the delta sigma modulator with leakage

Figure 4:16.

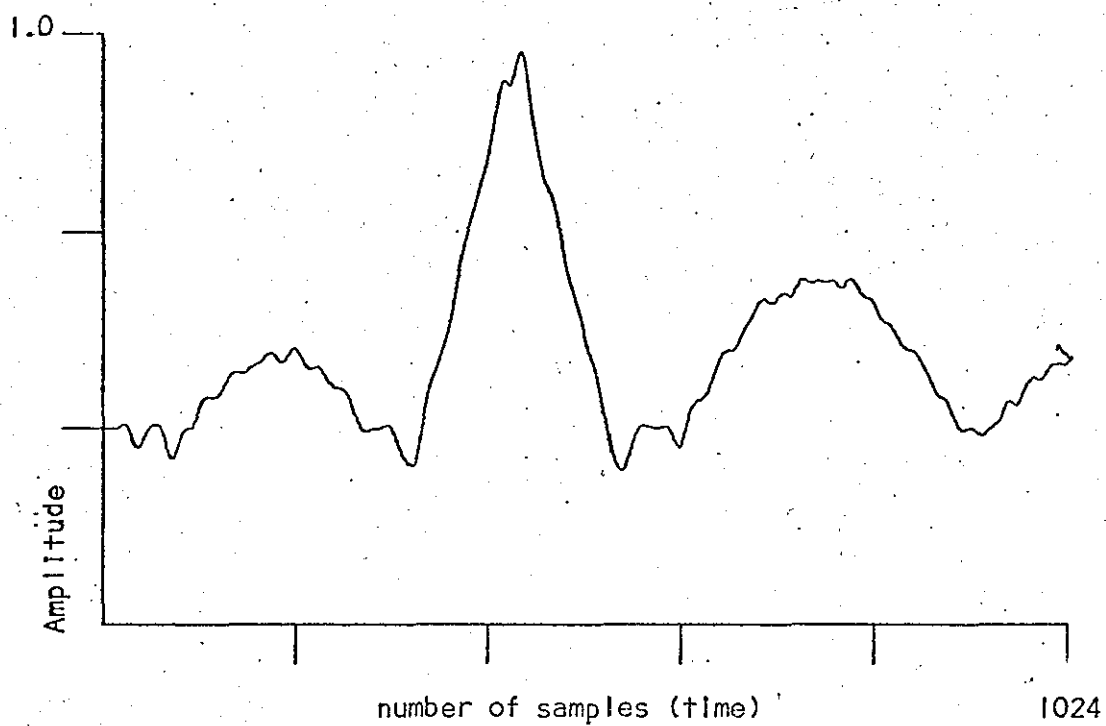
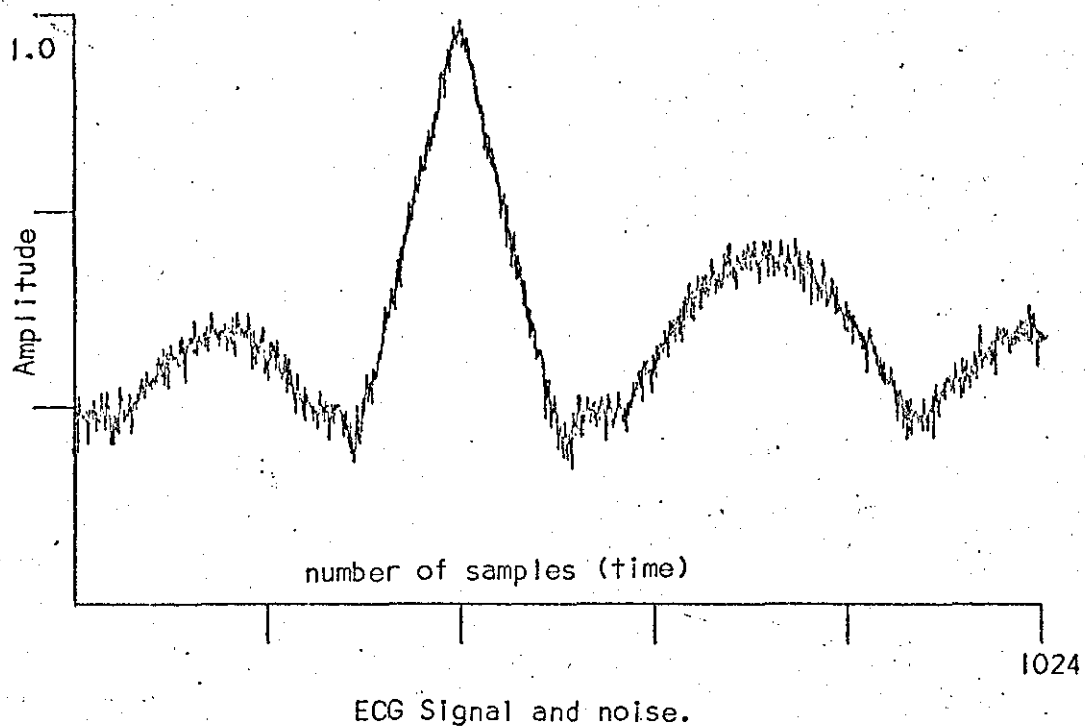


Figure 4.16(d) Decoded output of the delta-sigma modulator with noise.

An ECG waveform coded by a delta sigma modulator with a perfect integrator in the forward loop and decoded with a low pass filter showed transients at the start of the decoded waveform. This is shown in figure 4.9.

As a result a suitable value of leakage (as mentioned before) is required to minimise these transients. Various values of leakage were tried and an optimum value ($S = 0.985$) was reached which gave minimum transients in the decoded ECG waveform.

This is shown in figure 4.16.

4.3 Further Analysis

The above observations revealed that the ECG waveform encoded and decoded by the delta modulator showed no loss in any segment of the ECG waveform and it was free from any added noise or transients. This is shown in figures 4.13 and 4.14.

However, in the delta sigma modulator, despite choosing an optimum value of leakage for the integrator, the decoded ECG waveform showed transients at the start of the waveform. It further showed ripple-like noise at the slow varying edges of the P and T segment of the ECG waveform. This led to the further study of the process of coding and decoding of the ECG waveform. The study was undertaken by performing the following:

1. Observing the output pulse pattern for the ECG waveform as an input.
2. Observing the component of noise in the frequency domain.
3. Separating the noise components in the time domain.
4. Adding pseudo-random noise and observing its effect on the decoded output.

4.3.1 Pattern of Output Pulses

The output pulses of the delta sigma modulator (encoder) are termed as one as (+1) and zero (-1). Two ones or zeros appearing consecutively are termed as modulated pulses while one and zero appearing alternately are termed as unmodulated pulses or simply pulses.

The output pulse pattern of the P and T segments for the delta sigma modulator with the integrator having no leakage and for an optimum value of leakage ($S = 0.985$) is studied here.

P Segment

The P segment in the input ECG waveform has an amplitude of 0.2 as simulated in Section 4.1.2, having a shape of a half sine wave occupying 200 samples.

No Leakage ($S = 1$)

The output pulses for no leakage are shown in figure 4.17. A modulated pulse of two zeros corresponded to the start of the P segment and was followed by a modulated pulse of two ones. It was then followed by a modulated pulse of three zeros and a modulated pulse of two ones which appeared more frequently until it was repeated seven times separated by three unmodulated pulses.

The decoded P segment showed transients and ripple-like noise as mentioned before.

Leakage ($S = 0.985$)

In this case there appeared a long stream of unmodulated pulses before the occurrence of a modulated pulse of two ones. This modulated pulse recurred nine times, separated by three unmodulated pulses. This is shown in figure 4.18.



Figure 4.17 Pulse pattern of P segment with no leakage ($S = 1$)



Figure 4.18 Pulse pattern of P segment with leakage ($S=0.985$).

T Segment

The T segment had an amplitude of 0.4 with a shape of a half sine wave occupying 300 samples.

No Leakage

The pulse pattern is shown in figure 4.19.

The first modulated pulse of two ones appeared after 46 unmodulated pulses from the start of the T segment, followed by nine unmodulated pulses before the next modulated pulse of two ones. It was then followed by a modulated pulse of two ones which appeared more frequently until it repeated itself nine times separated by one unmodulated pulse. This pattern was followed by more modulated pulses of two ones and modulated pulses of three ones appearing occasionally. This was followed by the modulated pulse of two ones which repeated itself fifteen times, separated by one unmodulated pulse. The appearance of the remaining modulated pulses was less frequent with the decrease in the amplitude of the T segment.

Leakage $S = 0.985$

The pattern of the output pulse in this case was not very different. It is shown in figure 4.20.

QRS Complex A pulse pattern of QRS complex with and without leakage is shown in figure 4.21. There is no noise produced for this pattern.

Observations The following pulses form a certain pattern and this pattern repeats itself (periodic).

1. A periodic pulse pattern of two ones (two pulses) followed by three pulses (three pulses of alternate sign). This pulse pattern is situated corresponding to the slowly varying edges of the P segment near the peak. This is shown in figure 4.18.
2. A periodic pattern of two ones followed by one pulse corresponding to the slowly varying edge of the T segment. This is shown in figure 4.20.

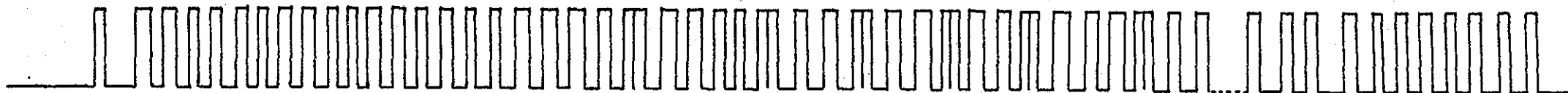
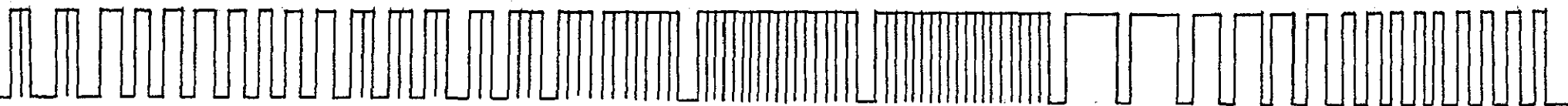


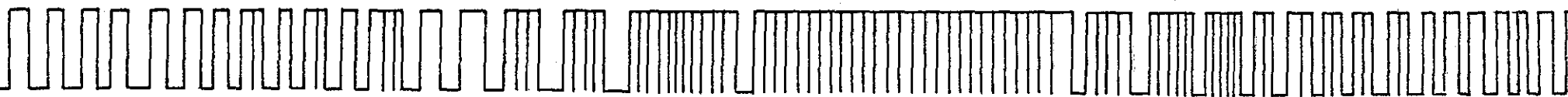
Figure 4.19 Pulse pattern of T segment with no leakage ($S = 1$)



Figure 4.20 Pulse pattern of T segment with leakage ($S = 0.985$)



(a) Pulse pattern of QRS complex with no leakage ($S = 1$)



(b) Pulse pattern of QRS complex with leakage ($S = 0.985$)

Figure 4.21

3. A periodic pattern of one and zero corresponding to the dc input: This pattern lasts as long as there is a dc input. The pulses when convolved with the impulse response of the filter give a decoded output.
4. Absence of zero modulated pulses in the case of leakage. It is observed from the decoded output that some components of noise appeared corresponding to the periodic pattern given above (1,2). Similarly there appeared some undershoots corresponding to the one and zero pattern of pulses for a dc input.

4.3.2 Frequency Domain Analysis

To establish the frequency contents of the noise appearing in the decoded output of the delta sigma modulator, a power spectrum of the output was taken. (Theory of spectrum analysis and DFT is given in Appendix F.). This is shown in figure 4.22. The power spectrum for the simulated input ECG waveform and decoded output signal from the delta modulator were also obtained as shown in figures 4.23, 4.24. It is observed from the power spectra that high frequency components are present in the decoded output of the delta sigma modulator compared with the other two cases. These components of high frequency are produced by the process of coding and subsequent decoding in the delta sigma modulation system.

4.3.3 Cepstral Analysis

Since the decoded output of the delta sigma modulator consists of a lower frequency decoded ECG signal and higher frequency noise, a technique is required in which the two are easily identifiable and

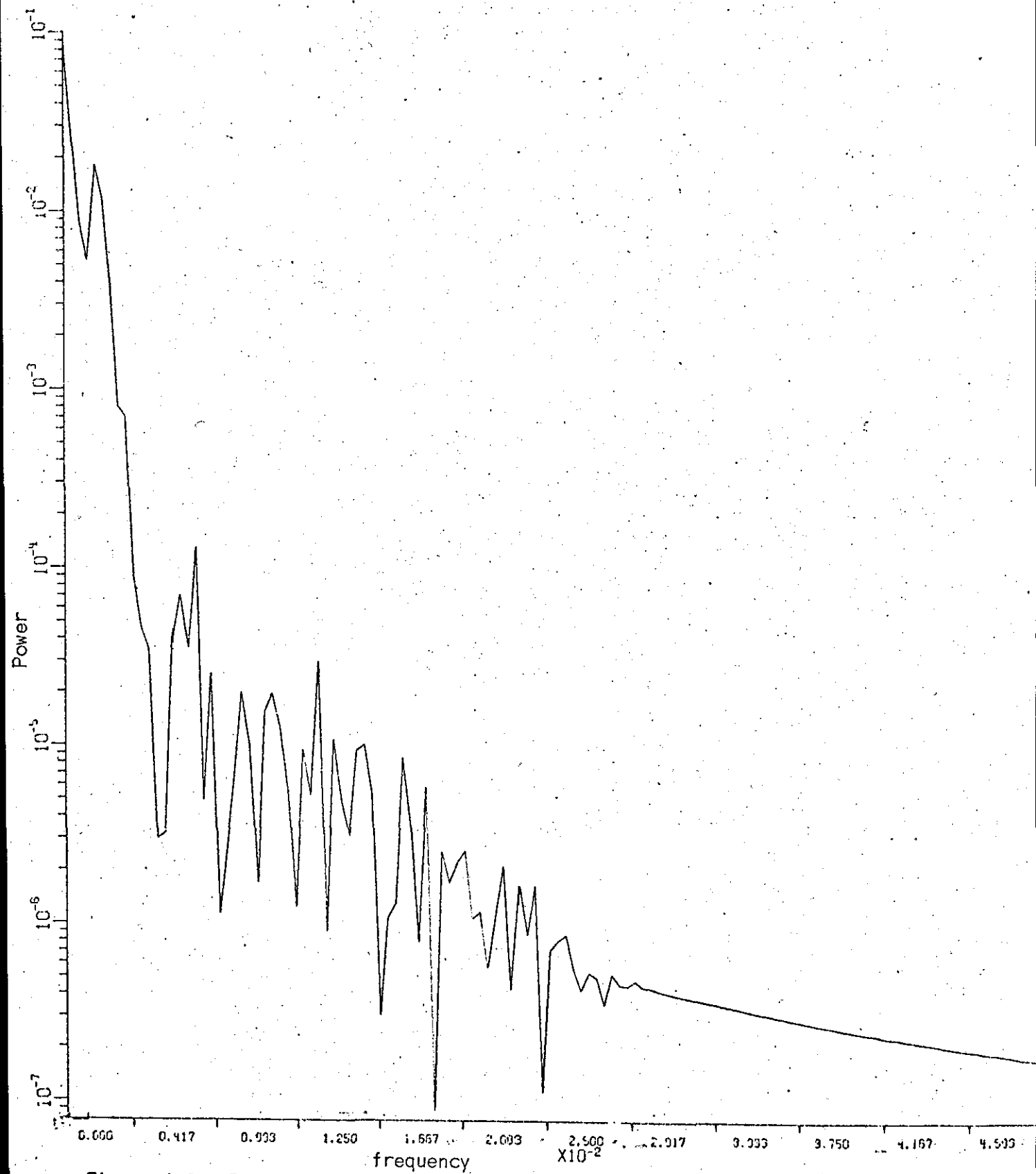


Figure 4.22 Power spectrum of the decoded ECG waveform from the delta sigma modulator (leakage $S = 0.985$)

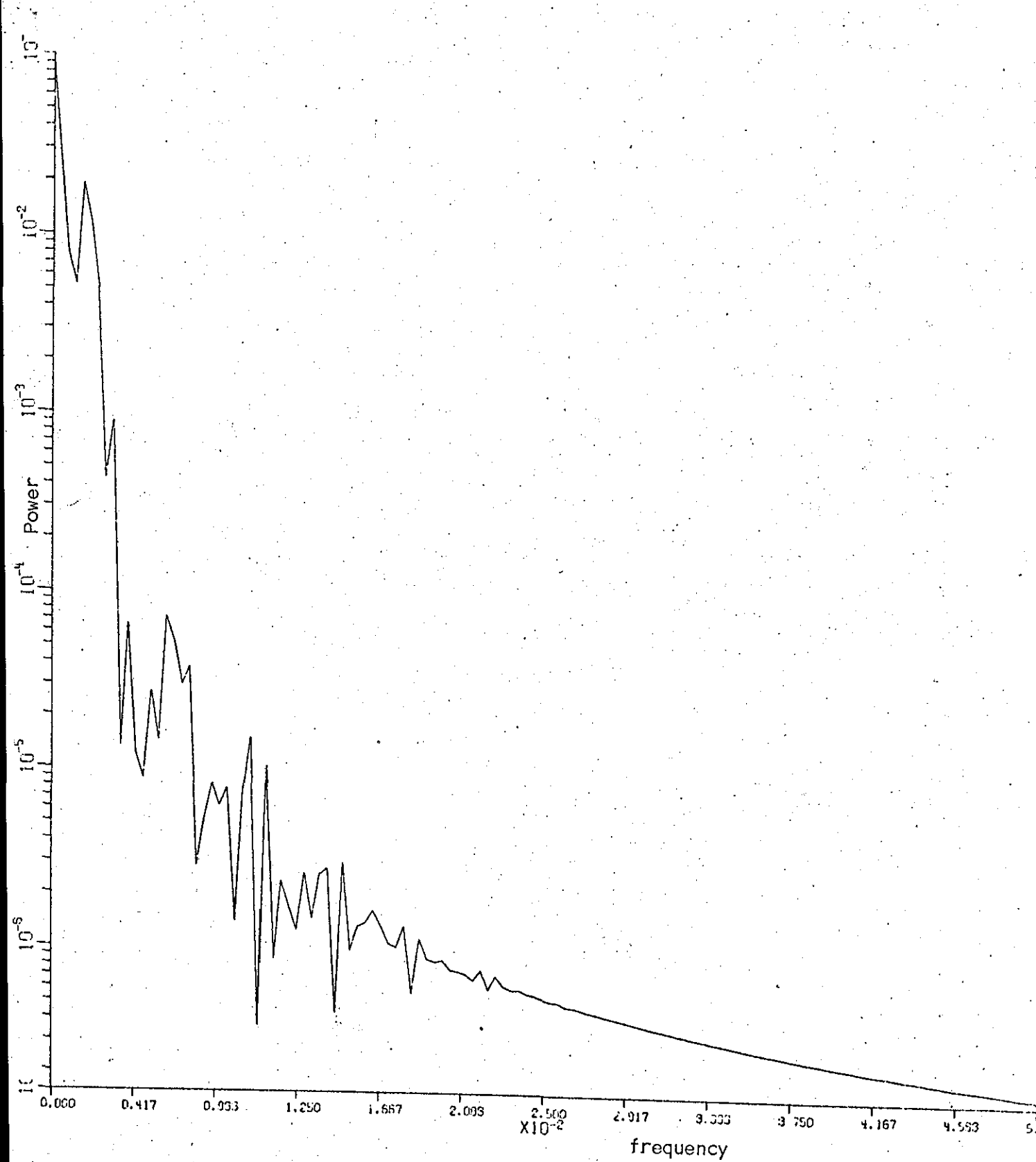


Figure 4.23. Power spectrum of the ECG waveform as an input signal

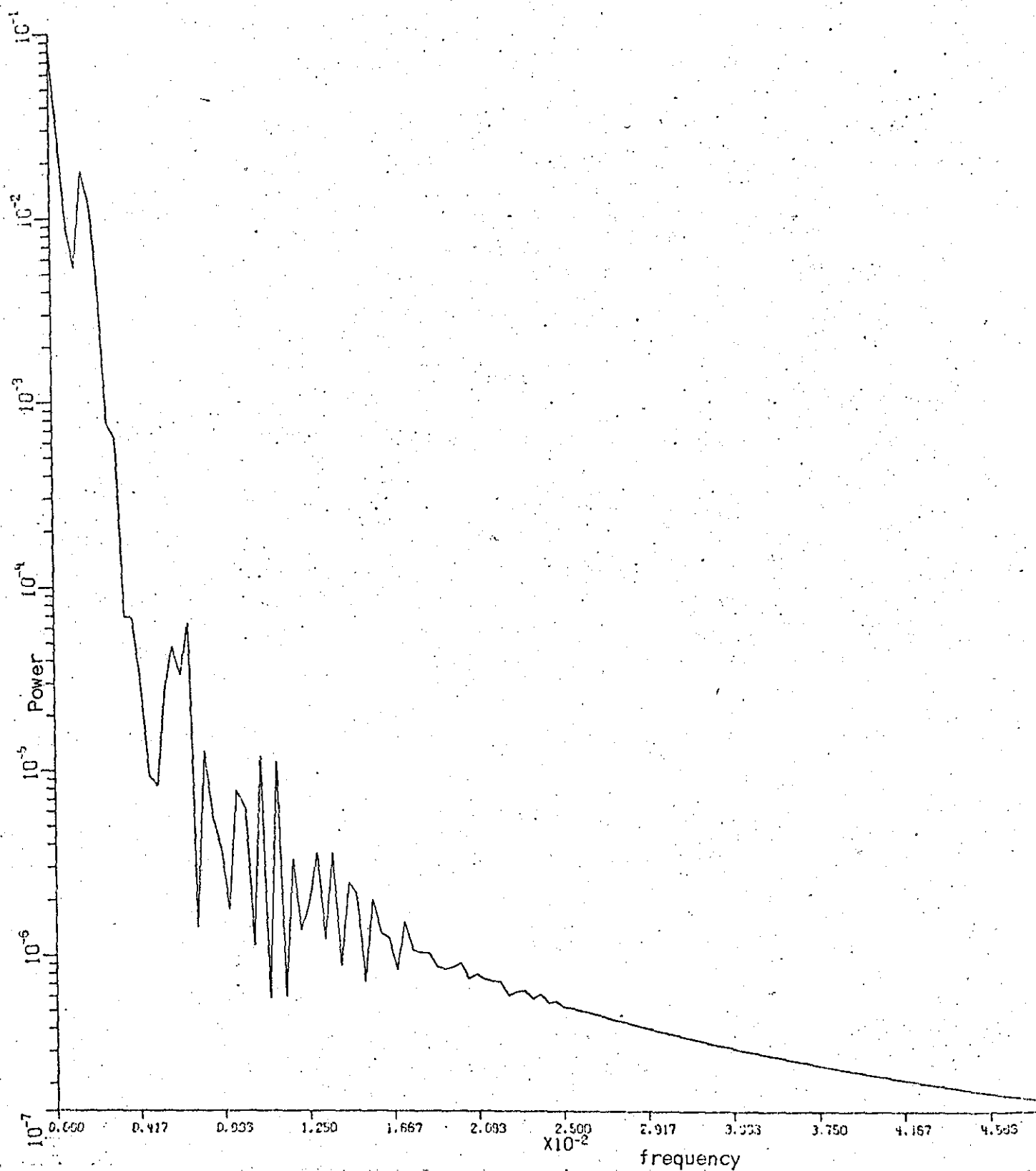


Figure 4.24 Power spectrum of the decoded output ECG waveform from the delta modulator (leakage $S=0.985$)

separated to obtain a better picture of the decoded waveform.

In the basic form the system for reproducing the output analogue signal consists of a delta sigma modulator as a coder giving digital pulses corresponding to the analogue input, and a low pass filter as a decoder. The digital sequence of pulses $l(t)$ contains some periodic pattern corresponding to the amplitude of the input signal. The function of the low pass filter as a decoder is specified completely by its impulse response $h(t)$, such that the decoded output ECG signal $o(t)$ in this case equals the convolution of $l(t)$ and $h(t)$ as shown in figure 4.25.

In the frequency domain if $L(\omega)$ is the spectrum of digital pulses and $H(\omega)$ is the spectrum of the low pass filter, then the spectrum of output ECG signal is the product of the two spectra.

$$O(t) = l(t) * h(t)$$

$$O(j\omega) = L(j\omega) \cdot H(j\omega)$$

$O(j\omega)$ is the fourier transform of $O(t)$, and $*$ denotes convolution.

The source of periodicity of high frequency noise is the periodic pattern of pulses present in the digital output, since the non-periodic changing pattern will give rise to a low frequency signal when decoded by the filter and is in the range of the peak formed by the resonant mode of the filter.

If the periodic pattern of the pulses is assumed constant, then the power spectrum of a quasi-periodic signal over a finite analysis is also periodic. The obvious way to observe this periodicity will be to take the fourier transform of the power spectrum, which will show a peak corresponding to the period of the power spectrum.



Figure 4.25 Basic Delta Sigma Modulator System

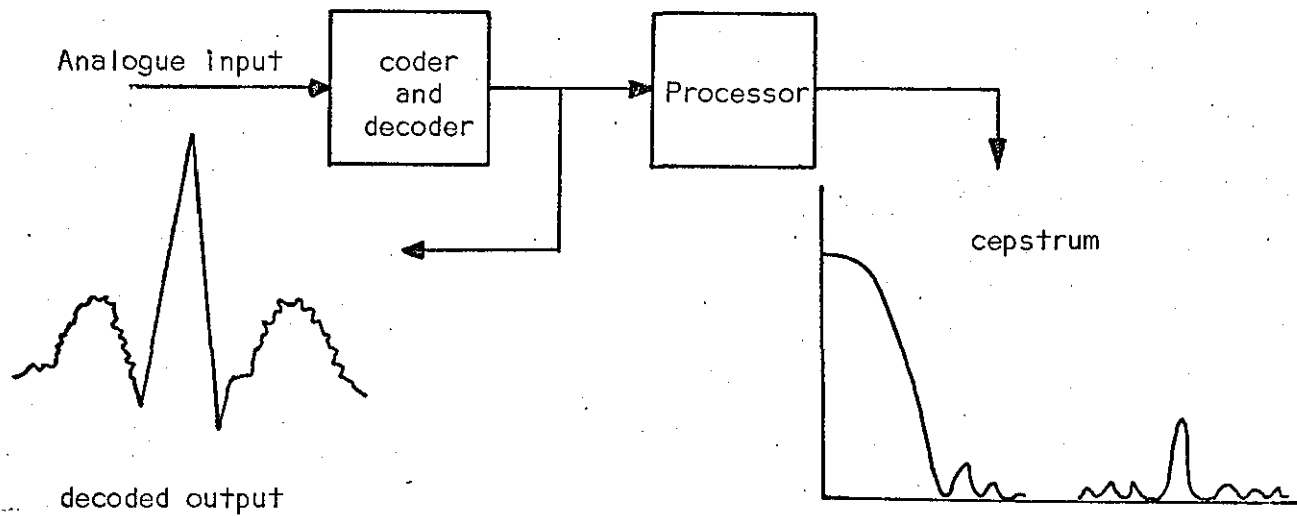


Figure 4.26 Cepstral Analysis of the decoded output

The fourier transform of the power spectrum is known as the autocorrelation function of the original time signal.

The power spectrum of the decoded output ECG signal is the product

$$|O(j\omega)|^2 = |L(j\omega)|^2 \cdot |H(j\omega)|^2$$

The fourier transform of a product is equal to the convolution of the fourier transforms of the two multiplicands. Thus for the convolution of the product of many signals, the transfer function $H(j\omega)$ is such that the resulting convolution gives broad peaks and, in some cases, multiple peaks. Hence the convolution becomes, in effect, a confusion.

However, Bogert et al⁷⁸ suggested that if the logarithm of the power spectrum is taken, the two spectra become additive. Hence, taking the log of the above equation :

$$\begin{aligned} \text{Log } |O(j\omega)|^2 &= \text{Log}\{|L(j\omega)|^2 \cdot |H(j\omega)|^2\} \\ &= \text{Log } |L(j\omega)|^2 + \text{Log } |H(j\omega)|^2 \end{aligned}$$

The log spectrum⁽⁷⁹⁾ of the output digital pulses containing the periodic pattern manifests itself as a high frequency ripple in this spectrum, while the effect of the filter and the non-periodic pattern (ECG waveform) is to produce a low frequency signal.

If the fourier transform or the power spectrum of the log spectrum is taken, it preserves the additive property and makes the effect of the two frequencies more obvious and easily distinguishable. The power spectrum of the log spectrum is called CEPSTRUM. It is shown in figure 4.26 and Appendix G.

Therefore, the spectrum of log spectrum has a sharp peak corresponding to the high frequency ripples in the log spectrum and a broader peak corresponding to the low frequency information in the log spectrum. A cepstrum of the decoded ECG waveform from the delta sigma modulator is shown in figure 4.27.

To prevent confusion between the usual frequency components of a time function and the frequency ripples in the log spectrum, a paraphrase word has been used⁽⁷⁹⁾ called Quefrequency to describe the frequency of spectral ripples. It has the units of cycles per hertz or simply seconds. Likewise the period of spectral ripples is called the Reperiod. Hence adopting this terminology the cepstrum consists of peaks occurring at high frequencies equal to the pitch period in seconds and low frequency information corresponding to the format structure in the log spectrum. Hence this information can be detected and measured.

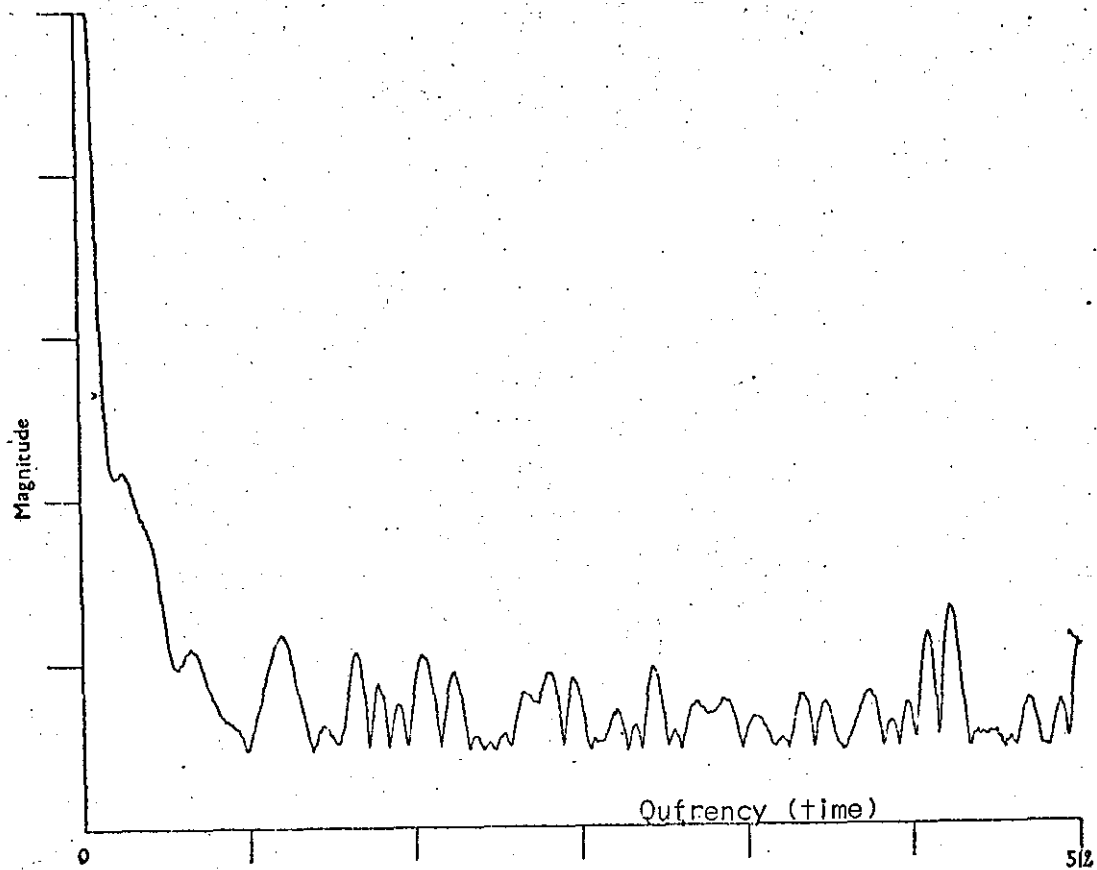
The cepstral analysis for the decoded ECG waveform from the delta modulator and the input ECG waveform were also obtained. These are shown in figures 4.28 and 4.29.

In the case of the cepstrum of the decoded ECG waveform from the delta sigma modulator, there appeared additional components of different periodicity than obtained in the cepstrum of the output ECG waveform from the delta modulator and input ECG waveform.

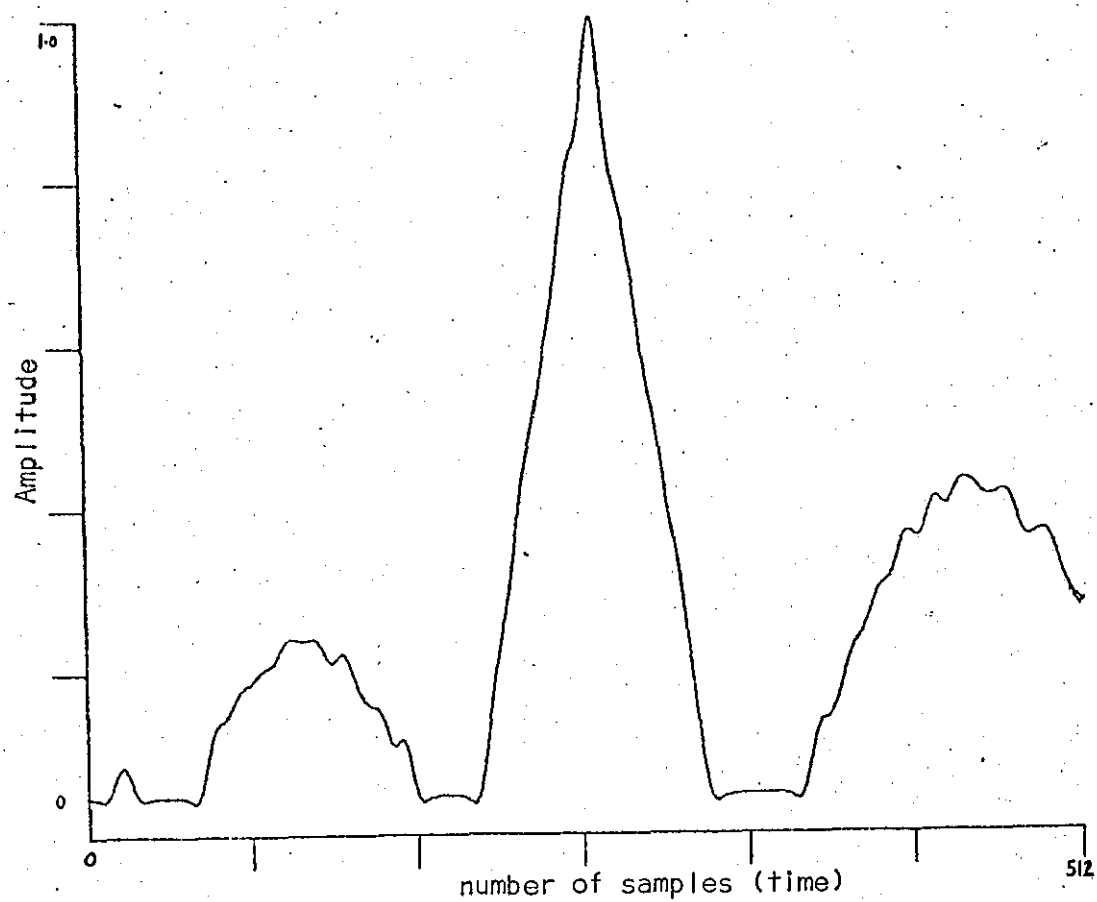
It is concluded from this comparison, therefore, that the decoded output from the delta sigma modulator contains noise which is separated in time domain.

4.4. Addition of Random Noise

Since there exists a periodic pattern in the output pulses of a delta sigma modulator for an ECG Waveform as the input, a noise is added to the input to get a non-periodic pattern of the output pulses.

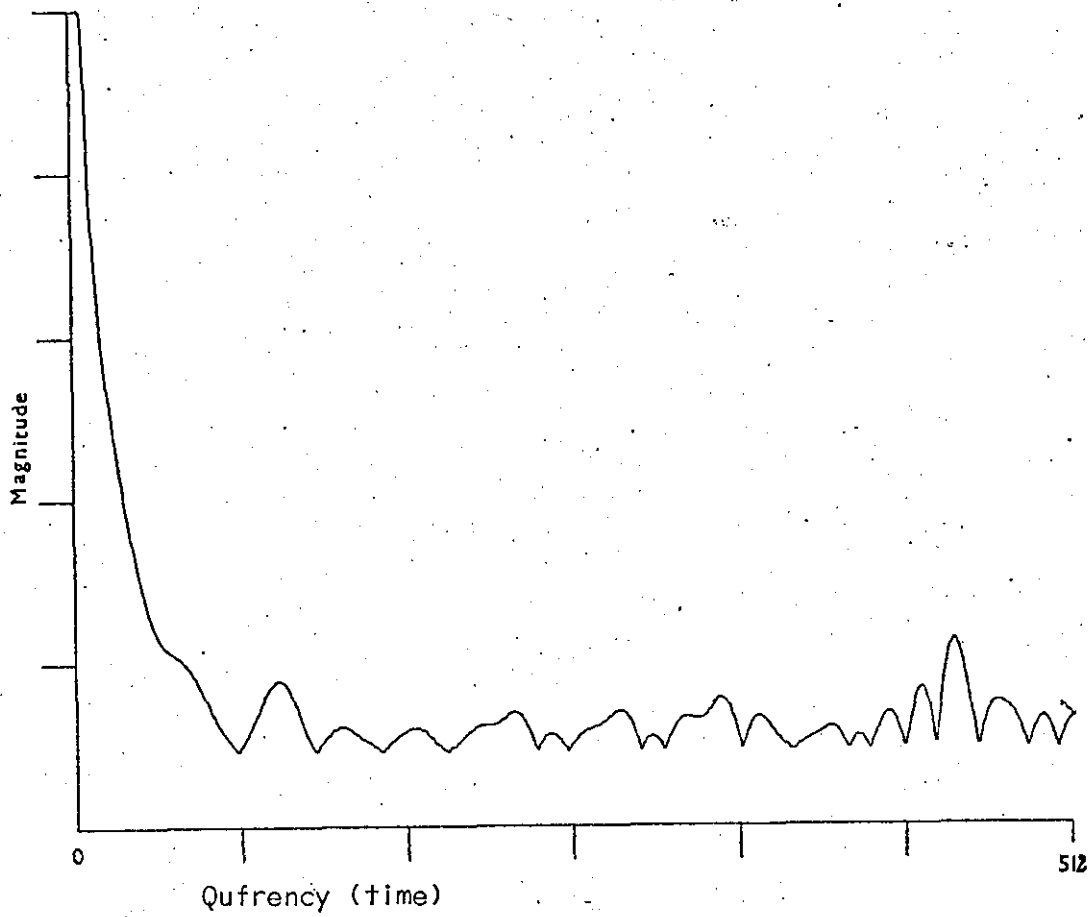


(a) Cepstrum of the decoded ECG waveform from the delta sigma modulator (leakage $S=0.985$)

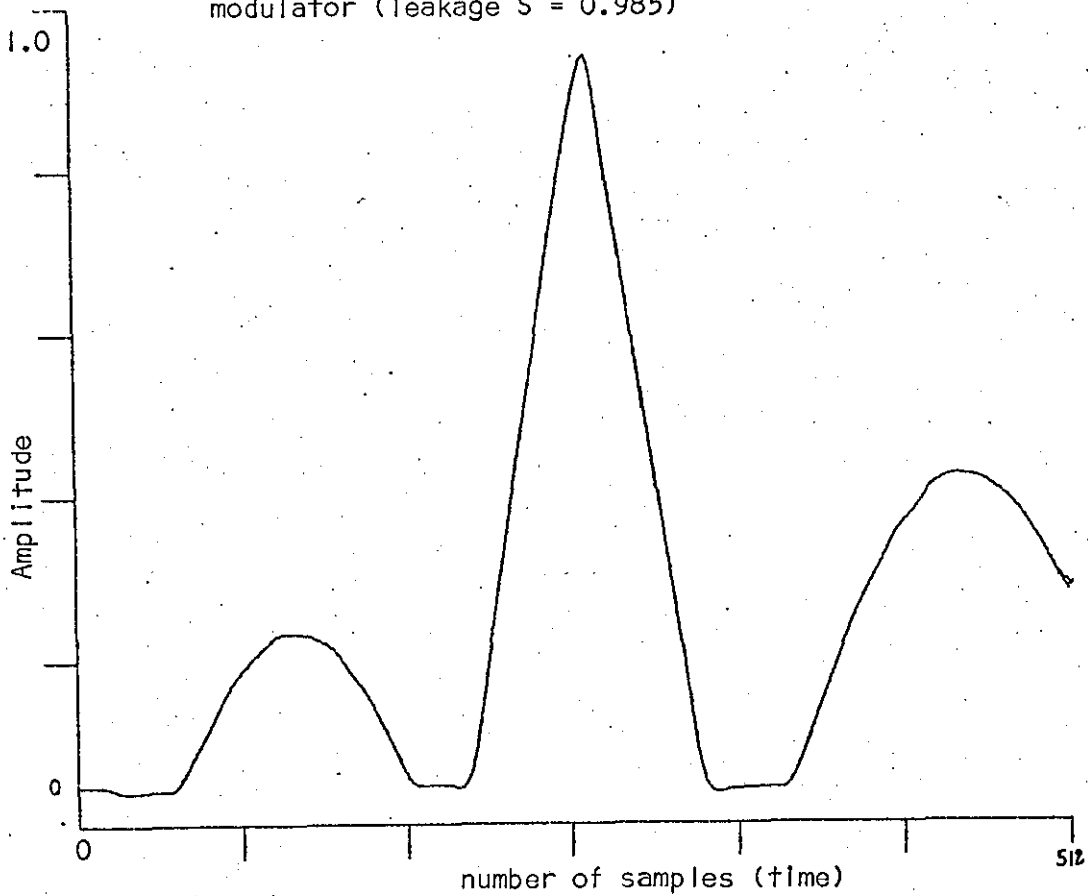


(b) Decoded ECG waveform from the delta sigma modulator

Figure 4.27

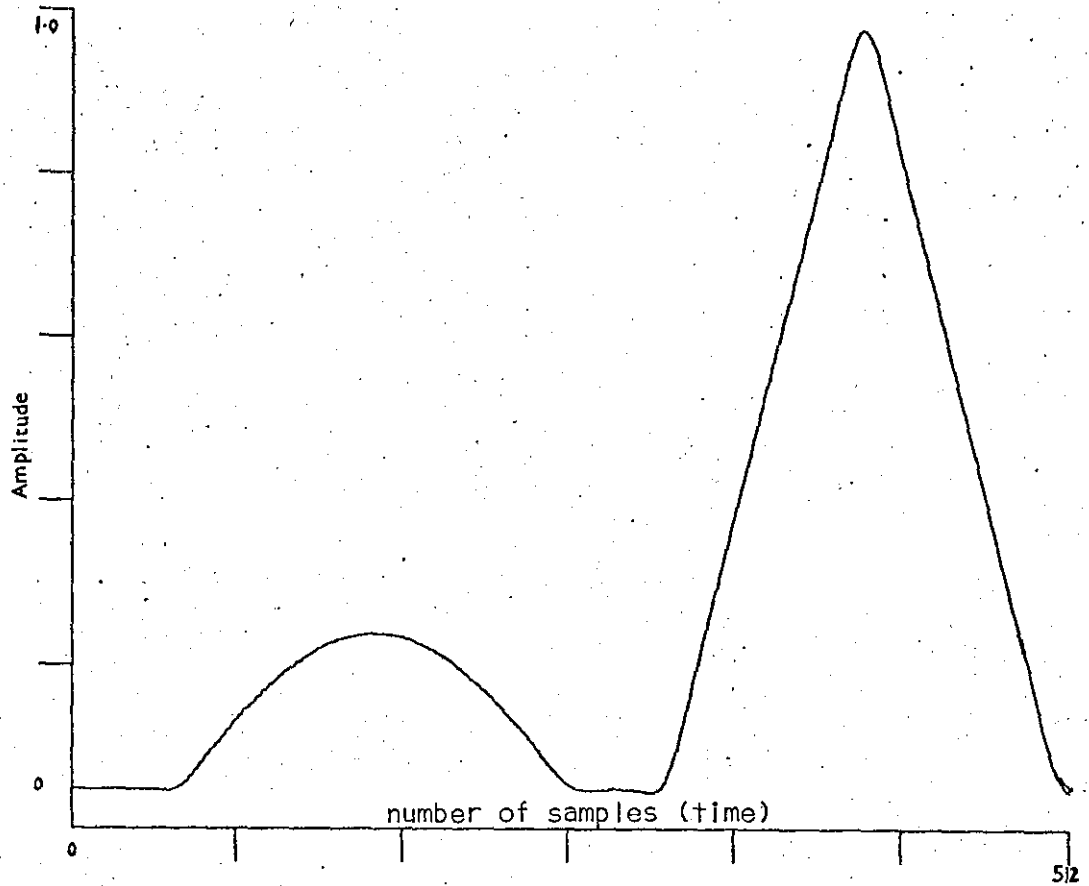


(a) Cepstrum of the decoded ECG waveform from the delta modulator (leakage $S = 0.985$)

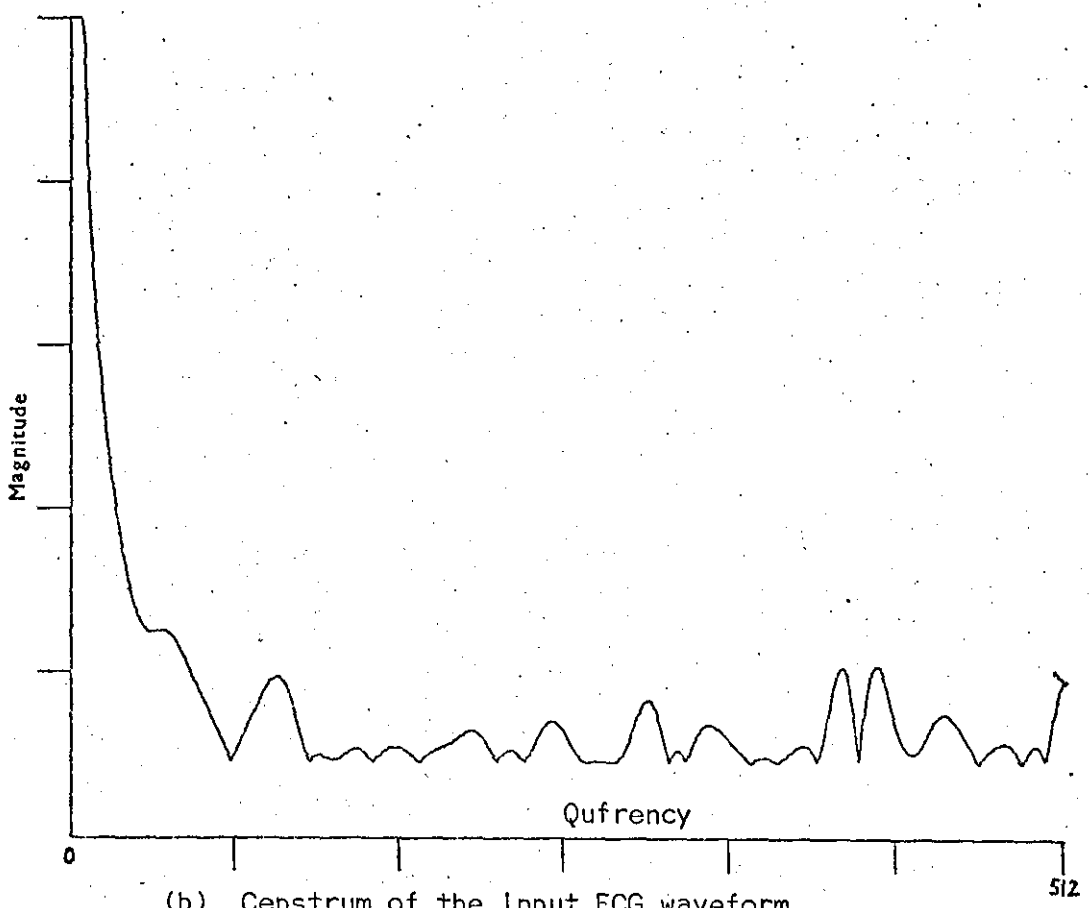


(b) Decoded ECG waveform from the delta modulator

Figure 4.28



(a) ECG waveform as an input signal (only half samples are shown)



(b) Cepstrum of the Input ECG waveform

Figure 4.29

When these non-periodic pulses are decoded, the resulting signal is markedly different from that in the previous case. This is shown in figure 4.16(d).

4.5 Discussion

The above study and analysis showed a certain pattern of pulses in the digital output of the delta sigma modulator. The spectral analyses showed that the decoded output waveform of the delta sigma modulator contained higher frequency components than the decoded output of the delta modulator and the input ECG waveform. The presence of these components were also confirmed in the time domain by the cepstral analysis. The presence of higher frequency components (noise) was due to the following features of the delta sigma modulator.

4.5.1 Nature of delta sigma modulator.

In the delta sigma modulator the additional RC circuit (integrator) at the coder attenuates the higher frequencies relative to the lower frequencies in the input signal. By removing the RC circuit (Integrator) in the decoder, higher frequencies are relatively enhanced. The presence of higher frequencies in the decoded output are shown in figure 4.22 by spectrum analysis. Also the quantization noise in the delta sigma modulator which is described in Chapter 3 and is given by

$$N_q^2 = \frac{4\pi^2 V^2}{9} \left(\frac{f_o}{f_s}\right)^3$$

N_q increases by 9 db/octave with increase in the bandwidth of the filter in the decoder. The quantization noise at the decoded output rises towards the top of the signal band. The coding threshold rises with increase in signal frequency.

The low pass filter simulated to decode the signal is not an ideal filter because an ideal filter cannot be implemented in practice. As a result, some of the higher frequency components produced in the process of coding, and part of the quantization noise, passes through to the resultant decoded waveform. A decrease in the cut-off

frequency of the filter reduces the high frequency components considerably, as shown in figure 4.9 compared to figure 4.8.

4.5.2 Filtering Action (Decoding)

In delta sigma modulation the output pulses carry the information corresponding to the amplitude of the input signal. If the amplitude of the input signal remains constant the output pulse pattern is a sequence of pulses of alternate sign. An increase in the input amplitude of the signal causes an increase in the rate of one pulses and a decrease of zero pulses. The reverse is the case by decreasing the amplitude of the signal. However, if the input signal consists of a constant amplitude or a slow varying signal, the output pulses are repeated in a certain pattern, followed by or preceded by different pulse patterns, depending on the input signal. On decoding, the filter treats the change from the repeated pattern to other pulses or vice versa as a transition or discontinuity and cannot respond quickly to the change. As the filter tries to overcompensate the change, it results in overshooting or undershooting, and ringing is produced.

The appearance of large transients in the beginning of the decoded output from a delta sigma modulator with a perfect integrator is observed, which reduces by putting a suitable leakage in the integrator.

There were some early pulses (one and zero) obtained with an integrator having no leakage, while with a leakage the first one is produced after some pulses. It is concluded, on the basis of this study, that the inherently higher frequency noise produced in delta sigma modulation appears at the decoded output. This is because the decoder (ideal filter) is more critical and difficult to design in practice. Hence for waveform preservation applications the delta modulator is simpler and better than the delta sigma modulator. The time-variant study of the delta modulator is given in the next section.

4.6 Time-Variant Delta Modulator

During the long time monitoring the ECG waveform may change (as mentioned earlier) due to the state of the heart and may also be accompanied by noise and interference. Some noise and interference may also be present due to power supply variations, component ageing and asymmetry of the quantizer in the coder. This makes delta modulation a time variant system. A biomedical telemetry system based on the delta modulator with the local integrator having a fixed constant step voltage is investigated here under conditions mentioned above. Histograms were used to study the time-variant effects of the delta modulator.

4.6.1 Methods of Investigation

Although the presence of noise and interference makes a system time-variant, large numbers of recordings for noise are taken to make an ensemble, and samples of the ensemble taken at a certain fixed time results in the same probability density function as that from samples taken at any other time⁽⁸⁰⁾. This sort of process is referred to as stationary and its statistics are time-invariant.

Although the noise is assumed random so that it cannot specify in advance particular voltage values as a function of time, it is assumed that the noise statistics are known. In particular it is assumed that the noise is zero-mean gaussian. It has a gaussian probability density function. If the noise is sampled at any arbitrary time $v(t_1)$ the probability that the measured sample $n(t_1)$ will fall in the range n to $n + dn$ is given by

$$f_n = \frac{e^{-n^2/2\sigma^2}}{\sqrt{2\pi\sigma^2}}$$

This is a statistical model for additive noise and a valid representation for actual noise present.

σ^2 , noise variance, a statistical constant can either be found out on the long time constant true meter or measured digitally.

The following digital technique can be used to measure σ^2 using the digital computer.

Now instead of estimating the probability of noise (error) over a single sample to lie in a certain amplitude, it was estimated over an ensemble or over one cycle of an ECG signal at one particular time. To make it more meaningful, an average over one cycle was taken which contained 851 samples and which was squared to obtain the mean square value of error (MSVE). This procedure was repeated over the other ECG signals constituting the long stream of signals taken for investigation. There are one hundred ECG cycles in the long stream of signals taken, each accompanying different patterns of noise having the same fixed variance. The number of ECG cycles taken and the time involved for computations was limited on the computer.

Having found the mean square values of error (MSVE) for each cycle of ECG waveform which were different, they were arranged to form a Histogram. Whatever variance of noise was added, the histogram of the Mean Square value of noise for the input noisy signal was obtained before it entered the delta modulator as the coder. This was obtained by subtracting the input signal from the noisy signal for each sample and squaring the mean over one cycle of ECG waveform. The histogram was obtained by arranging the number of times the MSVE occurred at a certain amplitude for different noisy waveforms. Similarly a histogram of MSVE for the decoded output signal for α

noisy input was obtained. To observe the action of a delta modulator as a coder the following different inputs were used:

- (a) A band-limited noise (Gaussian) (having $\sigma = 0.015$) smaller than the step voltage of the local integrator of the delta modulator.
- (b) A bandlimited Gaussian noise (having variance $\sigma = 0.05$) bigger than the step voltage of the local integrator of the delta modulator.
- (c) (a) and (b) above were repeated for the un-bandlimited Gaussian noise.

4.6.2 Nature of the Delta Modulator Noise

A delta modulator with a single integrator transforms a continuous input signal $h(t)$ to the binary sequences $a_{-1}, a_0, a_2, \dots, a_n$ where a_n may have the value $+1$ or -1 . The modulator generates binary symbols at T_s intervals according to sign of $e(t)$, the error signal. The error is the difference of $b(t)$ and $x(t)$, the integrated delta modulator signal generated in the modulator feedback loop. The term $x(t)$ is the integral of the binary pulses weighted by step size d . Thus $x(t)$ has a step $+d$ or $-d$ at each sampling instant and is otherwise constant.

At the delta modulator receiver, the integrated signal is recovered by a replica of the modulator feedback loop and analogue signal $b'(t)$ is generated by means of a low pass filter. The signal $b'(t)$ is an approximation of the system input.

The two important parameters of a delta modulator are the sampling interval (clock rate) T_s , and d , the step size.

The quantization noise decreases with increasing sampling rate $f_s = \frac{1}{T_s}$, while for a fixed rate the value of the step size determines the mixture of quantization noise and slope overload noise in the quantizing noise signal $b(t) - b'(t)$. In a practical system step size d is selected to provide a proper balance between quantisation noise⁽⁸¹⁾⁽⁸²⁾ (the predominant form for high values of d) and slope overload noise (the predominant form for low values of d).

In order to avoid overloading in a system the value of ' d ' is set so that $\frac{d}{T_s}$, the maximum average slope of integrated signal $x(t)$ is exceeded by the slope of input signal $b(t)$ with very low probability.

To do this Van de Weg⁽⁸³⁾ established the condition that $\frac{d}{T_s}$ is four times the root mean square slope of $b(t)$. For gaussian signals, the probability that the slope of $b(t)$ is greater than $\frac{d}{T_s}$ is less than 4×10^{-5} . If the rms slope of $b(t)$ is $2\pi s f_b$, then the condition that the maximum average slope of $x(t)$ is equal four times the rms slope of $b(t)$ may be expressed as

$$\frac{d}{T_s} = 8\pi s f_b \quad \text{where } f_b \text{ is the highest frequency in } b(t) \\ s \text{ is root mean square value of } b(t)$$

4.7 Experimental Arrangement for Simulation

In order to produce a stream of signals accompanied by noise on the computer, an ECG waveform of one cycle was generated in the computer and was mixed with noise of a certain variance. This process was repeated and noise was added from a pseudo random generator composed of shift registers. It was arranged in such a way that every time the noise generator was used, the distribution of random numbers

(which make the noise) was different, although the variance was the same. Hence the effect of a continuous long signal with varied noise in practice was obtained. This is shown in figure 4.30.

The signal with added noise can be filtered, and the filter used is the same as used in the decoder.

To obtain the mean square value of error, the difference between the decoded output for a noisy input and the input without noise was taken for each sample, comprising of one ECG signal at a time. This was added over one cycle, squared, and the mean was taken as follows:

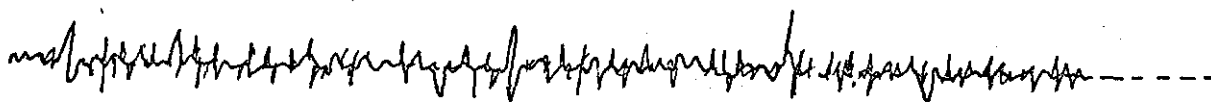
$$\begin{aligned} & \sum_{i=1}^{\text{No. of samples}} \frac{(\text{Output decoded signal} - \text{Input signal without noise})^2}{\text{Total samples in one cycle of ECG}} \\ &= \frac{1}{851} \sum_{i=1}^{851} \{Y(i) - X(i)\}^2 \end{aligned}$$

4.7.1 Noise Generator

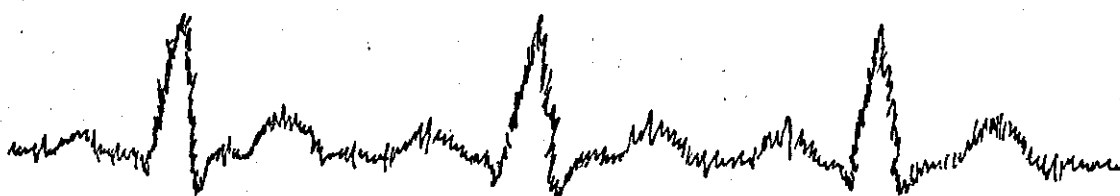
It is a pseudo random generator built in the computer composed of shift registers. The distribution of random numbers (noise) can be arranged in uniform or Gaussian fashion. As assumed earlier the noise added is to be Gaussian, which is a bell shaped curve of random numbers in the range -6.0 to +6.0 with a unit variance. In order to scale it down it is multiplied with a suitable number to get a required



(a)



(b)



(c)

- (a) Continuous ECG signal
- (b) Noise (Gaussian)
- (c) Continuous signal plus noise

Figure 4.30

variance.

As the ECG signal predominantly occurs in the positive direction, it was thought to put some -ve bias in the noise to make it more effective. Whatever the added noise characteristics might be, a histogram of this noise is obtained to get an idea in terms of the range, i.e. the difference between the maximum and minimum value for the amplitude of the mean square of error for the input noise, the shape of the histogram and where most of the noise occurs. The theory of the histograms is given in Appendix H.

4.7.2 Delta Modulator and Decoder

The delta modulator and its decoder was used as simulated earlier in Section 4.1.3. The delta modulator simulated had a constant step voltage of 0.02 in the local integrator.

4.8 Results

A time varying effect in delta modulation is obtained by adding Gaussian noise of different pattern of a fixed variance in an ensemble of ECG signals. The mean square value of error for each sample and hence for each cycle in the ensemble was obtained. As the values of mean square values of error for each sample averaged over the whole cycle were different, a histogram was obtained to show the number of times the error occurred in a certain amplitude chosen depending on the range of MSVE obtained.

The histograms of the MSVE for the added noise and the decoded signals for two cases of variance for both low pass bandlimited and wideband noise were obtained. These are shown in figures 4.31-4.38 in the Appendix along with their values. The ranges for these histograms are plotted on the diagram shown in figure 4.39. and Table 3.

No. of times mean square value of error occurs in certain ampli-

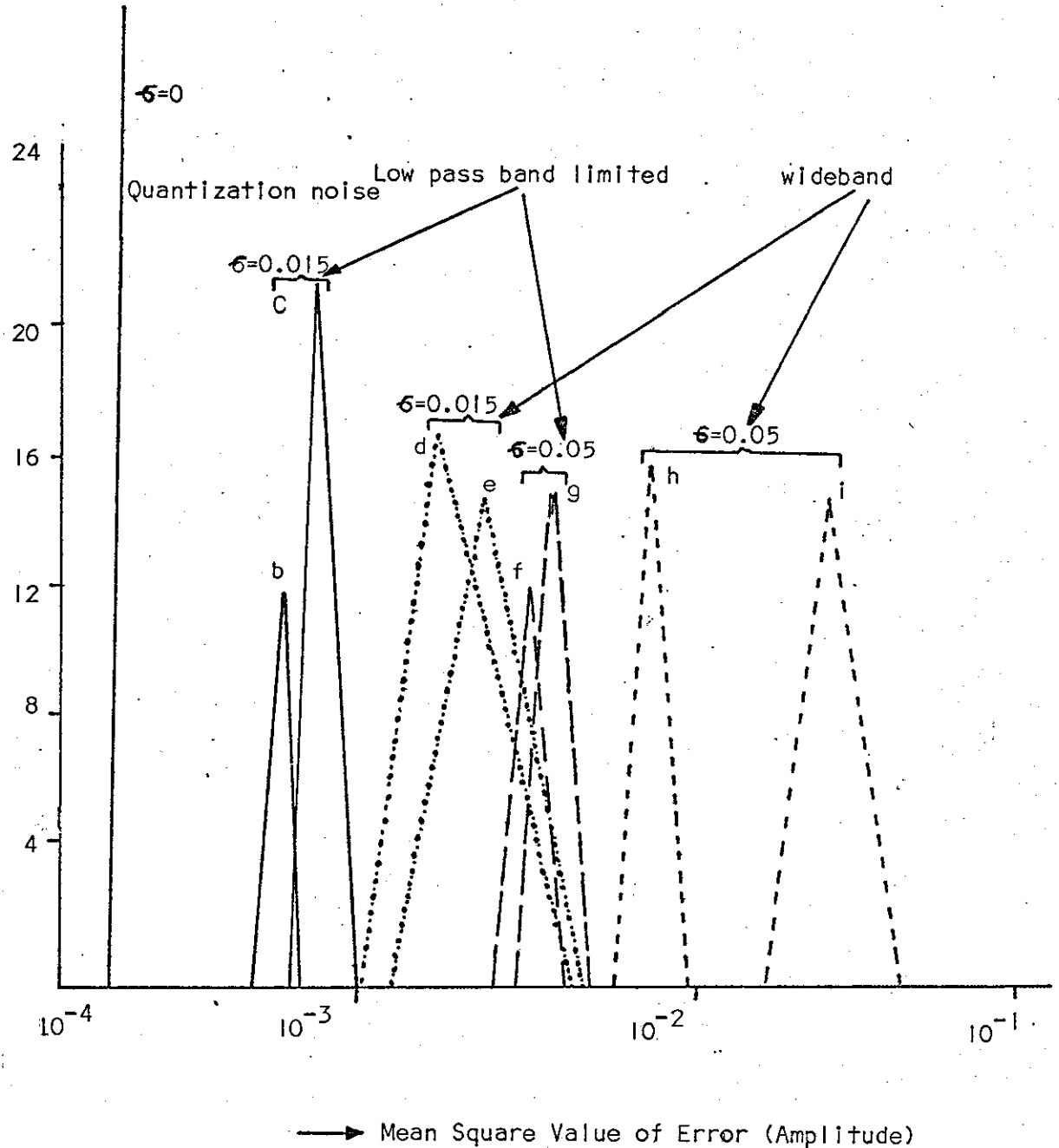


Figure 4.39 Diagram showing the range for histograms of low pass bandlimited and wideband noise of variance ($\sigma = 0.015, 0.05$)

Table 3

		Range	Max.No. of times noise occurs at certain ampl. Interval
<u>Variance = 0.015</u>			
Added noise (BL)	b	$.164 \times 10^{-3}$	12
Decoded noise (BL)	c	$.2433 \times 10^{-3}$	22
Added noise (WB)	e	$.325 \times 10^{-3}$	15
Decoded noise (WB)	d	$.5112 \times 10^{-3}$	17
<u>Variance = 0.05</u>			
Added noise (BL)	f	$.1844 \times 10^{-2}$	13
Decoded noise (BL)	g	$.2122 \times 10^{-2}$	15
Added noise (WB)	i	$.343 \times 10^{-2}$	15
Decoded noise (WB)	h	$.2922 \times 10^{-2}$	16

BL = Low pass bandlimited

WB = Wideband

It was observed that MSVE for the decoded output in the case of low pass bandlimited noise for both values of variance was more than the MSVE of added noise. It was also observed that the maximum number of times MSVE occurred at a particular range increased for the decoded signal and was significantly increased for the low values of variance (0.015). The MSVE for the decoded output when the input signal was not added with any noise was the single line shown on figure 4.39. That is all the values occurred at one point.

Quite different results were obtained for the MSVE of wideband noise. It was observed in this case that the range for the MSVE decoded signal decreased as the value of variance was increased. The maximum number of times MSVE occurred at a certain range for the decoded output increased slightly.

The ECG waveform with added low pass bandlimited and wideband noise were also decoded for one waveform and plots of these waveforms were obtained. This is shown in figures 4.40 - 4.45.

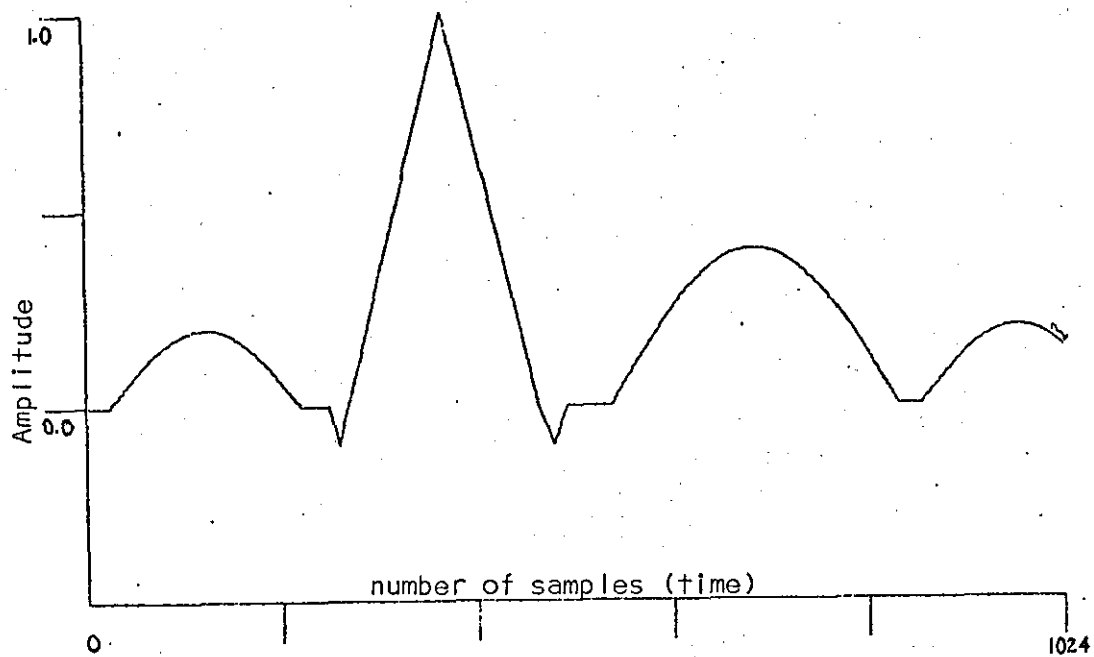
It was observed in the case of wide band noise that the decoded signal had less noise than was present in the input signal. The same was observed in this case even when the output signal was not finally low pass filtered.

4.9 Discussion

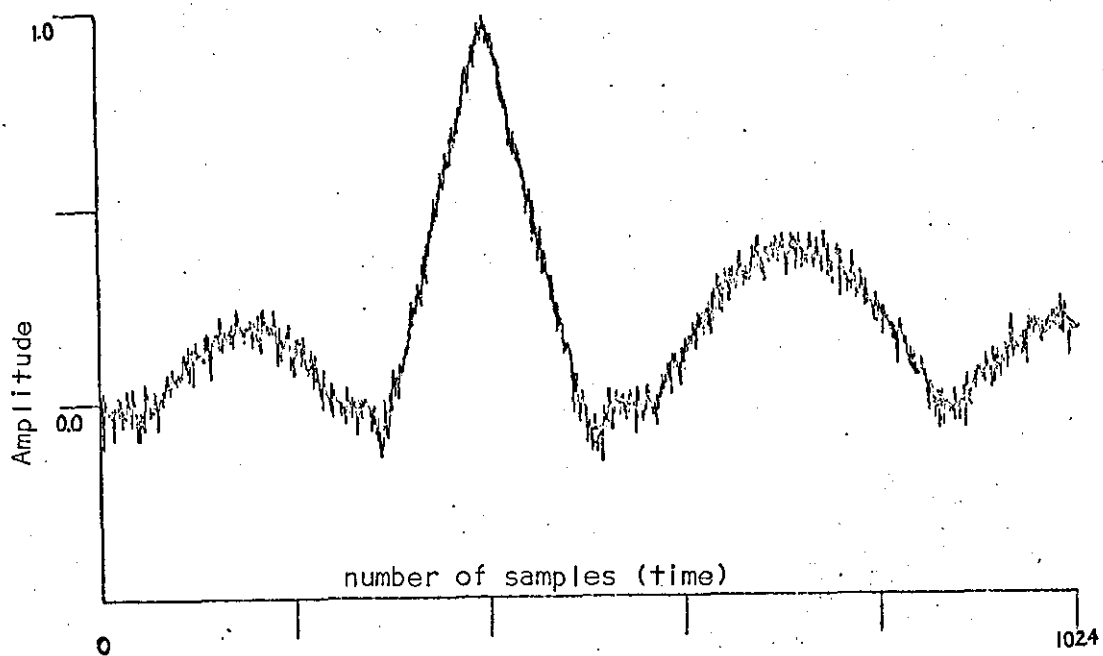
Bandlimited Noise

For bandlimited noise the range of MSVE of the decoded signal increased for both values of variance. The maximum number of times MSVE occurred in certain amplitudes also increased for the decoded signal.

The effect of bandlimiting the added noise with the low pass filter is to reduce the amplitude and filter the frequencies of noise above the cut off frequency of the filter. Due to the zero phase of the low pass filter used, the time distortion of low frequencies is avoided. Depending upon the amount of noise added, low pass

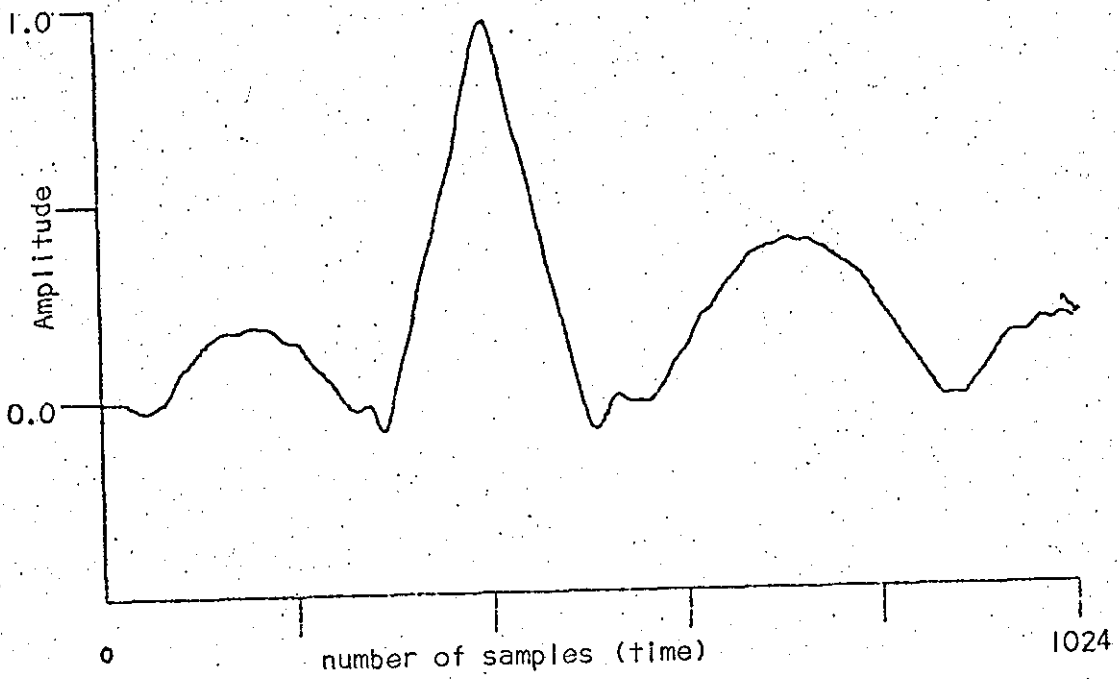


(a) Simulated ECG waveform

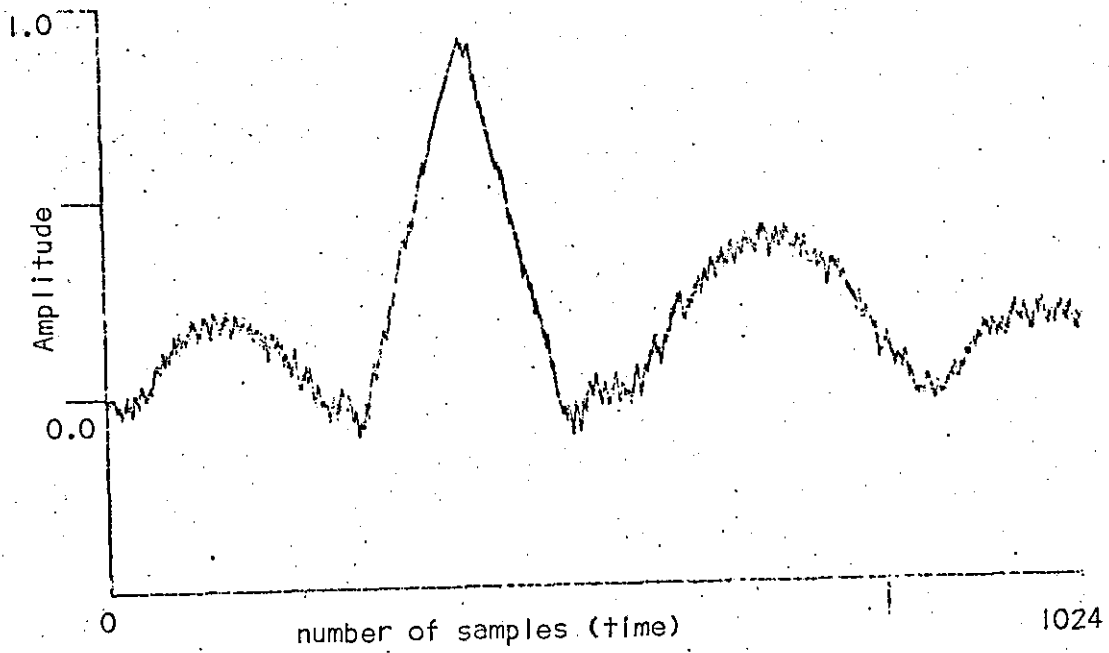


(b) Simulated ECG waveform with added noise of variance 0.015

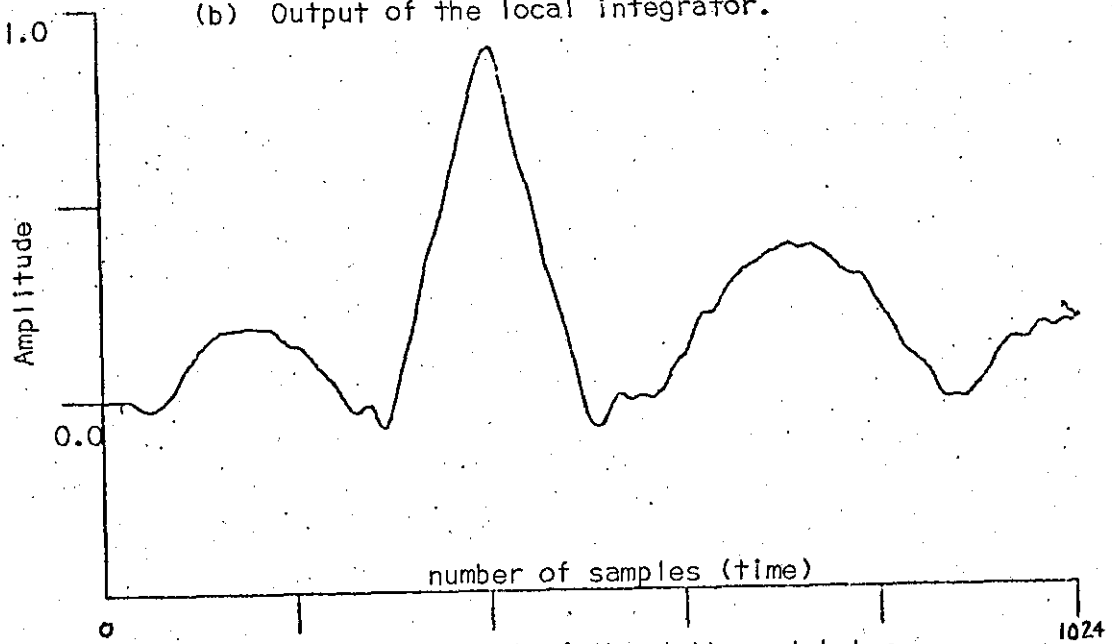
Figure 4.40



(a) Low pass bandlimited signal (ECG waveform and noise) as an input to the delta modulator.

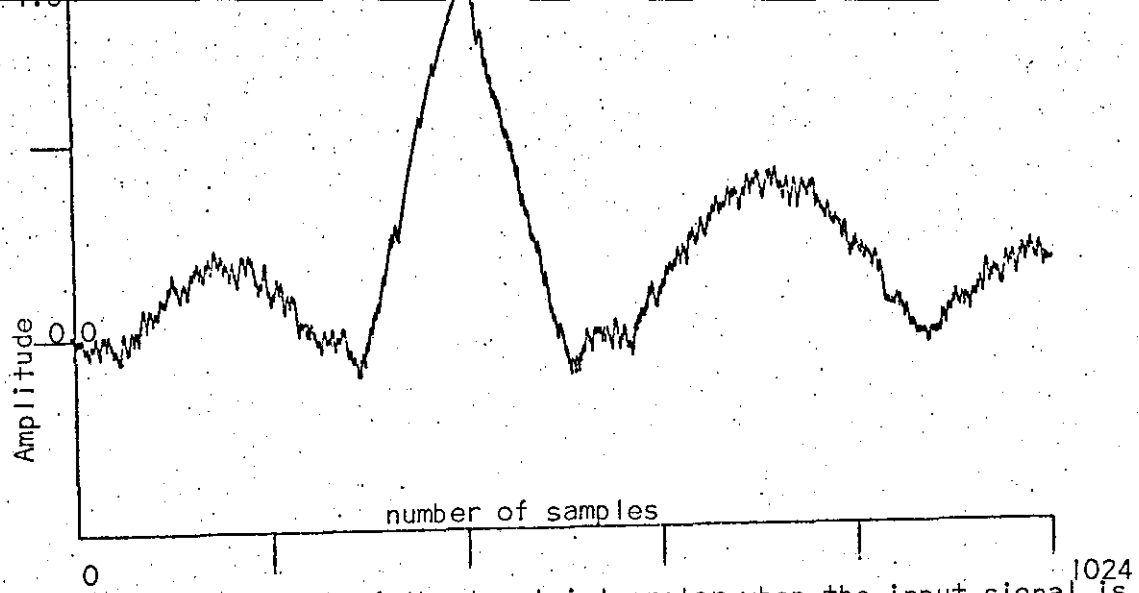


(b) Output of the local integrator.

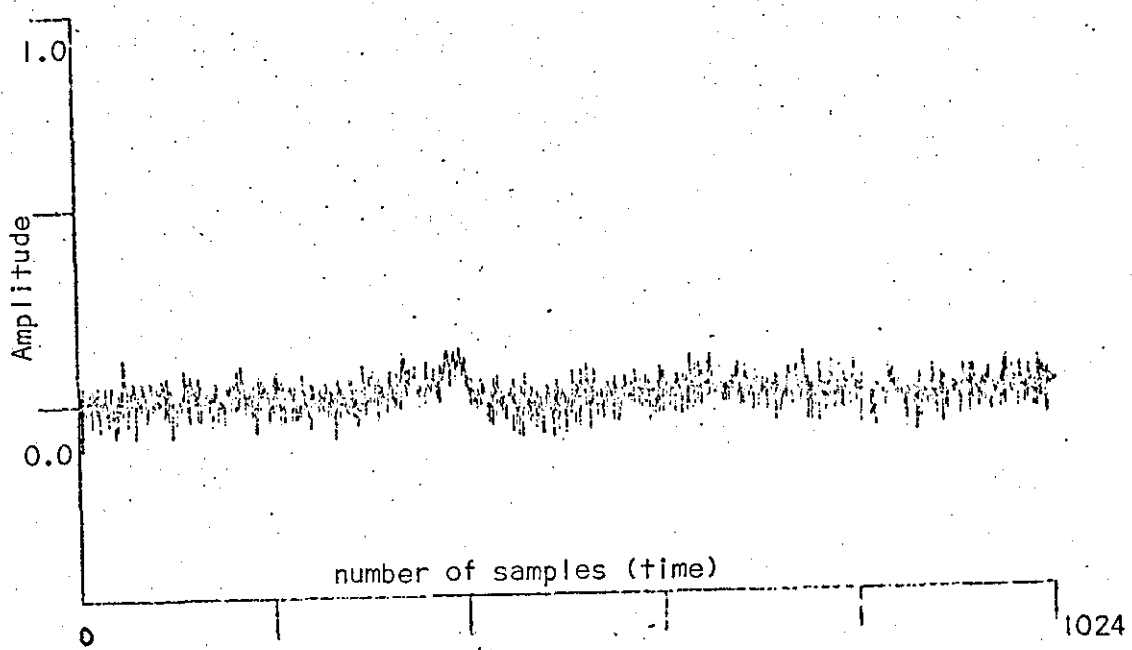


(c) Decoded output of the delta modulator

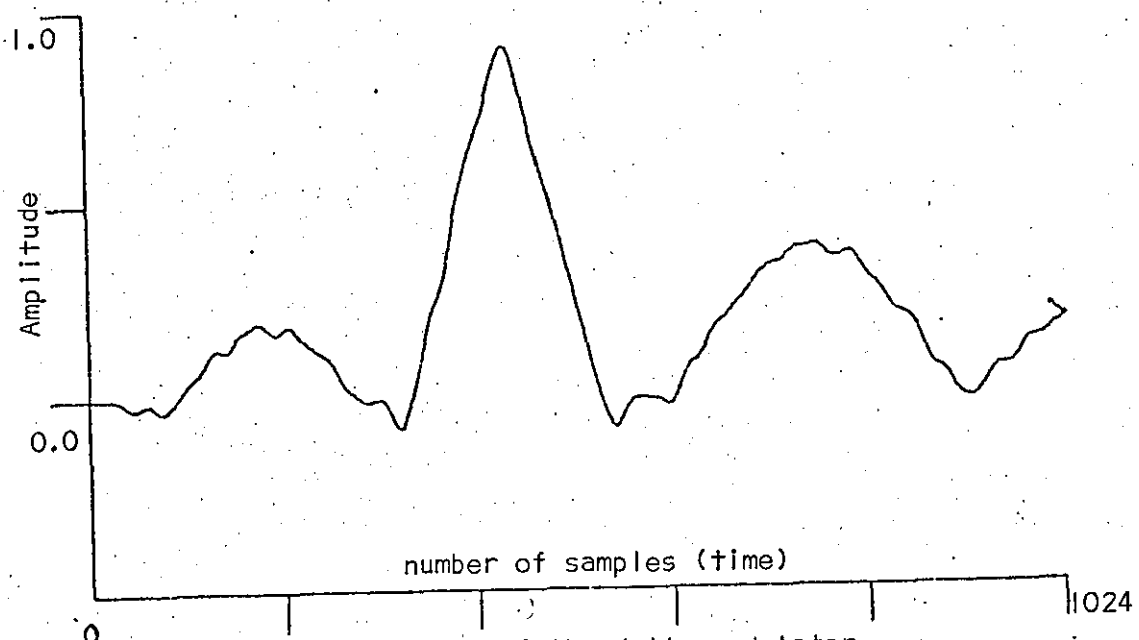
Figure 4.41



(a) Output of the local integrator when the input signal is accompanied with noise (wideband) of variance 0.015.



(b) Error waveform



(c) Decoded output of the delta modulator

Figure 4.42

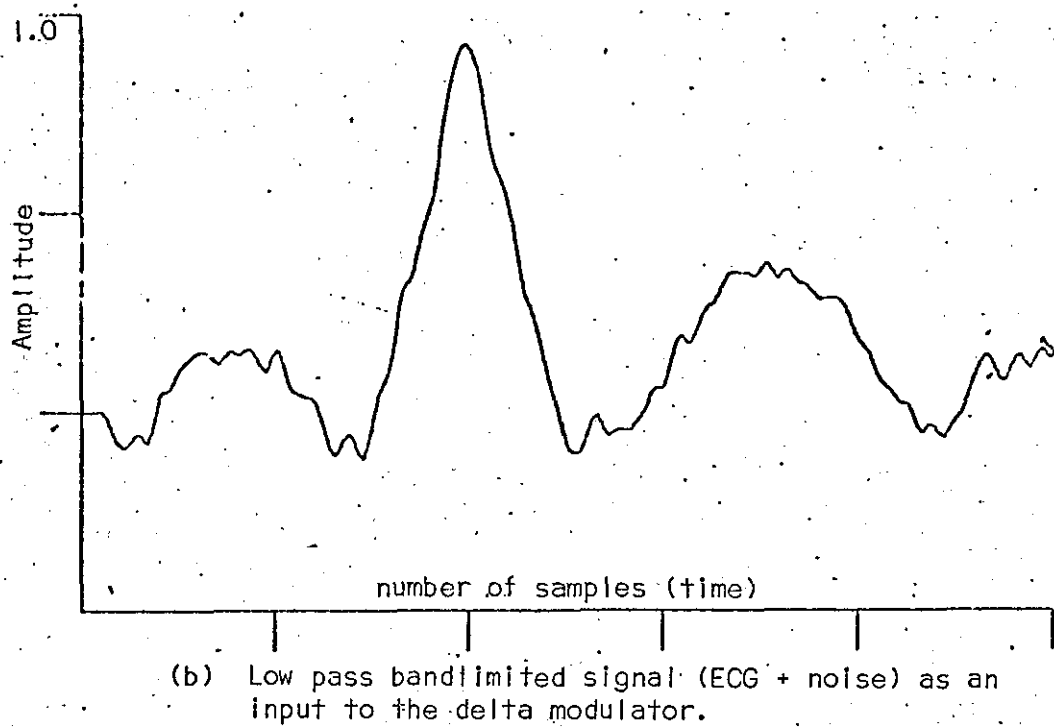
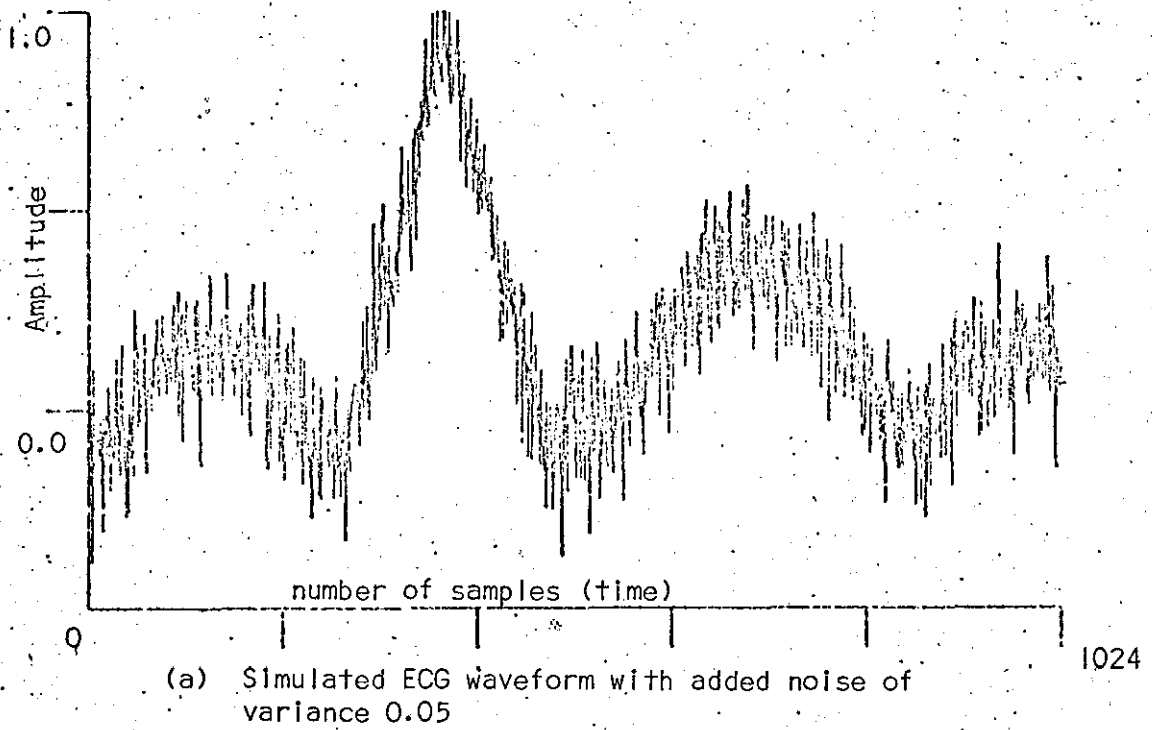
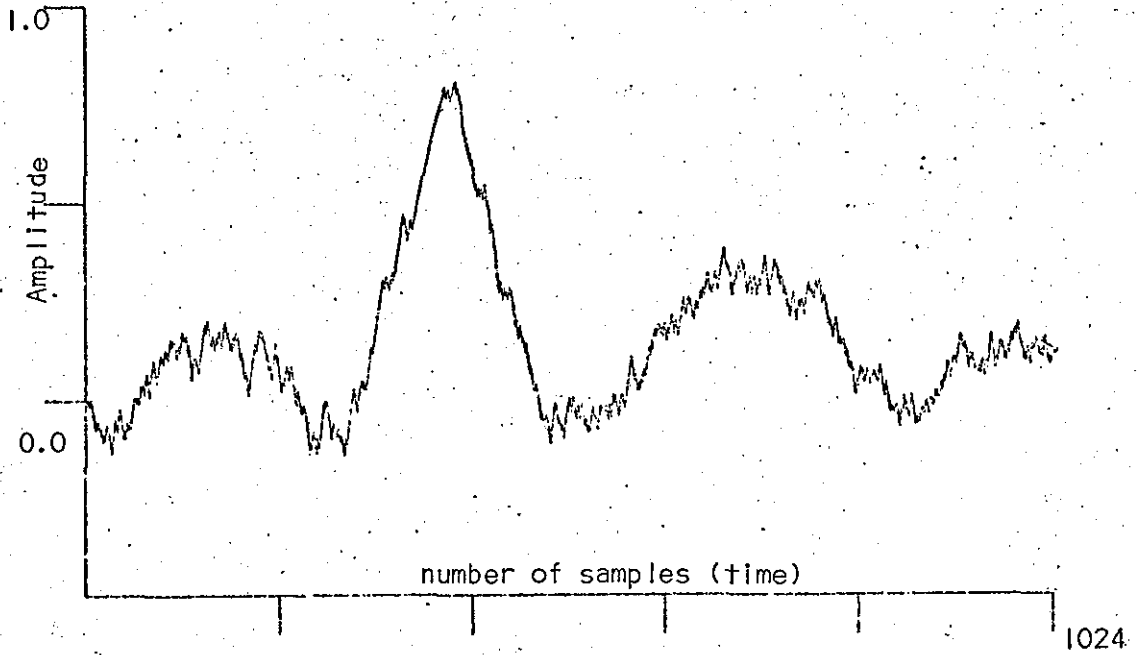
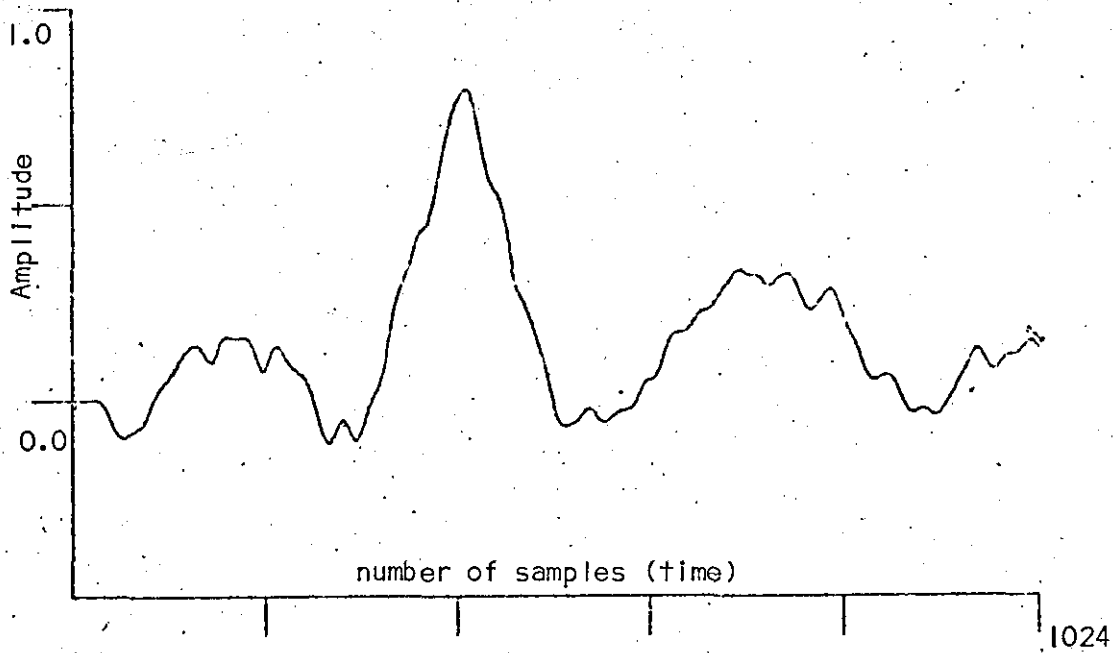


Figure 4.43

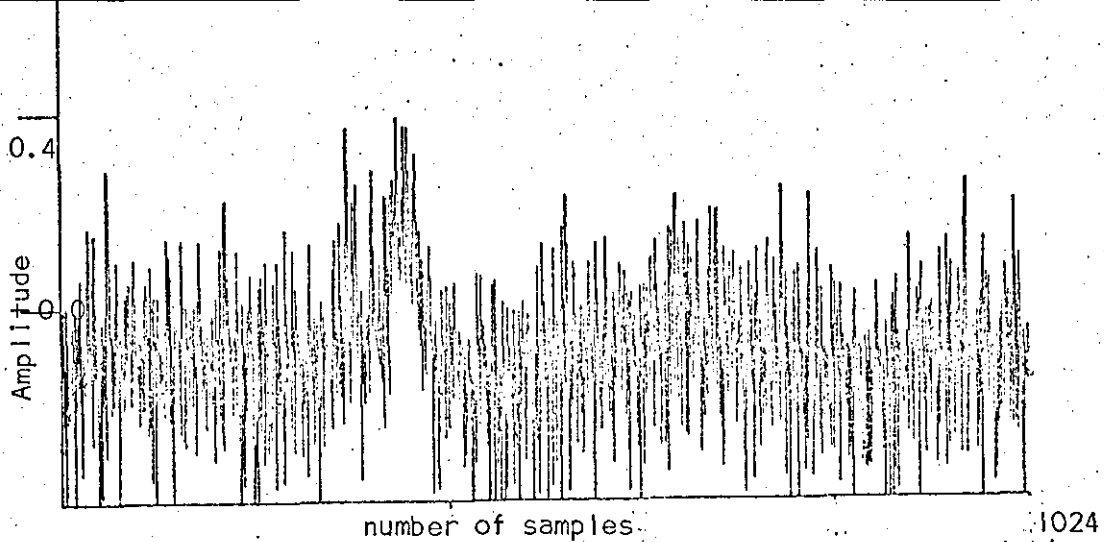


(a) Output of the local integrator.

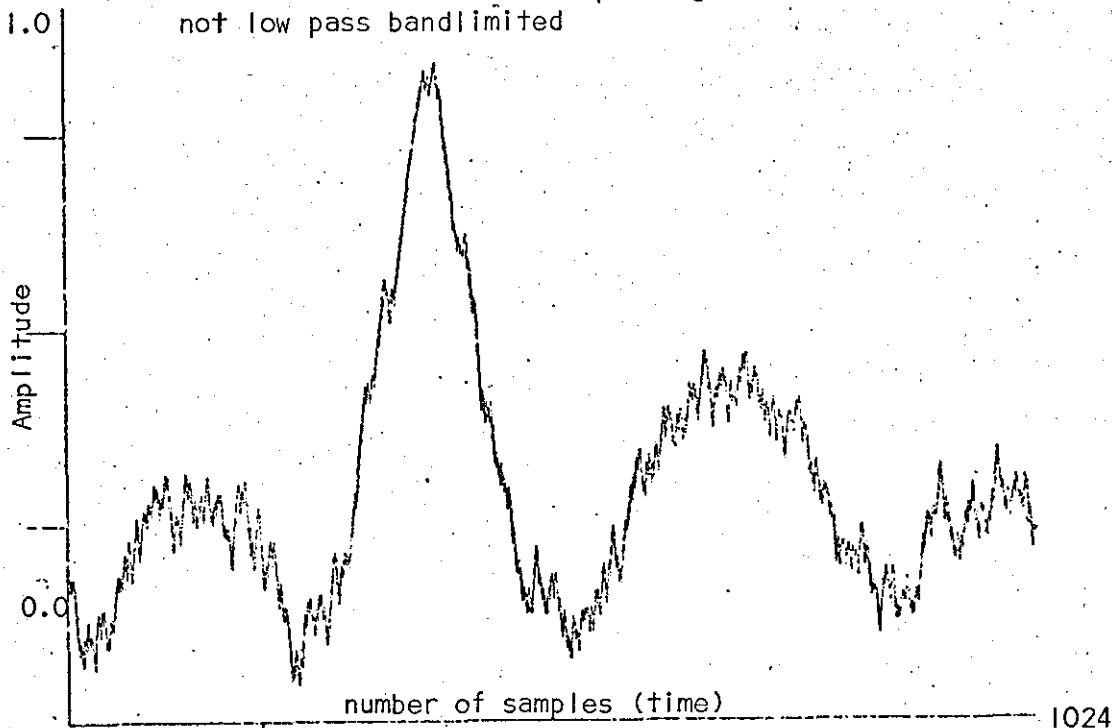


(b) Decoded output of the delta modulator

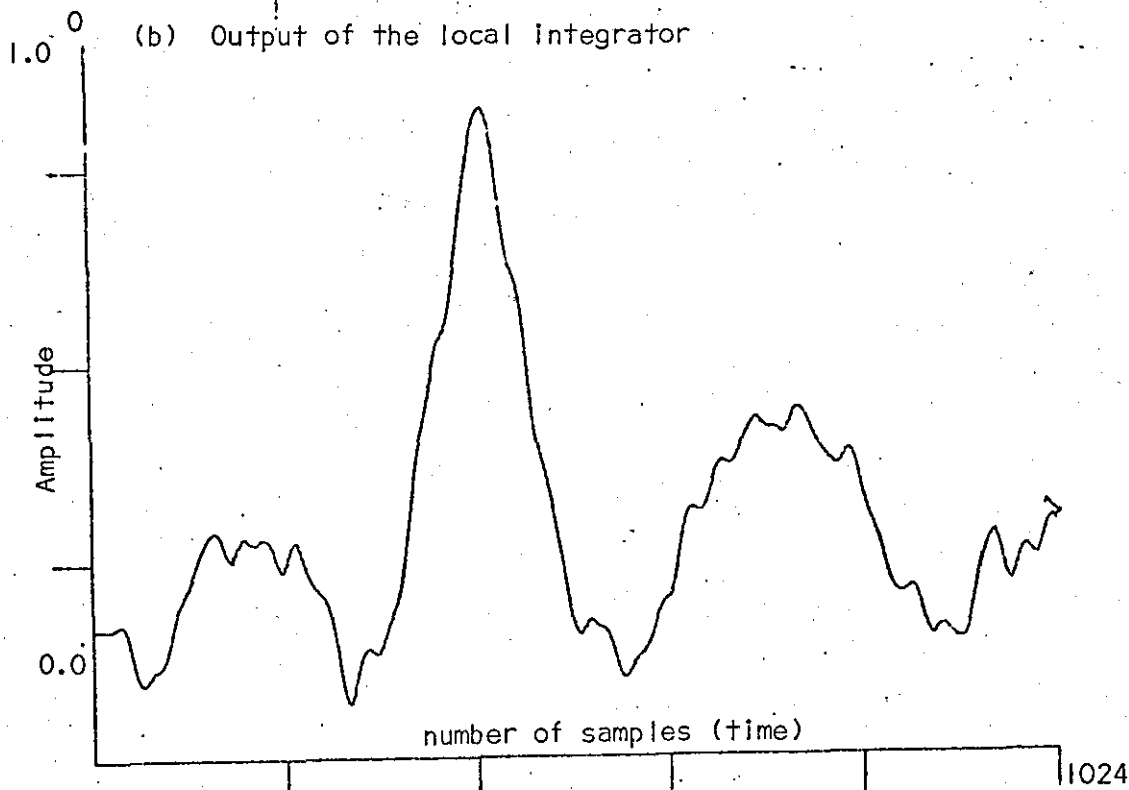
Figure 4.44



(a) Error waveform when the input signal (ECG + noise) is not low pass bandlimited



(b) Output of the local integrator



(c) Decoded output of the delta modulator

Figure 4.45

filtering of the added noise reduces the probability of slope overloading of the delta modulator. However, the inband noise on top of the signal is tracked accordingly. The decoded signal for a symmetrical coder, working below the slope overload condition differs from the input signal by only the quantization noise, but as the comparison is made between the histogram of MSVE for the added noise and that of the decoded output signal, the MSVE of the decoded output is more (added noise + quantization noise).

Wideband Noise

When the input signal to the delta modulator is Gaussian or if the signal is accompanied by Gaussian noise, such a signal when coded and decoded by a delta modulator may be accompanied by some noise. Two types of noise can be produced as mentioned in Chapter 3. To clarify the difference between these noises it is desirable to consider the spectrum of the noise introduced by the delta modulator. The simplest definition of noise is that noise is an error, that is, the difference between the input signal and the local output signal, as defined in Chapter 3. This error is correlated statistically with the input signal. In other words the error may be considered to be made up of two components, one linearly dependent on the input signal and the other linearly independent of the output signal.
(84)

The linearly dependent component may be regarded as being caused by passing the signal through a noise-free linear filter. The equivalent linear filter does not introduce noise but merely introduces frequency distortion, as for example in producing selective attenuation and phase shift, particularly for the higher frequency

components of the signal that the delta modulator cannot follow.

The noise component linearly independent of the signal may be viewed as equivalent to uncorrelated noise just as in the case of a non feedback type of pulse code modulation quantizer. Hence the presence of Gaussian wideband noise in relatively low frequency signals makes it prone to slope overloading in addition to producing quantization noise when decoded by the delta modulator. However in such a situation, the delta modulator eliminates the high frequency components and attenuates the amplitude due to the filtering action mentioned above. As a result MSVE for the decoded signal as observed and shown in figure 4.39(h) is less than the MSVE of added noise. In the time domain the signal with wideband noise is shown to be decoded in figure 4.45.

This showed that although the biomedical signals were accompanied with noise and interferences of higher frequencies than the delta modulator was designed to code, preservation of its waveform was achieved, while reducing the effect of noise.

4.10 Effects of Errors (Digital) on the Output Signal of the Delta Modulation

In the previous sections the effect of noise (generated in the system) or accompanying the input signal, on the decoded output was studied.

However, there are noise sources which affect the transmitted signal between the transmitter and receiver. In radio telemetry for example atmospheric transmission is generally subject to noise from natural and man-made sources. Similarly there is channel noise and noise found in the front part of the receiver before the decoder.

The effect of such a noise on the output signal-to-noise ratio, and on the decoded ECG waveform of the delta modulator was studied and is discussed here.

4.11 Theory

A block diagram showing the arrangement for studying the effects of noise in the transmitted signals on the output is shown in figure 4.46.

The encoded signal (digital) from the delta modulator to be transmitted has a polarity +1 (one) and -1 (zero). The noise present in the transmission path was assumed to be random, having a Gaussian distribution. The digital signal is received and the decoder is preceded by a decision detector. The function of the decision detector is to determine the state of each pulse (digit) out of two for a binary signal. It has a threshold level and any pulse appearing at the input of the decision detector greater than zero will be generated as +1(one) and -1 (zero) for a pulse less than zero. The decision

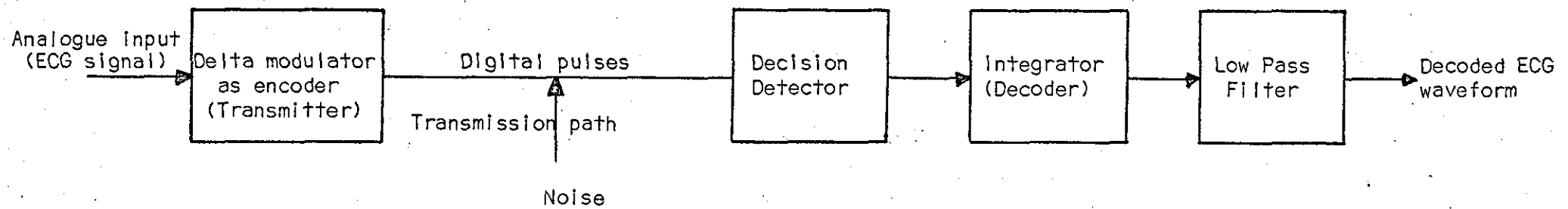


Figure 4.46 Block diagram showing the arrangement for studying the effects of errors (digital) on the output signal of delta modulation.

detector is followed by an RC integrator and a low pass filter to recover the analogue signal.

A typical binary signal before transmission and the corresponding waveform at the input to the detector is shown in figure 4.47. The amplitude levels of the received signal, if unaccompanied by noise, would be 1 (+1) and 0 (-1).

Assuming an equal probability of two binary states $P(1) = P(-1) = 0.5$, a threshold level is set at 0. At the instant of inspection the detector decides whether the signal plus noise is above or below the threshold level and generates the appropriate output of +1 or -1.

An error is said to be produced when noise on the signal is such that a wrong decision is made.

This is illustrated in figure 4.47 by the third digit in error.

Let us assume that received signal (x) at the input to the decision detector is the original signal (V) plus noise v , therefore

$$x = V + v$$

Probability of the noise voltage at any particular time having a voltage between v and $v + dv$ is

$$P(v) dv = \frac{1}{\sqrt{2\pi}\sigma} e^{-v^2/2\sigma^2}$$

σ = r.m.s. value of the noise voltage.

Thus for a binary polar signal, (as used in the present investigation) there are two possible probability density functions $q_1(x)$ and $q_0(x)$ for the value of x (signal + noise) at the instant of inspection. The probability density function actually obtained depending upon whether it is +V or -V. It is illustrated in

figure 4.48.

$$q_1(x) = \frac{1}{\sqrt{2\pi\sigma^2}} \exp\left(-\frac{(x-V)^2}{2\sigma^2}\right)$$

$$q_0(x) = \frac{1}{\sqrt{2\pi\sigma^2}} \exp\left(-\frac{(x+V)^2}{2\sigma^2}\right)$$

If a one (+1) was transmitted, the probability of an error is

$$P_{e1} = \frac{1}{\sqrt{2\pi\sigma^2}} \int_{-\infty}^0 \exp\left(-\frac{(x-V)^2}{2\sigma^2}\right) dx$$

If a zero (-1) was transmitted, the probability of an error is

$$P_{e0} = \frac{1}{\sqrt{2\pi\sigma^2}} \int_0^{\infty} \exp\left(-\frac{(x+V)^2}{2\sigma^2}\right) dx$$

Since there is equal probability of one or zero being transmitted

$$\begin{aligned} P_{e1} = P_{e0} &= \frac{1}{\sqrt{2\pi\sigma^2}} \int_V^{\infty} \exp\left(-\frac{v^2}{2\sigma^2}\right) dv \\ &= \frac{1}{\sqrt{2\pi}} \int_{\frac{V}{\sigma}}^{\infty} \exp\left(-\frac{v^2}{2}\right) dv = Q\left(\frac{V}{\sigma}\right) \end{aligned}$$

$Q\left(\frac{V}{\sigma}\right)$ is called Q-function.

If P_0 is the probability of a pulse '0' being transmitted, and P_1 the probability of '1', then the probability of an error is

$$P_e = (P_0 + P_1) Q\left(\frac{V}{\sigma}\right) = Q\left(\frac{V}{\sigma}\right)$$

There are standard tables for Q-function (also called error function

in a different form). Hence knowing the value of V and σ the probability of error pulses can be obtained.

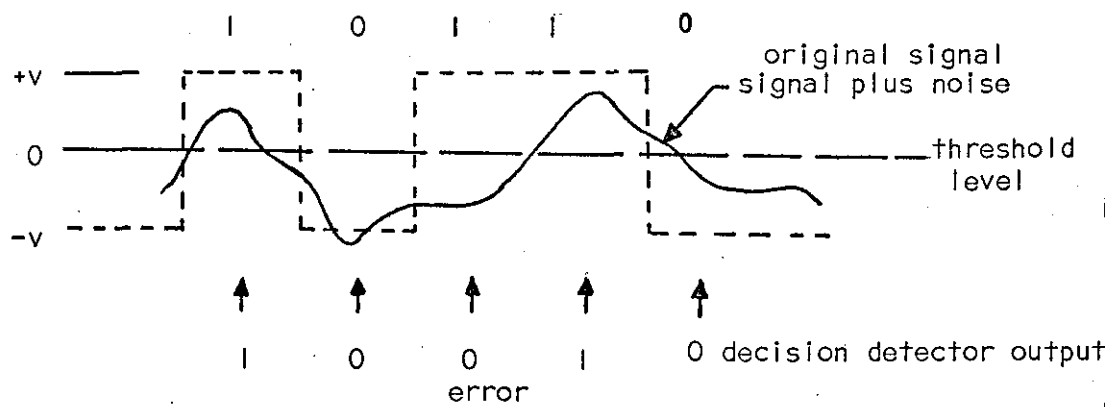


Figure 4.47 Decision detection - The effect of noise on pulse transmission

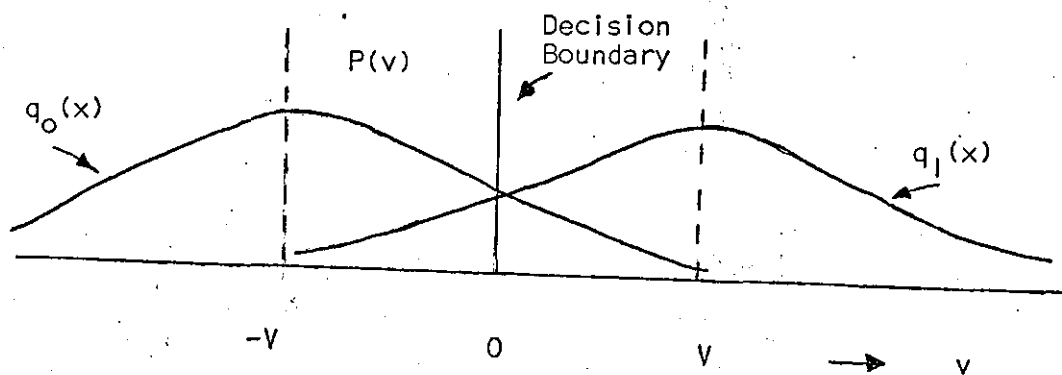


Figure 4.48 Error probability in receiver signal

Effect of Digital Error on the Decoded Output of
the Delta Modulator

The effect of digital errors on the output signal of the delta modulator can be determined by representing the received re-shaped pulse sequence on an error free pattern plus a randomly spaced series of rectangular pulses of amplitude $+2V$ or $-2V$, the latter depending upon whether a 1 or 0 is incorrectly received. It is assumed that the error free pattern, which is identical to the original transmitted signal, and the randomly spaced error pulses are received simultaneously. This is shown in figure 4.49.

Let the probability of an error be P_e , that is, error pulses occur on average once every $\frac{1}{P_e}$ digits. Half of the errors will give rise to $+2V$ pulses in the waveform (c) of figure 4.49 and the other half to $-2V$ pulses.

It is noted that the positive error pulses are associated with an original 0 of amplitude $-V$, becoming a 1 of amplitude $+V$, and similarly the negative error pulses are associated with 1's having become 0's.

The output of the system, therefore, consists of the result of putting the error-free digit pattern and the error pulses simultaneously through the RC network followed by the low pass filter. Since the RC network and the filter are both linear networks, it follows that the decoded output consists of the original input waveform plus the error pulses through the RC network and the filter.

Energy Contribution at the Output by the Error Pulses

Since the error pulses are of duration $\frac{1}{f_s}$ (where $f_s =$ sampling frequency) and are randomly distributed, Johnson⁽⁶⁵⁾ assumed that their long term energy spectrum is of the form

$$\left(\frac{\sin x}{x}\right)^2$$

with the first null at f_s . If the upper limit of the input frequency band is small enough in comparison with f_s the energy density of the error noise spectrum will be effectively constant over the frequency range of the input signal.

Since the amplitudes of the error pulses are $\pm 2V$ the mean square voltage of the error pulse stream is $4PeV^2$. Its energy density over the range of the output filter is thus

$$\frac{8 Pe V^2}{f_s}$$

The effect on the RC network as the decoder is to produce at its output an error noise having a frequency dependent spectrum. Hence its energy density is given by

$$\frac{8 Pe V^2}{f_s} \left(\frac{f_c^2}{f_c^2 + f^2} \right) \quad \text{at frequency } f$$

where $f_c = \frac{1}{2\pi RC}$

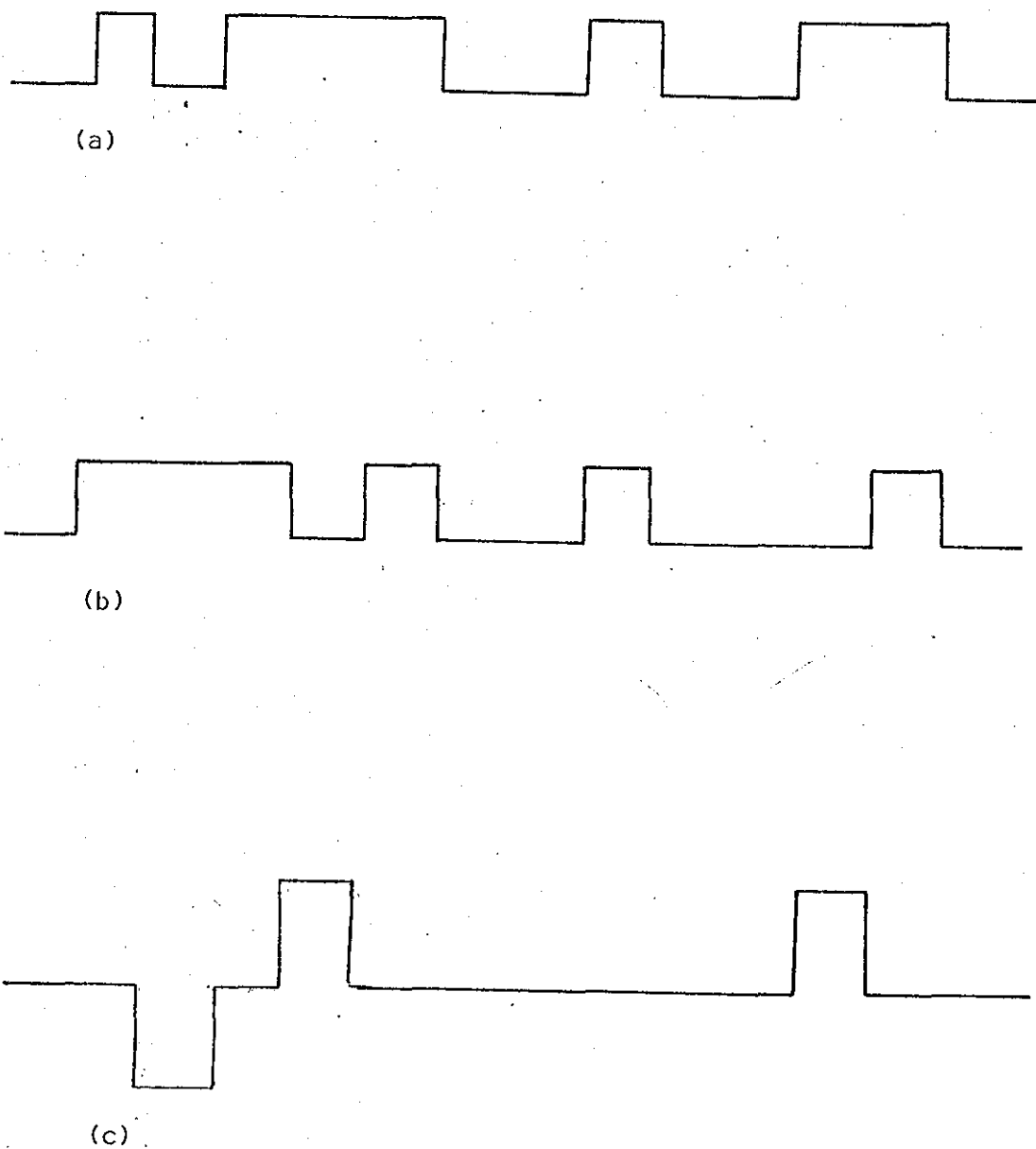


Figure 4.49 (a) Received pulse transmission
(b) Error-free sequence = original transmitted sequence
(c) Error-pulse sequence

Since the spectrum of biomedical signals starts practically from DC, the lowest frequency in the spectrum can be taken as zero. Hence the total mean square error noise voltage at the decoded output is

$$N_e^2 = \frac{8Pe V^2 f_c^2}{f_s} \int_0^{f_m} \frac{df}{f_c^2 + f^2}$$

If f_m is the highest frequency in the spectrum of biomedical signals.

$$N_e^2 = \frac{8 Pe V^2 f_c}{f_s} \left[\tan^{-1} \left(\frac{f_m}{f_c} \right) - \tan^{-1} \left(\frac{0}{f_c} \right) \right]$$

From the above formula error noise can be calculated at the output of the delta modulator. This does not include quantization noise. For a sine wave of peak amplitude V , the mean signal to error noise (or fluctuation noise) power ratio is given by

$$\left(\frac{S}{N_e} \right)^2 = \frac{f_s}{16 Pe f_c} \left[\tan^{-1} \frac{f_m}{f_c} \right]^{-1}$$

Assuming that the mean output signal power is $\frac{V^2}{2}$.

For a signal amplitude consistent with the condition of non-overloading

$$\left(\frac{S}{N_e} \right)^2 \approx \frac{f_s}{16Pe(1+\omega_m^2 T_c^2) f_c} \left[\tan^{-1} \frac{f_m}{f_c} \right]^{-1}$$

4.12 Results and Discussion

An ECG waveform was coded by the delta modulator and the effect of noise was studied at the decoded output waveform. The simulation is already discussed in section 4.1 and the arrangement for investigation is given in figure 4.46.

The digital pulses at the output of the decision detector were compared with the pulses obtained without noise and error pulses were detected. The error probability (error pulse) was also calculated from the formula given in the last section as

$$P_e = Q\left(\frac{V}{\sigma}\right)$$

$$V = 1 \text{ in the present case}$$

$$\sigma = \text{variance of added noise}$$

The standard table gives the probability of error pulses as

$$P(x) = 1 - Q(x) \quad \text{where } x = \frac{V}{\sigma}$$

The number of error pulses for noise of variance $\sigma = 0.4, 0.5$ obtained on the computer simulation were four and fifteen respectively out of 851 pulses. The calculated error pulses for these variances were six and twenty two out of 1000.

The following values of variance for noise were added to the digital pulses, and the decoded output for an ECG waveform was obtained. It is shown in figures 4.51 and 4.52. The added noise for variance $(\sigma) = 0.5$ and $\sigma = 0.75$ is also shown in figures 4.53 and 4.54.

Signal-to-noise ratio at the decoded output was also calculated at 8 Hz and is shown below

Noise Variance	Signal-to-Noise ratio at the input to decision detector	Probability of error pulses (P_e)	Calculated output signal to noise ratio (Does not include quantization noise)
0.4	7.94 dB	$P_e = .0063$ (6 error pulses in 1000)	49.03 dB
0.5	6 dB	$P_e = .022$ (22 error pulses in 1000)	38.12 dB
0.75	2.5 dB	$P_e = .0912$ (91 error pulses in 1000)	25.84 dB
1.25	1.92 dB	$P_e = .2119$ (211 error pulses in 1000)	18.5 dB

The signal-to-noise ratio at the output is calculated by using the formula derived in Section 4.11.2.

The above table and the figures illustrate the effect of error pulses at the decoded output of the delta modulator.

It is observed that in the case of $\sigma = 0.12$ and $\sigma = 0.4$, there is hardly any effect on the decoded ECG waveform (figure 4.51(b), (c)). However, on increasing the variance of noise to $\sigma = 0.5$ or $P_e = 0.022$ the amplitude of the P segments starts to be affected (figure 4.52(a)) but preserving the timing of the segments (PR and QT Interval). For $\sigma = 0.75$ or $P_e = 0.0912$ the amplitude of the P and T segments and both the intervals are affected, though the amplitude of the QRS complex is not much affected (figure 4.52 (b)). With $P_e = 0.211$ the whole of the decoded ECG waveform is corrupted.

It is concluded from this that the acceptable ECG waveform is obtained for a clinician when the value of P_e is between 0.006 (6×10^{-3}) and 0.022 (2.2×10^{-2}).

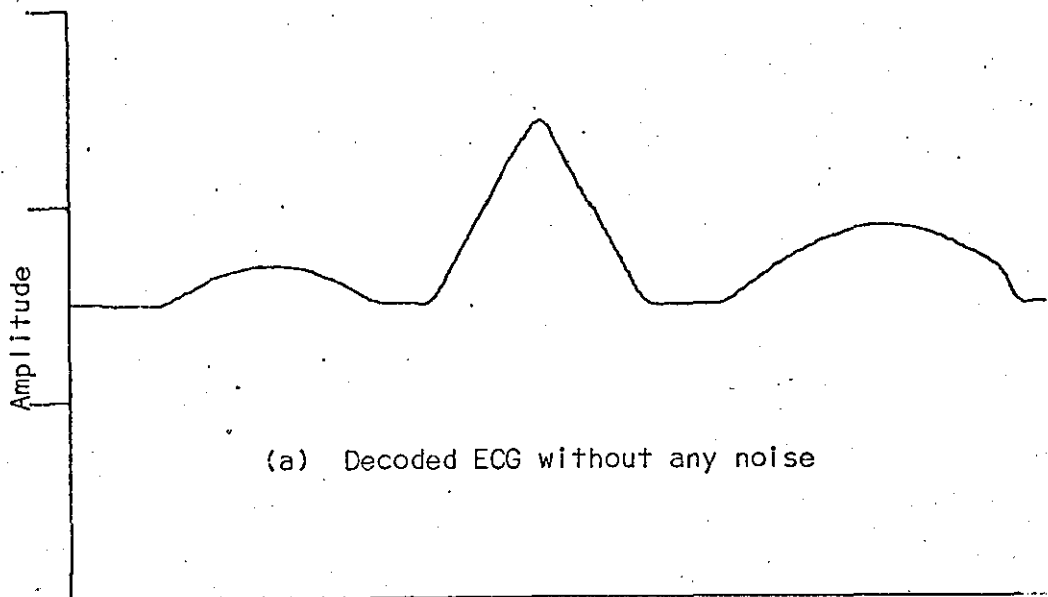


Fig.4-50

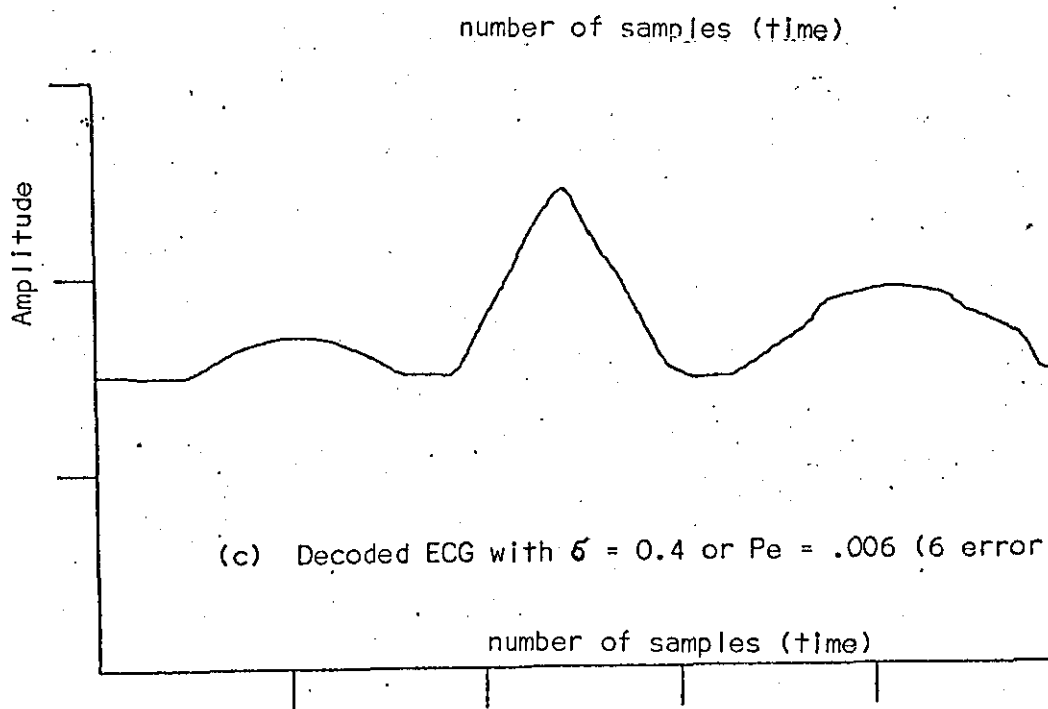
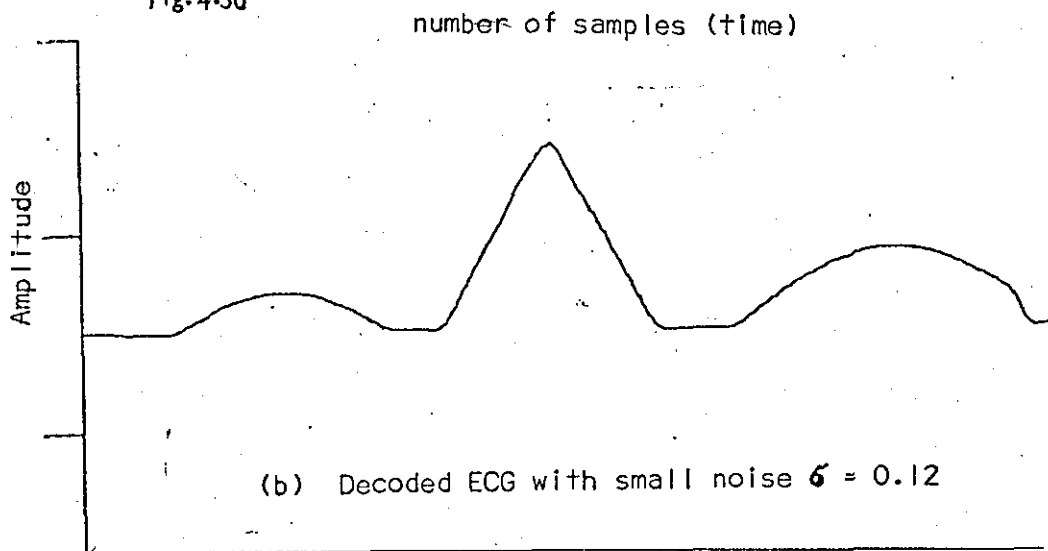


Figure 4.51 Effect of Error Pulses on the Decoded ECG waveform

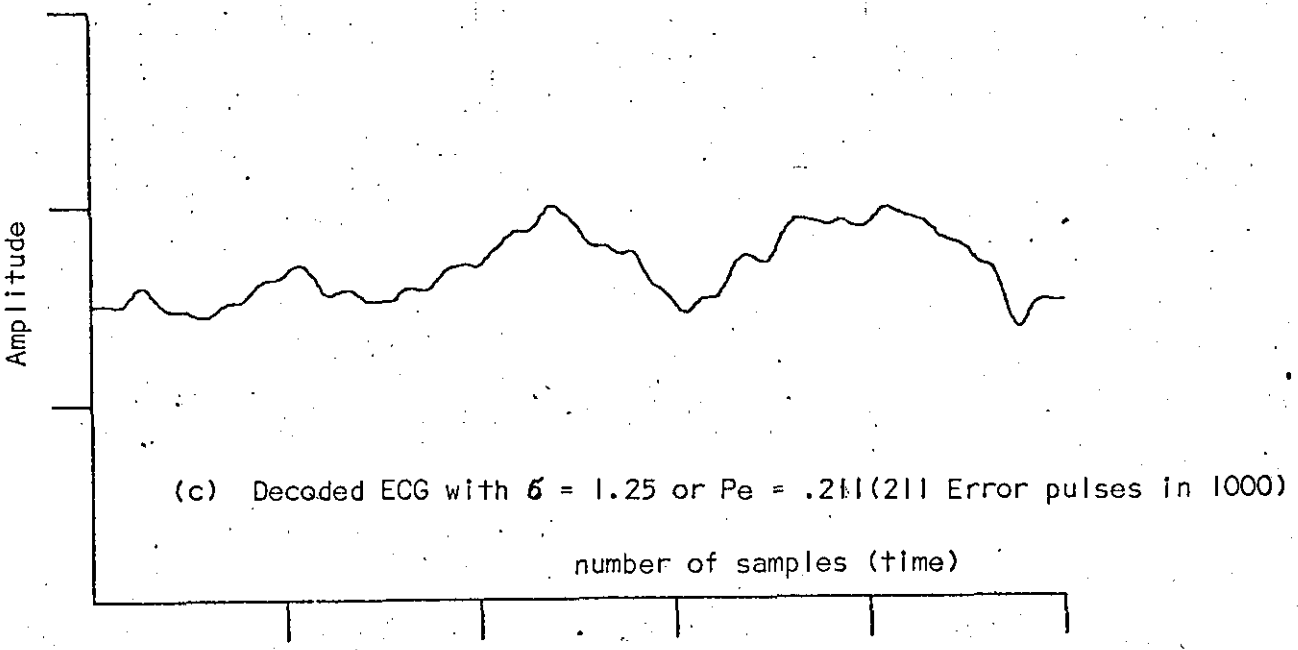
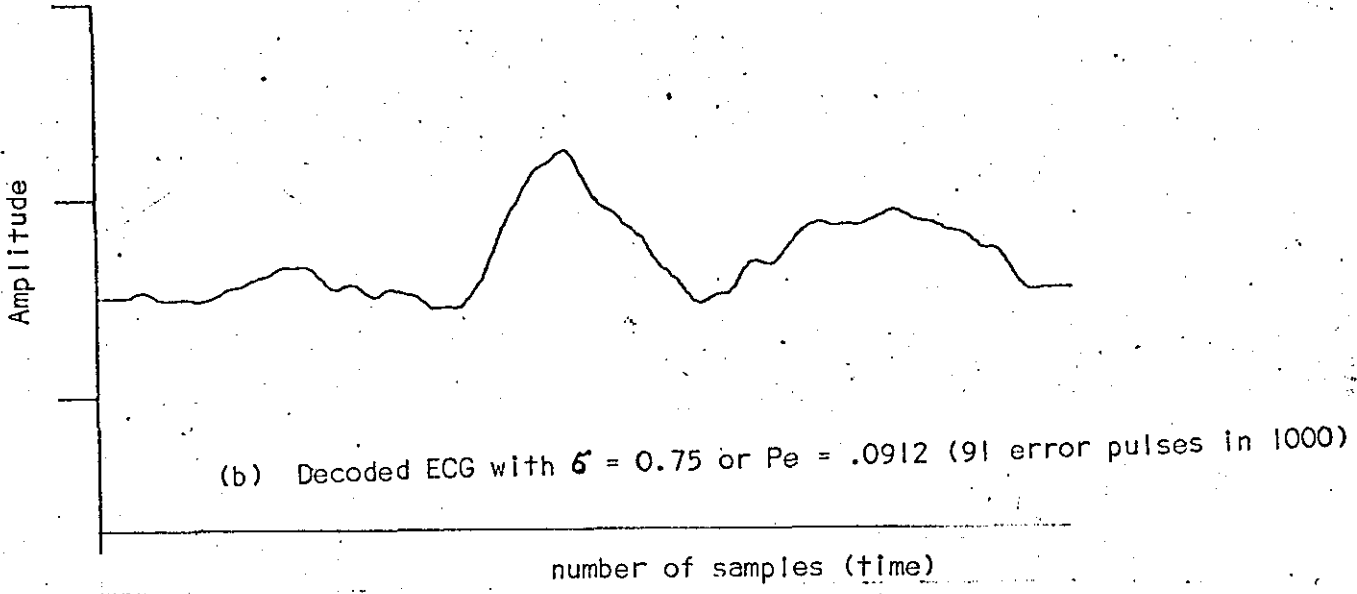
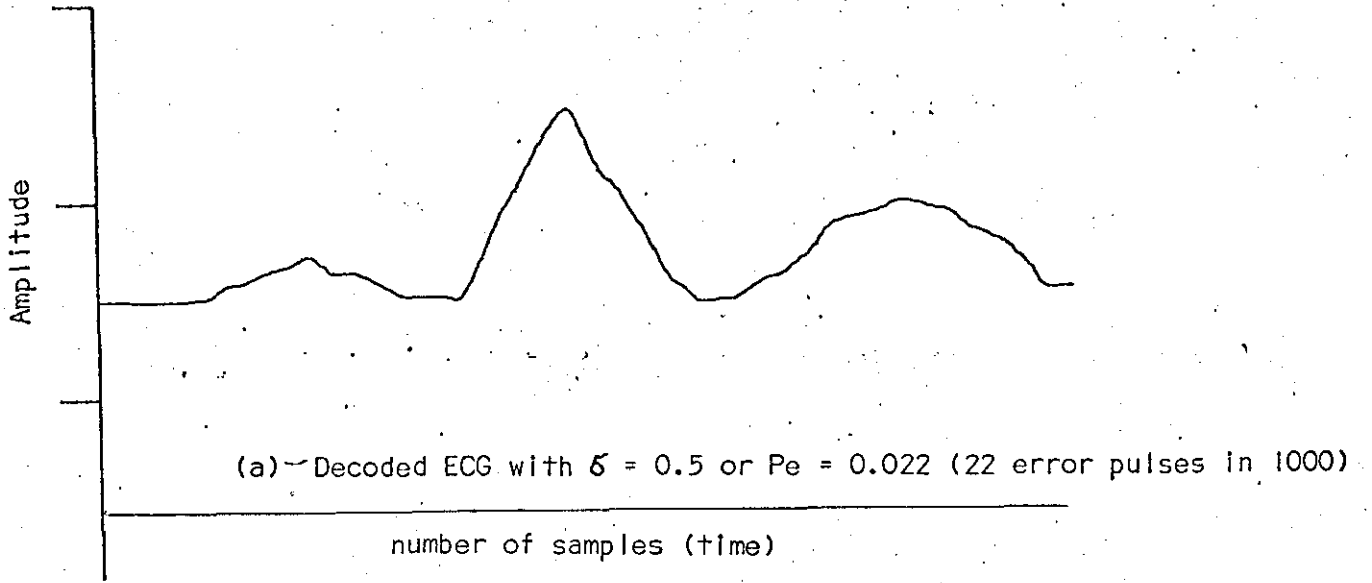
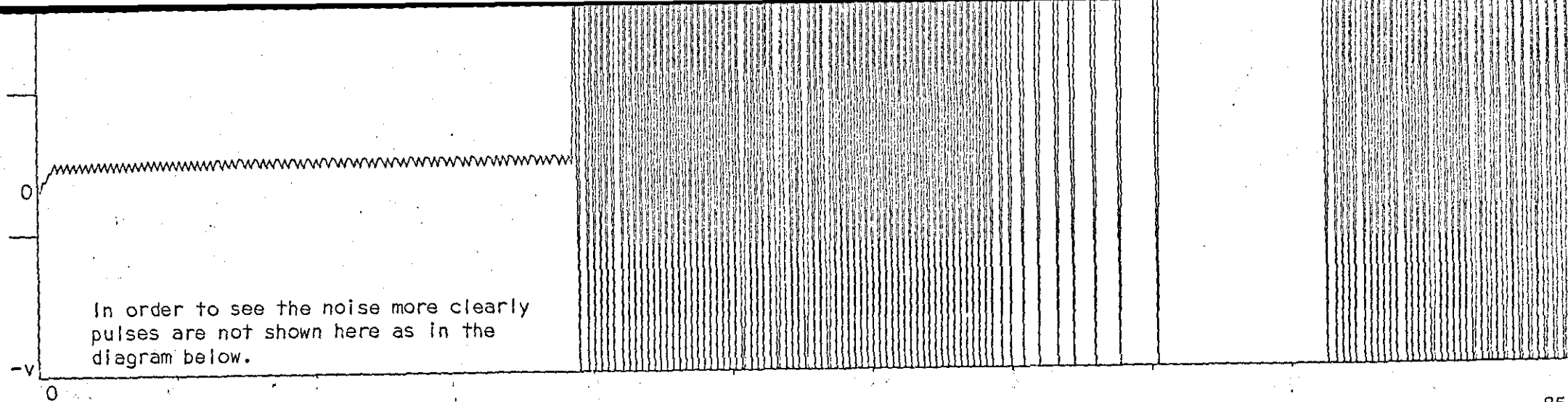


Figure 4.52 Effect of error pulses on the decoded ECG waveform



(a) Noise free output at pulses of the delta modulator (for ECG) at the input to the decision detector

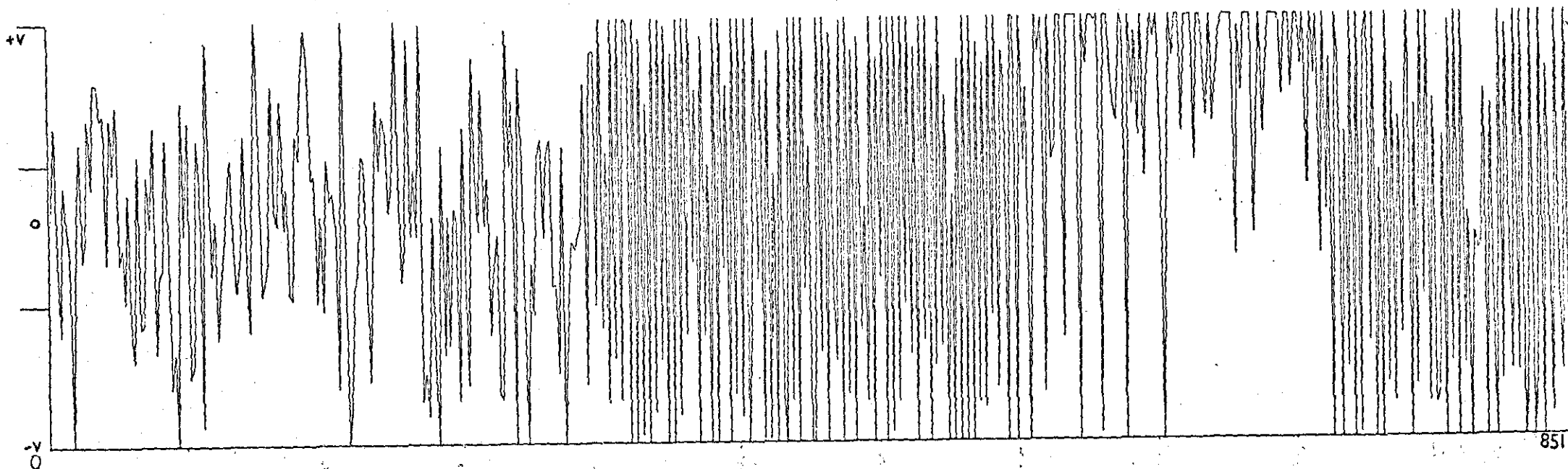
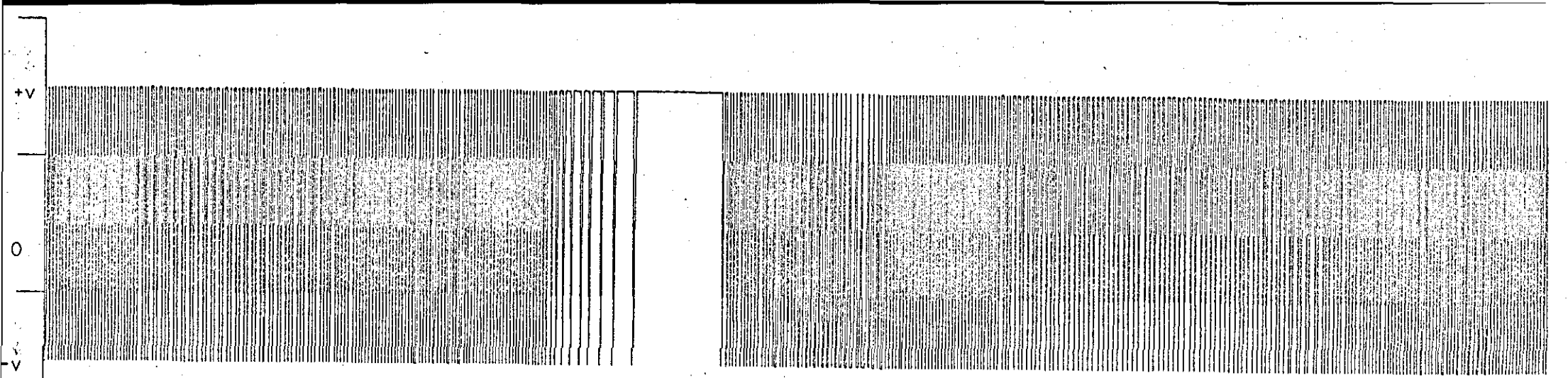


Figure 4.53 (b) Noise ($\beta=0.5$ or $P_e=0.022$) added to the above noise free pulses at the input to the decision detector.



(a) Noise free pulse of the delta modulator for (ECG waveform) at the input to the decision detector

851

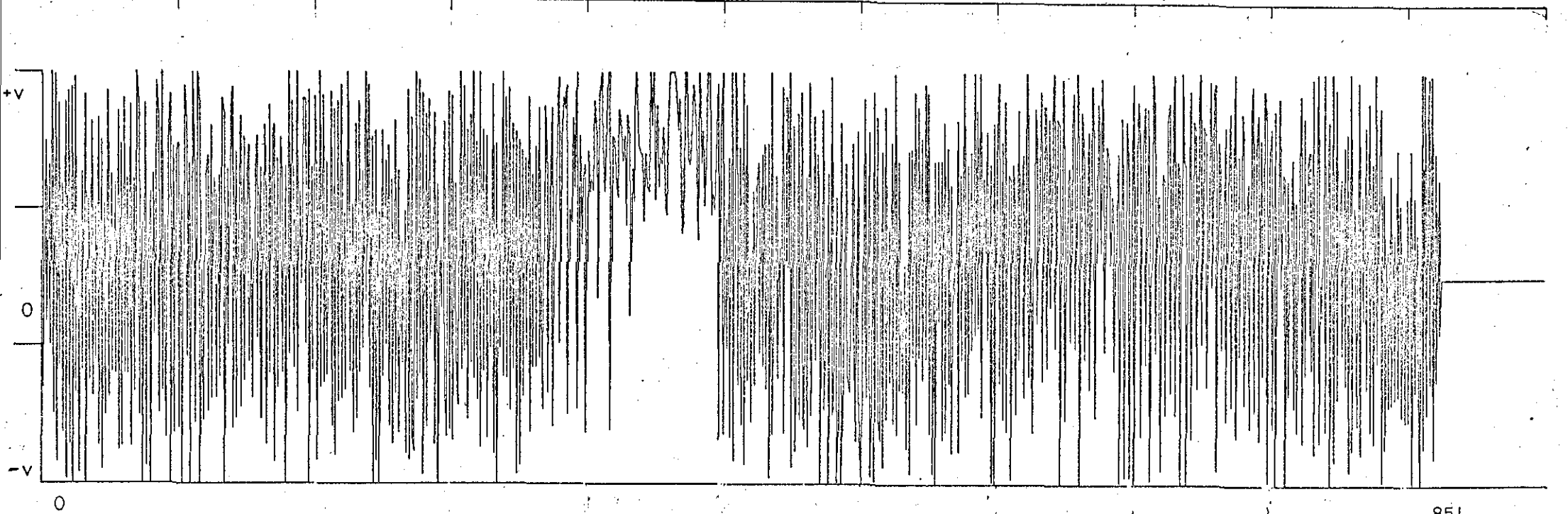


Figure 4.54 (b) Noise ($\beta = 0.75$ or $P_e = 0.0912$) added to the above noise free pulses at the input to the decision detector

851

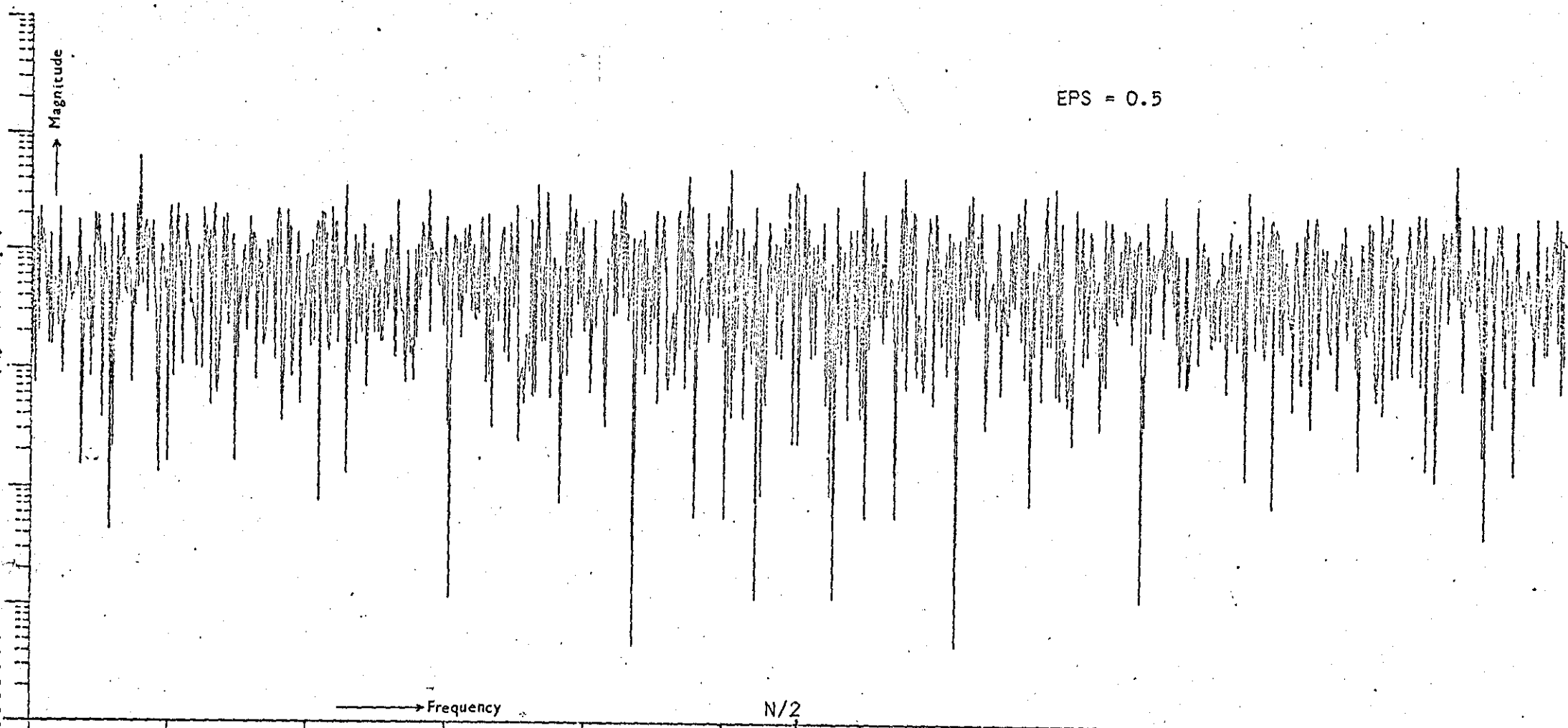


Figure 4.53 Full spectrum of digital signal with 22 error pulses

It is noted here that in pulse code modulation the effects of error pulses become significant when the error probability is 10^{-4} .⁽⁵⁷⁾ Hence delta modulator is superior to PCM in this aspect.

A spectrum of error pulses (22 pulses) for the noise variance = 0.5 was obtained and is shown in figure 4.53. The spectrum obtained looks like a Gaussian noise having a flat form. This is because the error pulses obtained have an impulse form and a spectrum of an impulse is flat.

Johnson⁽⁶⁵⁾ used rectangular pulses which have a spectrum of the form $\sin \frac{x}{x}$.

CHAPTER 5TRANSMITTING AND RECEIVING SYSTEMS5. Introduction

The biomedical signals in a biomedical telemetry system, after being coded and multiplexed, in the case of multichannel systems, are to be telemetered. The way of communicating these coded signals depends on the situation, and purpose of their information. This also depends on the availability of a transmitting link and the siting of the receiving stations. There are various ways in which the biomedical data can be telemetered.

1. Radio link
2. Line
3. Telephone
4. Tape recorder
5. Photocoupler
6. Acoustic or ultrasonic

5.1 Radio Link

A radio link can be successfully used to connect the subject to the display or the data-processing station. Apart from providing a link to inaccessible places (situations), radio telemetry offers a convenient method of eliminating otherwise essential connecting wires.

One of the most widespread applications of radio links has been in the telemetry of Electrocardiograms (ECG) in sports physiology and industrial medicine where direct links cannot be possibly used. Another relatively inaccessible location is within the body (though a short distance) from intestines, bladder, teeth, etc., also long distance situations where a radio link is used to a ship at sea, a pilot in flight or an astronaut in space. Another area where a radio link is useful is when the subject is situated in an area where the main powered measuring system is liable to disturbances

from capacitance coupling. Here the subject's life is also in danger when he is connected to the mains supply via a recording instrument.

Despite all these advantages, radio telemetry has its drawbacks.

1. More complicated than line telemetry
2. Sometimes more interferences from spark sources, spurious magnetic fields due to electrical environment, such as electrical machines and also other transmitters.
3. Prior permission is required to transmit the data and a limited range may be allotted.
4. Receiving stations can be difficult and expensive.

5.2 Radio Transmission System

The need to transpose a baseband signal to some other part of the spectrum is essential for radio transmission. Such a process is called modulation. Hence in a radio transmitting system the baseband signal (coded digital signals in the present case) modulates a carrier and transmits via a radio link at certain radio frequencies. The frequency range allocated by the Post Office in the U.K. is 102.2 - 102.35 MHz and 102.36 - 102.39 MHz.

There are various analogue and digital techniques of modulation. The most commonly used analogue modulation is frequency modulation and has the following advantages:

1. Frequency modulation is less sensitive to variations in amplitude of the transmitted signal so that there is less baseline variation due to changes in the subject's position.

2. It is inherently less noisy.
3. It requires less gain in the modulation amplifier, hence less power for a given transmission strength.

Although frequency modulation is very advantageous the bandwidth required to transmit the same information is larger than for amplitude modulation. For biomedical telemetry, when the range and power required is not very great, due to regulations of the Ministry of Radio and Telecommunications, narrow band frequency modulation may be employed.

5.2.1 Narrow Band Frequency Modulation (56)

Wide band frequency modulation (FM) can be analysed for two cases. The first is when the modulating signal ω_m (sinusoidal for example) modulates the carrier (ω_c) with modulation index

$$\beta = \frac{\text{frequency deviation in the carrier } (\Delta F)}{\text{frequency of modulating signal (FM)}}$$

greater than $\frac{\pi}{2}$ and second when β is less than $\frac{\pi}{2}$. Small modulation index (β) corresponds to narrow bandwidth, and FM systems with $\beta \ll \frac{\pi}{2}$ are thus called narrowband FM systems.

If ω_c is the radian frequency of the unmodulated carrier and ω_m is the radian frequency of the modulating signal, then the frequency modulated carrier for a sinusoidal signal is given by

$$\begin{aligned} F_c(t) &= \cos(\omega_c t + \beta \sin \omega_m t) \\ &= \cos \omega_c t \cos(\beta \sin \omega_m t) - \sin \omega_c t \sin(\beta \sin \omega_m t) \end{aligned}$$

Assuming $\beta \ll \frac{\pi}{2}$ which implies that the maximum phase shift of the carrier is much less than $\frac{\pi}{2}$ radians.

For $\beta \ll \frac{\pi}{2}$, $\cos(\beta \sin \omega_m t) = 1$, and $\sin(\beta \sin \omega_m t) = \beta \sin \omega_m t$. The frequency modulated wave for small modulation index thus appears in the form

$$F_c(t) = \cos \omega_c t - \beta \sin \omega_m t \sin \omega_c t \quad \beta \ll \frac{\pi}{2}$$

The above expression shows the presence of the original unmodulated carrier term ($\cos \omega_c t$) plus a term given by the product of the modulating signal and carrier. This form is similar to that of the output of a product modulator in the case of amplitude modulation.

For the sinusoidal modulating signal the product term in the above expression provides sideband frequencies displaced $\pm \omega_m$ radian from ω_c . The bandwidth of this narrowband FM signal is twice the highest frequency component of the modulating signal.

A similar expression for the frequency modulated carrier results when a general modulating signal instead of a sinusoidal modulating signal is used. In any case the spectrum of narrowband FM consists of the carrier plus two sidebands, one on each side of the carrier. Narrowband FM is thus equivalent in this sense to amplitude modulation (AM). Although narrowband FM and AM have similar frequency spectra and their mathematical representation is similar, they are distinctly different methods of modulation.

In narrow band FM the carrier amplitude is assumed constant but its phase (and effectively the instantaneous frequency also) varies with signal. In AM the frequency of the carrier remains unchanged but its envelope varies with the input signal. In narrow band FM the sideband term appears in phase quadrature with the carrier term while in the case of AM the carrier and sideband terms are in phase.

5.2.2 Digital Modulation

Another type of modulation exists when the RF carrier is to be modulated by a binary sequence or waveform. This is digital in nature and in this case the information to be transmitted is in the form of discrete amplitudes which is in contrast to the variable amplitudes of an analogue waveform. Since a finite set of discrete waveforms are transmitted the receiver has only to decide on two levels which makes the performance of the system dependent on the probability of error.

There are essentially three ways of modulating a sine-wave carrier by variation of its amplitude, its phase or its frequency in accordance with the information being transmitted. Similarly, in the binary case, this corresponds to switching the three parameters between either of two possible states.

Amplitude Shift Keying (ASK)

A sinusoidal carrier is pulsed so that one of the binary states is represented by the presence of a carrier and the other state is represented by its absence. Most commonly the amplitude switches to zero (off state) and some predetermined amplitude level (the on state). Such systems are then called on-off-keyed systems.

Phase Shift Keying (PSK)

The phase of the carrier switches by π radian or 180° . In a two phase system one phase of the carrier frequency is used to represent one binary state while the other at 180° is used for the second state.

Frequency Shift Keying (FSK)

In this case the carrier switches between two frequencies either by modulating one sine-wave generating source or by switching between two oscillating sources locked in phase.

The advantages and disadvantages of these modulations are given in detail in various books on this subject⁽⁵⁶⁾.

Phase modulation is equivalent to an amplitude modulated wave of twice the amplitude with the component at the carrier frequency suppressed. FSK systems are better for the optimum signalling of binary information in the presence of noise.

Phase synchronisation is quite difficult to obtain for detecting such signals, but coherent detection using phase lock loop techniques solve this problem.

5.2.3 Choice of Modulation Method

The requirements of the biomedical telemetry system envisaged are given in Chapter I. However, minimum transmitter power consumption, minimum bandwidth and simplicity of the receiver are some of the requirements.

The study of the digital modulations reveals that FSK is generally less effective in the presence of noise and requires wider system bandwidths, but is more effective over fading channels.

PSK, although generally most effective in terms of conserving power or minimizing errors, is difficult to use over fading channels, and its use introduces severe phase control problems for the receiver.

A narrow-band FM, however, employs smaller bandwidth and is easy to implement with minimum power consumption. The receiver for narrow-band FM is a domestic FM receiver and can be used effectively with some modification.

5.3 Frequency Modulation Transmitters (Radio Link)(85)

In the radio communication system, the information to be transmitted is first of all transformed into an electrical time varying quantity (a current or voltage) which comprises the signal.

In the frequency modulation transmitter the signal is used to modulate the output of a high frequency generator by varying its frequency according to the signal amplitude. Transmission then takes place by means of the modulated high frequency wave which is necessary for effective radiation of signals through air.

There are various FM transmitters as described in the literature, the principle is basically the same.

Transmitters for frequency modulation fall into two broad categories, depending on the technique employed to obtain the frequency deviation.

The first type employs a direct modulation process where the modulating signal directly controls the carrier frequency and is usually referred to as direct FM.

The second type obtains a frequency modulated wave indirectly after phase modulating the carrier.

Many circuits have been used to produce direct FM systems. In each case some form of reactance (inductance or capacitance) is shunted across the master oscillator circuit, and the effective inductance or capacitance value is made to vary in accordance with the modulating signal. The master oscillator is used to generate the carrier frequency by a high-Q resonant circuit.

There are various ways of obtaining a capacitance (or inductance) variation proportional to the signal intelligence. The most common involve the use of a capacitance plus a controlled source from an active circuit element. The examples are Miller-effect capacitance and a reactance tube.

One common method is to use, as the capacitance in the circuit, a back-biased varactor diode. The modulating signal controls the back-bias voltage, varying in turn the varactor capacitance.

Direct frequency FM systems have one inherent drawback. Since the frequency of the master oscillator is varied, this circuit cannot be a crystal oscillator. Therefore the transmitter centre frequency is subject to drift.

To overcome this problem either an extra facility called Automatic Frequency Control or a different technique using a crystal controlled oscillator is employed to stabilize the frequency.

The circuitry for the automatic frequency control can be complicated. The other technique to stabilize the frequency of the oscillator, is given in the following section.

5.3.1 Indirect Frequency Modulation

When the carrier is derived from a crystal controlled source, an indirect means of frequency modulation is necessary.

The well-established method known as the Armstrong modulator makes use of the similarity between full amplitude modulation (AM) and narrow-band angle modulation.

The Armstrong FM System

A block diagram of the Armstrong FM system is shown in figure 5.1.

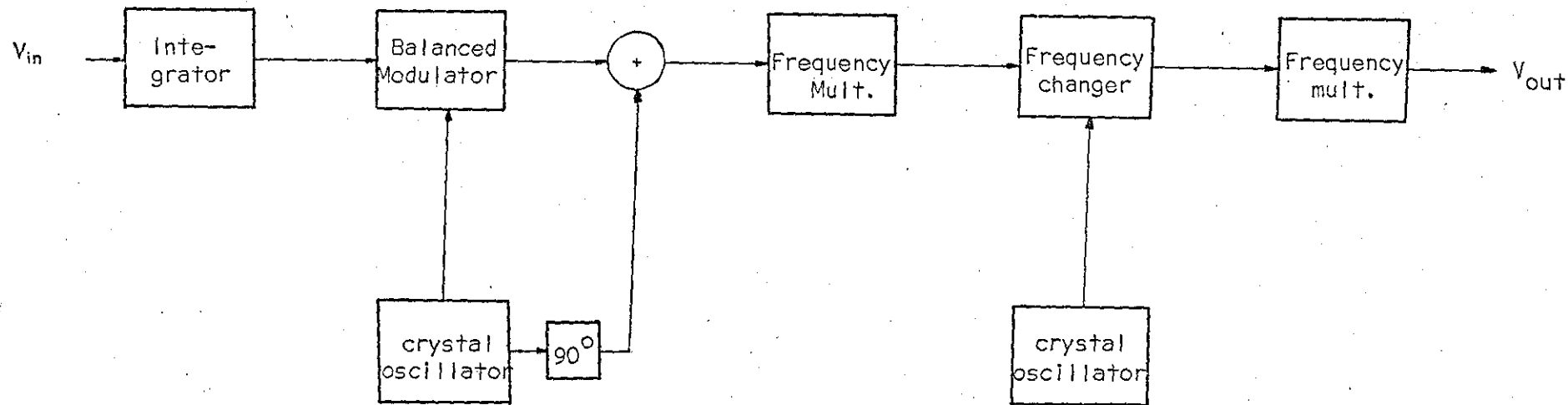
The carrier frequency is generated by the first crystal oscillator. The crystal output and the input signal (suitably corrected) are fed to the balanced modulator. The balanced modulator generates the upper and lower AM side frequencies and suppresses the carrier frequency, called double-sideband suppressed carrier (DSBSC) signal. In this signal all the power is conveyed in the sidebands.

The crystal oscillator signal is also fed to a phase shifting (R-C) network to produce a 90-deg phase shift. The outputs of the balanced modulator and the phase-shift network are fed to a combining circuit and the output is a frequency modulated wave.

The amount of deviation obtainable by this technique is very low, hence the output is effectively a narrowband FM when the correcting circuit preceding the balanced modulator is an integrator. A narrow band phase modulation (PM) is obtained, if the integrator is removed, since the phase displacement is directly proportional to the amplitude of input modulating signal. But this is true only for a phase displacement not exceeding 0.2 radian.

Due to the low frequency deviation, tremendous frequency multiplication, as shown in figure 5.1 is required to raise the deviation to an acceptable value for a frequency modulated system.

The biomedical telemetry system as mentioned in Chapter 1 requires simple and low power circuitry to make it economic, small and compact.



← Narrow band frequency modulator →

Figure 5.1 Armstrong Indirect Frequency Modulator

The indirect FM transmitter is more complicated and the circuitry consumes more power than the direct FM system, although it has a better stability.

However, better stability can be achieved in a direct FM transmitter by using a crystal controlled oscillator when a narrow band FM is required. Since the present biomedical telemetry system is not intended for a very long range and a limited bandwidth is available by the Post Office regulations, the narrow band FM can be used. A narrow band FM transmitter can be achieved with relative simplicity, economy and with minimum power consumption.

5.3.2 Narrow-band Frequency Modulation using Crystal Controlled Oscillator

Because the crystal in the oscillator is used to stabilize the frequency, it is difficult to modulate the frequency directly. However it is known that the frequency of a quartz crystal oscillator operating in the parallel mode can be changed slightly by varying the capacitance shunting the crystal. Any deviation produced can be used to communicate information.

Noble⁽⁸⁶⁾ (1966) has continuously varied the frequency of operation of a crystal one part in a thousand without material degradation of the frequency stability.

The most practical method of pulling the frequency of a crystal is by varying capacitance (using a varicap diode or ordinary diode) in series with the crystal.

5.4 Line Links

When a subject and the recording instrument, situated in different localities, are connected by a line, it is said to be using Line Telemetry. The line is a direct connection of some sort between the transmitting and receiving stations situated at different localities. The common line used may be a pair of wires, coaxial cables or telephone lines. The choice for the use, of course, depends upon the availability, ease, cost, location and the purpose of using the line telemetry.

Some of the examples for using line telemetry are given below:

- (a) In many cases when radio telemetry cannot be used due to interference from spark sources, spurious electromagnetic fields and interference from other transmitters.
- (b) It may be due to the difficulty of obtaining a suitable site for the transmitting and receiving antennae.
- (c) It might be that a patient is recovering or being treated at home and the effective clinical area is greatly enlarged by sending signals from patients at home to the central clinic via the local telephone lines. Another example of this kind of application is the on-line use of computer for the signal processing of the biomedical data and availability of analysis from the patients who might be in a different building.

Some of the basic considerations like the problem of transmitting information in the presence of noise are the same for both radio and line links. The main difference is due to the difference in the

properties of the propagation media between the transmitting and receiving systems which vary enormously over the range of frequencies used for transmission. The principles applied to the bandwidth and noise in relation to data input are the same as for a radio link.

5.4.1 Wire Link

An ordinary wire link consists of the line circuit which may be either a two wire or four wire configuration and the associated transmitting and receiving terminal equipment.

For short distances and comparatively simple forms of signals, a conventional pair of circuits can be used as for telephone working. The impedance taken for termination is 600 ohms, and the apparatus designed uses a characteristic impedance of 600 ohms.

5.5 Telephone Link

A telephone link is a form of line link where the biomedical data can be sent over the public telephone network.

Direct analogue transmission of biomedical signals on the ordinary or switched telephone network is difficult due to the low frequency attenuation characteristics of the system. This is due to the repeating coils and the use of series capacitors and shunt inductors for signalling and other purposes. There is relatively more attenuation at the lower and higher frequencies. However the telephone network can be modified to reduce frequency attenuation or specially rented telephone lines, available in the U.K., may be used for permanent short or long distance transmission.

Instead of using the telephone lines directly for transmission of physiological data, the signals can be changed into wavering audible tones. The audible tone is then transmitted through the

air to the telephone mouthpiece, where it is converted to an electrical signal for transmission in the same way that any voice signal is handled. The biomedical signal may be used to modulate a carrier frequency in the audio range and variation in the carrier (audio range) can be coupled to any telephone.

5.6 Tape Recorder

A tape recorder may be used to record the biomedical signals and these can be processed later with the computer. These signals may also be transmitted via a telephone.

A tape recorder is also used as a data storage device carried by the subject in certain circumstances when radio telemetry cannot be conveniently used. The situation may arise when the distance to be covered is too great for efficient radio telemetry or if the subject must be left to himself for a long period and able to move about freely.

The present quality of the pocket-sized miniature tape recorders for entertainment purposes, with the addition of a simple modulating device, makes ECG storage possible. Such a system was described by ⁸⁷Hertsler (1967) and ⁸⁸Livingstone (1968) and was manufactured by Depex.

A further advantage of this recording device is that only one central playback and processing installation need be used for various recording units. In this way many subjects can be treated by different investigators at the same time.

5.7 Photocoupler

There are some situations and areas where both line and radio telemetry are not very practical to use. This sort of situation may arise in an operating theatre where interference and spurious disturbances from numerous electric equipment makes radio telemetry impossible. This situation may also make line telemetry impractical and hazardous due to connecting cables.

The photocoupler, which is a much more simple and reliable means of wireless connection, finds its use in these situations.

89

(Van der Weide et al, 1968).

5.8 Acoustic or Ultrasonic Link

Telemetering of physiological data is often required from the subjects under water to the monitoring station over the surface. It was found, by Anderson²⁶ (1970), that an ultrasonic or acoustic link provides the longest range in water. The velocity of sound is independent of frequency but the attenuation increases with increase of frequency. The use of sound signals for the transmission of information under water means that a signal may arrive at a particular receiving point over several paths. Since the different paths will generally have different lengths, the arrival over a range of time can seriously distort the signal. Slow transmissions are less attenuated than fast ones and the magnitude of this problem generally increases with increasing range. Frequency Modulated signals are less affected by multipath problems than the amplitude modulated signals. However, the problems of multipath reception echoes and background noise are improved by transmitting the physiological data slowly and in digital form.

5.9 The Receiver System

The function of any receiver system is to extract the intelligence from the transmitted signal at some remote station. A typical receiving system usually has a receiving link followed by some sort of amplifier and a waveshaper. Once the incoming signal is given a proper waveshape, then it is decoded and displayed on a convenient recording instrument. The receiving end depends on the transmitting link. If the transmitting link is radio, the receiving system will have a radio receiver followed by an amplifier, waveshaper and decoder. If the transmitting system has a line link then the receiving end is simply a decoder with some sort of buffer amplifier.

5.10 Radio Receiver

Conventional superhetrodyne receivers are commonly used for radio telemetry work. They combine the advantages of a fixed frequency receiver with variable tuning. The incoming signal is combined with a signal from a local oscillator in a mixing device and the output is obtained at another frequency (the intermediate frequency). Most of the radio frequency amplification is obtained at the fixed intermediate frequency. A diode detector may be used to obtain the demodulated signal from the radio frequency signal.

A frequency modulated receiver is used as a receiver for the frequency modulated transmitter. It consists basically of a receiving aerial, frequency tuner, intermediate frequency amplifier, limiter and detector. Although these are the basic parts, the receiver may have other added circuits such as automatic gain control (AGC), automatic frequency control (AFC) and a phase lock loop.

5.10.1 Phase Lock Loop

Very weak signals can be picked out from the output of the receiver by using a phase lock loop. This is also known as correlation or synchronous detection. The basic idea of using an oscillator in the receiver synchronised with the received signal was first proposed by Woodyard in 1937 but the present technique of the phase locked loop was developed mainly in recent years for colour television and telemetry.

It is a closed loop system which compares the phase of the local signal with the incoming signal and forces the local signal into step with the incoming signal from the transmitter. The oscillator produces a reference signal for comparison with the incoming signal. The arrangement is shown in figure 5.2.

A filter that will pass only slow changes (low pass filter) prevents any rapid changes in the locally generated sine wave in response to momentary disturbances in the received signal. A clear signal comes out with an indication of frequency and phase changes due to modulation. The inability to shift suddenly is equivalent to rejecting noise by a very narrow band filter adjusted around the transmitter carrier frequency. If fading suddenly removes several cycles completely they will be inserted at their proper place by the local oscillator and a few extra impulses added by noise will not appear in the output.

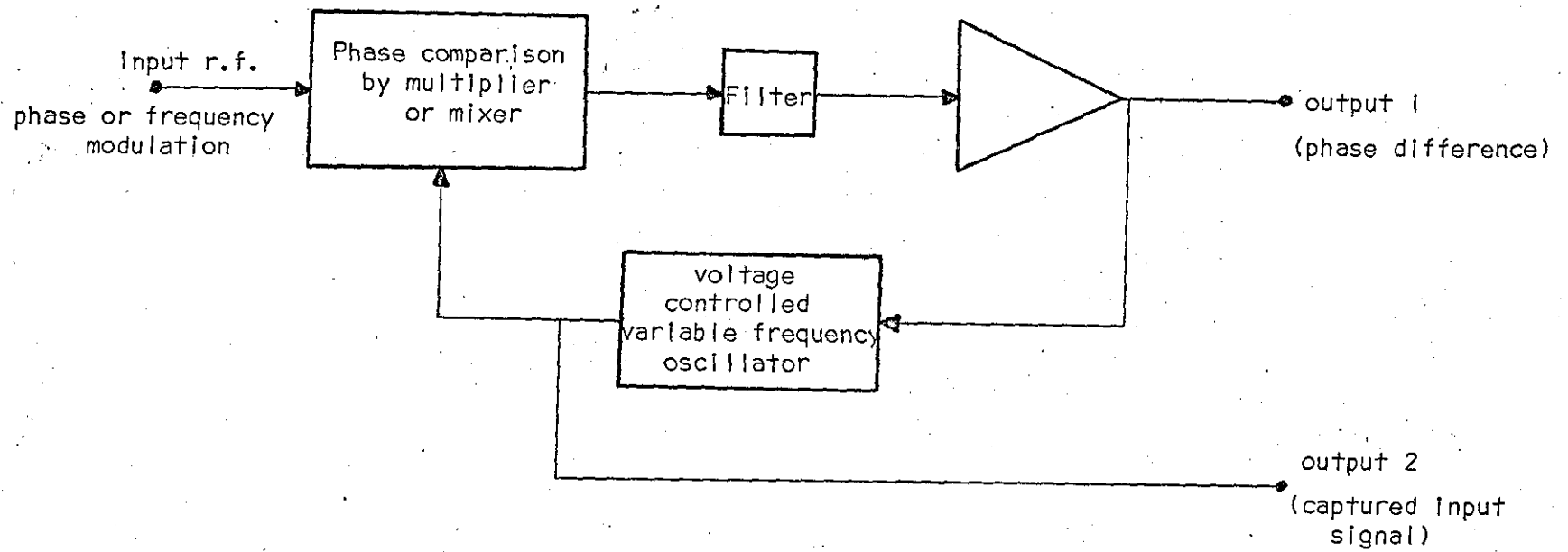


Figure 5.2 Phase Lock Loop

5.11 Antenna

In the transmission of biomedical data using a radio link, the antenna at the transmitting end is situated in the radio frequency transmitter. At the receiving end it is situated in the input to the radio receiver.

The purpose of the transmitting antenna is to radiate the transmitter output power in the desired direction with as high an efficiency as possible.

Since the transmitting antenna may be situated close to a human body, (in the case of a transmitting system carried by a mobile subject), it is desirable to study the influence of the human body on the performance of the antenna.

5.11.1 Effect of Human Body on the Performance of Antenna

Krupka⁽⁹⁰⁾ investigated the effects of the human body on the performance of a small sized communication system with a whip antenna in the frequency range of 30 MHz to 150 MHz.

Magoye⁽⁹¹⁾ and Buchanan et al⁽⁹²⁾ investigated the effects of the human body in the range of 45 MHz - 102 MHz at 102 MHz, 450 MHz, 800 MHz and 6 - 280 MHz respectively.

However, the effects of the human body on the performance of an antenna is studied as follows.

The proper radiation arrangement of a transmitting system, without the effect of the human body, consists of the whip antenna and the outer surface of the conductive system box. It may be schematically represented as shown in figure 5.3.

A current I_g flows from the generator to the whip radiating element and I_s is the reverse current which flows from the inner surface of the system box to the outer surface. These currents may

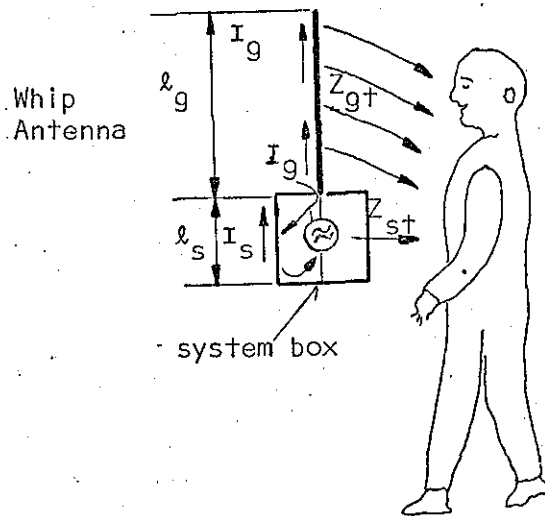


Figure 5.3

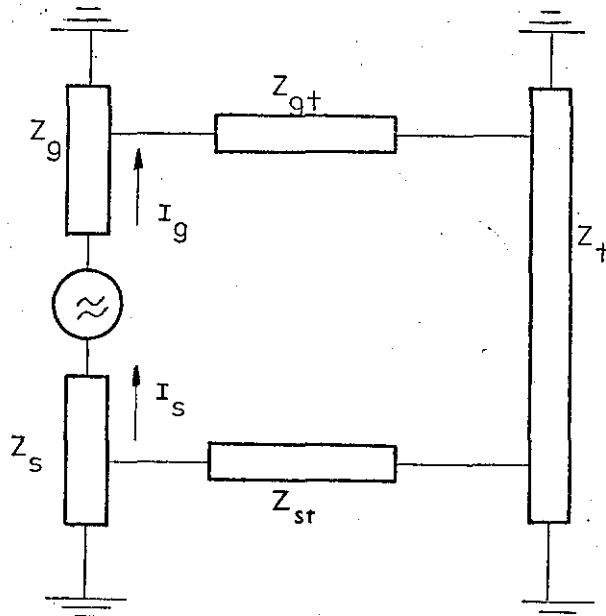


Figure 5.4

Figure 5.3 Basic Small-sized Telemetry system arrangements.

Figure 5.4 Approximate Equivalent Circuit of small-sized telemetry system in proximity to the human body.

be considered as in-phase antenna radiative currents. In principle this configuration is similar to an asymmetrical sleeve dipole. Hence the input impedance may be approximated by the sum of the upper whip antenna impedance

$$Z_g = R_g + jX_g$$

and the outer conductive box surface impedance

$$Z_s = R_s + jX_s$$

in series.

The human body is a very complex structure but from some known properties of the human tissue an equivalent electric circuit of the body can be approximated.

Schwan⁽⁹³⁾⁽⁹⁴⁾ has measured tissue impedance using d.c. and a.c. currents. Current flowing through body tissue causes local heating and other effects. The d.c. and a.c. effects observed in the body are different. The body response to a.c. currents is an indication that the body is frequency dependent. It may be deduced from this that the human body contains imperfectly conducting components which, among others, give rise to an external real resistance and are more or less distributed among components having a dielectric character. The electrical length of imperfectly conducting components has a value comparable to the wavelength of higher frequencies. Therefore, it is clear that the current flowing through them must radiate, and radiation necessitates the existence of an impedance. Hence, it may be supposed that the human body is electrically equivalent to a circuit consisting of :

- 1) A real dissipative resistance (R_d)
- 2) A real radiation resistance R_r
- 3) A reactance jX_r

The detailed information concerning the values of these three impedance components is not obtainable. It may be reasoned that R_r and $R_d \neq 0$ and jX_+ as an antenna reactance may take on various positive and negative values including zero in its dependence on frequency. An interesting assumption is that $jX_+ = 0$ for a certain frequency. This may be considered as a "human body resonance". On the above assumption a human body represents a radiating element for higher frequencies, surrounded or permeated by a dielectric medium and strongly damped by a dissipative resistance. If a whip antenna is situated in close proximity to such an element, a coupling arises. Since the antenna proper consists of two elements, (the whip and the box), there also exist two different couplings.

1. Whip-to-human body coupling

It is shown in figure 5.3 and may be characterized as similar (in principle) to each of two coupled cylindrical radiating elements. The first is the whip which is a driven element and the other (the body) is a passive one. For a short distance between these elements of 0.03λ to 0.1λ in the frequency range 30 to 150 MHz, this coupling is strong.

2. Box-to-human body coupling

This coupling, from the box to the body, is shown in figure 5.3. It is mostly capacitive in nature, resembling a lumped form.

From these considerations an approximate equivalent circuit of a small sized transmitting system in proximity to the human body is established as shown in figure 5.4. The input impedance of such a system is determined by the impedance at the generator terminals of this circuit.

It also follows from these facts that a complete antenna circuit of a pocket-sized or portable system consists of two radiating elements.

1. A proper antenna circuit consisting of a whip radiator and a system box, similar to an asymmetrical sleeve dipole.
2. The subject's body.

This appears to be a two-element array built up in a rather unusual manner. Krupka⁽⁹⁰⁾ found that the human body acted as a director at frequencies below 60 MHz. That is, the maximum signal was received when the body was interposed between the transmitting and receiving antenna; while the minimum signal was received when the body was not interposing. Krupka further established that the body resonant frequency lies between 60 MHz and 80 MHz, and at 150 MHz it acted as a reflector. When acting as a reflector, the maximum signal is received without interposing the body between the transmitting and receiving antenna.

Magoye⁽⁹¹⁾ found that the body acted as a director between 45 MHz - 55 MHz and a reflector above 60 MHz including a frequency of 102 MHz. He also found that the body acted as an antenna - a poor antenna, at all the frequencies. It was a comparatively better antenna at 450 and 800 MHz than at 102 MHz.

Buchanan et al⁽⁹²⁾ also found that the body acts as a director between 6-60 MHz and a reflector above 60 MHz in the range of 6-103 MHz.

5.11.2 Problems of Biomedical Telemetry Antennae

A biomedical telemetry antenna presents certain problems when used on a mobile subject close to the body.

1. Length of Biomedical Telemetry Antenna with Respect to the Wavelength.

The antenna must be a reasonable fraction of a wavelength for it to radiate efficiently to a point in space far from the radiating elements. It is usually short with respect to the wavelength⁽⁴⁷⁾. As a result it can resonate with loading which introduces some resistance in the resonant circuit. The presence of resistance will reduce the antenna efficiency whereby r.f. power will be dissipated as heat instead of being radiated.

2. Proximity of the Antenna to the Human Body.

The effects of the human body on the performance of a biomedical telemetry antenna is described earlier.

3. Movement of Antenna

The movement of an antenna on a mobile subject varies the capacitance coupling between aerial and electrodes. This becomes more serious when the reference point of the circuit is connected to an electrode, as in the case of ECG telemetry. The body-earth capacitance in this case is seriously increased, which increases the transmission loss. Moreover, the orientation is varying, not only in time but also from case to case.

However, no theoretical considerations appear to be applicable as yet⁽⁴⁷⁾. The literature on radio propagation, though adequate for many radio transmission situations, is not adequate for even the average situation in biomedical telemetry.

Using a formula for field strength at the receiver antenna given by Buchard⁽⁹⁶⁾

$$E_o = k \cdot \frac{\sqrt{f N_t h_t h_r}}{R^2}$$

f = frequency

N_t = transmitter output power

h_t, h_r = transmitter and receiver-antenna heights

R = range

The difficulty lies with the factor k, which is a sort of antenna efficiency and is in most cases less than 0.1. The efficiency depends not only on the position of the antenna, but also on its length in proportion to the wavelength and to the subject's dimension and on the shape of the antenna.

There are various positions of mounting and types of antennae. The most commonly used biomedical telemetry antenna is a whip antenna. A vertical whip antenna allows a suitable signal to be directed outward along all directions on the surface of the earth. This can be used at the back of the subject or can be fixed (stationary) between the shoulder and waist.

Krupka⁽⁹⁰⁾ carried out transmission measurements with a whip antenna at various positions and heights. He established that the gain of any antenna system is determined by two factors.

- (a) Antenna directivity
- (b) Antenna efficiency

The antenna directivity cannot be expected to be high, for the most part it should be close to that of a dipole, efficiency should therefore play the main role. The antenna efficiency is affected by the magnitude of radiation and dissipative resistances

(given in the last section), the magnitude of the coupling impedance (between the antenna circuit and the body), and the general circuit configuration. The efficiency may be improved by the increase of the radiation resistance R_g of the radiating element. That is, by a prolongation of the element length. R_g reaches its maximum when the whip antenna operates in the region of first parallel resonance.

A cable from the waist to shoulder can be used as an antenna for biomedical telemetry systems.

Shepherd and Chaney⁽⁹⁷⁾ recommended an earpiece cable connected to a ferrite core as the best construction for a frequency of 40 MHz.

In some situations, such as the personal ECG transmission where biomedical telemetry systems are required, the antenna severely limits the achievable antenna efficiency. A protruding antenna which changes a person's outline may be dangerous during the movement of the subject.

Magoye found that at 102 MHz, the physical size of the driven antenna is such that it is most inconvenient for the subject to carry. However, modified forms like the Marconi and loaded antennae could be used. He also found that at 450 MHz and 800 MHz (and other higher frequencies) the size of the driven element is small compared with the height of the subject and when these antennae are used, virtually no restriction is placed on the movement of the subject.

On the basis of his work he suggested that 450 MHz and 800 MHz frequencies are preferable to 102 MHz allocated by the Post Office (in the U.K.) for biomedical telemetry.

Krupka justifies the use of this frequency but Kupier's⁽⁹⁸⁾ experience indicates the opposite. He found that at the higher frequencies the transmission performance is of inferior quality, but the quality of reception can be optimised.

5.11.3 Receiving Antenna

In some ways the receiving antenna does not present as many problems as the transmitting antenna. This is mainly due to the situation and mounting position. In normal circumstances the receiving antenna is not moved and will not be close to any medium which can have any effect on the electromagnetic radiation.

CHAPTER 6PRACTICAL SYSTEM6. Introduction

The multichannel biomedical telemetry system to be described is a four channel system using delta modulators as the encoders for analogue signals from transducers. The physiological data from different channels are multiplexed by time division and may be telemetered by radio or a line link. Both essentially consist of a transmitting and receiving system.

The transmitting system to be described refers to the whole unit. This encodes the input physiological signals, the coded signals are then multiplexed and combined with a synchronisation pulse to form a time division multiplexed signal to be telemetered.

Similarly the receiving system refers to the whole unit which receives the time division multiplexed signal from the transmitting link, demultiplexes and decodes it to obtain the analogue signals.

6.1 Design of the System

In order to design and construct a compact portable multi-channel biomedical telemetry system the following points were taken into consideration:

1. The system was designed and constructed so that the circuitry was kept simple with minimum components to reduce the size and power consumption. The low power TTL micrologic available at that time was used to implement the circuitry.
2. The frequency for the transmission of the biomedical signals via a radio link was chosen to be between 102.2 MHz and 102.4 MHz. for class III devices as allocated by the Post Office in the U.K. This range lies in the domestic frequency modulation range of transmission (88-108 MHz). Hence a domestic FM receiver was used to receive the transmitted biomedical data.

3. The important frequencies (given below) associated with the system based on delta modulation for telemetering biomedical data were chosen as follows:

- (i) The bandwidth of the low pass filter in the decoder of the delta modulator (f_o)
- (ii) The clock frequency (f_s)
- (iii) The characteristic frequency (f_c) or the break frequency of the overload characteristic. (That is of the RC circuit in the feedback loop).

(i) Bandwidth of the Low Pass Filter (f_o)

The expression for the signal-to-noise ratio in terms of filter bandwidth (f_o) and other frequencies as derived in Chapter 3 is given by

$$\frac{S}{N_q}^2 = \frac{3}{8\pi^2} \frac{f_s^3}{f_o f_m^2} \quad (5.1)$$

This shows that the signal-to-noise ratio of the delta modulator improves by 3 db/octave with a decrease in the filter bandwidth (f_o). Hence the bandwidth of the filter is chosen to be as small as possible which makes it equal to the highest frequency in the input signal.

Most of the biomedical signals except the electromyogram (EMG) have a frequency range below 100 Hz. However, for clinical investigations the frequency range of the EMG can be taken to be quite adequate between 50 Hz and 200 Hz⁽⁵²⁾. As a result, the bandwidth of the filter in the decoder of the delta modulator was chosen to be 200 Hz.

(ii) Sampling or Clock Frequency

Having decided the bandwidth of the low pass filter in the decoder or the spectrum of the input signal to be coded the sampling frequency (f_s) was chosen as follows:

The expression for signal to noise ratio (equation 5.1) shows that the signal to noise ratio increases by 9 db/octave with increase of f_s . Hence for higher input signal to noise ratio and large amplitude range the sampling frequency is increased but that increases the bandwidth of the system. The sampling frequency is also related to the quantization step size (d) of the integrator as

$$f_s = \frac{2 f_c v}{d} \quad f_c = \frac{1}{2\pi RC}$$

For a fixed value of f_o and v , an increase of f_s decreases the step voltage but contributes to the slope overload noise. While higher values of the step voltage and hence smaller values of the sampling frequency contribute to the quantization noise. Hence in a practical system the value of f_s is chosen to provide a balance between quantization noise and overload noise. The value of f_s was chosen to be 20 times the highest frequency in the spectrum of the input signal to be coded. For each channel the sampling frequency was taken to be 4 kHz. Since the frequency of the synchronisation pulse is equal to the bandwidth of one channel, the frequency of the master clock in a four channel system was fixed as 20 kHz.

(iii) Characteristic Frequency of RC Integrator

In the basic delta modulator f_c is chosen in accordance with the spectrum of the input signal. The spectrum of the input signal has two features to be taken into consideration. First it has the maximum

permissible amplitude set by the condition to avoid overloading, secondly it represents the highest input frequency that would be accommodated in a practical system. This is due to the overload characteristic of the delta modulator with an RC integrator. In practice it is desirable to work as closely as possible to the overload condition in order that the signal-to-noise ratio may be kept as high as possible. Hence f_c is made equal to the highest frequency in the input signal at which its amplitude just overloads and beyond this frequency the amplitude of the signal falls.

However, an expression for dynamic range in terms of f_c as derived in Chapter 3 is given by

$$\frac{V_{\max}}{V_{\min}} = \frac{f_s}{\pi(f_c^2 + f_m^2)^{\frac{1}{2}}}$$

This expression shows that for a higher f_c , a lower amplitude range (the ratio of the sinusoidal amplitude which must causes overload, to the threshold amplitude) is obtained. The overload characteristic of the RC integrator shows that a higher f_c allows a larger amplitude of the input signal to be accommodated for a given frequency.

Lower values of f_c give a better dynamic range and improve on the signal-to-noise ratio, especially when the input signal is subject to amplitude limiting.

Hence the choice of f_c is a compromise. For the delta modulator to have an approximate slope overload characteristic for all frequencies in the spectrum of the input signal, it was chosen to be equal to 8 Hz.

6.2 Transmitting System

In the case of the multichannel transmitting system, using the radio link, the encoded time division multiplexed signal frequency modulates the carrier. The transmitting system consisted of the following and is shown in figure 6.1.

1. Transducers and signal conditioners
2. Encoders
3. Clock
4. Multiplexing unit and combining circuit
5. Transmitting link

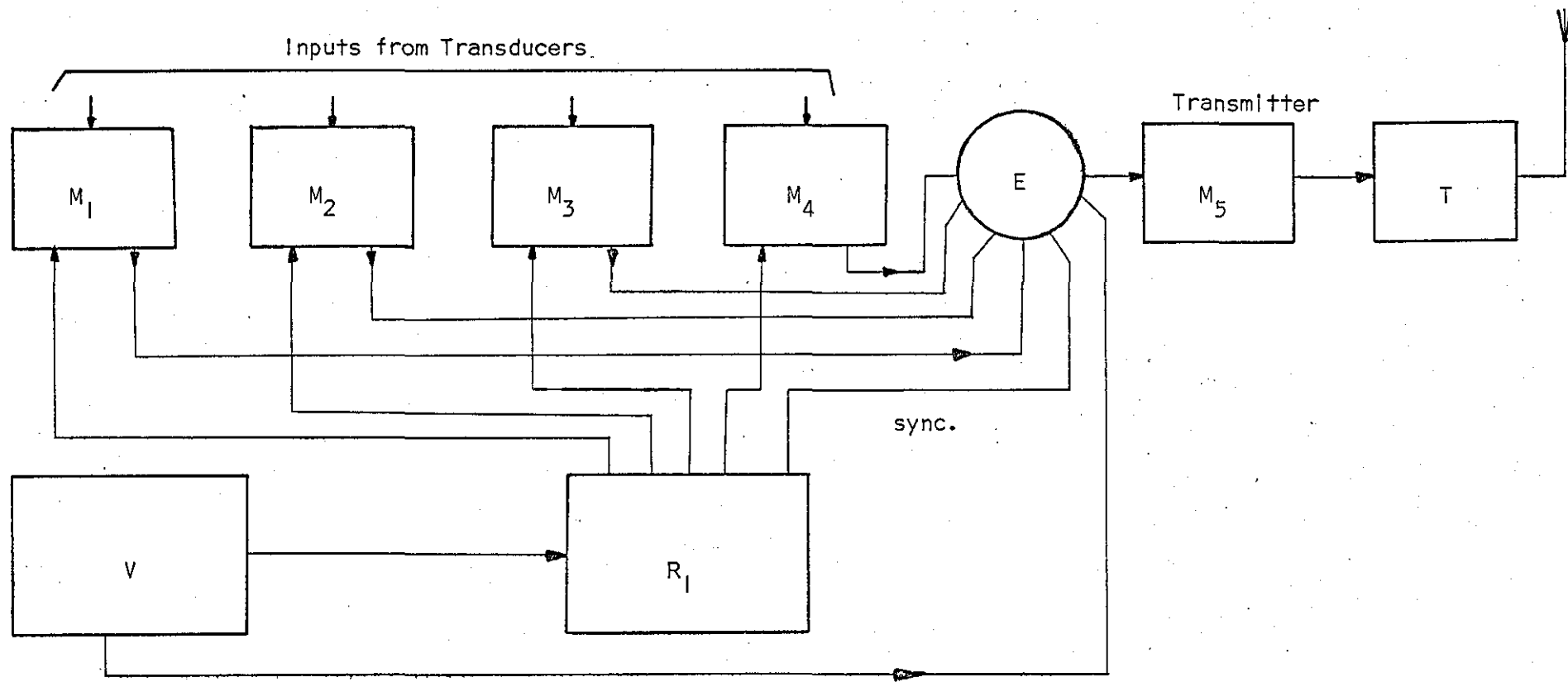
6.2.1 Electrodes and Signal Conditioners

The electrodes and transducers used to acquire the biomedical signals are described in Chapter 2. The signals obtained by using these electrodes often need to be properly amplified before coding. The amplifier used for this purpose is also described in Chapter 2.

6.2.2 Encoders (Modulators)

The analogue biomedical signals obtained are amplified and need to be coded in a suitable form prior to actual transmission. The coder used in this multichannel system is a delta modulator for each channel. The delta modulator or modified delta modulator as used is described in Chapter 3.

The practical modified delta modulator uses an operational amplifier as the amplitude quantiser and comparator, a D-type flip flop with an RC integrator as a zero order sample and hold circuit, two resistors as a Kirchoff's adder and a reference voltage. This is shown in figure 6.2 with the values of components.



- | | |
|---|---------------------------------|
| $M_1 - M_4$ Encoders (Delta Modulators) | E - Combining Unit |
| V - Astable Flip Flop as Clock | M_5 - Frequency Modulator |
| R_1 - Ring Counter | T - Radio Frequency Transmitter |

Figure 6.1 A Block Diagram of Four Channel Transmitting System.

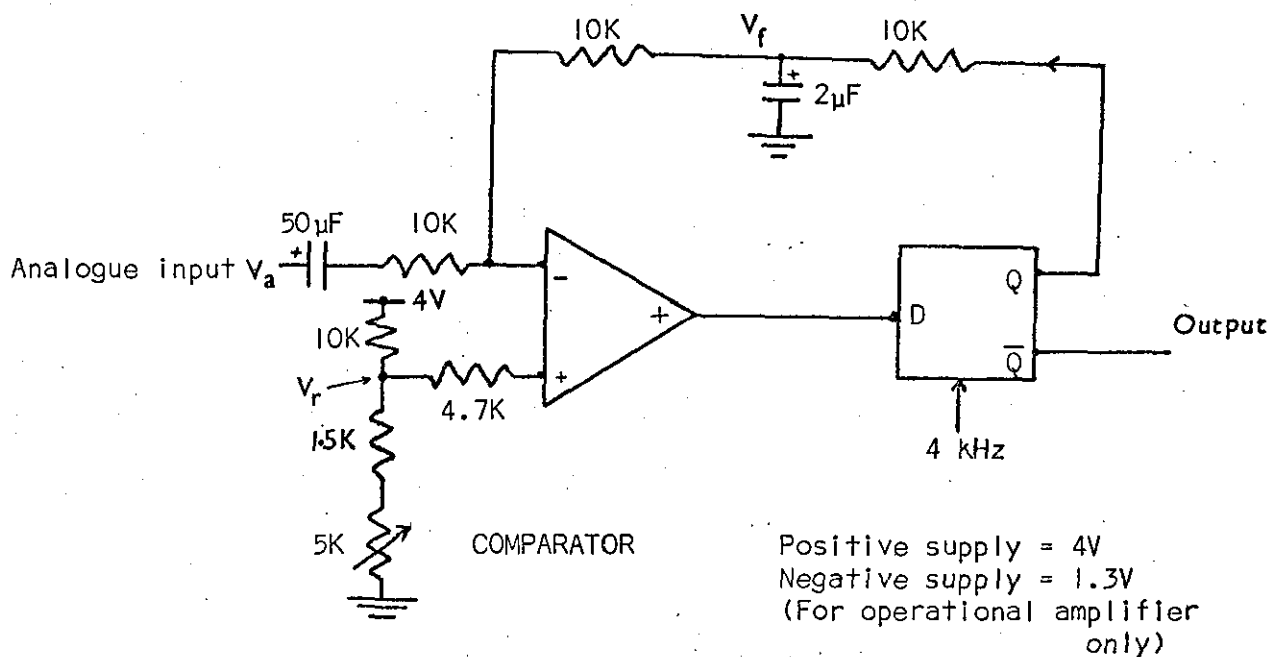


Figure 6.2 Practical Delta Modulator.

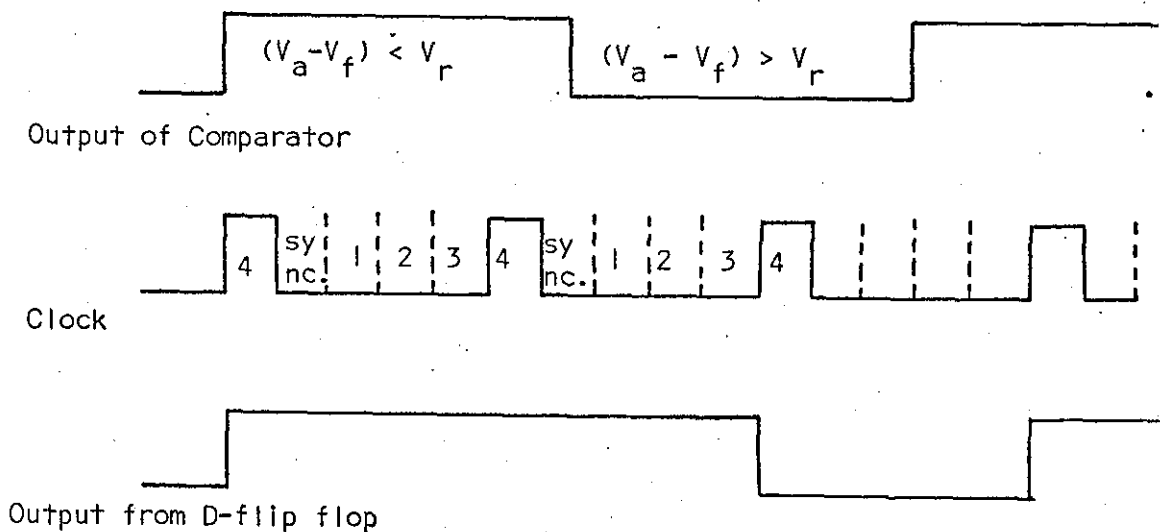


Figure 6.3 Waveform of Delta Modulator.

The digital output from the D flip flop is integrated by the RC integrator. Instead of using a subtractor to form an error, an adder is used and the zero state of the flip flop is fed back to the RC circuit. The voltage across the capacitor is presented to one half of the Kirchoff's adder, the other input to this adder is compared with the reference voltage in the comparator and, depending on whether the difference is greater or smaller than the reference voltage, one or zero is transmitted. While the flip flop receives its next pulse, it takes the state of the comparator as shown in figure 6.3. Dual in-line packages (DIP) are used (Hoare, Ivison and Qazi)⁽⁹⁹⁾ to achieve a small and low power system.

6.2.3 Clock

The clock initiates the action of the ring counter which in turn provides a clock pulse for the sample and hold circuit of the modified delta modulator. The clock also helps to provide a synchronisation pulse in the time division multiplexed signal for a multichannel system. The frequency of the clock should be short term stable, and immune to changes in temperature and power supply variations. A multivibrator circuit can normally fulfil the requirements of a clock but its circuitry involves more components and hence uses more power. It is also more sensitive to the changes of temperature and power supply variations. Various other circuits were tried to obtain the characteristics mentioned above.

Practical Circuit

Finally the practical circuit was developed and used as shown in figure 6.4. It makes use of two of the four gates in one single Integrated Circuit (IC) circuit SN7400LN. This IC is a quadruple 2-input nand gate and is a low power TTL logic Dual-in-line package.

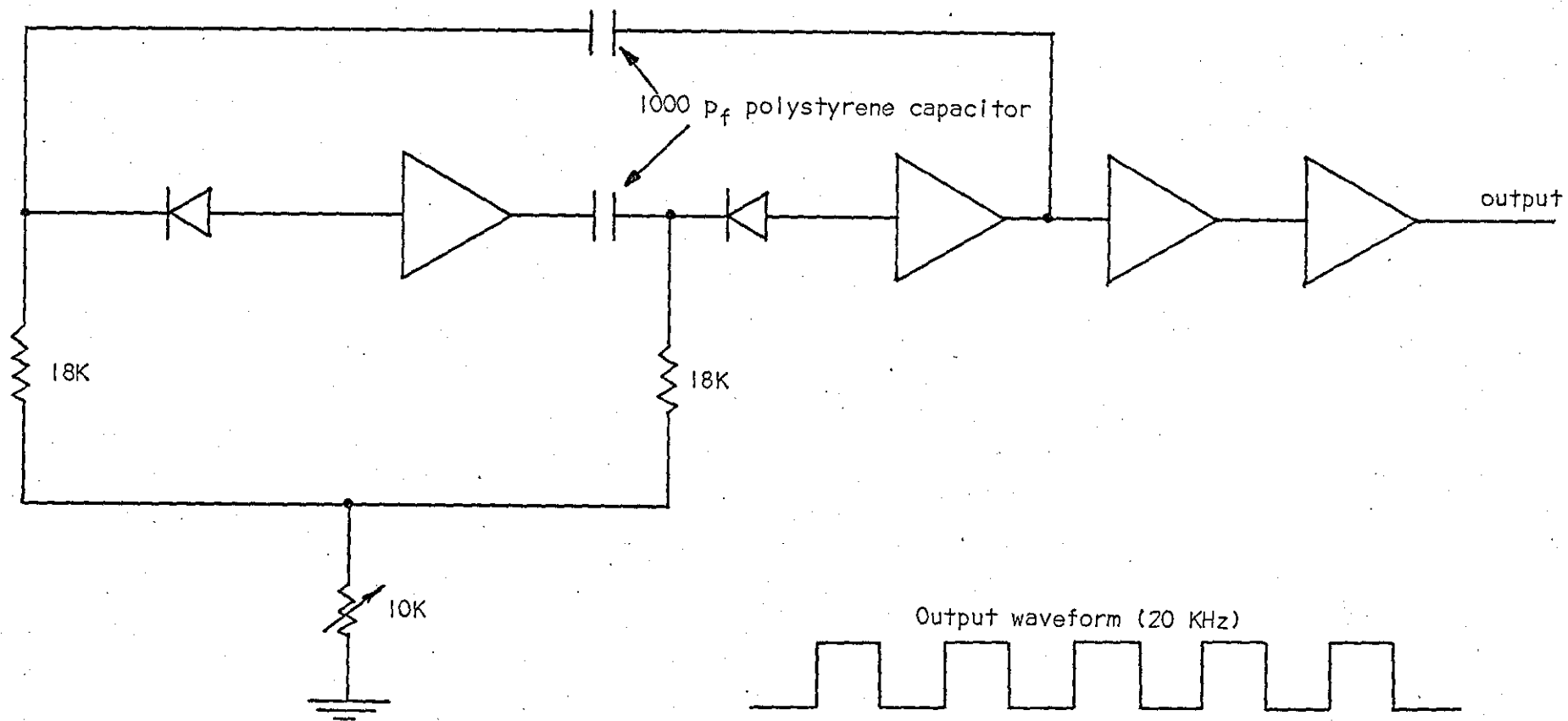


Figure 6.4 Low Power Astable Multivibrator used as a Clock

The effect of temperature on the frequency is shown as follows:-

At ambient temperature (23°C) frequency = 20.00 kHz.

At 48°C frequency = 20.45 kHz

At 60°C frequency = 20.88 kHz

Supply voltage = 4V

Current consumed = 0.72 mA

The effect of these temperature variations on frequency was better than with the other circuits tried. The potentiometer (10 kohms) was used to adjust any variations in the frequency required.

6.2.4 Multiplexing Unit

A time division multiplexing unit is basically a counting or sequencing device and a combining unit. The sequencing is accomplished by using an electronic counter and the combining unit uses NOR gating circuits.

A chain of binaries in which the first is coupled to the second, the second to the third, and so on, with the last coupled back to the first, is called a ring counter. In such a counter each binary device receives its triggering signal directly from the external triggering source. The coupling between the flip flop is not for the purpose of triggering but rather for the purpose of favouring or priming only one binary so that it alone will respond to the triggering signal. One stage of a ring counter is in the state one (1) and all other stages are in the state zero (0). With each successive trigger the '1' state moves to the following flip flop.

The time division scanning is obtained by the master frame generator driven from the system clock. Hence the sequential pulsing unit fed from the frame rate generator is therefore held to the system clock frequency.

The other aspect of the time division multiplexing system which is required in the simple system, is one synchronisation pulse transmitted per frame to give the reference to which the remainder of the frame is locked.

A Nand gate is connected to the output of each individual flip flop in the counter. The number of flip flops (stages) in the counter corresponds to the number of channels. When the desired number has been reached, forming one complete cycle of the counter, the output of the Nand gate inhibits the input to the counter. The output of the Nand gate is used to provide a signal to the start of the counter and is used as a synchronisation pulse for one cycle.

Practical Circuit

The four D flip flop SN74L74N, connected as in figure 6.5 forms the four stages of the ring counter. The input to the first stage of the counter is obtained by anding the inverted output of each D flip flop in the counter. Each flip flop of the counter is supplied with the trigger pulse from the master clock (20 kHz) of the system. The Nand gate used is an SN74L20N and its output is inverted to provide a synchronisation pulse.

6.2.5 Combining Unit

As mentioned earlier a time division multiplexed signal is a composite signal composed of a number of data channels and a synchronising pulse, each appearing at a time slot allocated for it. The signals to be multiplexed are the outputs of the delta modulators and the synchronisation pulse. The outputs of the delta modulators are supplied with a clock pulse generated from the D flip flops and sequenced by a ring counter. Each cycle of the ring counter clocks once each channel delta modulator. When each delta

modulator is clocked the output is logically 'ANDED' with the clock signal. This is further combined with a synchronising pulse achieved via a logical 'OR' gate to form a composite signal. On each cycle of the ring counter a 'one' is always present at the multiplexed signal in the synchronisation position. The signal obtained is transmitted on the radio link or line link. The four channel encoder and multiplexer is shown in figure 6.5.

Practical Circuit

The output of each delta modulator is gated with the corresponding clock obtained from the output of the counter. The SN7400LN microcircuit, having four gates on one IC, is used for four channels. The output of these gates is combined by using a SN 7420N and finally a SN7400LN is again used to form a composite time division multiplexed signal.

6.3 Modulator and Radio Frequency Transmitter

The time division multiplexed signal in this multichannel system is to be sent either via a radio or a line link. Various types of modulation can be used for the radio link as described in Chapter 5. Due to the advantages mentioned in Chapter 5, narrowband frequency modulation is used as a mode of transmission for the time division multiplexed system.

The time division multiplexed signal is coupled to the radio frequency transmitter via a coupling network and modulates the carrier generated in the radio frequency oscillator. This is shown in figure 6.6.

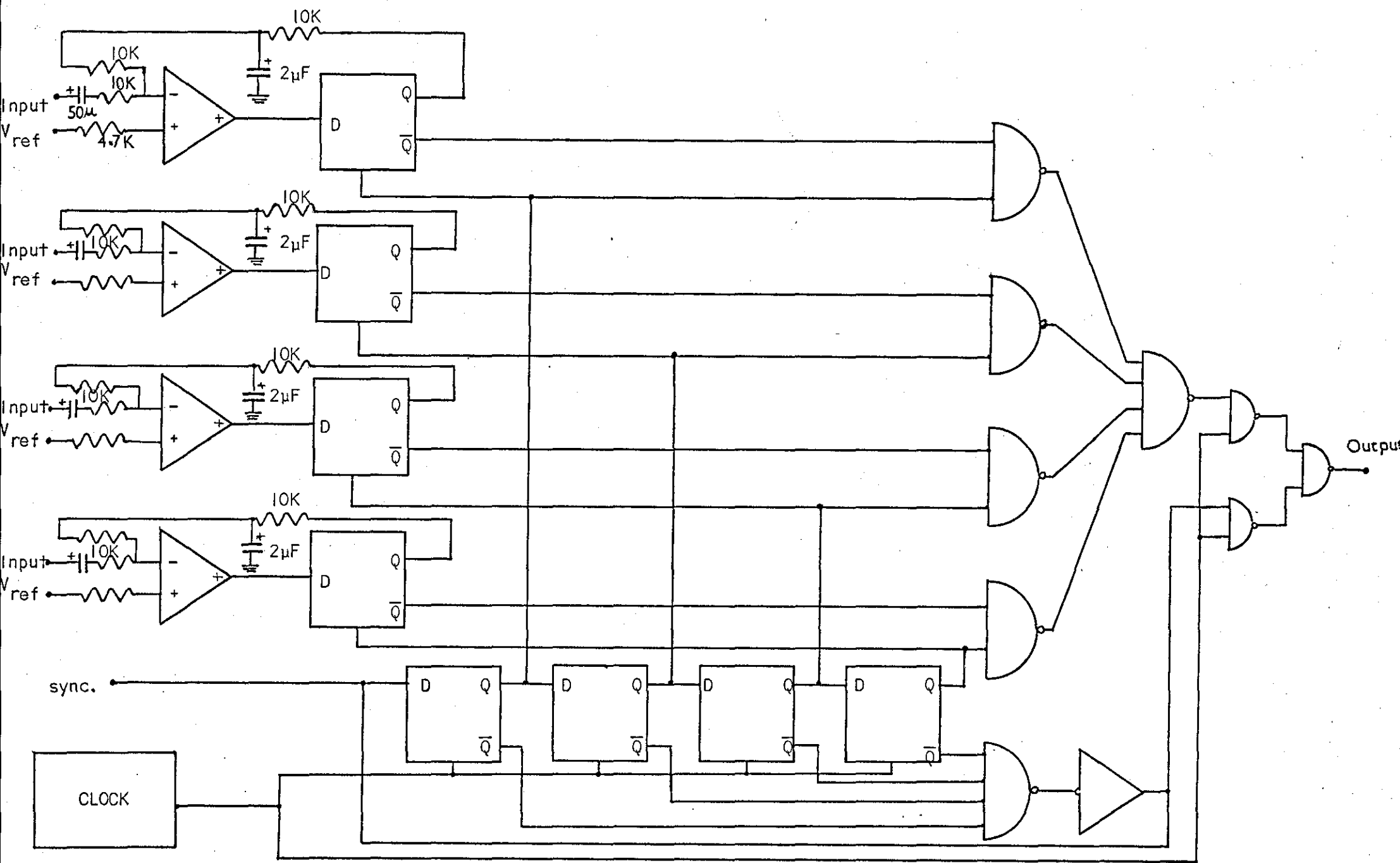


Figure 6.5 Four Channel Encoder and Time Division Multiplexer.

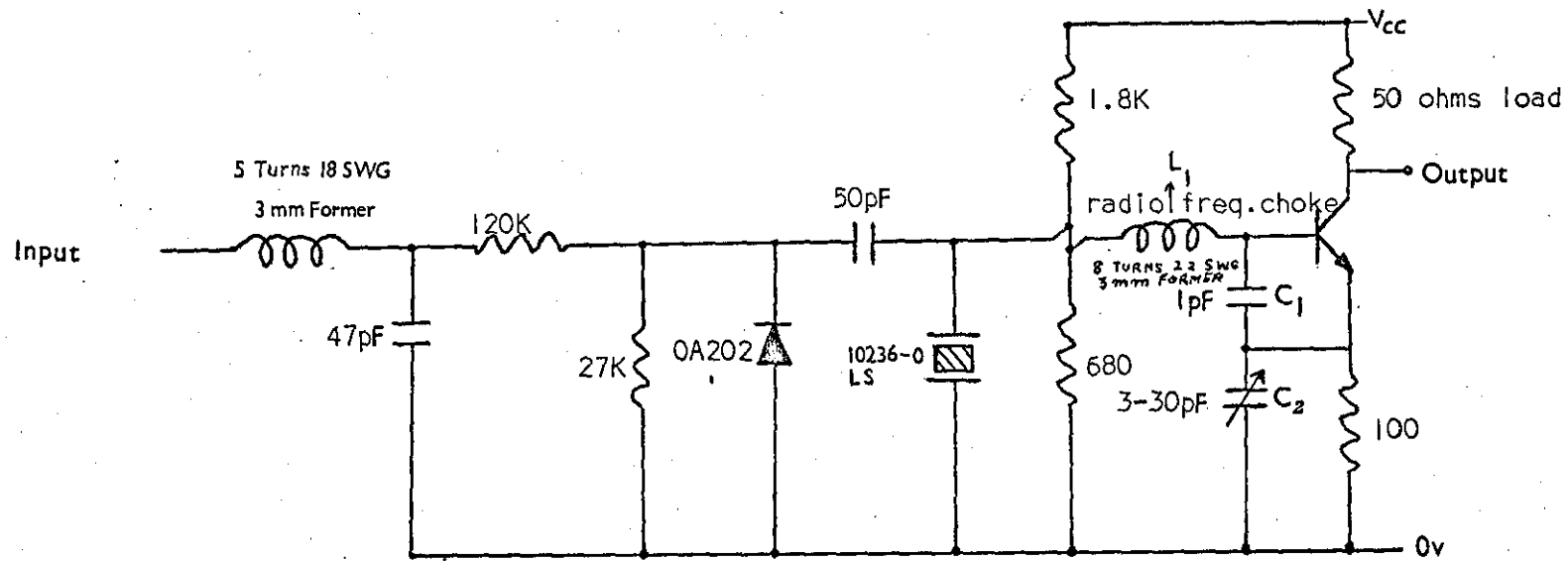


Figure 6.6 Coupling Network, Modulator and Radio Frequency Oscillator.

6.3.1 Radio Frequency Oscillator

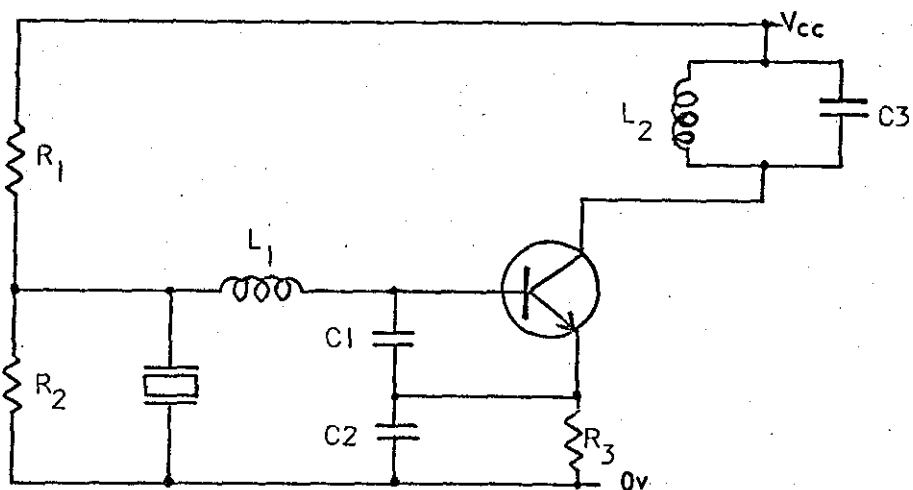
It consists of a crystal controlled oscillator where the crystal oscillates at the series resonance of the fifth overtone with a frequency of 102.35 MHz. The crystal controlled oscillator gives a better frequency stability. The circuitry used is that of a derived Colpitts oscillator.

The inductance L_1 together with the capacitance C_1 and C_2 in series makes the series selector tank circuit oscillate at the fifth overtone, in series resonance with a frequency of 102 MHz. This is shown in figure 6.7. The base-emitter capacitance C_1 , in conjunction with C_2 forms an impedance divider. By neglecting the earth connections, C_1 and C_2 can be taken in series with the crystal and feedback occurs between the emitter and the base of the transistor through the crystal. C_1 also acts to minimise the effects of transistor junction capacitance on the frequency of oscillation.

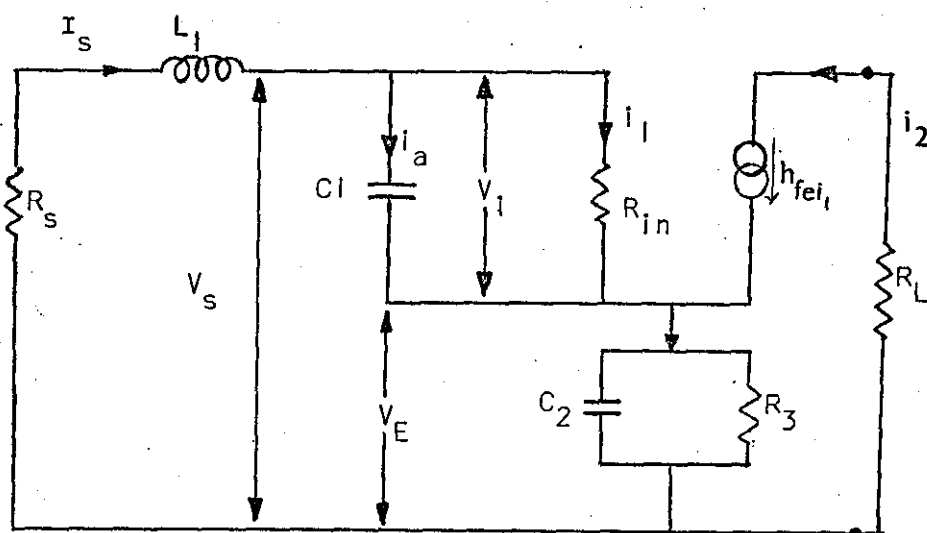
Practical Circuit

The frequency modulated transmitter consists of a crystal controlled oscillator, modulating circuit, coupling, and matching circuit to the antenna. As mentioned earlier, a frequency modulated system works on the principle that the frequency of the radiated signal is deviated from the central carrier frequency by an amount proportional to the instantaneous amplitude.

One way of achieving this is to deviate the frequency of the resonant circuit of the carrier oscillator by the modulating signal, using a voltage variable capacitor connected across the tuned circuit of the transmitter oscillator.



(a) 102 MHz Crystal Controlled Oscillator.



(b) A.C. Equivalent circuit of 102 MHz Oscillator

Figure 6.7

A reverse biased semiconductor diode has a depletion layer that acts as a capacitor. The capacitance value of this depletion layer depends on the value of the applied voltage. Junctions can be designed to have a large value of capacitance that can be varied over a wide range by comparatively small voltage changes. Since a small deviation in the carrier only is required to achieve a narrow-band frequency modulation, an ordinary reverse bias diode is used for this purpose.

The carrier frequency oscillator, as described earlier, is a crystal controlled derived Colpitts oscillator. It is usually more difficult to deviate the oscillator frequency by varying the capacitance across the tank circuit. However, varying the voltage across the diode with the modulating signal causes the instantaneous capacitance to vary in sympathy and deviate the carrier frequency enough for our purpose.

Direct narrowband frequency modulation is obtained when an oscillator is modulated by the variable voltage capacitor. The circuit used is shown in figure 6.6. The output from the combining unit is applied to the crystal controlled oscillator via a coupling network shown in fig. 6.6. The analysis for the oscillator is given in Appendix I. The digital multiplexed signal is coupled by a choke and a capacitor to earth, to remove any high frequency component present in the signal. The two resistors, forming a potentiometer network, are used to bring the varying input signal voltage to a suitable value to be applied to the reverse biased diode. The varying signal voltage applied across the diode changes the capacitance and hence deviates the frequency of the crystal controlled oscillator. A 3-30 PF

variable capacitor is used to adjust the frequency of the oscillator. In order to reduce the interference from the oscillator to the modulators, it is necessary to keep the two units at some distance.

6.3.2 Coupling and Matching of the Antenna

With an effective tank circuit, Q , of 12 or thereabouts in the transmitter, the impedance ratio at resonance to that at the overtone frequencies is not very high. As a result there develops a harmonic voltage for radiation purposes across the circuit. The modern regulation permits a maximum radiated level of 40 db below fundamental or 200 mW (whichever is less) for individual harmonics. To comply with this it is necessary to devise an antenna coupling circuit which discriminates against the higher frequencies. Also, the place where radio frequency power is generated is very frequently not the place where it is to be utilised. This is the case with the transmitter and antenna. In order to transfer the maximum power, a matching or coupling network to the antenna is used in the transmitter, as shown in figure 6.8. The coupling is achieved by another resonant circuit. In order to remove very high frequencies produced due to overtones, one end of the resonant circuit is connected to earth via a 22 pF capacitance. It is also connected to the supply voltage with a radio frequency choke so that the supply voltage is only used for the D.C. biasing and operation of the transistor.

The variable capacitor can be used to tune to the antenna. From the transmitter to the antenna an impedance matching condition must exist between the output of the transmitter and antenna. Since a given antenna has a given value of impedance, some sort of impedance transformation is needed for the matching.

A number of impedance transformations exist, the choice of which depends on the antenna impedance, the transmitter output impedance and the frequency, etc. of operation.

The method used here is the tapping of the capacitance of a parallel LC resonant circuit situated in the output of the transmitter. This is shown in figure 6.9. The equivalent circuit of the matching unit is also shown. It can be shown that

$$\frac{Z_{2,3}}{Z_{1,3}} \approx \left(\frac{C_1}{(C_1 + C_2)} \right)^2$$

The antenna (monopole) is connected at the point common to both capacitors connected in series. The tuned circuit serves the double purpose of the matching unit and also for selecting the carrier frequency. These two functions of the circuit can be expressed mathematically

$$f_0 = \frac{1}{2\pi} \sqrt{\frac{(C_1 + C_2)}{LC_1 C_2}}$$

f_0 is the transmitter centre frequency 102 MHz.

$$Z_{out} = \left(\frac{C_1 + C_2}{C_1} \right)^2 Z_L$$

If R_L is the load (i.e. aerial) resistance, R_{out} is the output impedance of the transmitter at anti-resonance, then

$$R_{out} = \left(\frac{C_1 + C_2}{C_1} \right)^2 R_L$$

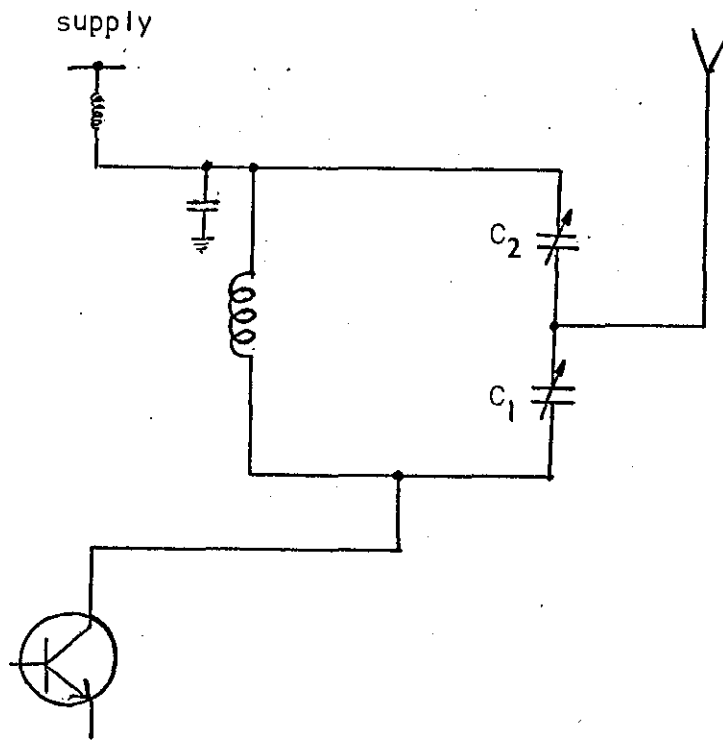


Figure 6.8 Matching or Coupling Circuit in the Output of Transmitter.

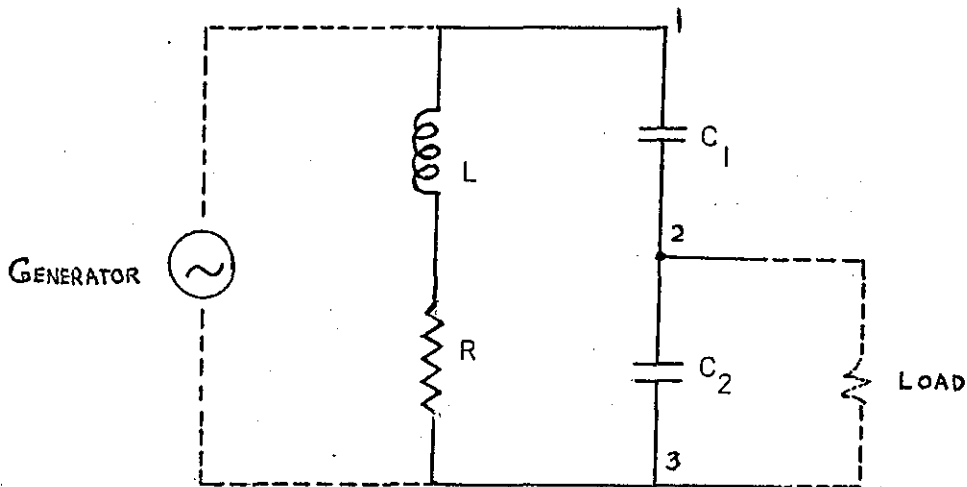


Figure 6.9 Capacitance Tapped Matching or Coupling Circuit.

6.4 Receiving System

In the case of a transmitting system using a radio link, the receiving system consisted of a FM receiver (RF/IF unit), used in conjunction with a discriminator, a waveshaping unit, a demultiplexer and decoders. This is shown in figure 6.10. The time division multiplexed signal is then applied to the JK flip flops together with a strobing signal from the ring counter which is correctly timed. The outputs from the JK flip flops are converted to analogue form by RC integrators. The high frequency components, due to the clock, are removed by passing it through the low pass filter. Hence the receiving system consists of the following:

1. RF/IF unit with discriminator
2. Waveshaping unit
3. Synchronisation unit
4. Demultiplexer
5. Decoders
6. Filters

6.4.1 FM Receiver (RF/IF Unit) and Waveshaping Unit

A Pye FM tuner was used to receive the multichannel biomedical data from the radio link and the output was taken from the output of the discriminator in the tuner. Since this output is the result of converting small changes in frequency into corresponding output voltage changes, the output obtained needs to be properly waveshaped before demultiplexing and changing it into the analogue form. Hence the waveshaping unit filters the undesired frequency components from

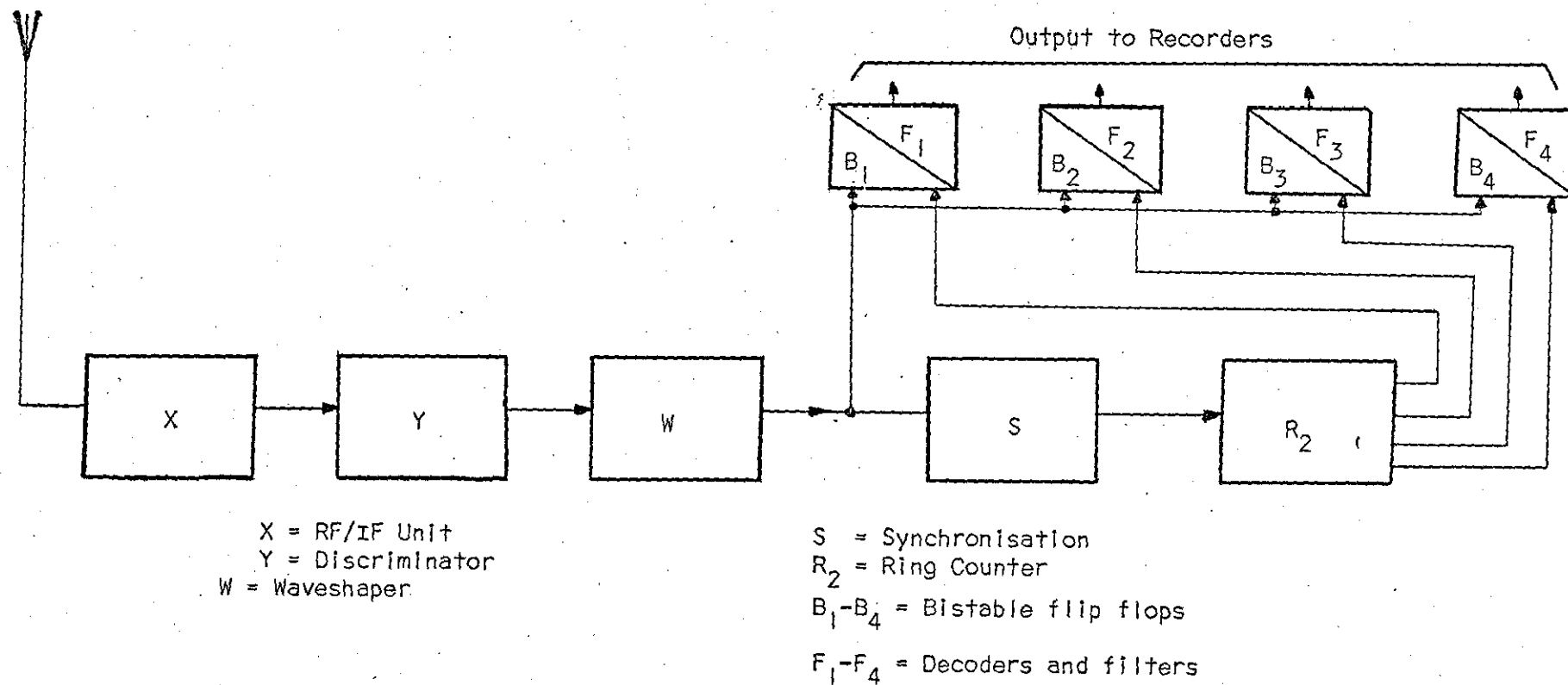
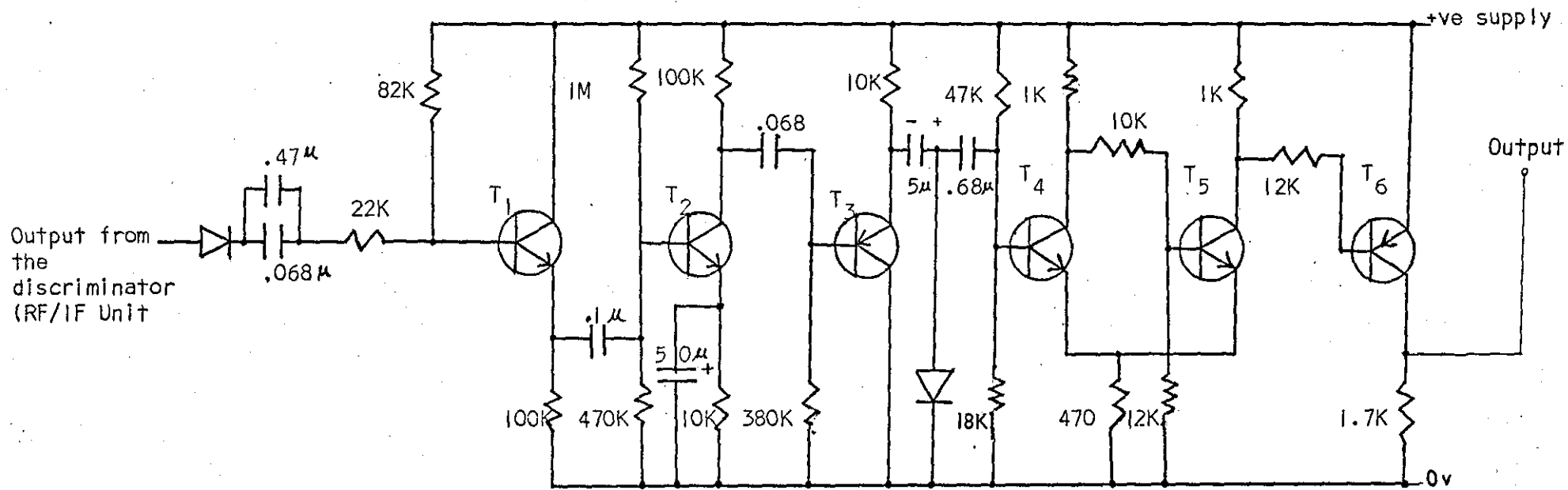


Figure 6.10 A Block Diagram of Four Channel Receiving System.



Emitter follower

Amplifier

Schmitt trigger

Inverter

- T_1, T_4, T_5 = NPN ZTX 301
- T_2 = NPN ZTX 302
- T_3, T_6 = PNP ZTX 501

Figure 6.11 Waveshaping Circuit.

the output of the discriminator, amplifies it with an A.C. coupled amplifier and changes it into square waveform using a Schmitt trigger. This is shown in figure 6.11.

Practical Circuit

The output of the discriminator is coupled to the emitter follower by a series diode and a capacitor. This ensures the D.C. level of the signal and removes the hum and low frequency components. A small capacitance across the diode filters the high frequency components.

Amplifier

An emitter follower before the amplifier serves as a buffer between the tuner discriminator and the rest of the circuitry of the receiver system. Its high input impedance minimises the loading on the receiver, while its low output impedance ensures the matching with the amplifier that follows.

The amplifier is a two stage high gain A.C. coupled amplifier. The transistor used is a ZTX 302 (NPN) for the first stage of amplification. This is followed by a ZTX 501 (PNP) transistor used for the second stage of amplification. The output of the amplifier is coupled to the Schmitt trigger via a capacitor. A diode is connected to earth to restore the D.C. value lost in the capacitor coupling.

Schmitt Trigger

The amplified signal needs to be converted to a square waveform. A Schmitt trigger employs two ZTX 301 (NPN) transistors and converts the signal into a square wave. The square waveform is inverted to match the logic circuitry to follow. The waveform is inverted by a single ZTX 501 (PNP) transistor.

6.4.2 Synchronisation and Demultiplexing

In time division working, synchronisation has to be maintained between the master rate of the multiplexing sequence and the slave rate of the related channel separation process (demultiplexing) at the receiving end. Hence the demultiplexing process is the reverse of multiplexing. In order to demultiplex correctly a synchronisation pulse is added after the completion of every group of channels in the multichannel data on the transmitting end. On the receiving end, once the data is properly synchronised or locked, the demultiplexing is simply a matter of separating the respective channels.

This is achieved by using the received data to obtain clock pulses on the receiving end and using this clock to drive a ring counter. The output of the ring counter is then used to strobe the pulses from the received multiplex data into the flip flop, and is demultiplexed. Synchronisation is achieved by allowing the ring counter to proceed only at the end of a cycle, providing a '1' is present on the received data.

The practical circuits and their operation are given in the following sections. The circuit of the four channel demultiplexer and decoder is shown in figure 6.12.

6.4.3 Clock

The clock on the receiving end is used for driving a ring counter, hence for better synchronisation the received multichannel data is used for obtaining these clock pulses. The time-division multiplexed data, having been waveshaped, is integrated to remove any spikes present, and passed through a buffer gate. It is then applied to the J-K flip-flop and the nand gate for demultiplexing and synchronisation. The time division multiplexed data is also

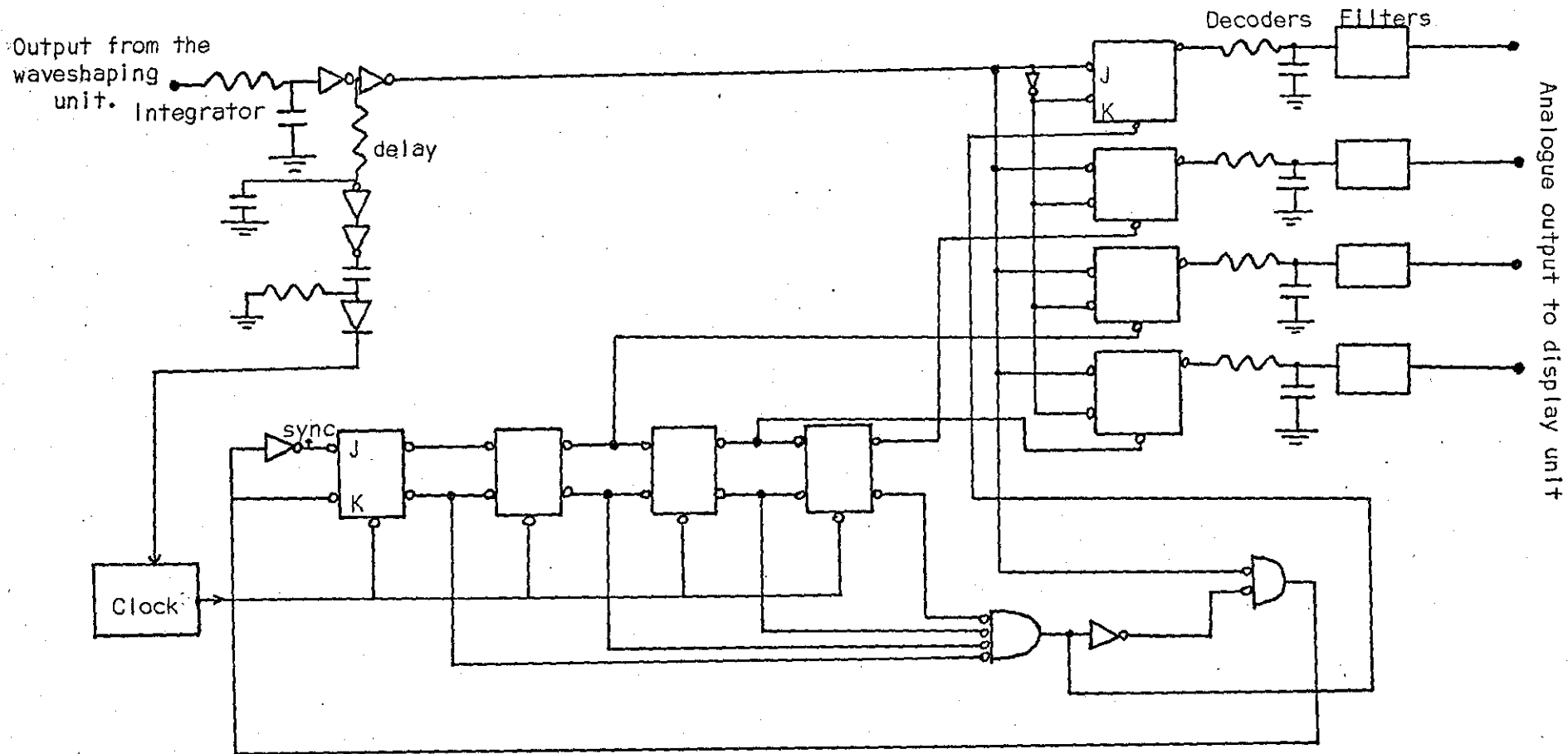


Figure 6.12 Circuit of Four Channel Demultiplexer and Decoder.

delayed to make the timing certain, differentiated and rectified to obtain only the positive pulses. This is shown in figure 6.12

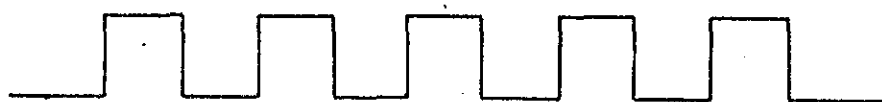
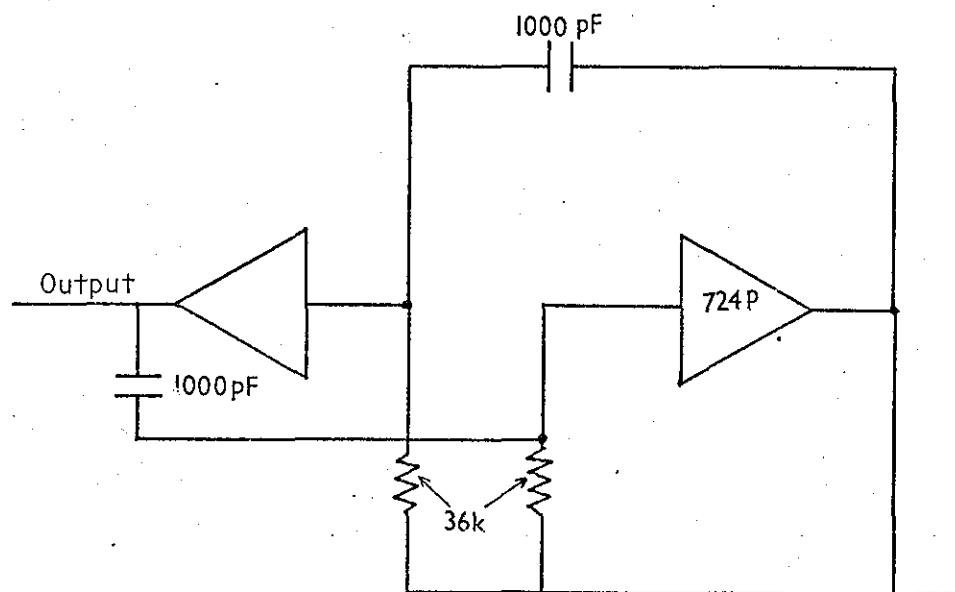
The positive pulses thus obtained are applied to the base of one of the gates in the local multivibrator used for generating the clock pulses. The clock pulses are then generated in the conventional resistance capacitance coupled multivibrator shown in figure 6.13 in accordance with the received time division multiplexed data.

The circuitry at the receiving end is not very critical for power requirements, hence the microcircuits used are of medium power resistor transistor logic (RTL). The integrated circuit (IC) used for the buffer gate is an MC 799P. The clock circuit uses MC 725 Nor gates and the values of the resistor and capacitance are chosen to give a clock frequency of 20 kHz. The remaining gates in the clock circuitry are used to buffer the output of the multivibrator for increasing the fan out.

6.4.4 Synchronisation Circuitry

The transmitting system in a time division multiplexed signal supplies a synchronisation pulse after the completion of a group of channels in the system. The synchronisation pulse in the present system is always a logical one (1) and is used on the receiving end to mark the beginning and end of every group of channels.

The synchronisation on the receiving end is obtained by a closed loop circuit in conjunction with the ring counter and two And gates. This is shown in figure 6.14.



Output waveform (20 KHz)

Figure 6.13 Clock Circuit and Waveform.

The Nand gates A and B, shown in the figure, followed by Nor gates, act as And gates. The progress of the counter is inhibited when the input to the counter is in the state One which is obtained when all the four inputs to the gate B are Ones. This state only arrives at the end of the cycle of all channels. Hence when the received signal contains a '1' at the space allocated for the synchronisation pulse, and provided that '1' is present at the other input to the gate A, an output of '1' will be obtained. This is the input to the counter and the counter will be allowed to proceed only at the end of each cycle. It is seen that with every synchronisation pulse a logic pulse opens the And gate to allow the data to be sent to the appropriate channel. The '1' present in the synchronisation process may, in certain cases, be due to the overload and data channels. In this case it usually takes a few cycles before the '1' locks to the synchronisation pulse. The probability of such a case is not very high.

6.4.5 Demultiplexer

In order to separate or demultiplex the multichannel data, sequential pulses are obtained from the outputs of the ring counter for each channel to be separated. The demultiplexing is finally achieved by using J-K flip flops, where the input to these devices is the multichannel data and clock pulses are taken from the different stages of the ring counter. The channels are separated depending upon the time of the clock pulse taken from the ring counter. The four flip flops used for the four stage ring counter are medium power logic MC 790P and the four flip flops used for the demultiplexing of the four channel data are also MC 790P. The ring counter is driven by a 20 KHz clock as mentioned before.

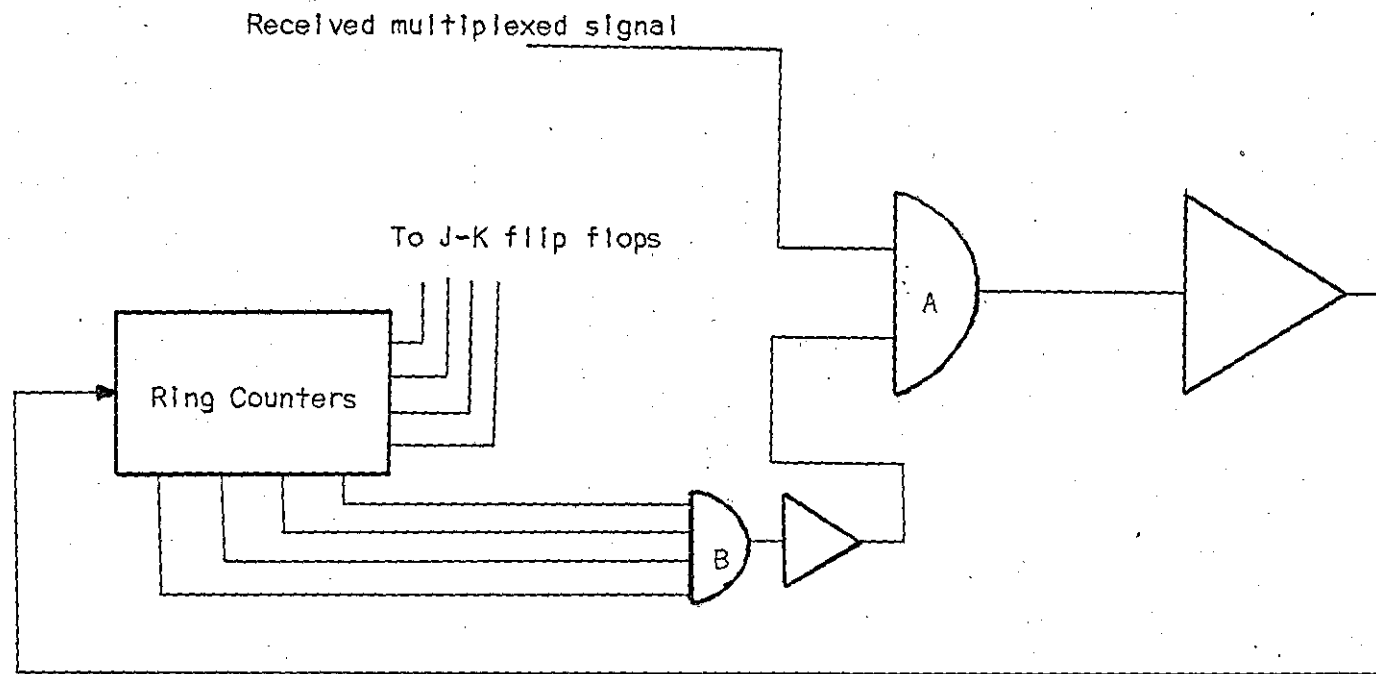


Figure 6.14 Synchronisation Circuit.

6.4.6 Decoder

The demultiplexed signal, which is still in digital form, needs to be brought into analogue form for each channel. As mentioned earlier the decoder for the signals encoded by the delta modulator is an integrator. An RC integrator is used for this purpose and it is the same in principle and circuitry as the one used in the encoder.

6.4.7 Low Pass Filter

The recovered analogue signal at the output of the decoder contains inherent high frequency components due to the high sampling frequency. A low pass filter is used to filter out these high frequency components. The bandwidth of the low pass filter is equal to the highest frequency present in the analogue signal.

The simplest type of low pass filter is the Rc network shown in fig.6.16

If the total impedance = Z

$$\text{Then } Z = \sqrt{R^2 + Z_c^2}$$

$$\text{where } Z_c = \frac{1}{2\pi f c}$$

Since the network is merely a voltage divider

$$e_{\text{out}} = Z_c/Z \cdot e_{\text{in}}$$

If A is the gain of the network

$$A = e_{\text{out}}/e_{\text{in}}$$

Filters can be directly connected to one another with little loss in effectiveness if each has the same RC product, but R is increased, as for example the one shown in figure 6.15.

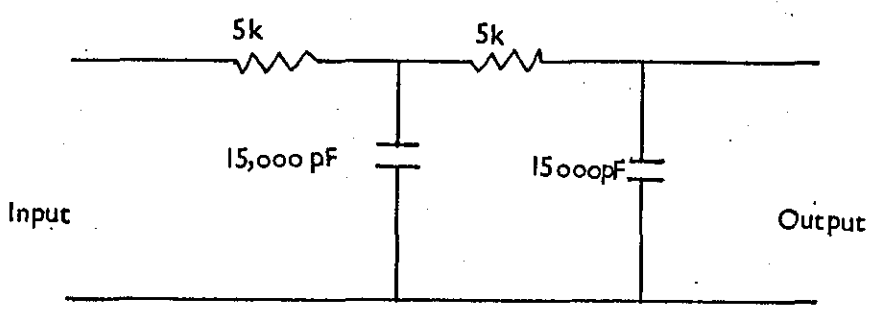


Figure 6.15 Practical Low Pass Filter.

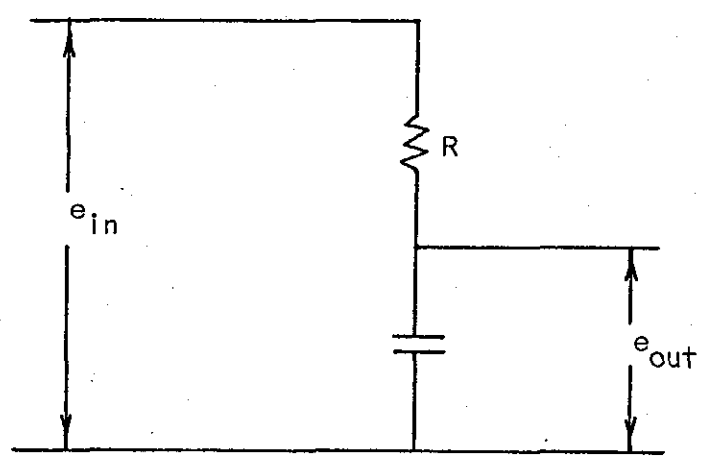


Figure 6.16 A Low Pass RC Filter.

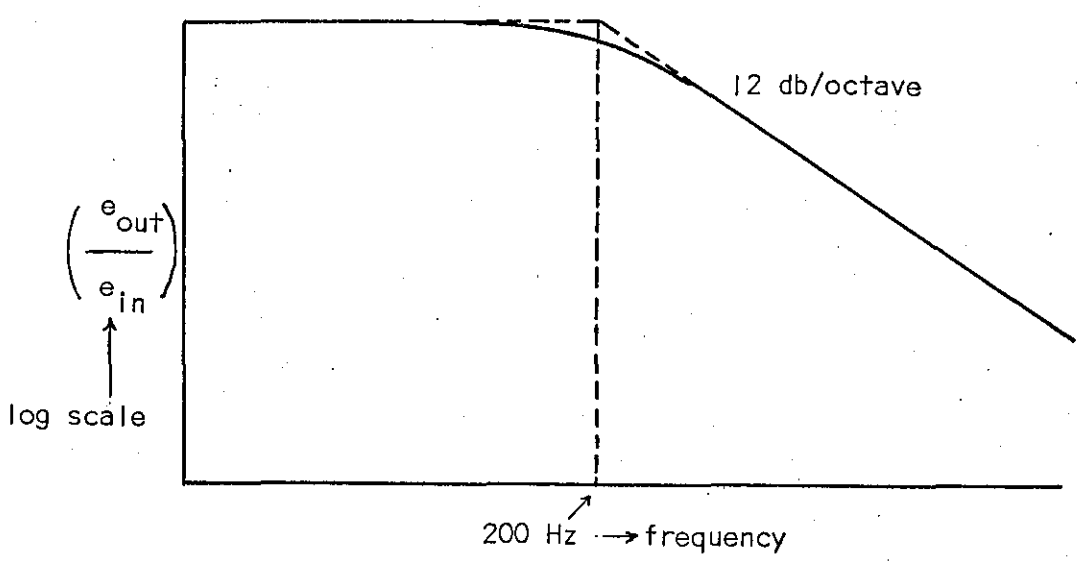


Figure 6.17 Characteristic of Low Pass RC Filter.

Practical Low Pass Filter

A simple low pass filter from discrete components was designed to filter the high frequency due to sampling. The filter designed is a π -section with a bandwidth of 200 Hz as shown in figure 6.17

6.5 Single Wire Time Division Multiplexing System

Any occasion when a wire can be attached, line telemetry is used. However, if many subjects need to be monitored in a central monitoring room in a big hospital or, if a clinic is to be connected to the central computer for on-line processing or storing the biomedical data, one of the prime requirements is the availability of many channels. A novel technique (Hoare, Qazi, Ivison)⁽¹⁰⁰⁾ is developed for obtaining many channels using a single wire and time division multiplexing (TDM). It is a digital interrogative system which works on the principle similar to the address/reply system. It is a two way transmission process where the interrogating pulses travel from the decoder (receiver) end to the encoder (transmitter) end, and the data pulses travel in the opposite direction, one at a time. The pulses travel along the line with a velocity of approximately 5ns/metre, and the fact that it is an interrogative system makes it slow for very long distance transmission.

It is anticipated that the available bandwidth per channel will be sufficiently large to overcome the problem of noise and thereby improve the threshold of encoding. For example, if 100 metres of co-axial cable is used, the clock pulse repetition rate could be 1 MHz. For twenty signals being multiplexed there would be approximately 50,000 pulses per signal. This gives a high ratio of clock pulses to maximum signal frequency for many biomedical signals.

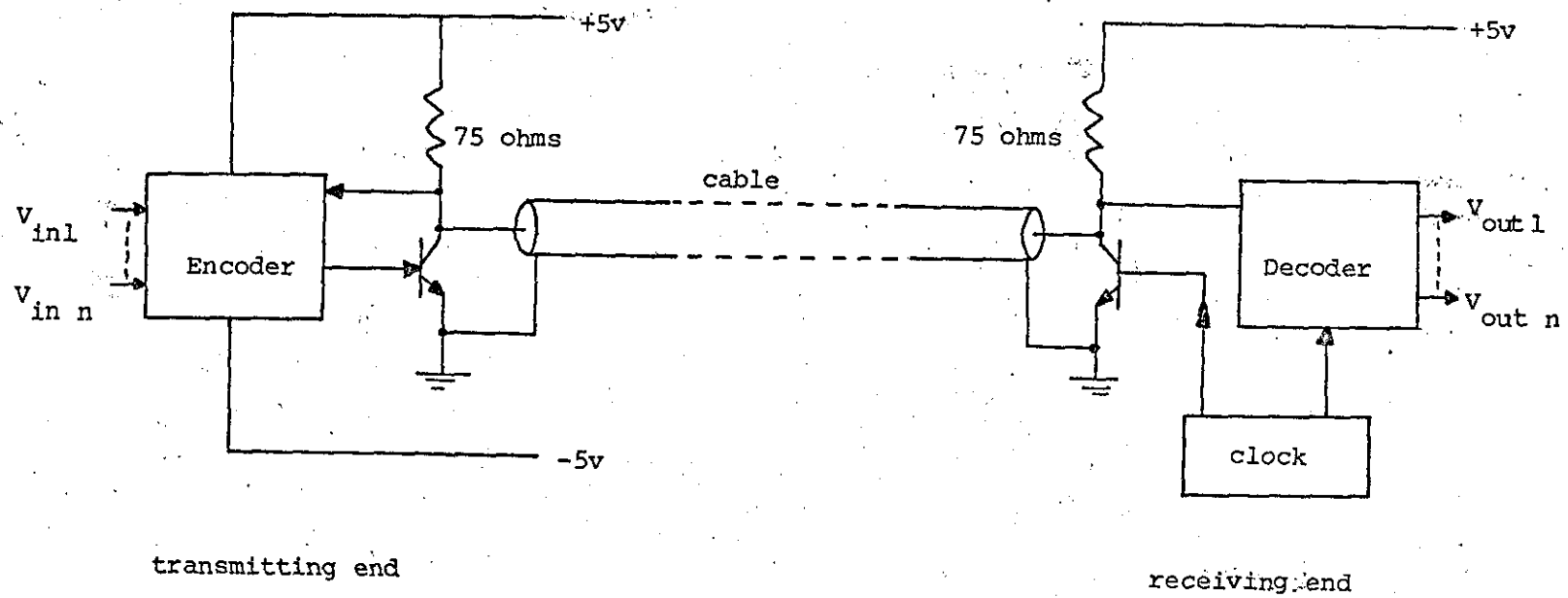


Figure 6.18 Block diagram of a single wire time division multiplexed system

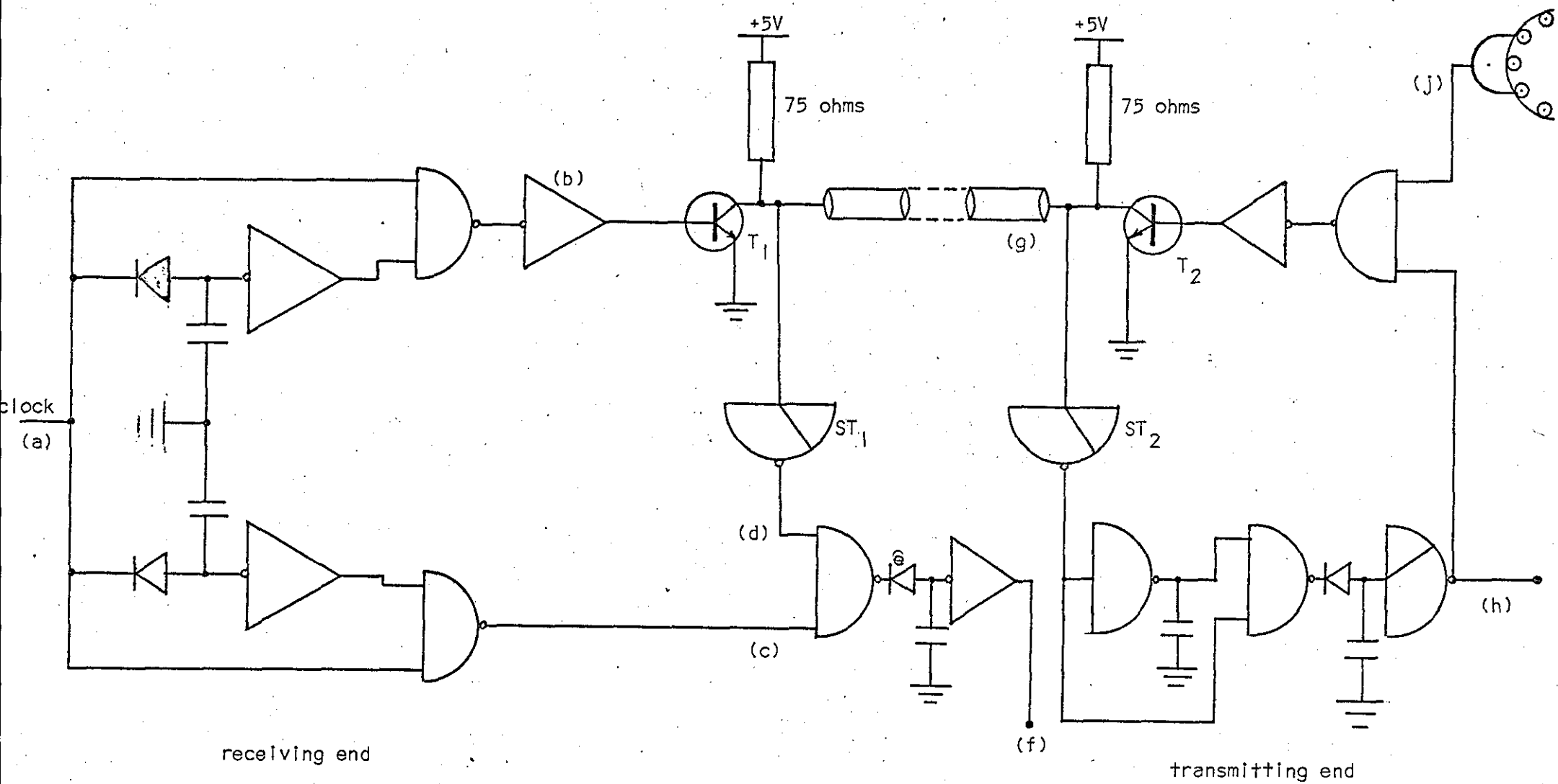


Figure 6.19 Cable and Control Circuits for Single-wire Telemetry System.

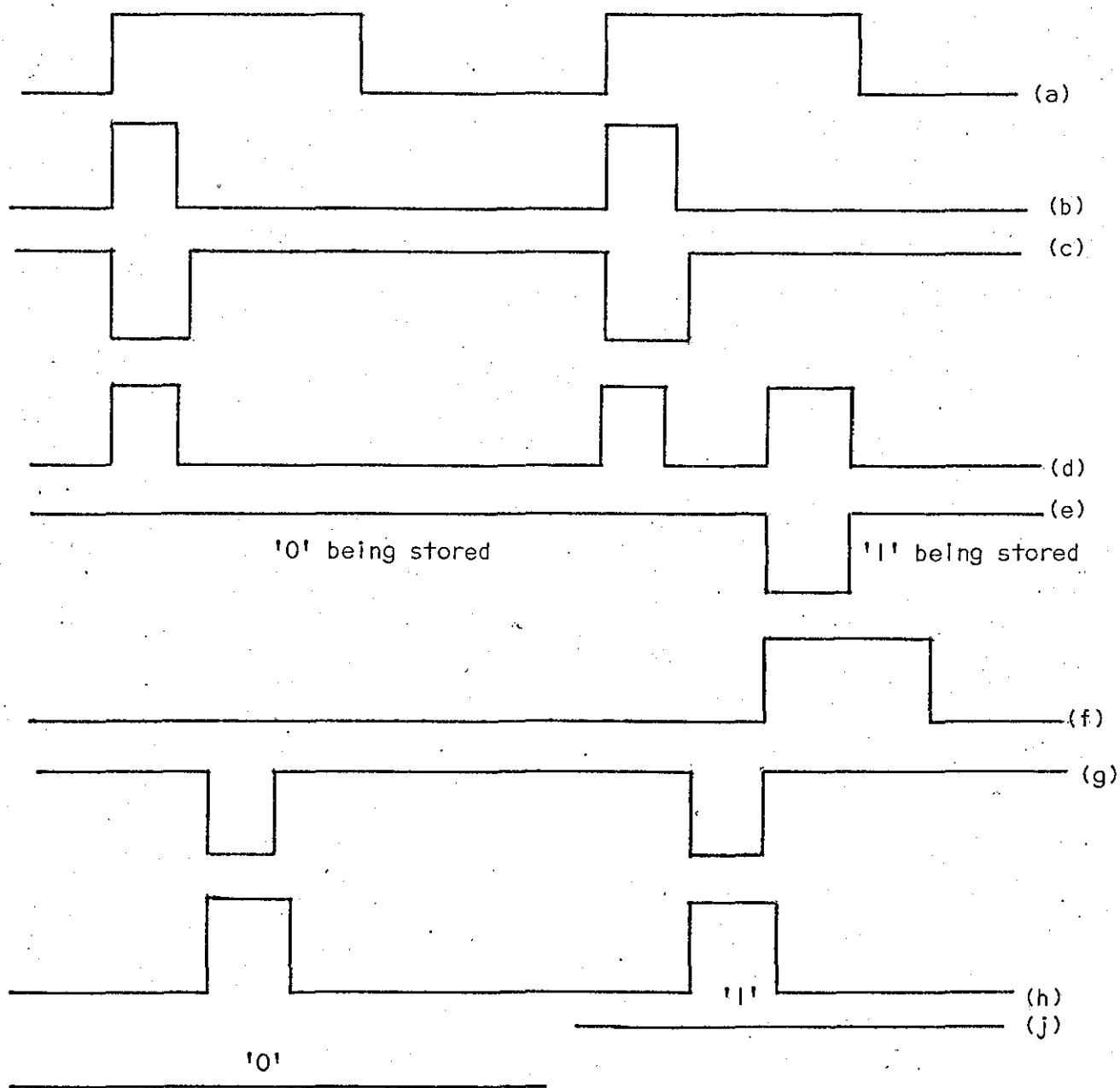


Figure 6.20 Waveforms for Single-wire Telemetry System.

6.6 Practical System

Biomedical signals encoded by delta modulation are telemetered by means of a single coaxial cable. The theory and design of the delta modulator is given in Chapters 3 and 6. The block diagram of the multichannel time division multiplexed system using a coaxial cable is shown in figure 6.18.

Both ends of the cable are connected to encoders and decoders via a transistor switch. The clock is situated on the decoding (receiving) end and is also used to generate pulses to switch the transistor. The cable is normally correctly terminated. However, when the pulse from the clock switches the transistor on, the cable is short circuited for a short period and a pulse travels along the line towards the encoder (transmitting) end. This pulse determines the state of data stored in '1' or '0' states, it also causes the next signal to be selected. If a '1' is being stored, the encoder end of the line is maintained at earth potential for a further period of time and causes a signal to travel back along the line where it is detected at the decoder.

The system is described by dividing it into the following. Associated circuitry for multiplexing and demultiplexing is described in Sections 6.2 and 6.4.

1. Clock and control circuitry
2. Transmitting circuitry and encoders
3. Receiving circuitry and decoders

6.6.1 Clock and Control Circuitry

The control circuitry and waveforms are shown in figures 6.19 and 6.20. The clock waveform shown in figure 6.20(a) initiates the operation of the control circuitry and various waveforms used in the system (marked) are obtained. The control circuitry is used to

send a pulse from the receiving end along the line towards the transmitting end. Depending on the state of the data on the transmitting end, a pulse travels back and the information is transmitted and decoded on the receiving end. Failing to do that, the interrogative pulse waits for the right state of the data to be transmitted. The pulse 'h' used to switch the transistor switch on the transmitting end is also used to drive a ring counter for clocking the delta modulators on this end. In order to achieve this, there is a control circuitry associated with the transmitting and receiving end as shown in the figures.

The interrogating pulse starts from the receiving end and initiates the transmitting system. In order to do that a short duration (200 n sec) of pulse 'b' is produced from the positive going clock pulse 'a' by the following arrangement. The positive pulse of the clock waveform is stretched (delayed) with the forward biased diode, capacitor to earth, and the Nor gate. This is further nanded with the clock pulse to give the required waveform after inversion. The output of the transistor switch is connected to both the cable and the other part of the circuitry in order to receive the data pulses and steer them to the decoder. It is important to suppress any signal getting through to the decoder when a pulse is travelling on the line towards the encoder. This is done by stretching (delaying) the clock pulse when it is positive, nanding it with the clock pulse to get the waveform 'c'. This is further nanded with 'd' to get 'e', where 'd' is the output of Schmitt trigger ST_1 when a pulse is travelling along the line and the transistor T_1 is on. The negative pulse 'c' is used to suppress the output 'd' from the Schmitt trigger.

6.6.2 Control Circuitry on the Transmitting End

On the other side of the cable is connected a transistor switch and associated control circuitry, to obtain a positive pulse which allows the data to be handed out and pass through the transistor switch along the cable where it will be decoded. This is done as shown in figure 6.19. The received pulse on this cable side is detected by a Schmitt trigger, the output of which is stretched and handed to give a pulse 'h'. The 'h' is connected to the one input of nand gate, the other input being connected to the multiplexed signal, i.e., the information to be transmitted which is stored in the form of a DC level, as shown in figure 6.20(j)

If a zero is stored, the 'h' will be inhibited and will not pass through the gate, and the transistor switch remains non-conducting and the line remain terminated by 75 ohm. If the information stored is one, the pulse 'h' will pass through the gate and causes the transistor T_2 to switch to conduct, and a pulse is transmitted back along the line. This is the first reflection or reply when the interrogating pulse is first applied. During this time the output of ST_2 is held and the pulse travels back where it is detected by the Schmitt trigger ST_1 . Its output is handed by the clock pulse, and output pulse 'e' is obtained due to the right polarity of inputs. The output pulse is further stretched to give a pulse 'f' to make it less critical for the length of line.

6.6.3 Transmitting Circuitry

The signal encoders are the basic delta modulators used to code the analogue signal into digital form. Time division multiplexing is achieved by using a ring counter with the number of stages equal

to the number of channels, as shown in figure 6.21. The received pulses 'h' are used to drive a ring counter and each cycle of the ring counter clocks each delta modulator once in turn. When the cycle is finished and each delta modulator is clocked, the output is logically Anded with the clock signal. It is further passed through an Or gate and all the outputs are combined to form the signal 'j'. The 'j' signal also contains a synchronisation pulse which is a one in each cycle of the ring counter. The synchronisation is obtained by Nanding all the pulses used to clock the delta modulators obtained from the flip flops.

6.6.4 Receiving Circuitry

The receiving system is situated on the clock side where all the control pulses originate. The data to be decoded only arrives on the receiving end when an interrogating pulse is sent from this side to the transmitting end. If the data to be transmitted is in the right state, it is transmitted towards the receiving end.

Normally data consists of ones and zeros, depending on the input signal and always a one in the synchronising position. The received multiplexed data is demultiplexed by driving another ring counter using the clock pulses from 'a'. This is done by strobing the multiplexed data into flip flops by the outputs of the ring counter from each stage. The receiving system is shown in figure 6.22.

Synchronisation is achieved by allowing the ring counter to proceed only at the end of a cycle providing a 'one', which is a synchronisation pulse is on line f. The signal may go out of synchronisation due to the 'one' present in the data.

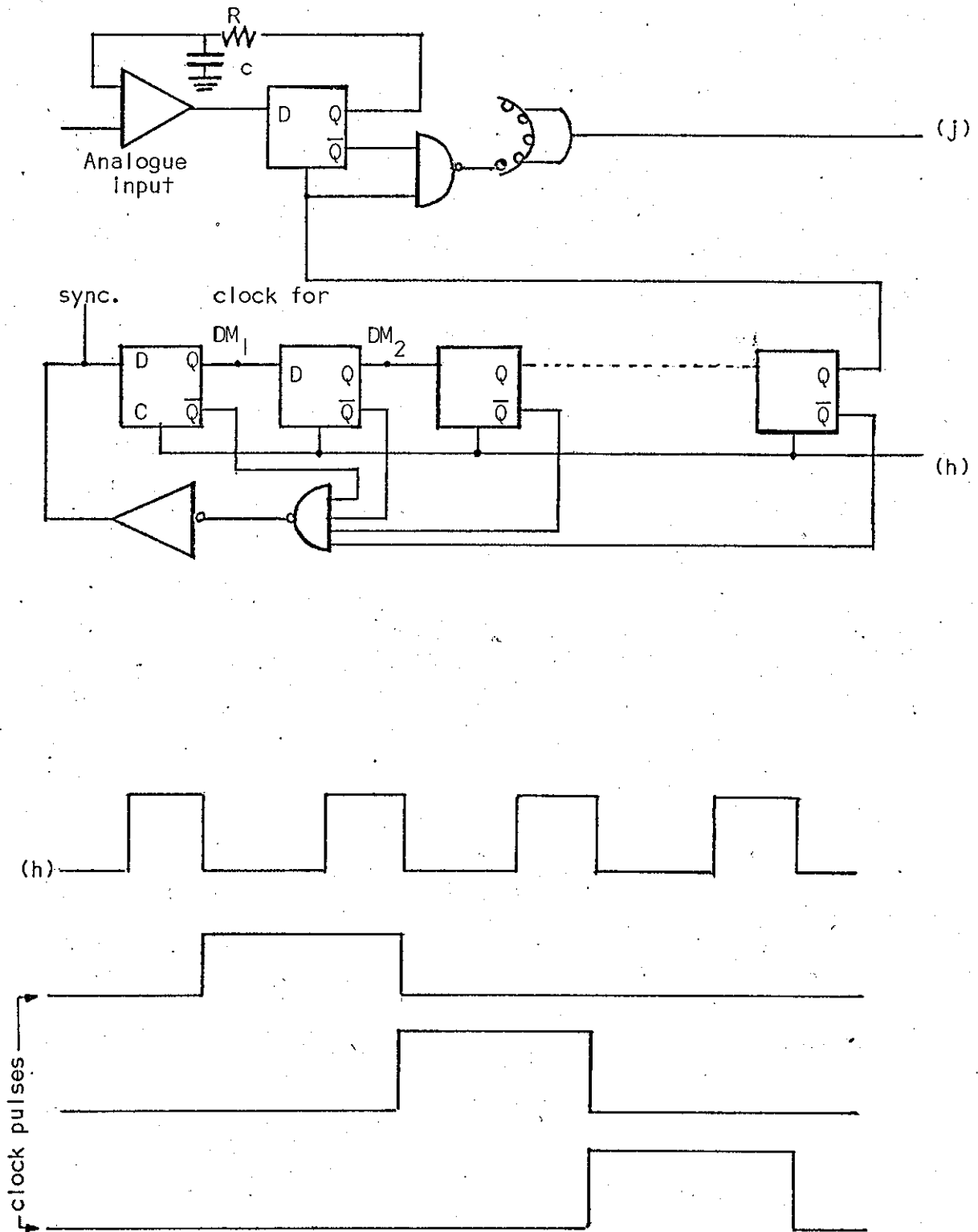


Figure 6.21 Transmitter Circuit for Single-wire Telemetry System.

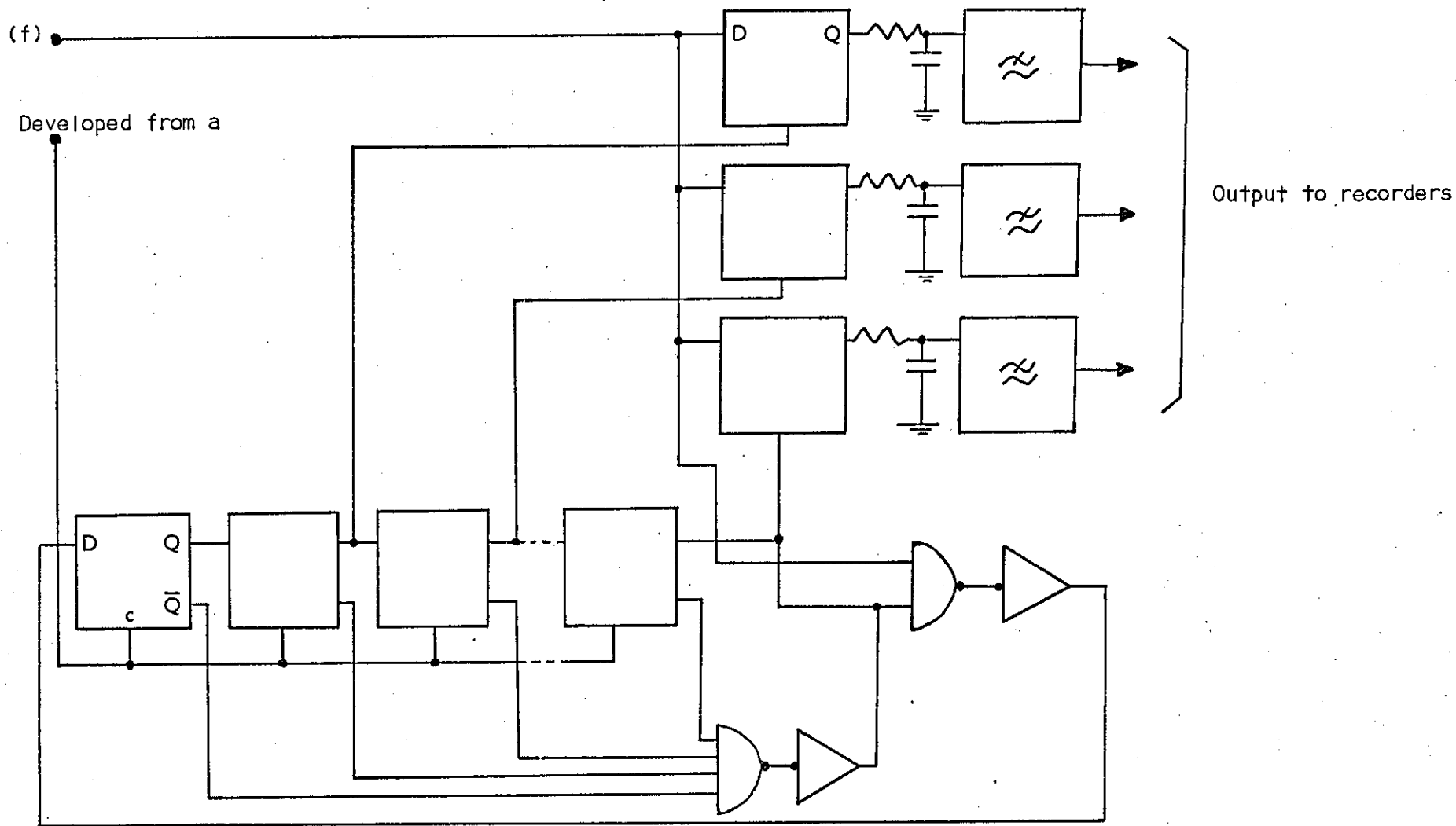


Figure 6.22 Receiver circuits for single-wire telemetry system

This only happens when switching the ring counter 'on' but it comes back in synchronisation after a few cycles.

The data is demultiplexed as explained in Section 6.4.5 and the output of the flip flops is passed through the RC network as an integrator to recover the analogue signal. The higher frequency components due to sampling are eliminated by passing through the low pass filter.

The system performance is based on the following :

1. Overload Characteristic

$$\frac{\text{Maximum input voltage at } f_m}{\text{Maximum input at low frequency}} = \left(1 + \left(\frac{f_m}{f_c}\right)^2\right)^{-\frac{1}{2}}$$

2. Quantization Noise

$$\text{for } f_m > f_c \text{ Maximum signal to noise ratio} = \frac{0.2f_s^{3/2}}{f_c f_o^{1/2}}$$

$$\text{for } f_m < f_c \text{ maximum signal to noise ratio} = \frac{0.2f_s^{3/2}}{f_m f_o^{1/2}}$$

f_m = signal frequency

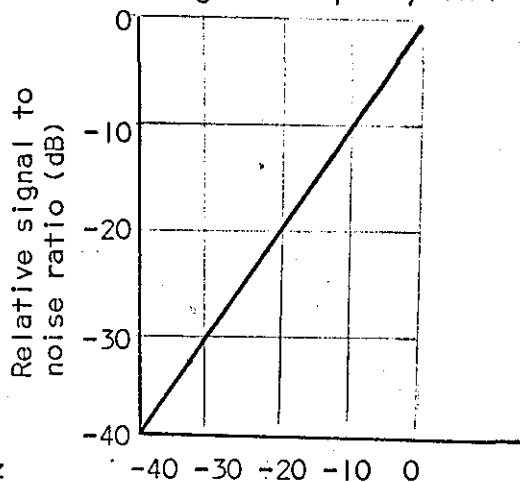
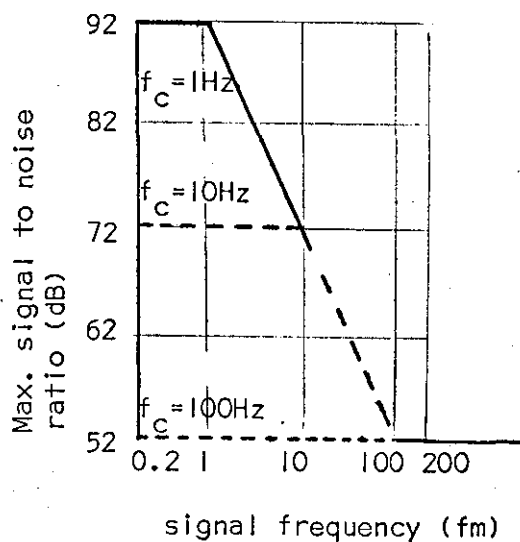
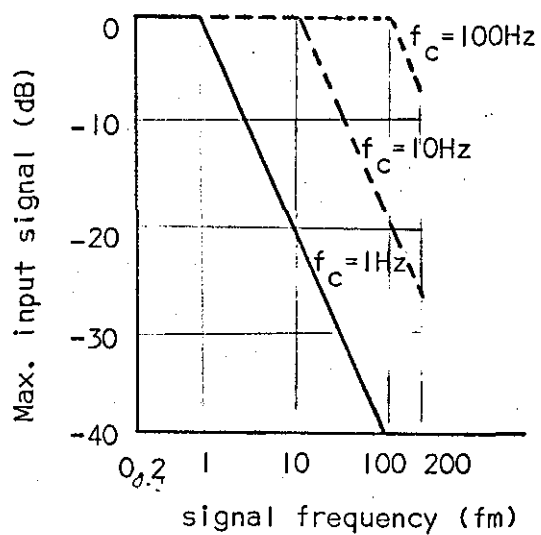
$$f_c = \frac{1}{2\pi RC}$$

f_o = bandwidth of low pass filter

f_s = clock frequency

Typical characteristics of the system performance are shown in figure 6.23.

Another possible application of the system described is the remote monitoring of group of signals as shown in figure 6.24.



Clock frequency (f_s) = 20kHz

Bandwidth of low pass filter = 200 Hz

number of channels = 24

$$f_c = \frac{1}{2\pi R_c}$$

Input signal level relative to maximum input (dB)

Figure 6.23 Typical System Performance Characteristics.

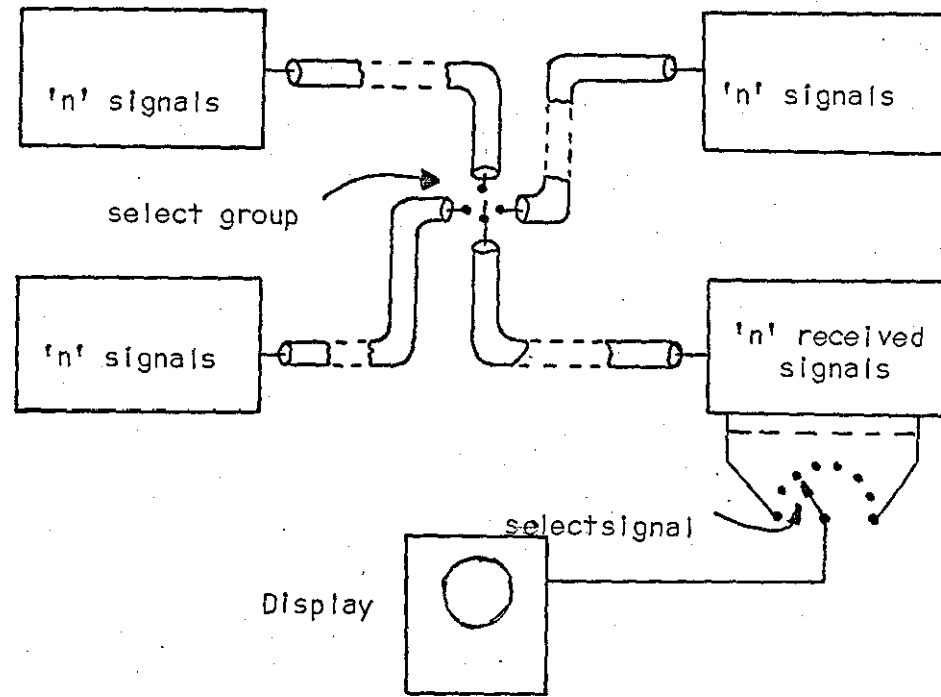


Figure 6.24 Application of Single-wire Telemetry System.

6.7 Performance and Characteristics of the System

The four channel biomedical telemetry system was constructed and contained in two packs. The four channel encoder and multiplexer was contained in one pack and a domestic soap box of 2.5" x 3.5" was used to house it. The radio frequency transmitter was housed in the separate soap box, though both can be accommodated in one box in two layers. Silicon rubber was used to set them.

The picture of the units are shown in figures 6.25 and 6.26.

The following characteristics were evolved and are discussed here.

- (i) Bandwidth of the system
- (ii) Noise
- (iii) Power consumption
- (iv) DC input-output characteristic and drift
- (v) Size, weight and range of transmission

6.7.1 Bandwidth of the System

The bandwidth of the multichannel system depended on the following:

- (i) Bandwidth of the encoder (delta modulator)
- (ii) Number of channels
- (iii) Type of modulation (narrow frequency modulation)
used for radio transmission

(i) In delta modulation the digital output of the encoder appears in one's and zeros depending on the input signal. The fastest rate at which one's and zero's can appear is at the clock rate and their distribution is random. However, the spectrum of a digital output employing rectangular pulses is of the form $\sin \frac{x}{x}$ with its first null at the clock frequency. Hence the clock frequency was taken as the bandwidth of the encoder which is 4 kHz for each channel.

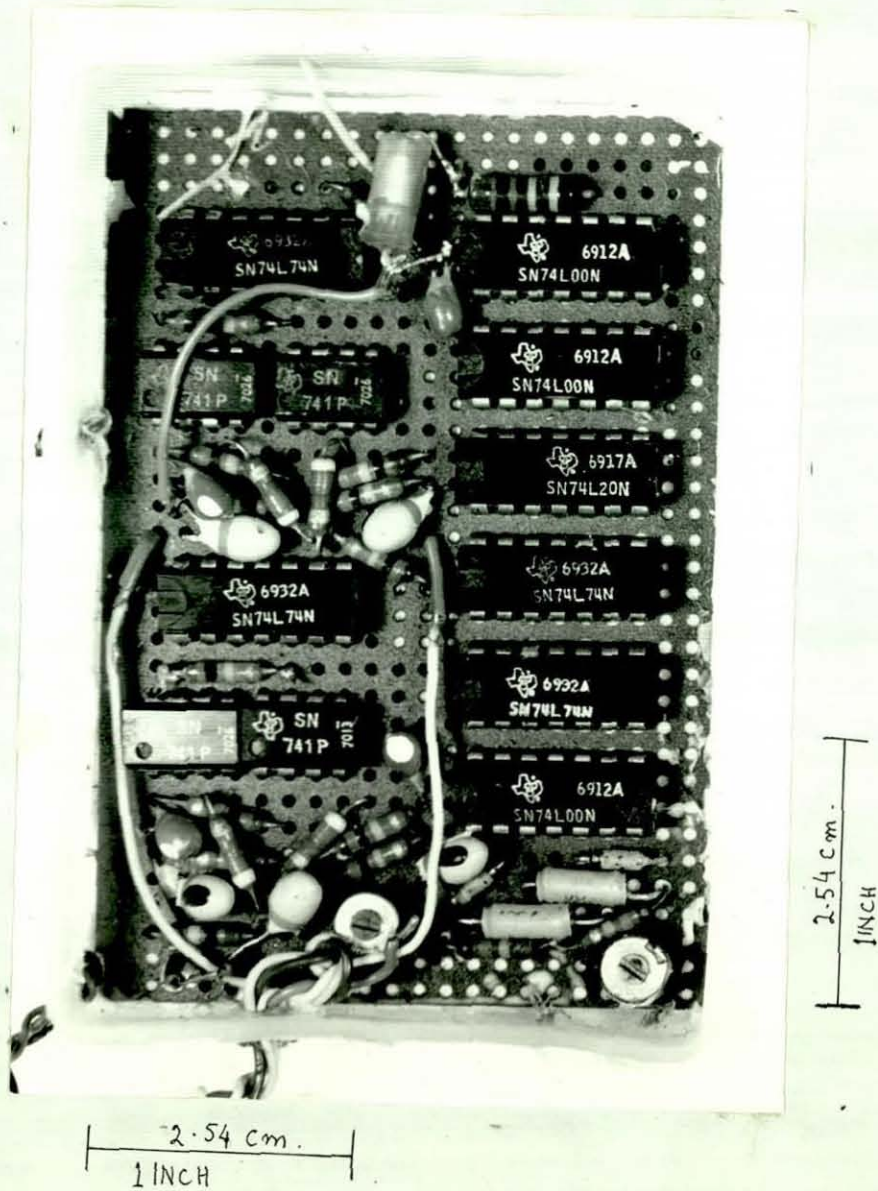


Figure 6.25 Photograph of the four channel encoder and multiplexer.

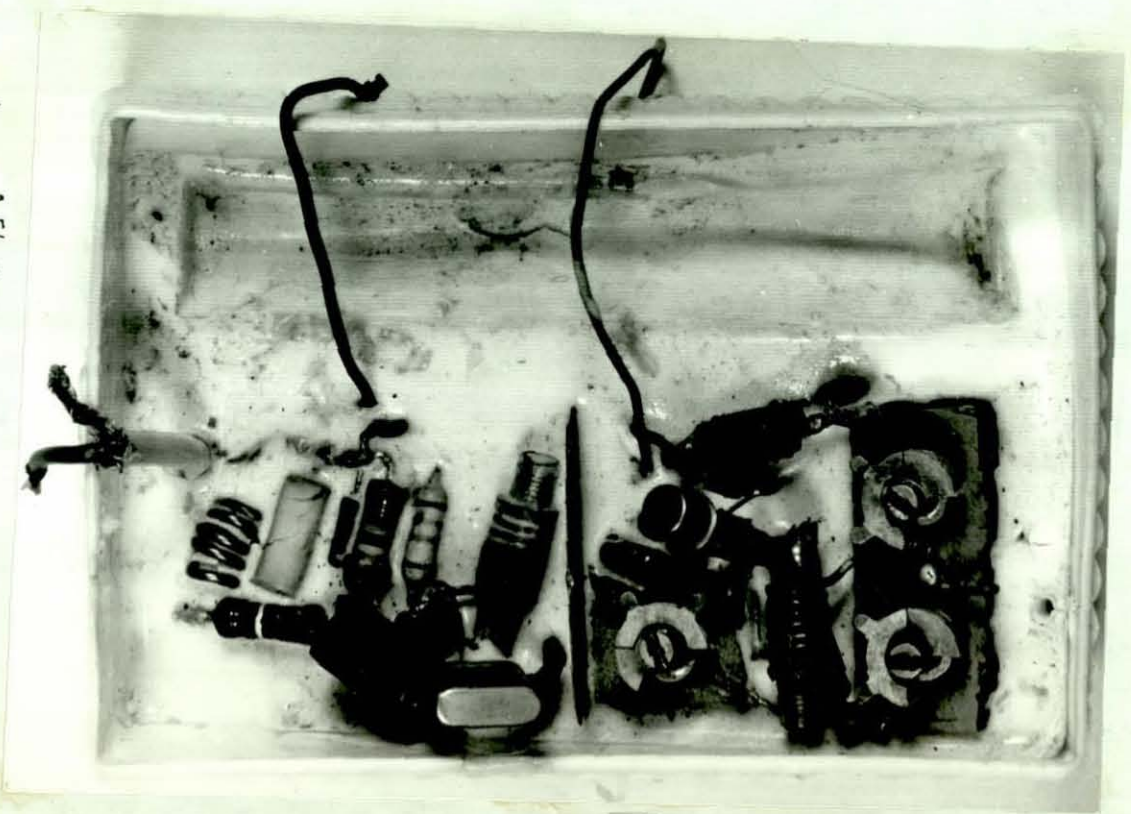


Figure 6.26 The radio frequency transmitter

A spectrum of the digital output for an ECG waveform as an input was taken on the computer and is shown in figure 6.27. The spectrum gives the maximum energy at the clock frequency and also energy at the low frequencies due to the low frequencies present in the ECG waveform. The clock frequency in the computer simulation was chosen to be 1 kHz for investigation as explained earlier.

(ii) The number of channels in a time division multiplexed system increases the bandwidth linearly. This is given by the product of the number of channels and the clock frequency chosen for each channel. Hence the bandwidth of four channels + one channel due to synchronisation = $5 \times 4 = 20$ kHz.

(iii) The bandwidth of narrow band frequency modulation is twice the frequency of the modulating signal (Section 5.2.1). In order to measure the bandwidth of the multichannel system a Hewlett Packard spectrum analyser was used as shown in figure 6.28. The spectrum obtained is shown in figure 6.28. It showed one main sideband on each side of the carrier displaced by 20 kHz. There were other sideband present but with insignificant energy. Hence the bandwidth of the four channel system using a radio link = 40 kHz.

It is noted here that the bandwidth of the system is well within the limit (200 kHz) for class III devices) of the Post Office (in U.K.) regulations and allows the number of channel to be increased if desired.

6.7.2 Noise

The following are the sources of noise in a multichannel system using a radio link.

- (1) Quantization noise
- (2) Overload noise

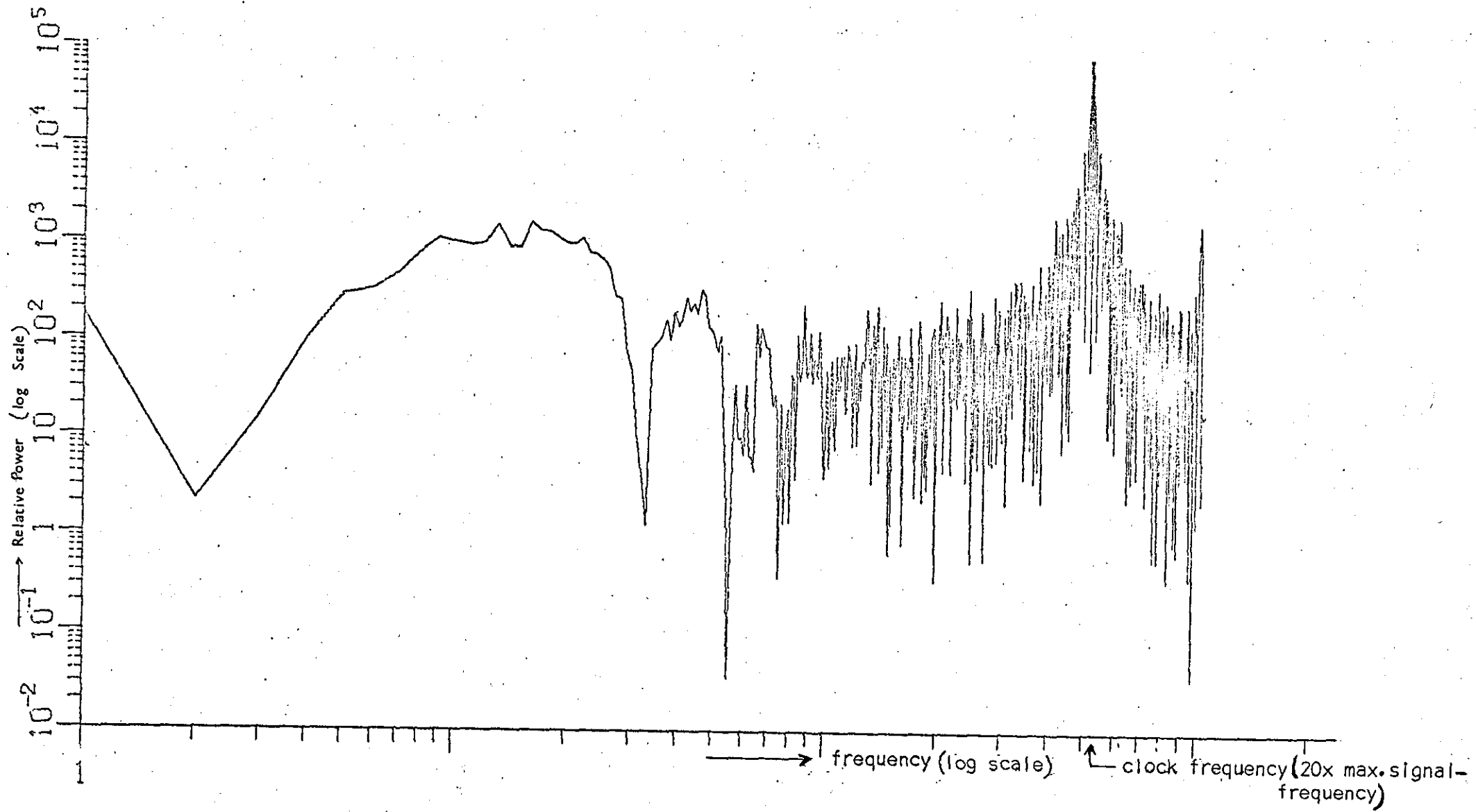
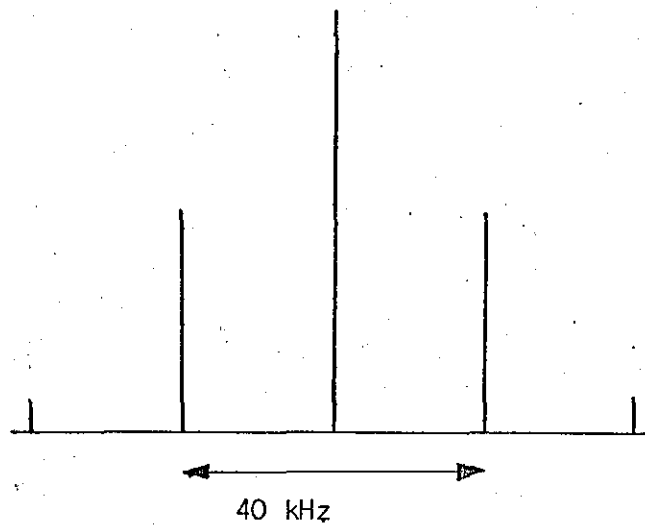


Figure 6.27 Spectrum of digital output of delta modulator for ECG input



(a) Measurement of Bandwidth



(b) Spectrum of Transmitted Signal (Radio link)

Figure 6.28

- (3) Noise due to error pulses (fluctuation noise)
- (4) Idle channel noise
- (5) Noise due to multiplexing

The first three sources of noise have been discussed in Chapter three and Chapter four (4.10). Idle channel noise is produced at the output of a delta modulator when there is no real input signal. It is caused by the presence of any noise in the input when the step sizes of the quantizer are unequal. It can be eliminated by adjusting to make the step size of the quantizer equal.

Noise in a multiplexed system may be due to interference, jitter or cross talk and any synchronisation error in demultiplexing. However, maximum signal to noise ratio is obtained (Chapter 3) when the input signal to the delta modulator is just below the overload condition, the only source of noise being the inherent quantization noise. Hence noise was measured at this condition and compared with the following:

- (i) Noise of the single channel system with a direct link and the radio link using the same and different clocks on both ends
- (ii) Noise of the multiplexed system with a direct link and the radio link using the same and the different clocks on both ends.

Measurement of Noise

The noise was measured by varying the amplitude of the input signal (sine wave) until overloading occurs. The arrangement for the measurement of noise is shown in figure 6.29.

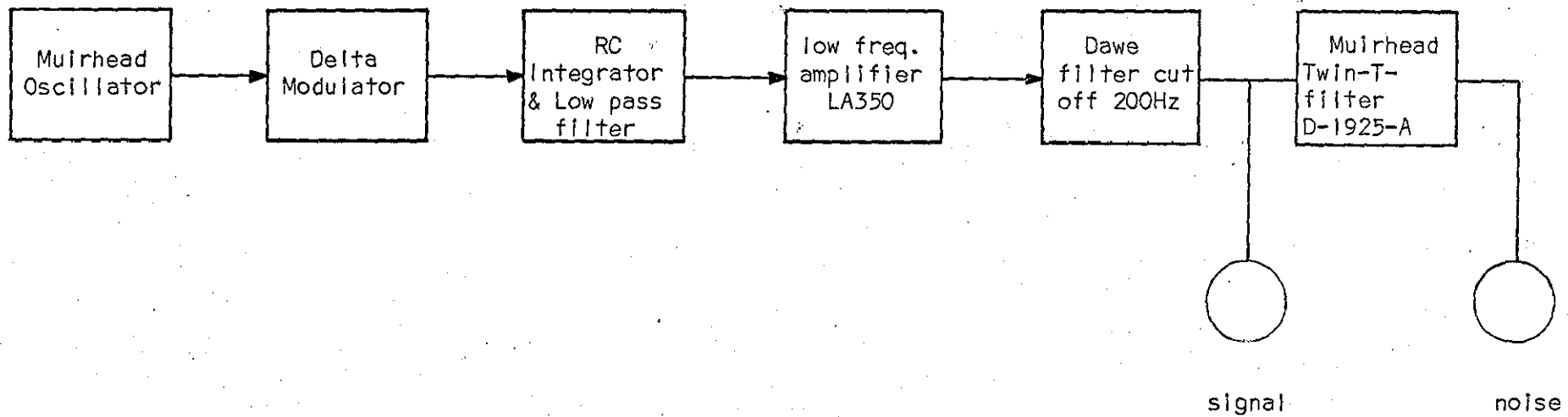


Figure 6.29 Measurement of noise

The frequency of the input signal was fixed at 5 Hz, and the relative noise power was obtained from the decoded signal through a 5 Hz rejection amplifier composed of a twin T network. Since the measurement was for comparison purposes and amplification of the signal had taken place, the values of noise obtained are not a figure of noise for the system.

Results

The relation between the amplitude of the input signal and noise measured is shown in figures 6.30 and 6.31. It is observed that in the multiplexed system using a direct link, the noise measured was more than the single channel system when the clock on both ends was different. However using the same clock in the above cases the noise measured for both the systems was lower at a smaller input signal level. Beyond this region (shown in figure 6.30) the noise was the same in both the systems. Near overloading the noise in the multiplexed system with the same clock was less.

In the multiplexed system using a radio link and employing different clocks on both the ends the noise was nearly the same as for a direct link. The Noise measured by using the radio link was at a distance of ten feet in the same room.

However using the same clock on both ends in the above case the magnitude of the noise was smaller (shown in figure 6.31).

6.7.3 Power Consumption

Power consumption determines the size, life and reliability of a portable system. These requirements make it necessary to design the system for low power consumption compatible with the available low power logic and power source.

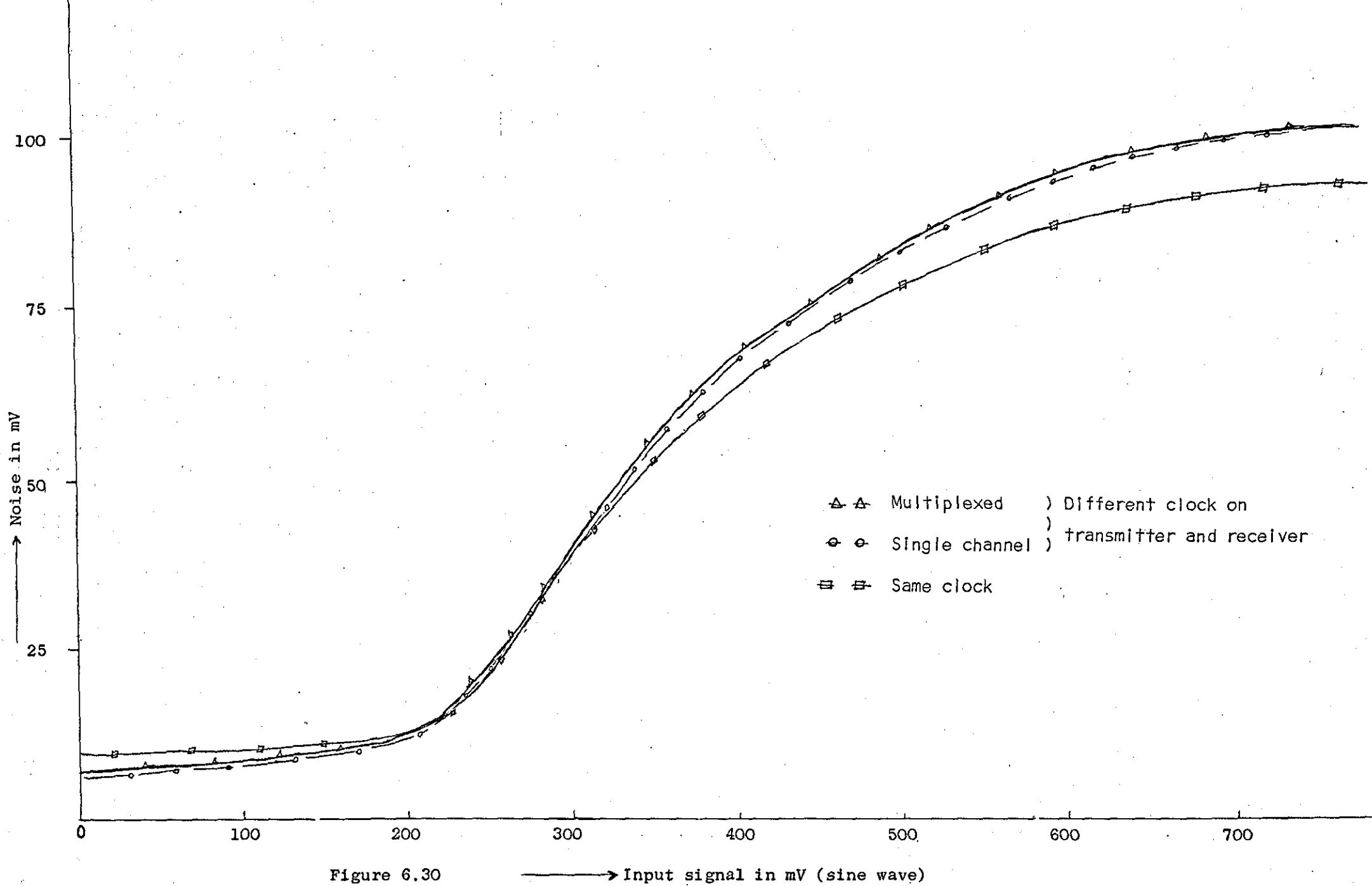
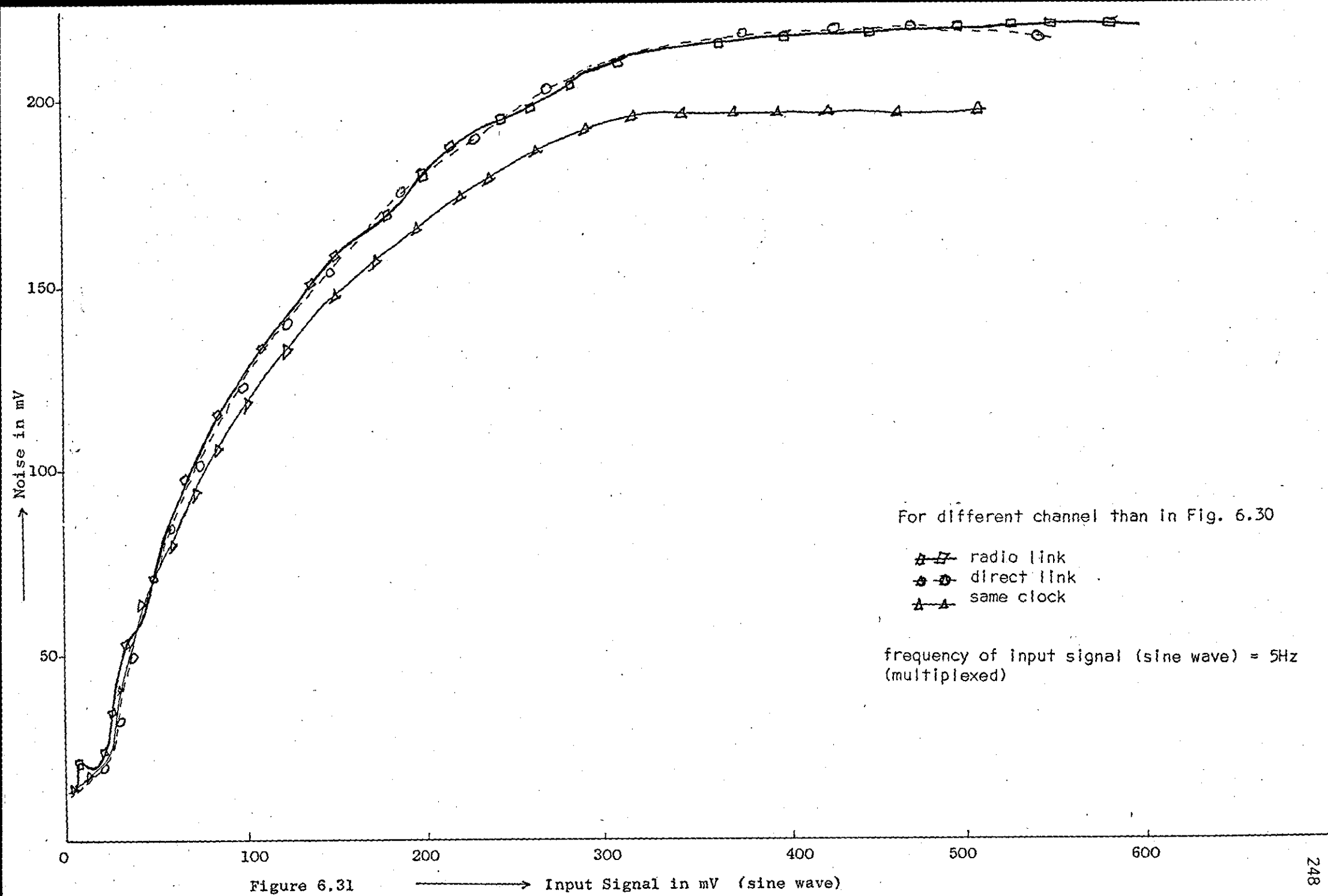


Figure 6.30

→ Input signal in mV (sine wave)



The system (described in this chapter) was first designed and tested for RTL medium power logic using a mains powered supply. The final system was then designed for low power TTL logic available at the time. The battery used for the supply was a TR-133R Mallory.

Power consumed is as follows:

Four Channel Encoder and Multiplexer

Positive supply = 4V
 Negative supply = -1.3V
 Current in the positive rail = 8.2 mA
 Current in the negative rail = 0.76 mA

RF Transmitter

Supply voltage = 4V
 Current = 5.5 mA

Total Power Consumption of the System

Supply voltage = 4V and -1.3V
 Current = 14 mA and 0.77 mA
 Total power is about 57mW

With the given current capacity of the TR-133R battery, the expected life of the system is about 70 hours. A holder was designed to house the positive and negative supply source in the same enclosure.

6.7.4 DC Input-Output Characteristic and Drift

A relationship between a dc input voltage and the output voltage was obtained to see the linearity of the single channel delta modulation system. This is performed by removing the input coupling capacitor as shown in figure 6.32.

The input level of a dc voltage was varied between the negative supply voltage and positive supply voltage and the output voltage was measured at the output of the low pass filter. The characteristic obtained is shown in figure 6.33.

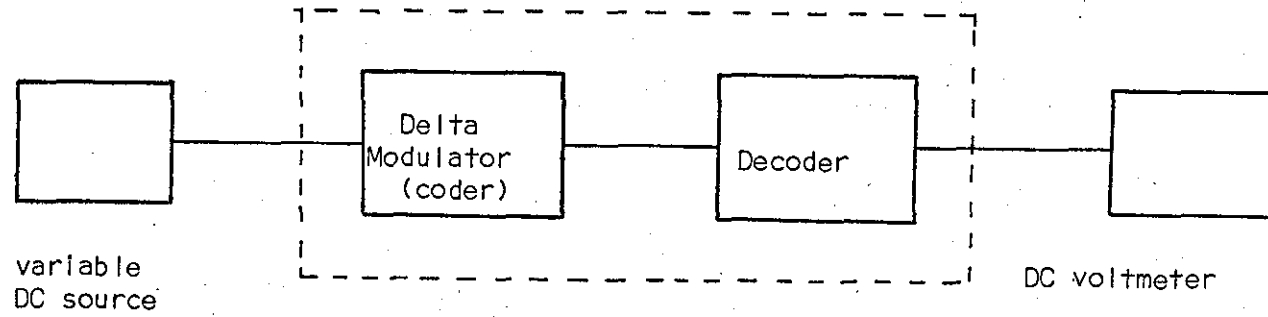


Figure 6.32 DC Input-output characteristic

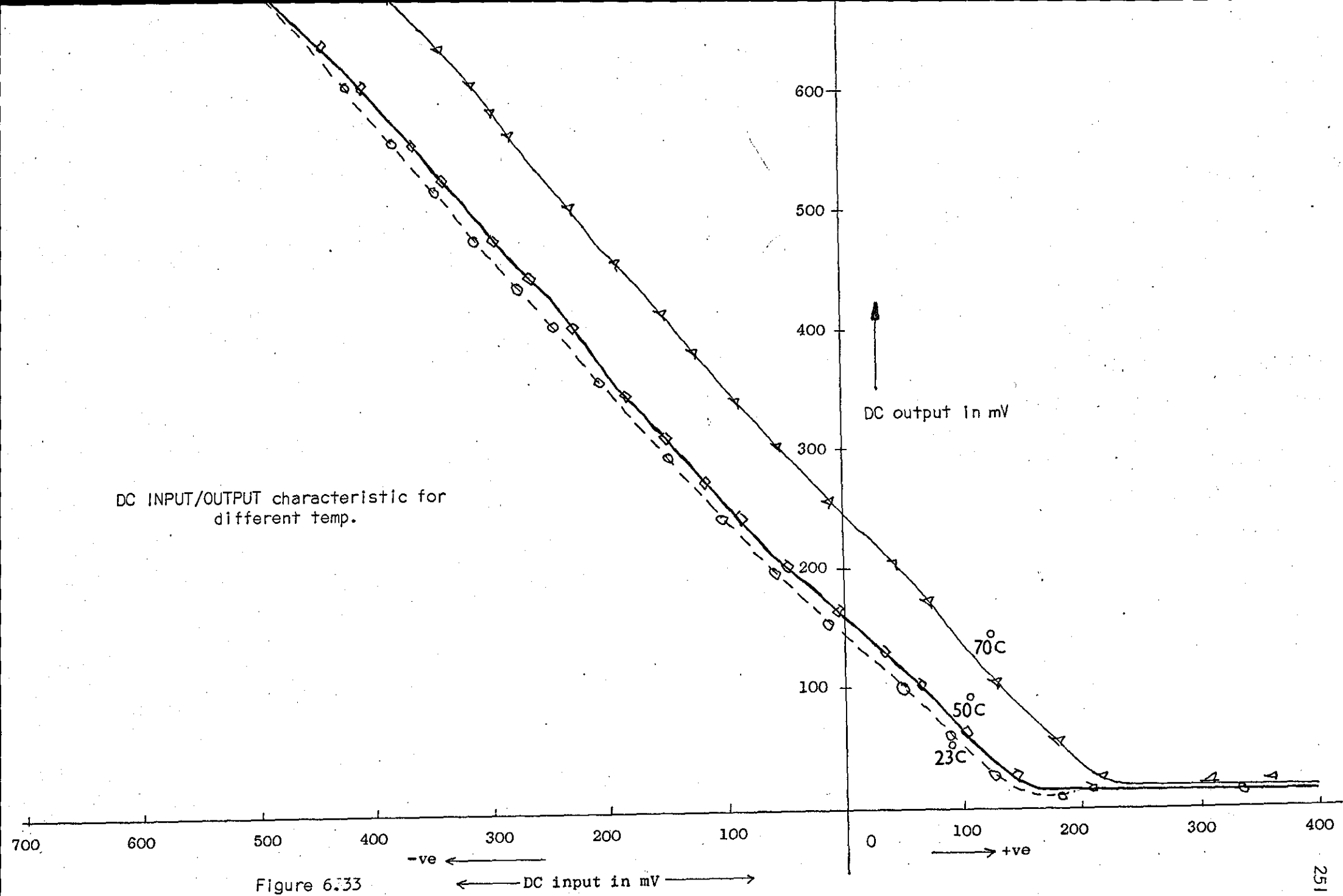


Figure 6.33

Drift

Drift is referred to as a slow change in the quiescent point of a device which can arise from changes in temperature or variations in supply voltage.

Digital techniques of modulations are usually less sensitive to changes in temperature and supply voltage. However, the analogue part associated with the system is more susceptible to these variations and gives rise to drift. To study the drift the arrangement used is shown in figure 6.32 and the dotted position of the system was placed in an oven. The DC input-output characteristics were obtained at 23°C (ambient temperature), 25°C and 70°C. The characteristics are shown in figure 6.33. The characteristics show a drift, though the linearity of the system was the same. Therefore, the drift measured at 70°C is 2.11 mV/C°.

6.7.5 Size, Weight and Range of Transmission

As mentioned earlier the system is housed in two soap boxes as shown in figures 6.25 and 6.26. The dimensions are 89 x 63 mm. The weights of these units are as follows:

Weights of four channel multiplexer and encoder including soap box = 3¼ oz or 81 grammes

Weight of four channel encoder + multiplexer and RF transmitter in one soap box = 5 oz or 135 grammes

(These weights do not include the battery).

Weight of the whole system with battery in two soap boxes = 7 oz or 200 grammes

Range of Transmission

The range of transmission of the system was measured to be between 100 and 200 yards with a transmitted power equal to 1.5mW. The power

was measured by a Hewlett Packard 431 c power meter.

6.8 Discussion and Conclusion

The price of the system (components only) was £20 at the time of development. The weight and size achieved enables a subject to carry it without any strain or hazard. The size and power consumption can be further reduced by using recently developed micrologic.

The life of the system is about 70 hours from a mercury battery of 100 mA-hour capacity

It was observed in the noise measurement that it was reduced by using the same clock on both the ends. In order to achieve better locking of the incoming signal, before demultiplexing, a phase lock technique was employed but was not finished in time. The radio link employed was not very effective for longer distances and a better technique for the radio link was developed later on in the Department of Electronic and Electrical Engineering, Loughborough University of Technology, by Ivison and Robinson⁽¹⁰⁾.

CHAPTER 7CONCLUSIONS

From the foregoing work the following conclusions may be drawn.

1. On the basis of the theoretical study of digital modulation techniques for biomedical signals, it was found that the coded techniques are more reliable, have a better signal-to-noise ratio and use less bandwidth. It was also concluded that delta modulation is simpler, easier to implement and is more suited for a small compact multichannel biomedical telemetry system.
2. Computer simulation in Chapter 4 enabled the investigation of the delta modulator and the delta sigma modulator for their suitability to the preservation of the ECG waveform. It was concluded that the decoder (filter) in the delta sigma modulator is more critical to design and inherent noise gets through to the decoded output. Further analysis showed that the delta modulator is easier to design and is a better system for the preservation of the ECG waveform.
3. The computer investigation also showed that in the long term monitoring of ECG signals, the effect of high frequency noise was considerably reduced due to the filtering action (RC Integrator in the feedback loop) of the delta modulator. The histogram technique used to study the long term monitoring of ECG signals may prove useful in certain situations for patient monitoring.
4. The computer investigation into the effect of error pulses in the digital output for the delta modulator showed that the decoded ECG waveform becomes corrupted when the error probability was greater than 2 error pulses in 100. This figure of error probability is found to be better than pulse code modulation.

5. The digital nature of the system and the investigation in Chapter 4 indicates that the system can be incorporated in an on-line system and real time processings of the physiological signals can be carried out.
6. The signal processing techniques developed and employed for the processing and analysis of ECG signal are useful for diagnostic and data analysis purposes of biomedical signals.
7. The design and construction of the practical multichannel system showed compactness, economy and simplicity of the system.
8. Narrow band frequency modulation (radio link) achieved by pulling the frequency of the crystal controlled oscillator, used a smaller bandwidth but was not very effective for long range transmission.
9. Finally, a single wire time division multiplexed system was designed showing attractive features for short range transmission where radio telemetry is not necessary.

REFERENCES

1. Johnston, E.B. 'Telemetry of Physiological Data',
ITT Federal Laboratories, San Fernando,
California.
2. Einthoven, W. 'Die Galvanometrische Registrirung des
Menschlichen Electrokardiogramms, (etc)',
Arch. Ges. Physiol. 99, 472, (1903).
3. Barker, L.F. 'Electrocardiography and Phonocardiography',
A collective review, Johns Hopkins
Hospital Bulletin, 20, 358, (1910).
4. Scientific American 'A Telephone Stethoscope', Scientific
American, 102, 496, (1910).
5. Ray, C.D. and 'Electroencephalographic and Response-
Bickford, R.G. averaged Bioelectric Data Transmitted
via Telephone Link', Proc. National
Telemetry Conf., U.S.A. (1963).
6. Stander, R.W., Barden, 'Telemetry of Physiological Data during
T.P. & Hagan, W.K. Parturition', Proc. National Telemetry
Conf., U.S.A. (1963).
7. Levine, I.M., Jossman, 'Monitoring Spasticity - Home Telephone
P.B., De Angelis, V., Telemetry vs Direct Laboratory Testing',
Tursky, B., & Meister, Proc. National Telemetry Conf., U.S.A.
M. p. 86 (1966).
8. Berson, A.S., Stallman, 'Telephone Transmission of Electro-
F.W., Brodes, J.H., & cardiograms and on-line Computer
Pipberger, H.K. Diagnosis', Amer.J.Med.Electron., 4,
p.35 (1965).

9. Hill, D.W. 'Transmitting Physiological Signals by Telephone', World Med. Electron., 4, p.108, (1966).
10. Kamp, A. 'Eight Channel E.E.G. Telemetry', E.E.G. Clin. Neurophysiol., 15, P.164, (1963).
11. Prescott, G.B. 'Bell's Electronic Speaking Telephone' Appleton, New York, P.79, (1884).
12. Winters, S.R. 'Diagnosis by Wireless', Sci. Am. 124, 465, (1921).
13. Caceres, C.A. Biomedical Telemetry, Academic Press, New York and London (1965)
14. Breaksell, G.C. & Parker, C.S. 'Radio Transmission of the Human Electroencephalogram and other Electrophysiological Data', Electroencephalog: Clinical Neurophysiol. 2, 243, (1949).
15. Holter, N.J. & Gengerelli, J.A. 'Remote Recording of Physiological Data by Radio', Rocky Mountain Med. Jnl., 46, 749, (1949).
16. Holter, N.J. 'Radioelectrocardiography: A New Technique for Cardiovascular Studies', Ann. N.Y. Acad. Sci., 65, 913, (1957).
17. Holter, N.J. 'New Method for Heart Studies', Science 134, 1214, (1961).
18. Winsor, T. et al. 'Electrocardiograms by Telemetry', Calif. Med. 94, 284, (1961).

19. Bellet, S., Deliyannis, S. & Ellakin, M. 'The Electrocardiogram during Exercise as Recorded by Radioelectrocardiography: Comparison with the Post-exercise Electrocardiogram (Master Two-step Test)'; *Am. Jnl. Cardiol.* 8, 395, (1951).
20. Hess, O.W. 'Instrumentation of (1) Radio-fetal-electrocardiography and (2) Radio Transmission of Intrauterine Pressure', *Proc. Nat. Telemetry Conf.*, Albuquerque, New Mexico, pp.8, (1963).
21. Larks, S.D. 'Foetal Electrocardiograph', Thomas, Springfield, Illinois, CAT (Mnemetron Div. Technical Measurements Corp.) (1961)
22. Mackay, R.S. & Jacobson, B. 'Endo Radio Sonde', *Nature*, 179, pp.1239, (1957).
23. Barr, N.L. 'Radio Transmission of Physiological Information', *Military Med.* 114, 79, (1954).
24. Kousnetzov, A.G. 'Some Results of Biological Experiment in Rockets and Sputnik II', *Jnl. Activation Med.* 29, 781, (1958).
25. Baldwin, H.A. *Bioscience*, 15, 95-97 (1965).
26. Anderson, V.C. 'Acoustic Communication is Better Than None', *IEE Spectrum*, pp.63-68, October 1970.
27. Hoare, D.W. & Ivison, J.M. 'Measuring the Heart Rate of an Active Athlete', *Electronic Engineering* 33, pp.6-8, January 1961.

28. Kamp, A., & Storm Van Leeuwen, W. 'A Two Channel EEG Radio Telemetering System', *Electroencephalog. Clin. Neurophysiol.* 13, 803 (1961).
29. Hambrecht, F.T., Donahue, P.D. & Melzack, R. 'A Multiple Channel EEG Telemetering System' *Electroencephalog. Clin. Neurophysiol.* 15, 323, (1963).
30. Marko, A.R. & McLennan, M.A. 'A Seven Channel Personal Telemetry System using Pulse Duration Modulation', *Proc. 16th Ann. Conf. Eng. in Medicine & Biology, Baltimore, Nov., 1963*, pp.154, (1963).
31. Murray, R.W., Marko, A., Kissen, A.T. & McGuire, D.M. 'A New Versatile Miniature Multi-Channel Personal Telemetry System for Medical Research', *Proc. of the Nat. Telemetry Conf., U.S.A.*, pp.152 (1967).
32. Robock, R.B., & Ko, W.H. 'A Six Channel Physiological System', *IEEE Trans., BME-14*, P.40 (1967).
33. Fischer, F., Peled, N., & Yerushalmi, S. 'FM/FM Multiplex Radio Telemetry System for Handling Biological Data', *IEE Trans., BME-14*, pp.30, (1967).
34. Rokushima, H. 'A Multichannel PWM/FM Radiotelemetry System for EEG', *Proc. 22nd Ann. Conf. on Engineering in Medicine and Biology (Chicago, Ill., 1969)*.
35. Skutt, H., Richard, Fell, Roger, B & Kertzer, R. 'A Multichannel Telemetry System for use in Exercise Physiology', *BME-17*, No. 4, pp.339-349, Oct. 1970.

36. Weller, C. & Manson, G. 'A Three Channel Telemetry System Compatible with the British Medicine & Biological Telemetry Regulation', Int. Biotelemetry Symp., Nijmegen, The Netherlands, pp.13-20, May 5-8, 1971.
37. H.M.S.O. 'Medical & Biological Telemetry Devices', H.M.S.O., London 1968.
38. Zerzawy, R. & Bachmann, K. 'A Programmable Four Channel System for Long-time Radio Telemetry of Biomedical Parameters', Int. Biotelemetry Symp., Nijmegen, The Netherlands, pp.49-56, May 5-8, 1971.
39. Ijzenbrandt, H.J.B., Kimmich, H.P. & Van Den Akker, A.J. 'Single to Seven Channel Lightweight Biotelemetry System', Int. Biotelemetry Symp., Nijmegen, The Netherlands, pp.57-64, May 5-8, 1971.
40. Skutt, H.R., Roger, Fell, B. & Hagstrom, E.C. 'A Multichannel Ultrasonic Underwater Telemetry System', Int. Biotelemetry Symp., Nijmegen, The Netherlands, pp.30-38, May 5-8, (1971)
41. Wen, H. Ko. 'Biomedical Engineering Systems', McGraw-Hill Book Co., Chapter 3, pp.69, (1970).
42. Marko, A., McLennan, M.A. & Correll, E.C. 'Research and Development on Pulse-Modulated Personal Telemetry Systems', Aerospace Med. Res. Labs., AMRL-TDR-64-96, pp.1-19, (1963).

43. Farrer, J.F., Zworykin, V.K. & Baum, J. 'Pressure Sensitive Telemetry Capsule for the Study of Gastrointestinal Mobility', *Science*, 126, pp.975, (1957)
44. Nicholas, N.H. & Rauch, L. 'Radio Telemetry', Wiley, New York, (1956)
45. Cromwell, L., Weibell, F.J., Pfeiffer, E.A. & Usselman, L.B. 'Biomedical Instrumentation & Measurements', Prentice Hall Inc., Englewood, New Jersey, Chap.3, (1973)
46. Waller, A. 'A Demonstration of Electromotive Changes Accompanying the Heart Beat', *J. Physiology*, London, 8, 229, (1887)
47. Kupier, J. 'Medical Telemetry Systems', IEE Medical Electronics Monographs, 1-6, Edited by B.W. Watson & D.W. Hill, pp. 111-144, (1971)
48. Bendersky, D. 'A Muscle Accelerometer and Spray-on Electrocardiogram Electrodes', 7th International Conf. on Medical & Biological Eng., Stockholm, pp.413 (1967).
49. Patten, C.W., Ramme, F.B., & Rowan, S. NASA Tech. Note D-2312 (May 1966)
50. Cromwell, L., Weibell, F.J., Pfeiffer, E.A. & Usselman, L.B. 'Biomedical Instrumentation & Measurements', Prentice Hall, Inc., Englewood, New Jersey, Chapter 4 (1974)

51. Greatbatch, W. 'Fundamental Properties of Physiological Electrodes', IEE Medical Electronics Monograph 7-12, Edited by D.W. Hill & B.W. Watson, pp. 27-41, (1974)
52. Pacela, A.F. 'Collecting the Body's Signals' Medical Electronics:2, Electronics pp.103-112, July (1967)
53. Boter, J., Den Hertog, A. & Kupier, J. 'Disturbance-Free Skin Electrodes for Persons During Exercise', Med. & Biol. Engng. 4, pp.91-95, (1966)
54. Hill, D.W. & Khandpur, R.S. 'The Performance of Transistor ECG Amplifier', World Medical Instrumentation, pp.12-22, May (1969)
55. Towers, T.D. 'High Input Impedance Amplifier Circuits', Wireless World, 74, 197 (1968)
56. Schwartz, M. 'Information Transmission, Modulation and Noise', McGraw-Hill Book Co., (1959)
57. Betts, J.A. 'Signal Processing Modulation and Noise' The English Universities Press Ltd., London (1970)
58. Zetterberg, L.H. 'A Comparison between Delta and Pulse Code Modulation' Ericsson Technics, 11, No. 1, pp 95-154, Jan. 1955.
59. Maschhoff, R.H. 'Delta Modulation' Electrotechnology, pp 91-97, January 1964.

60. Deloraine, E.M., Van Merlo, S. and Derjavitch, B. 'Method and System of Impulse Transmission' French patent No. 932, pp 140, August 10, 1946.
61. de Jager, J. 'Delta Modulation, a Method of PCM Transmission using 1-unit Code', Philips Res.Rept., No. 7, pp 442, 422-446, (1952).
62. Brotin, S.J. and Brown, J.M. 'Companded Delta Modulation for Telephony, Trans. I.E.E.E., Vol. COM-16, No. 1, pp 157-162, Feb. 1968.
63. Cutler, C.C. 'Differential Quantization of Communication Signals', U.S. Patent No. 2605, 361 applied for June 29, 1950, issued July 29, 1952.
64. Inose, H., Yasuda, Y. and Murakami, J. 'A Telemetering System by Code-Modulation - Delta-Sigma Modulation', IRE Trans. on Space Electronics and Telemetry, No. 8, pp 204-209, September 1962.
65. Johnson, F.B. 'Calculating Delta Modulator Performance' Trans. on Audio and Electroacoustics, Vol. AU-16, No. 1, pp 121-129, March 1968.
66. Abate, J.E. 'Linear and Adaptive Delta Modulation' Proc. IEEE, Vol. 55, pp 298-308, March 1967.

67. O'Neal, J.B., Jr., 'Delta Modulation Quantizing Noise Analytical and Computer Simulation Results for Gaussian and Television Signals', Bell System Technical Jnl., 45, No. 1, pp 117-141, Jan. 1966.
68. Flood, J.E. 'Time Division Multiplex Systems' Electronic Engineering, Jan. 1953.
69. Herbert, T.E. 'Telegraphy', Pitman 1930
70. Tomozawa, A. and Kaneko, H. 'Companded Delta Modulation for Telephone Transmission', Trans. IEEE, Vol. COM-16, No.1, pp 149-157, Feb. 1968
71. Steele, R. Symposium on Digital Communications, Loughborough University of Technology, U.K., 1974
72. Lockhart, G.B. 'Non-Recursive Filtering, Introductory Course on Digital Filtering', Imperial College, London, July 1970
73. Ackroyd, M.H. 'Digital Filters', Edited by D.W.Hill, Butterworth 1973
74. Rabiner, L.R., Gold, R. and McGonegal, C.A. 'An Approach to the Approximation Problem for Non-recursive Digital Filters', IEEE Trans. on Audio Electro-Acoustics, Vol. AU-18, No. 2, pp 83-106, June 1970
75. Kaiser, J.F. 'Digital Filters in System Analysis by Digital Computer', F. Kuo and J.F. Kaiser, Eds., New York, Wiley, 1966

76. Martin, M.A. 'Digital Filters for Data Processing' Missile and Space Division, General Electric Co. Tech. Information Series Report 62 - SD 484, 1962
77. Gold, B. and Jordan, K.L. 'A Direct Search Procedure for Designing Finite Duration Impulse Response Filters', IEEE Trans. Audio and Electroacoustics, Vol. AU-17, March 1969
78. Bogert, B.P., Healey, M.R. and Tukey, J.W. 'The Quefrency Analysis of Time Series for Echoes: Cepstrum, Pseudo-Autocovariance, Cross-Cepstrum and Saphe Cracking', Proc. of the Symps. on Time Series Analysis by M. Rosenblatt, Ed. (John Wiley & Sons, Inc., New York) pp 209-243 (1963)
79. Michall Noll, A. 'Cepstrum Pitch Determination', The Jnl. of Acoustical Society of America, Vol. 41, No. 2, pp 293-309 (Feb. 1967)
80. Bendat, J.S. and Piersal, A.G. 'Analysis of Random Data', Wiley Interscience, 1971.
81. Protonotarias, E.N. 'Slope overload noise in differential pulse code modulation', The Bell System Technical Jnl., 46, No.9, pp 2119-2162, Nov. 1967
82. Goodman, D.J. 'Delta Modulation Granular Noise', The Bell System Technical Jnl., pp 1197-1220, May-June 1969

83. Van de Weg, H. 'Quantization Noise of a Single Integration Delta Modulation System with an N-digit code', Philip Research Reports 8, No. 5, pp 367-385, Oct. 1953.
84. Aaron, M.R., Fleischman, J.S., McDonald, R.A. and Protonotarios, E.N. 'Response of Delta Modulation to Gaussian Signals', The Bell System Technical Jnl., pp 1167-1195, May-June 1969
85. De France, J.J. 'Communications Electronics Circuits', Holt, Rinehart and Winston, Inc., U.S.A. 1966
86. Noble, F.W. Proc. Inst. Elect. Electron. Eng., 54, pp 1976-1978 (1966)
87. Hertsler, E.C. 'Electrocardiogram Recording System for Ambulating Subjects', J. Appl. Physiol., 23, pp 998 (1967)
88. Livingstone, S.M. and Crecraft, D.I. 'A simple Physiological Recording System', 6, pp 337, 1968
89. Van der Weide, H. and Van Bommel, J.H. 'A Photon-Coupled Amplifier for the Transmission of Physiological Signals', Med. & Biol. Eng., Vol. 6, pp 447-448, 1968
90. Krupka, Z. 'The Effect of Human Body on Radiation Properties of Small-sized Communication Systems', IEEE Trans., Vol. AP-16(2), pp 154-163 (1968)

91. Magoye, J.O.L. 'Biomedical Telemetry Aerials', M.Sc. Thesis, University of Technology, Loughborough, 1972.
92. Buchanan, H., Moore, W.F., and Richter, C.R. 'Human Body Effect on Signal Patterns of Personal Telemetry Transmitters', USAF School of Aerospace Medicine, Report No. SAM-TR-70-4, Jan. 1970.
93. Schwan, H.P. 'Capacity and Conductivity of Body Tissue at UHF', Proc. IRE, pp 1735-40, Dec. 1953.
94. Schwan, H.P. 'Determination of Biological Impedances' Future Advances in Bio-medical Engineering, pp 323-407, (1963)
95. Oliver, B.M., Pierce, J.R. and Shannon, C.E. 'The Philosophy of PCM' Proceedings of the I.R.E., pp 1324-1332, November 1948.
96. Burchard, D. 'Die Überschlagige Berechnung der Reichweite von Kleinsendern Funkschau 16, pp 515 (1966)
97. Shepherd, N.H. and Chaney, W.G. 'Personal Radio Antennas' IRE Trans., VC-10, pp 23 (1961)
98. Kupier, J., Bosman, J. and Boter, J. 'Improvement in Measuring Physical Load by Wireless Transmission of the ECG', World Med. Electron., 4, pp 304, 1966
99. Hoare, D.W., Ivison, J.M. and Qazi, S. 'A Multichannel Biomedical Telemetry System using Delta Modulation', 8th Intern. Conf. on Med. and Biological Engineering, Session 30-8, July 1969.

100. Hoare, D.W., Ivison, J.M.
and Qazi, S. 'A Time-Division Multiplexed Radio
or Single-Wire Telemetry System using
Delta Modulation' Int. Symp. on
Biotelemetry, Nijmegen, The Netherlands,
May 1971.
101. Ivison, J.M. and Robinson,
P.F. 'A Digital Phase Modulator and
Demodulator for a Biomedical Telemetry
System'; Jnl. of the International
Federation for Medical and Biological
Engineering, Jan. 1974.

APPENDIX A

RADIO FREQUENCIES FOR LOW-POWER NON-SPEECH DEVICES

As there are only a limited number of frequencies available for these types of service the use of radio can only be agreed where alternative methods of communication (eg lines, ultrasonics or light beams) cannot reasonably be employed. Applicants may be asked to investigate the possibility of using alternative methods. Each application will be considered on its merits.

Under the Wireless Telegraphy Act 1949 all users of radio require a licence issued by the Minister of Posts and Telecommunications. Development of radio apparatus must be authorised by a Testing and Development Licence. Such a Licence must be applied for even if work is to be carried out under suppressed radiation conditions. Once equipment has been developed it must be submitted to the Ministry of Posts and Telecommunications for type approval tests to be carried out. A Licence for the use of such a system will only be issued where type approved equipment is to be used.

Medical and Biological Telemetry

There are three specifications for medical and biological telemetry equipment covering three separate classes of device. The relevant specification numbers are W.6802, A.6803 and W.6804. These are published by the Stationery Office in one booklet, SO code No. 88-5438, price 15p(3s)

- a. Class 1. This relates to very low power devices, operating between 300 kc/s and 30 Mc/s normally wholly contained within the body of an animal or man, (eg radio pills). The normal transmitting range should not appreciably exceed 5 feet.

b. Class II equipment must operate in the band 102.2 - 102.4 Mc/s. The range over which this class of equipment may be used would not normally exceed 50 feet.

c. Class III devices also operate in the 102.2 - 102.4 Mc/s. A more stringent specification applies, and consequently a greater range, up to 200 yards is permissible with equipment meeting this specification. The precise range depends largely on the sensitivity of the receiver used.

Note:

The information above is correct at the time of going to print, but may be subject to alteration from time to time. Specific enquiries and requests for application forms should be addressed to:

Ministry of Posts and Telecommunications
Radio Regulatory Division,
Waterloo Bridge House
Waterloo Road,
LONDON SE1

November 1969

In the U.S.A., U.K., Germany and the Netherlands it is possible to rent telephone lines for permanent short or long distance use for signal transmission, with single or multichannel working.

APPENDIX B

Integrator in the Encoder

The delta modulator becomes a closed loop system by the addition of a RC integrator. The RC integrator has a leakage in the practical circuit.

In the analogue form the transfer function can be written as

$$G(s) = \frac{a}{s + a} \quad (1)$$

where $a = \frac{1}{RC}$

Also for a RC network shown in figure B.1, the transfer function is

$$\begin{aligned} H(j\omega) &= \frac{\frac{1}{j\omega C}}{R + \frac{1}{j\omega C}} \\ &= \frac{1}{1 + j\omega CR} \end{aligned} \quad (2)$$

Discrete Form

In order to simulate a delta modulator and hence an RC integrator on the digital computer a discrete representation is required.

The representation is shown in figure B.2.

If 'T' is the sampling period, the z^{-1} block delays the signal by T seconds.

$$E(z) = B(z) + F(z) = B(z) + H(z)C(z)$$

$$C(z) = E(z) z^{-1}$$

$$E(z) = B(z) + H(z)E(z) z^{-1}$$

$$E(z) (1 - H(z) z^{-1}) = B(z)$$

$$G(z) = \frac{E(z)}{B(z)} = \frac{1}{1 - H(z)z^{-1}} \quad (3)$$

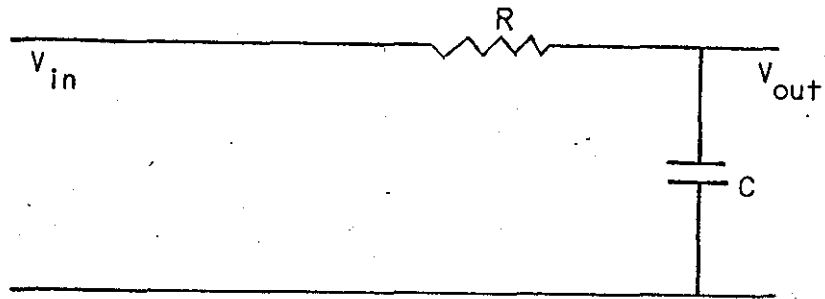


Figure B.1 RC Network

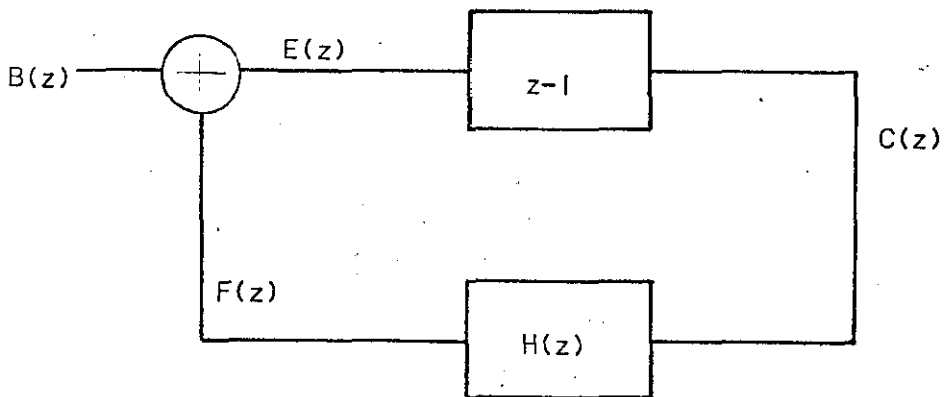


Figure B.2 Discrete Representation of Integrator

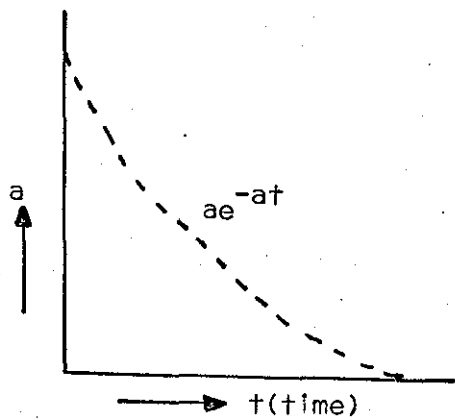


Figure B.3 Impulse Response of RC network

Comparing this result with the analogue form and ignoring a in the equation (1), the z-transform of $G(s) = \frac{1}{(s+a)}$ is

$$G(z) = \frac{1}{1 - e^{-aT} z^{-1}} \quad (4)$$

Comparing equation (3) and (4) it is observed that they are identical if $H(z) = e^{-aT}$.

The sampling period T and $a = \frac{1}{RC}$ are constant.

Hence $H(z)$ is also constant say μ

$$G(z) = \frac{a}{1 - \mu z^{-1}} \quad (5)$$

a is reintroduced to get $G(z)$ for the RC network (5) and can be expanded as

$$\begin{aligned} G(z) &= a\{1 + \mu z^{-1} + \mu^2 z^{-2} + \mu^3 z^{-3} + \dots\} \\ &= a \sum_{k=0}^{\infty} \mu^k z^{-k} \quad \mu < 1 \end{aligned} \quad (6)$$

$$G(z) = \sum_{k=0}^{\infty} e(kT) z^{-k} \quad (7)$$

This is obtained by the application of the discrete convolution technique.

$e(kT)$ is the value of the output of the pulse transfer function at time kT , i.e., the output signal is $e(t)$ defined at times T seconds apart.

From equation (6) and (7),

$$e(t) = a \mu^k = a e^{-aTk},$$

corresponding to a time signal $a e^{-at}$, defined at times T seconds apart.

$$a e^{-at} = \frac{1}{RC} e^{-t/RC} = \frac{1}{RC} e^{-kT/RC}$$

where $t = kT$

The curve of figure B.3. can easily be shown to be the impulse response of an RC network.

From equations (3) and (6)

$$E(z) = a \sum_{k=0}^{\infty} e^{-kaT} z^{-k} B(z)$$

$$E(z) = a \sum_{k=0}^{\infty} e^{-akT} z^{-k} \quad (8)$$

If $B(z) = 1$

$B(z) = 1$, if $b(t) = \delta(t)$ an impulse

$G(z) = E(z)$ and $e(t)$ is defined by the curve shown in figure B.3.

The magnitudes of $e(t)$ at successive sampling periods

$$a, a\mu, a\mu^2, a\mu^3, \dots$$

or $a, ae^{-aT}, ae^{-2aT}, ae^{-3aT}, \dots$

APPENDIX C

Theory of Non-Recursive Filters

The digital version of a transversal filter is termed non-recursive filter since each output number depends only on the input sequence. This is shown in figure C.1. and the equation

$$y(t) = \sum_{n=0}^{N-1} a_n x(t - nT) \quad (1)$$

The Digital version of the transversal filter or non-recursive filter employs an N stage digital delay line which holds successive numbers (generated by the analogue to digital converter) and shifts the sequence by one stage on the arrival of a clock pulse every T seconds. Since all operations in p are performed digitally the part between input X(KT) and output Y(KT) is a digital filter. The input X(KT) and output Y(KT) are number sequences where K = -1, 0, +1, The input sequence in general is conceived as a sampled and digitized version of an analogue signal but in practice it need not be derived in this way.

The value of an output number Y(KT) from the figure is related to the input sequence by

$$Y(KT) = \sum_{n=0}^{N-1} a_n x\{(K-n)T\} \quad (2)$$

This expression is analogous to the analogue transversal filter input/output relation given in equation (1). It should be noted however that the accuracy to which weighting coefficients can be set in the digital case depends on the number of digits employed. The

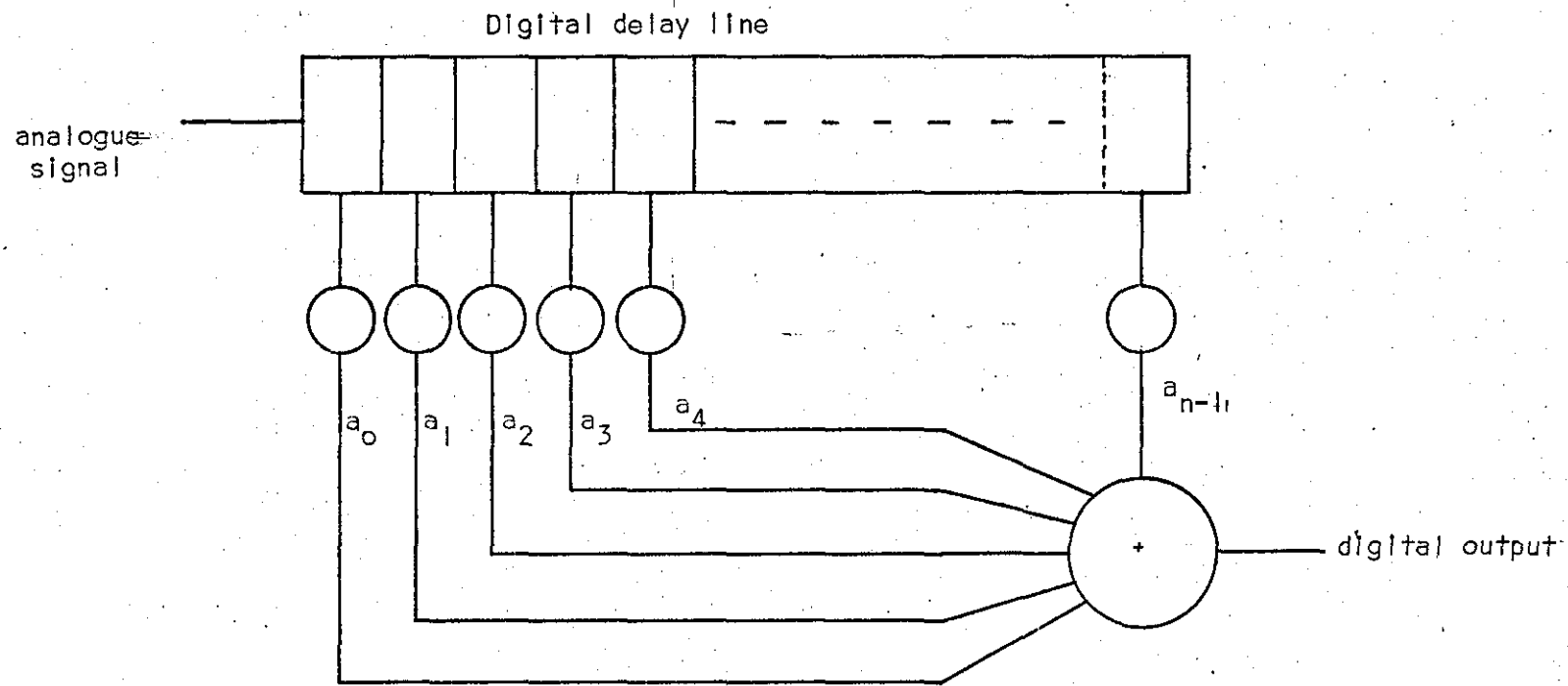


Figure C.1 Digital non-recursive filter

multiplication by digital arithmetic usually involves round-off errors which can be interpreted as noise.

Impulse Response of the Non-Recursive Filter

The impulse response is formed from the set of 'N' weighting constants. Since the number of delay elements N, must always be finite, then the impulse response of a non-recursive filter must always be limited in time. This property is common to all types of non-recursive filters and contrasts with the theoretically infinite impulse response of the recursive filter.

Frequency Response

The output of a non-recursive filter is given by

$$Y(KT) = \sum_{n=0}^{N-1} a_n x\{(K-n)T\}$$

Suppose that the input sequence is a sampled and digitized consinusoid of constant frequency ω rad/sec., then

$$x(KT) = \cos K\omega T$$

The output sequence $Y_\omega(KT)$, $K = \dots -1, 0, +1, \dots$

is determined by substituting the above expression for $x(KT)$ in the above = n of the filter.

$$\therefore Y_\omega(KT) = \sum_{n=0}^{N-1} a_n \cos(K-n)\omega T$$

Since $2 \cos \omega n T = \exp(j\omega n T) + \exp(-j\omega n T)$

$$= \text{Re} \sum_{n=0}^{N-1} a_n e^{j(K-n)\omega T}$$

Re is the real part

$$Y_\omega(KT) = \text{Re} \cdot e^{j\omega K T} \sum_{n=0}^{N-1} a_n e^{-j\omega n T}$$

$$= R e^{jK\omega T} \cdot I(e^{-j\omega T})$$

$$\text{Where } I(e^{-j\omega T}) = \sum_{n=0}^{N-1} a_n e^{-j\omega T n}$$

$$Y_{\omega}(KT) = \text{Re} \left\{ I(e^{-j\omega T}) e^{j(K\omega T + \theta_1)} \right\}$$

$$\text{Where } I(e^{-j\omega T}) = |I(e^{-j\omega T})| e^{j\theta_1}$$

Taking the real part

$$Y_{\omega}(KT) = |I(e^{-j\omega T})| \cos(K\omega T + \theta_1)$$

Thus the response of the filter to a cosinusoid of frequency ω is a consinusoid of the same frequency but with values of magnitude and phase determined by $I(e^{-j\omega T})$ and θ_1 respectively. $I(e^{-j\omega T})$ is therefore the frequency characteristic of the filter.

Computing the Ideal Weighting Sequence

Subroutine fast fourier transform given in the Appendix can be used to compute approximately the Ideal weighting sequence from the required frequency response characteristics. The subroutine computes the direct or inverse discrete fourier transform of an array of complex numbers. The DFT of an array of N complex numbers $(X_0, X_1, X_2 \dots X_{N-1})$ is another array of N complex numbers $(X_0, X_1, X_2, \dots X_{N-1})$ whose element is given by the formula

$$x_r = \sum_{k=0}^{N-1} a_k e^{-j2\pi rk/n} \quad r = 0, 1, 2, \dots N-1$$

The inverse of the discrete fourier transform allows the array $(X_0, X_1, \dots X_{N-1})$ to be computed from $(X_0, X_1, \dots X_{N-1})$, the inverse is given by

$$a_k = \frac{1}{N} \sum_{r=0}^{N-1} x_r e^{j2\pi rk/n} \quad k = 0, 1, 2, 3, \dots N-1$$

Synthesis of Non-Recursive Filters by Frequency Sampling

The frequency sampling technique is a general procedure which may be usefully applied to most filter requirements.

The frequency characteristic of an N -stage non-recursive filter is given by

$$I(e^{-j\omega T}) = \sum_{n=0}^{N-1} a_n e^{-j\omega n T} \quad (3)$$

Suppose this characteristic is sampled at intervals of $1/NT$ Hz along the frequency axis. If the samples are $X_0, X_1, X_2 \dots X_{N-1}$, then

$$\begin{aligned} X_r &= I(e^{-j\frac{2\pi r}{N}}) \quad r = 0, 1, 2, \dots, N-1 \\ &= \sum_{n=0}^{N-1} a_n e^{-jn\frac{2\pi r}{N}}, \quad r=0, 1, 1, 2, \dots, N-1 \end{aligned} \quad (4)$$

The above expression relates the N coefficient settings, a_0, a_1, \dots, a_{N-1} to the N frequency samples X_0, X_1, \dots, X_{N-1} .

Thus if there are N coefficients to be set there is freedom to choose the values of ' N ' independent points on the frequency response.

Equation (4) expresses a Discrete Fourier Transform (DFT). The set of frequency samples X_0, X_1, \dots, X_{N-1} is in fact the DFT of the set of coefficient values a_0, a_1, \dots, a_{N-1} . It follows that the coefficient set may be obtained from the set of frequency samples by application of the inverse DFT.

$$a_k = \frac{1}{N} \sum_{r=0}^{N-1} x_r e^{jr\frac{2\pi k}{N}} \quad k=0, 1, \dots, N-1$$

The evaluation itself may be performed by a fast fourier transform subroutine.

As the weighting coefficients are real numbers the frequency samples must exhibit the usual symmetry about zero frequency as shown in figure C.2.

It is then possible to specify independent $N/2$ complex values (usually magnitude and phase) of the frequency response at intervals of $\frac{1}{NT}$ Hz, extending from zero frequency to $\frac{1}{NT}$ Hz below the Nyquist frequency.

The procedure for the design of non-recursive filter from the frequency sampling technique is given below.

1. If the non-recursive filter has N taps, $N/2$ samples of the required frequency response at intervals of $\frac{1}{NT}$ Hz are selected along the frequency axis.
2. An inverse DFT computer programme is used to obtain the N values of coefficient setting from the $N/2$ frequency samples.

If it can be assumed that the finite precision of the non-recursive filter coefficients setting causes negligible error, then the frequency sampling technique guarantees that the frequency characteristic will equal $N/2$ specified values at equidistant points along the frequency axis.

There is however little control over behaviour between these points where sidelobe ripple may be unacceptably high.

Such difficulties are overcome by the following techniques.

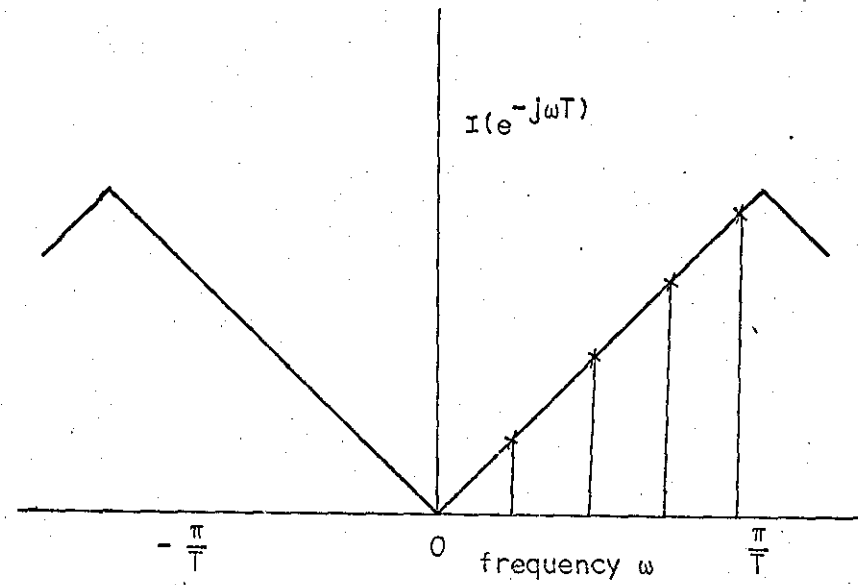


Figure C.2 Specification of $\frac{N}{2}$ frequency samples on a required characteristic

Fast Fourier Transform (FFT) and Discrete Fourier Transform (DFT)

The discrete fourier transform is the sampled data equivalent to the conventional fourier transform. The fast fourier transform is not a transform as such but a collective term for a number of algorithms which facilitate the efficient computation of discrete fourier transforms of N samples in $N \log_2 N$ operations where N is a power of two.

Cooley and Tuckey⁽¹⁹⁶⁵⁾ published a paper outlining this method. At the time it was thought to be a new method of computing a DFT because the DFT of N samples took something proportional to N^2 operations, the constant of proportionality depending on the symmetries of the sine and cosine in the weighting functions. Computer algorithms based on this N^2 method took up a great deal of computational time.

Soon after the publication of this paper it was realised that it was in fact a rediscovery of a method, in general terms, used by Danielson and Lanczos in 1942 who refer to a German paper by Ronge and Konig in 1924. The paper by Ronge and Konig describes in terms of sine and cosine series a method of transforming N points where ' N ' is a power of 2. This is done by forming $\log_2 N$ sub-series, and the algorithm doubles to form this DFT in $\log_2 N$ doublings. Thus a total number of operations of $N \log_2 N$ is necessary.

In those days of elementary computing machinery the saving of time was very small because of the small number of samples possible. Thus the algorithm was forgotten, until the advent of modern computing machinery.

If the DFT is computed without using the FFT algorithm the number of arithmetic operations involved with 'N' samples is proportional to N^2 . With use of the FFT algorithm, the number of operations is now proportional to $N \log_2 N$.

The factor of improvement is therefore

$$\frac{N^2}{N \log_2 N} = \frac{N}{\log_2 N}$$

With large sample number, the improvement can be very large.

APPENDIX D

DISCRETE CONVOLUTION

Any input sequence to the filter may be regarded as a sum of impulse sequence each applied at different sampling instances.

The general expression for the output of a linear system in terms of the input and the impulse response can readily be obtained.

A unit input sample, preceded and succeeded by zeros results in outputs h_0, h_1, \dots, h_r as it moves from delay to delay. Thus the impulse response is $h_r, r = 0, 1, \dots$. If the input sequence is $x_n, n = \dots, -2, -1, 0, 1, 2, \dots$, then the output is

$$\begin{aligned} y_n &= \sum_{r=0}^{\infty} h_r x_{n-r} \\ &= \sum_{r=-\infty}^n h_{n-r} x_r \end{aligned}$$

$$y_n = h_n * x_n$$

The output sequence can therefore be regarded as the input sequence convolved with the impulse response.

The input/output relation of the non-recursive filter is an expression of a discrete convolution between the input sequence and impulse response.

If transform methods are applied such convolution operations in the time domain may be replaced by multiplication in the frequency domain.

```

0107      SUBROUTINE NLOGN (N,X,LX,DIR)
0108      COMPLEX X,WK,HOLD,Q
0109      C      NMAX=LARGEST VALUE OF N TO BE PROCESSED
0110      C      NONDUMMY DIMENSION M(NMAX)
0111      C      FOR EXAMPLE, IF NMAX = 25 THEN
0112      DIMENSION M(25)
0113      C      DIMENSION X(2**N)
0114      DIMENSION X(LX)
0115      DO 1 I=1,N
0116      1 M(I)=2**(N-I)
0117      DO 4 L=1,N
0118      NBLOCK=2**(L-1)
0119      LBLOCK=LX/NBLOCK
0120      LBHALF=LBLOCK/2
0121      K=0
0122      DO 4 IBLOCK=1,NBLOCK
0123      FK=K
0124      FLX=LX
0125      V=DIR*6.28318531*FK/FLX
0126      WK=CMPLX(COS(V),SIN(V))
0127      ISTART=LBLOCK*(IBLOCK-1)
0128      DO 2 I=1,LBHALF
0129      J=ISTART+I
0130      JH=J+LBHALF
0131      Q=X(JH)*WK
0132      X(JH)=X(J)-Q
0133      X(J)=X(J)+Q
0134      2 CONTINUE
0135      DO 3 I=2,N
0136      II=I
0137      IF (K.LT.M(I)) GO TO 4
0138      3 K=K-M(I)
0139      4 K=K+M(II)
0140      K=0
0141      DO 7 J=1,LX
0142      IF (K.LT.J) GO TO 5
0143      HOLD=X(J)
0144      X(J)=X(K+1)
0145      X(K+1)=HOLD
0146      5 DO 6 I=1,N
0147      II=I
0148      IF(K.LT.M(I)) GO TO 7
0149      6 K=K-M(I)
0150      7 K=K+M(II)
0151      IF (DIR.LT.0.0) RETURN
0152      DO 8 I=1,LX
0153      8 X(I)=X(I)/FLX
0154      RETURN
0155      END

```

END OF SEGMENT, LENGTH 429, NAME NLOGN

APPENDIX FSPECTRAL ANALYSIS

The spectrum is obtained on the computer using the Fast Fourier Transform algorithm (FFT) and $N \log N$ subroutine. Before an FFT algorithm can be performed on a data array, a time function must be sampled at discrete intervals. For spectral analysis the sampling rate (f_s) must be at least twice the maximum frequency (f_M) encountered in the time function. That is,

$$f_s = 2f_M$$

The number of samples required is proportional to the resolution Δf desired. Δf may be precisely described as the frequency spacing between Fourier coefficients.

Total number of samples is related to Δf by

$$N/2 = f_M/\Delta f$$

$$f_s = 2f_M$$

This relation holds because the FFT of 'N' samples sampled at f_s yields $N/2$ coefficients equally spaced on the frequency axis at points located at

$$f = n\Delta f$$

where $n = 0, 1, 2, 3, \dots, N/2$

The length of the sampling interval t and N are related as

$$t = N/f_s$$

$$t = 2f_M/\Delta f/f_s$$

$$t = 1/\Delta f$$

The total number of samples taken for the analysis of the ECG waveform is 1024, that is,

$$N = 1024$$

For 1024 samples, the ECG waveform is taken more than a cycle lasting for 800 m sec.

Duration of ECG taken = 800 m sec.

$$\begin{aligned}\text{Sampling frequency} &= 1024 \cdot 10^3 / 800 \\ &= 1.28 \text{ kHz} \\ &1.3 \text{ kHz}\end{aligned}$$

Also,

$$\begin{aligned}1/\Delta f &= 800 \cdot 10^{-3} \\ \Delta f &= 10^3 / 800 \\ &= 1.25 \text{ Hz}\end{aligned}$$

Therefore

$$\begin{aligned}f &= n\Delta f \\ f_1 &= 1.25 \text{ Hz} \\ f_{512} &= 1.25 \cdot 512 \\ &= 640 \text{ Hz}\end{aligned}$$

APPENDIX G

Cepstrum

This is easily implemented using the FFT processor and the peripheral computer to perform a computation.

The process is :-

- (1) Form the FFT process on a time series $x(t)$
- (2) Re-order the output of the processor
- (3) The answer formed is in a complex form $a + ib$, thus to use the definition of cepstrum from signal analysis, the computer now takes the logarithm of this complex number.

$$a + ib = R e^{i\theta} \text{ where } R = \sqrt{a^2 + b^2}$$

$$\text{and } \theta = \tan^{-1} \left(\frac{b}{a} \right)$$

$$\text{So } \log_e(a+ib) = \log_e R + i\theta$$

This is only performed on the first $N/2$ answers.

- (4) Place in the real register in a frequency order the sequence $\log_e R$, and in the imaginary register θ
- (5) Perform an FFT on this frequency ordered sequence to form the quefrequency series.
- (6) Re-order into a quefrequency ordered sequence.

The reasoning behind the use of only $N/2$ of the 'samples' from the first pass of the FFT is equivalent to the Nyquist sampling criteria upon a time ordered series.

If the highest resolvable frequency is f say, then the quefrequency series will be based upon the inverse of this, i.e. $1/f$ as its 'frequency'. The cepstrum thus forms the series.

$$\left(0, \frac{1}{f}, \frac{2}{f}, \dots, \frac{f/2}{f} \right) \text{ sec. as the quefrequency series.}$$

Thus the largest quefrequency resolvable is $\frac{1}{2}$ sec. i.e.

2 Hz in the spectrum if $f < 1$.

APPENDIX H

Theory of a Histogram

As shown before, a long stream of signal is taken which is accompanied by a Gaussian noise. This can be treated as one long signal monitored for a long time consisting of many ECG signals. Similarly the decoded signal and the difference of the two signals will be in that form. The difference between the decoded signal with the noisy signal as an input and the signal without any noise called the Error or Distortion is also expected to have characteristics similar to the noise added in the input or the system, that is, time-invariant and stationary.

Consider there are N data values (S_n) , $n = 1, 2, 3 \dots N$ of the noise (error) obtained from a transformed record $S(t)$ which is also stationary having zero mean \bar{S} . That is, a probability density measurement of a single sample time history record $S(t)$ from a stationary random process $\{S(t)\}$. The probability that $S(t)$ assumes a particular amplitude between $S - (w/2)$ and $S + (w/2)$ during a time interval T may be estimated by

$$p(s, w) = \text{prob}\left\{S - (w/2) \leq S(t) \leq (S + w/2)\right\}$$

$$= \frac{1}{T} \sum \Delta t_i = \frac{T_x}{T}$$

Δt_i is the time spent by $S(t)$ in this amplitude range during the i^{th} entry into the range, and $T_x = \sum \Delta t_i$ the ratio $\frac{T_x}{T}$ is the total fractional portion of the time spent by $s(t)$ in the range $\{s - (\frac{w}{2}), s + (\frac{w}{2})\}$ it should be noted that T_x will usually be a function of the amplitude s . This estimated probability $p(s, w)$ will approach the true probability, $P(s, w)$ as T approaches infinity. Also this

estimated probability is an unbiased estimate of true probability,

hence

$$P(s,w) = E\{P(s,w)\} = \lim_{T \rightarrow \infty} P(s,w) = \lim_{T \rightarrow \infty} \frac{T_x}{T}$$

The probability density function $p(x)$ is defined

$$P(s) = \lim_{W \rightarrow 0} \frac{P(s,w)}{W} = \lim_{\substack{T \rightarrow \infty \\ W \rightarrow 0}} \frac{P(s,w)}{W} = \frac{T_x}{TW}$$

This is a sample estimate of $p(x)$.

It follows from the last equation that the probability density function of $s(t)$ can be estimated by

$$p(x) = \frac{N_x}{NW}$$

W is a narrow interval at s and N_x is the number of data values which fall within the range $x \pm \frac{W}{2}$. Hence an estimate $p(s)$ is obtained digitally by dividing the full range of s into an appropriate number of equal width class intervals, tabulating the number of data values in each class interval and dividing by the product of class interval width w and the sample size N . The estimate $p(s)$ is not unique, since it clearly is dependent upon the number of class intervals and their width is selected from the analysis.

If K denotes the number of class intervals selected to cover the entire range of the data values from 'a' to 'b', the width of each interval is given by

$$W = \frac{b-a}{K}$$

and the point of i^{th} interval is defined as

$$D_i = a + iw \quad i = 0, 1, 2, \dots, K$$

$$D_0 = a \quad D_K = b$$

Now sequence of $K + 2$ number is given by N_i , $i = 0, 1, 2, \dots, K+1$,
by the conditions

$N_0 =$ (number of x such that $x \leq D_0$)

$N_1 =$ (number of x such that $D_0 < x \leq D_1$)

⋮

$N_i =$ (number of x such that $D_{i-1} < x \leq D_i$)

⋮

$N_k =$ (number of x such that $D_{k-1} < x \leq D_k$)

⋮

$N_{k+1} =$ (number of x such that $x > D_k$)

This procedure will sort out the 'N' data values of 'x' so that the number sequence (N_i) satisfies

$$N = \sum_{i=0}^{K+1} N_i$$

One method of sorting this on a digital computer is to examine each value S_n , $n = 1, 2, 3, \dots, N$ in turn as follows

(a) If $S_n \leq a$, add the integer one to N_0

(b) If $a < S_n \leq b$, compute

$$l = \frac{S_n - a}{w}$$

then select 'l' as the largest integer less than or equal to l,
add the integer one to N_l .

(c) If $S_n > b$, add the integer one to N_{k+1}

Four output forms for the sequence (N_i) can be used. The first output is the Histogram, which is simply the sequence (N_i) without changes. The second output is the sample percentage of data in each class interval defined for $i = 0, 1, 2, \dots, K+1$, by

$$p_i = \text{Prob} (D_{i-1} < s \leq D_i) = \frac{N_i}{N}$$

The third output is the sequence of sample probability density estimates (p_i) defined at the midpoints of the K class intervals in (a,b) by

$$p_i = \frac{P_i}{w} = \frac{(N_i)}{(N)} - \frac{K}{b-a} \quad i = 1, 2, \dots, K$$

The fourth output is the sequence of sample probability distribution estimates

$$P(i) = \text{Prob} (-\infty < s \leq D_i) = \sum_{j=0}^i p_j = w \sum_{j=0}^i P_j$$

The Histogram and Probability Density Functions specify the probability of the variable being within a particular portion of its range and therefore they should provide sufficient information to enable the average value of the variable to be determined.

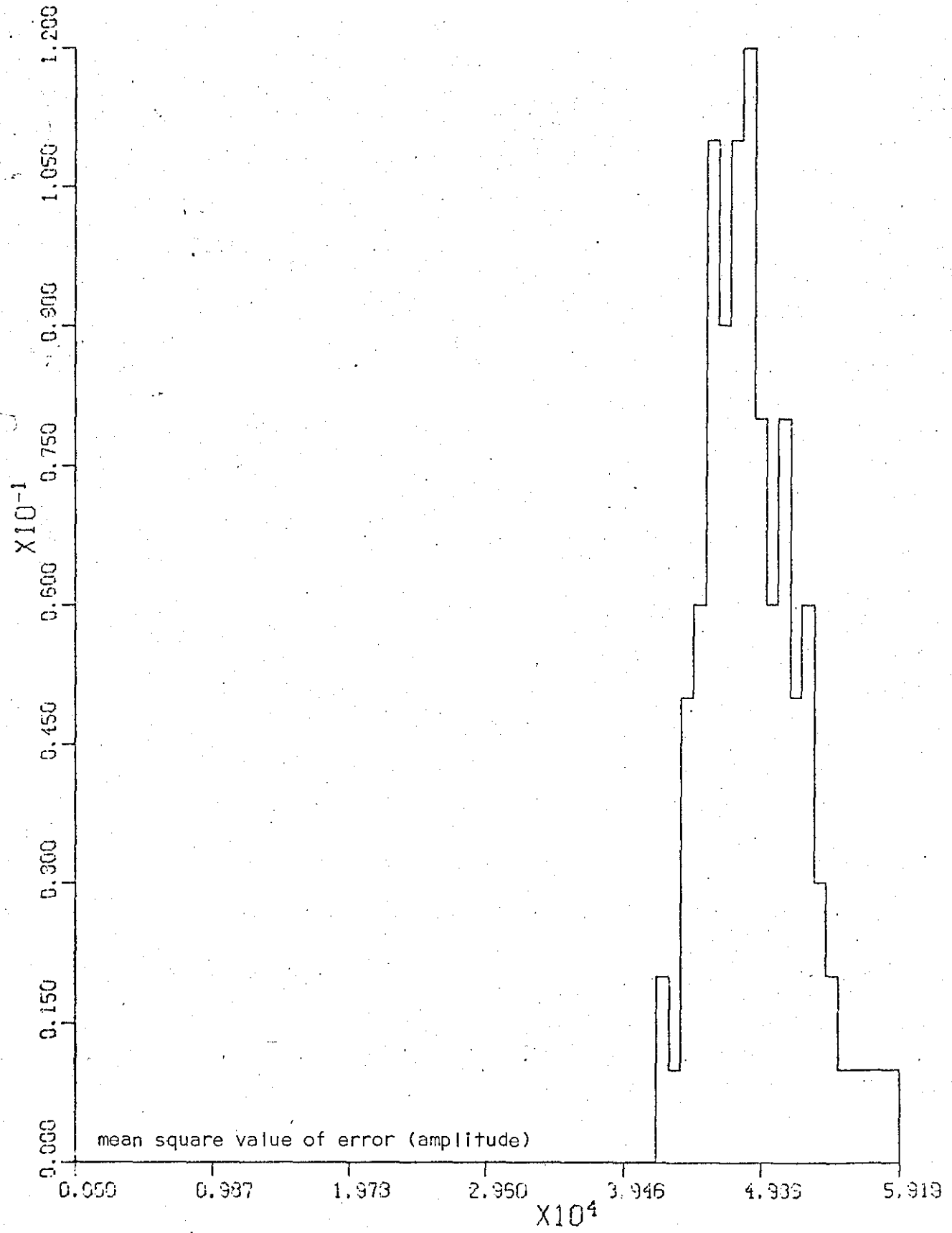


Figure 4.31 Histogram of input low pass bandlimited noise of variance 0.015

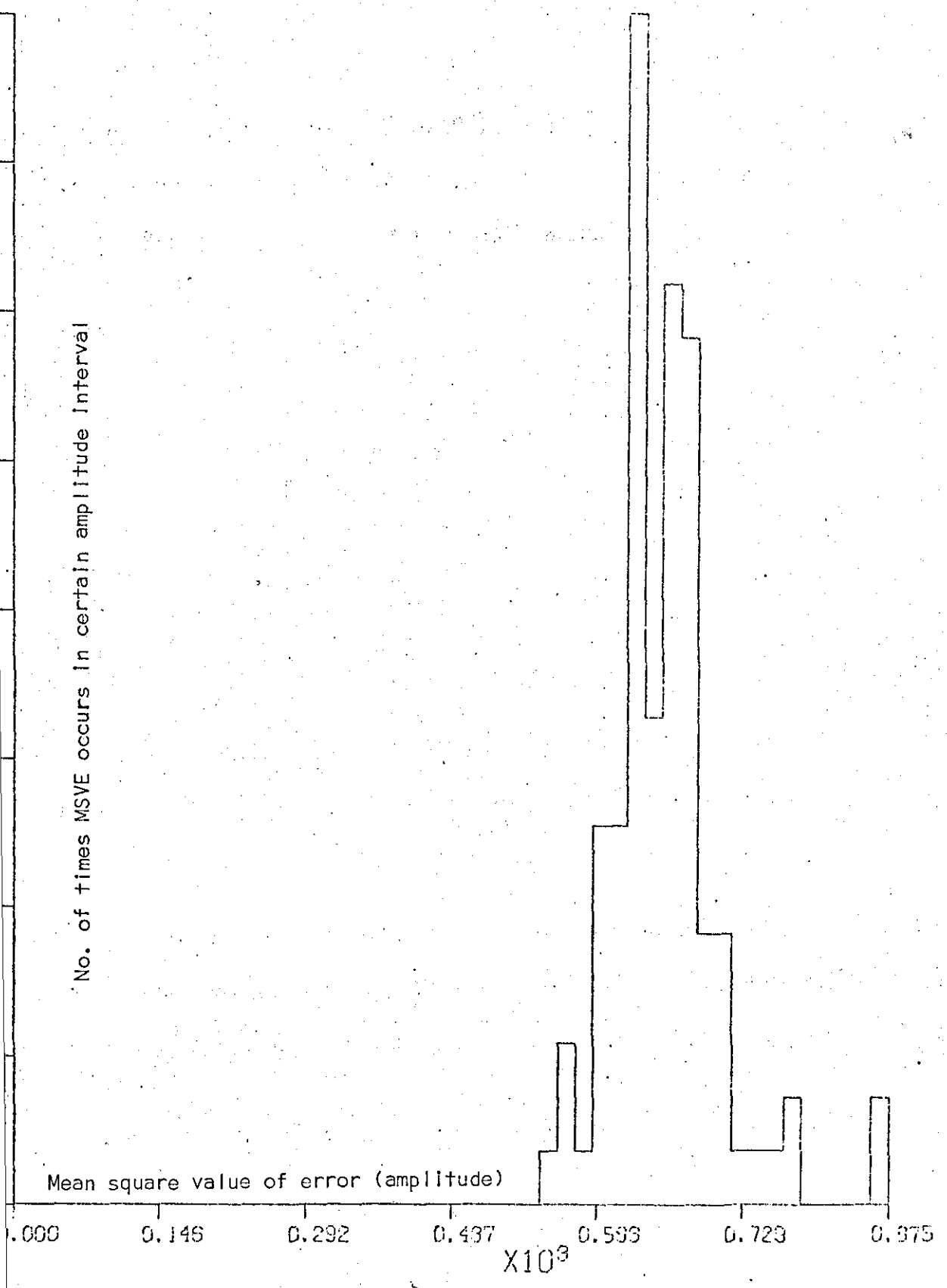


Figure 4.32 Histogram of the coder noise when the input signal has a low pass bandlimited noise of variance 0.015

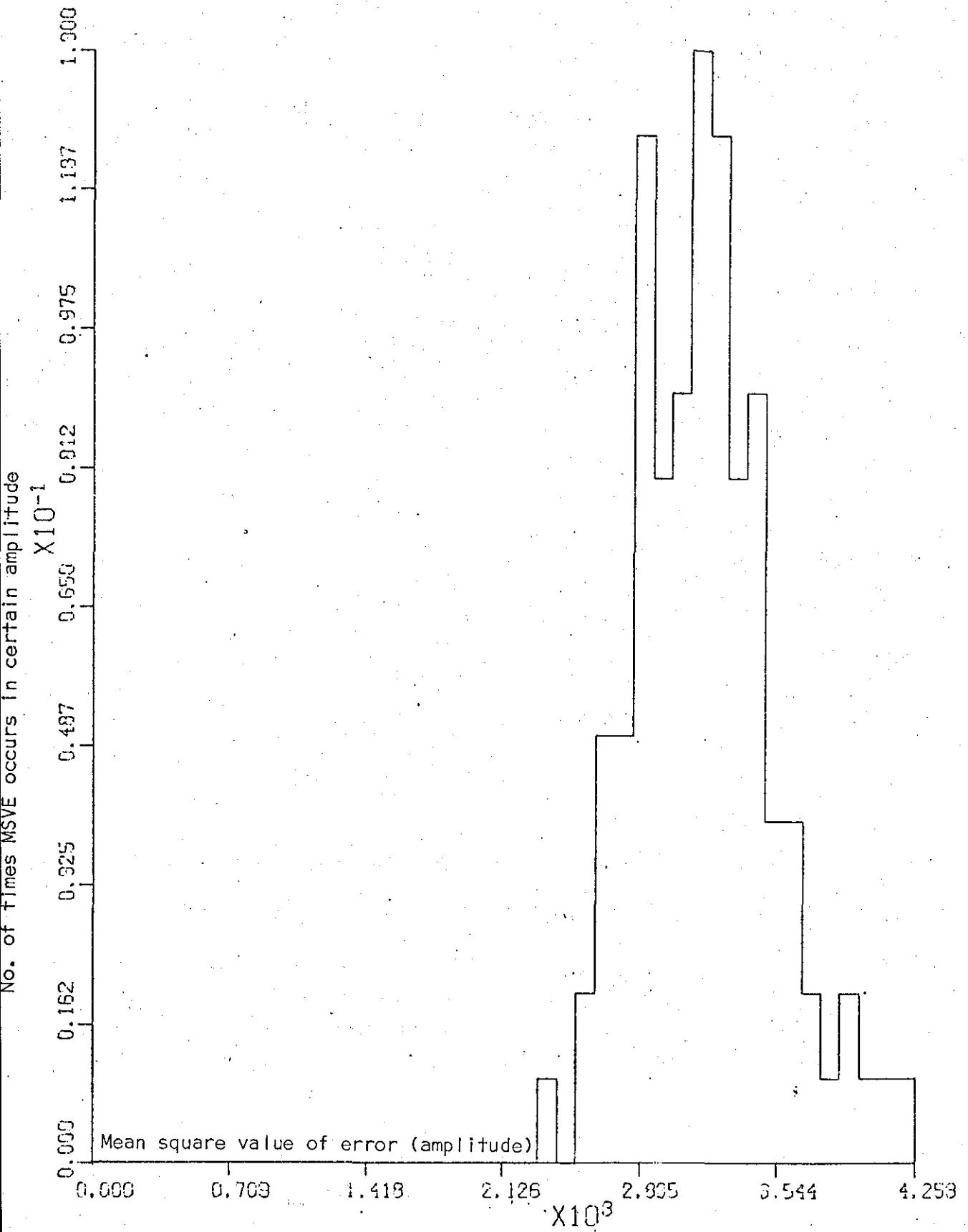


Figure 4.33 Histogram of input low pass bandlimited noise of variance 0.05

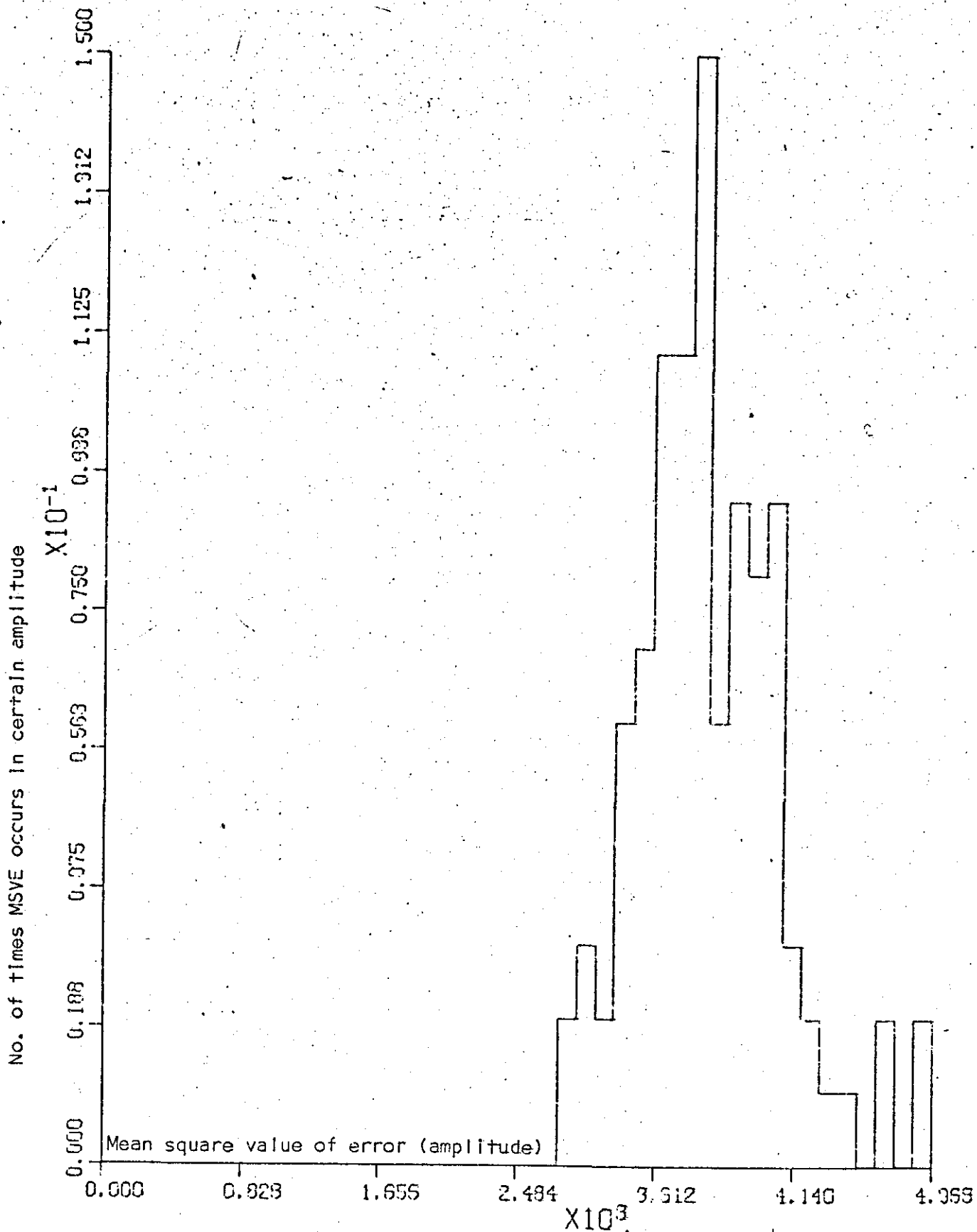


Figure 4.34 Histogram of the coder noise when the input has a low pass bandlimited noise of variance 0.05

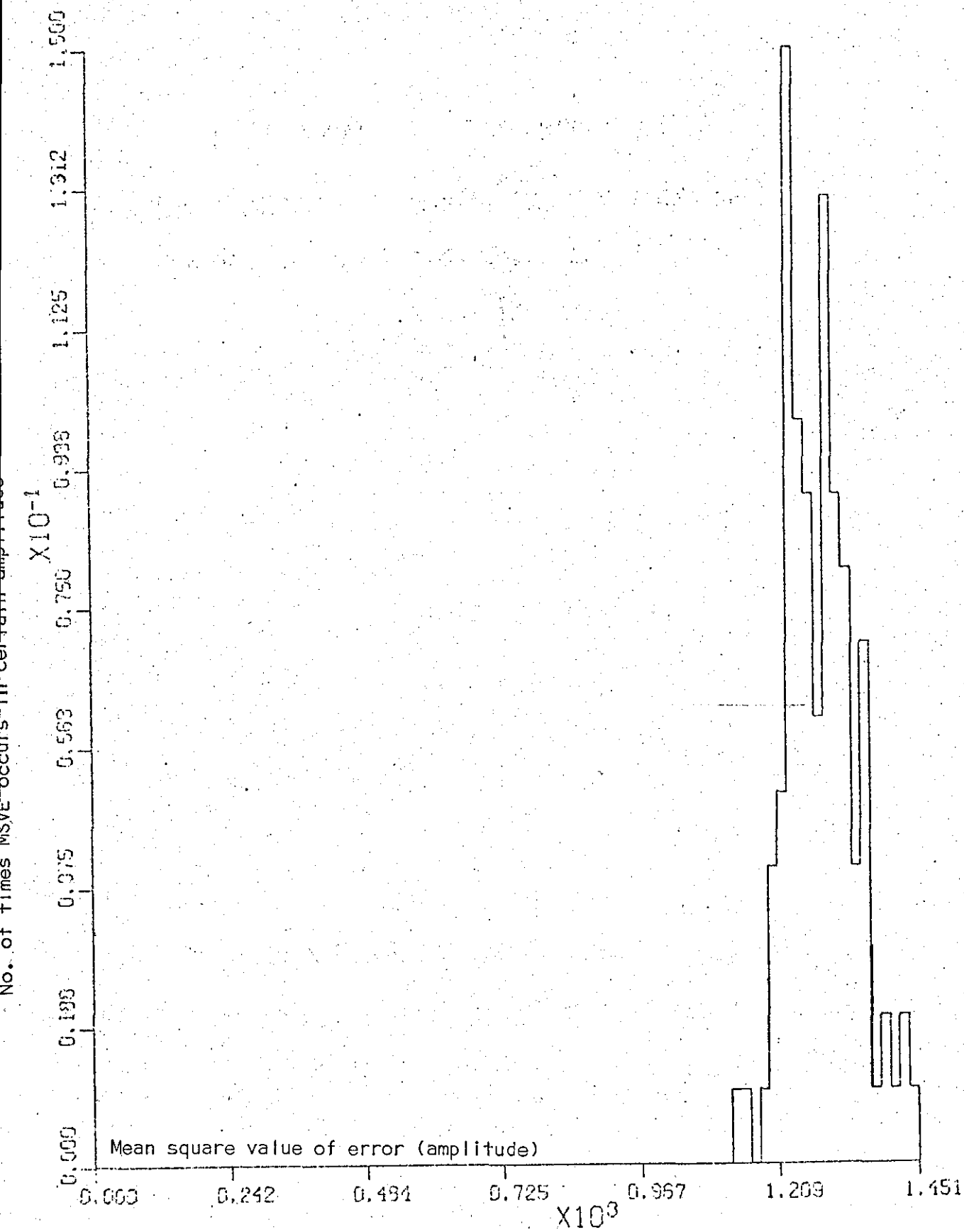


Figure 4.35 Histogram of input wideband noise of variance 0.015

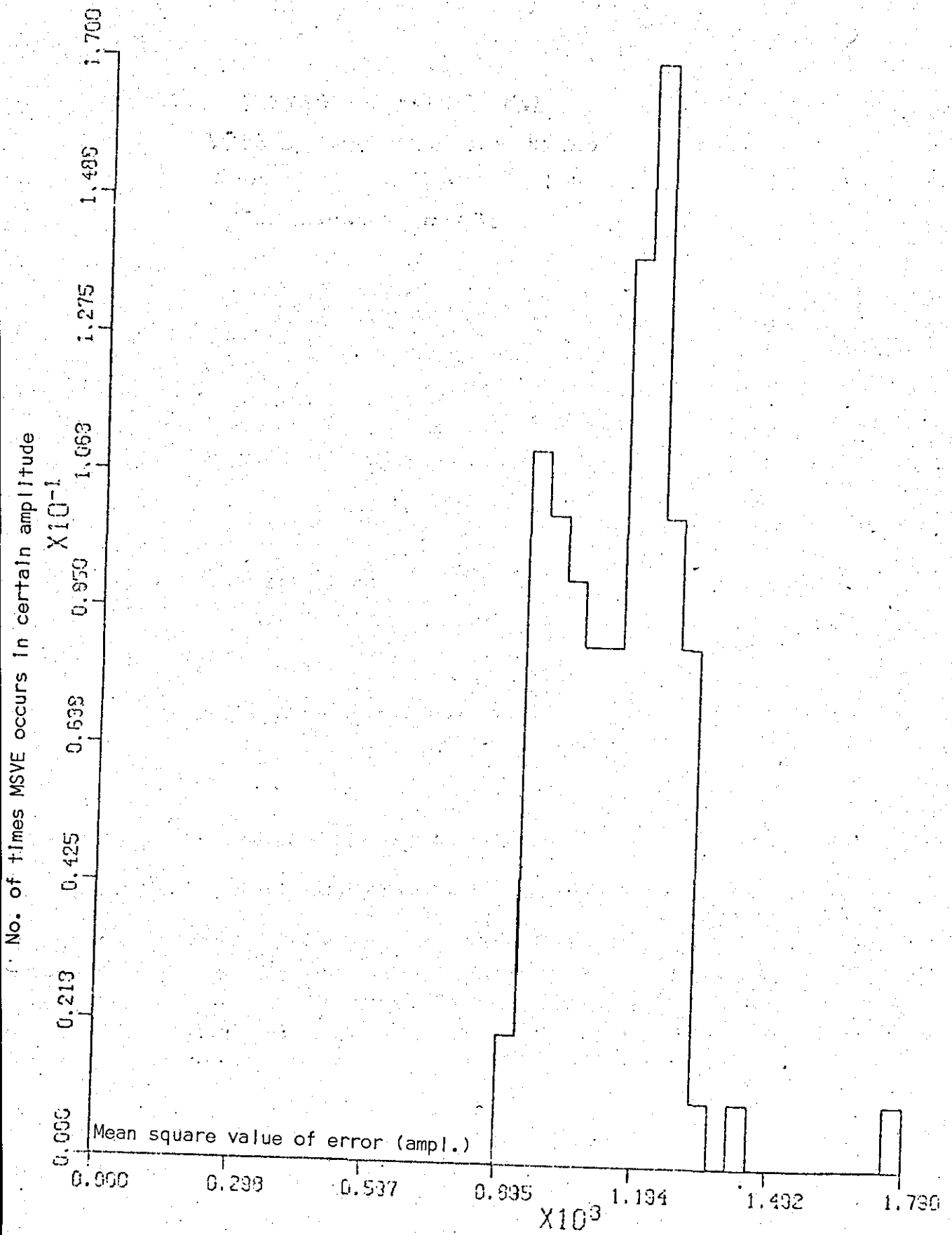


Figure 4.36 Histogram of the coder noise when the input has a wideband noise of variance 0.015

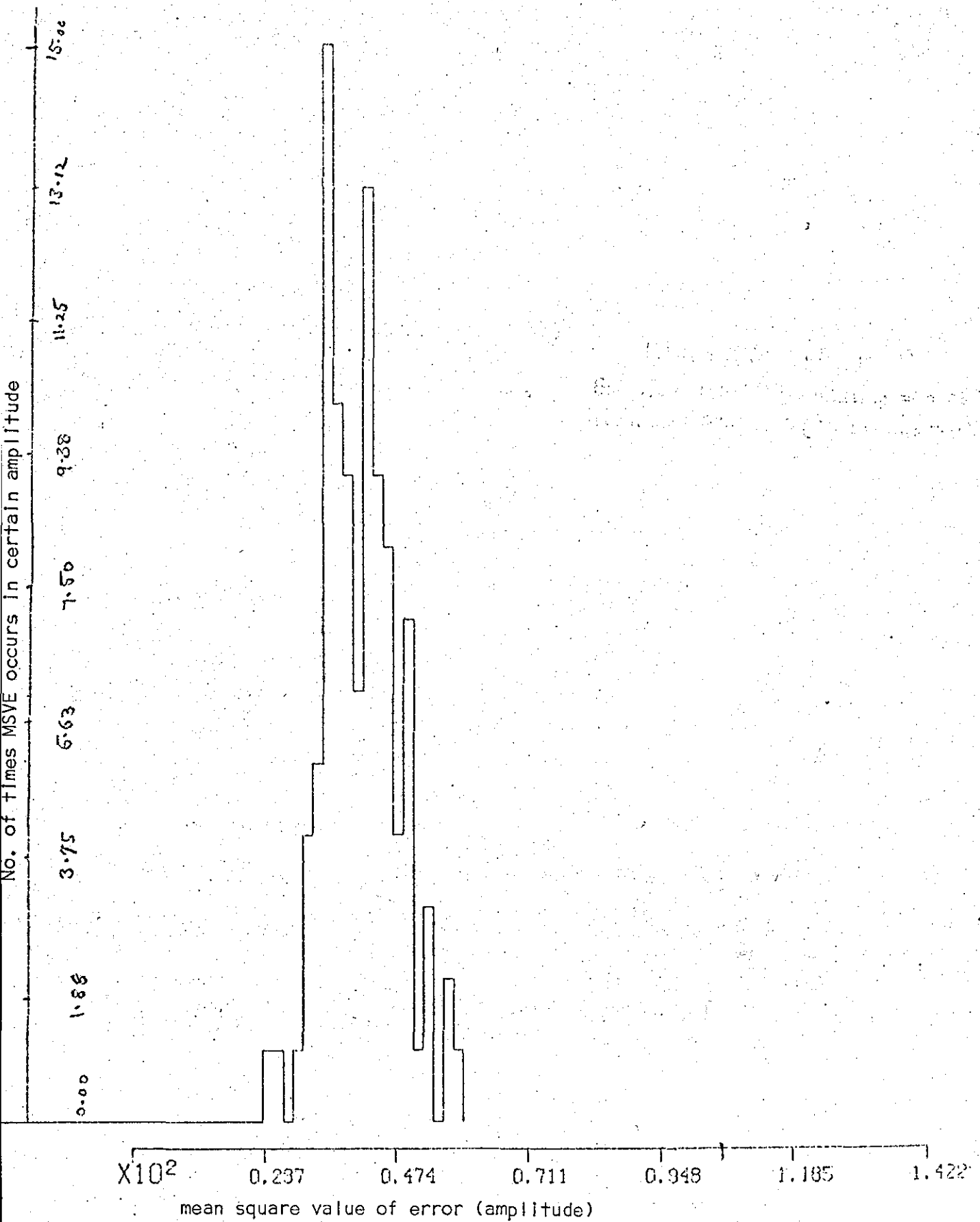


Figure 4.37 Histogram of input wideband noise of variance 0.05

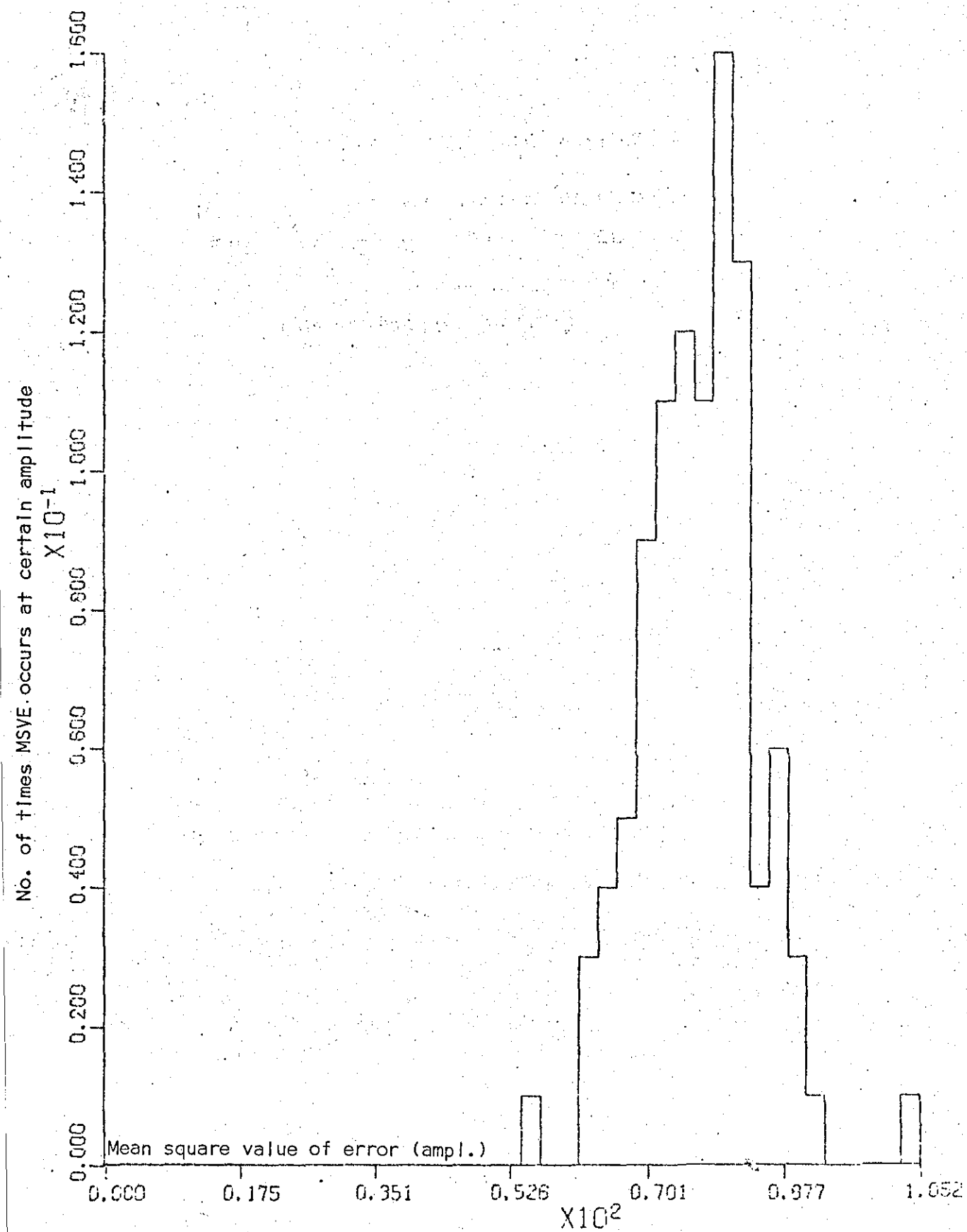


Figure 4.38 Histogram of coder noise when the input has a wideband noise of variance 0.05

Low Pass Bandlimited Noise Variance 0.015

<u>Mean Square Value of added noise</u>	<u>No.of times it occurs In an amplitude inter.</u>	<u>Mean Square Value of coder noise</u>	<u>No.of times it occurs in an amplitude inter.</u>
0.0000 00	0.000 00	0.000 00	0.000 00
0.4184×10^{-3}	0.2000×10	0.527×10^{-3}	0.1000×10
0.4271×10^{-3}	0.1000×10	0.5445×10^{-3}	0.3000×10
0.4357×10^{-3}	0.5000×10	0.5619×10^{-3}	0.1000×10
0.4444×10^{-3}	0.6000×10	0.5793×10^{-3}	0.7000×10
0.4531×10^{-3}	0.110×10^2	0.5967×10^{-3}	0.7000×10
0.4618×10^{-3}	0.9000×10	0.6141×10^{-3}	0.2200×10^2
0.4704×10^{-3}	0.1100×10	0.6314×10^{-3}	0.9000×10
0.4791×10^{-3}	0.1200×10^2	0.6488×10^{-3}	0.1700×10^2
0.4878×10^{-3}	0.8000×10	0.6662×10^{-3}	0.1600×10^2
0.4965×10^{-3}	0.6000×10	0.6836×10^{-3}	0.5000×10
0.5051×10^{-3}	0.8000×10	0.7010×10^{-3}	0.5000×10
0.5138×10^{-3}	0.5000×10	0.7184×10^{-3}	0.1000×10
0.5225×10^{-3}	0.6000×10	0.7357×10^{-3}	0.1000×10
0.5312×10^{-3}	0.3000×10	0.7351×10^{-3}	0.1000×10
0.5398×10^{-3}	0.2000×10	0.7705×10^{-3}	0.2000×10
0.5485×10^{-3}	0.1000×10	0.7879×10^{-3}	0.0000
0.5572×10^{-3}	0.1000×10	0.8053×10^{-3}	0.0000
0.5659×10^{-3}	0.1000×10	0.8226×10^{-3}	0.0000
0.5745×10^{-3}	0.1000×10	0.8400×10^{-3}	0.0000
0.5832×10^{-3}	0.1000×10	0.8574×10^{-3}	0.2000×10
0.5919×10^{-3}	0.0000	0.8748×10^{-3}	0.0000

Wideband Noise Variance 0.015

<u>Mean Square Value of error of added noise</u>	<u>No. of times it occurs in an amplitude Inter.</u>	<u>Mean Square Value of error of coder noise</u>	<u>No. of times it occurs in an amplitude Inter.</u>
0.0000 00	0.000 00	0.0000 00	0.000 00
0.1126×10^{-2}	0.100×10	0.8958×10^{-3}	0.200×10
0.1142×10^{-2}	0.100×10	0.9384×10^{-3}	0.110×10^2
0.1158×10^{-2}	0.000 00	0.9810×10^{-3}	0.100×10^2
0.1175×10^{-2}	0.100×10	0.1024×10^{-2}	0.900×10
0.1191×10^{-2}	0.400×10	0.1066×10^{-2}	0.800×10
0.1207×10^{-2}	0.500×10	0.1109×10^{-2}	0.800×10
0.1223×10^{-2}	0.1500×10^2	0.1151×10^{-2}	0.1400×10^2
0.1240×10^{-2}	0.100×10^2	0.1194×10^{-2}	0.1700×10^2
0.1256×10^{-2}	0.900×10	0.1237×10^{-2}	0.100×10^2
0.1272×10^{-2}	0.600×10	0.1279×10^{-2}	0.800×10
0.1288×10^{-2}	0.1300×10^2	0.1322×10^{-2}	0.100×10
0.1305×10^{-2}	0.9000×10	0.1364×10^{-2}	0.0000 00
0.1321×10^{-2}	0.800×10	0.1407×10^{-2}	0.1000×10
0.1337×10^{-2}	0.400×10	0.1450×10^{-2}	0.000×00
0.1353×10^{-2}	0.700×10	0.1492×10^{-2}	0.000×00
0.1370×10^{-2}	0.100×10	0.1535×10^{-2}	0.000×00
0.1386×10^{-2}	0.200×10	0.1577×10^{-2}	0.000×00
0.1402×10^{-2}	0.100×10	0.1620×10^{-2}	0.000×00
0.1418×10^{-2}	0.200×10	0.1663×10^{-2}	0.000×00
0.1435×10^{-2}	0.100×10	0.1705×10^{-2}	0.000×00
0.1451×10^{-2}	0.000 00	0.1748×10^{-2}	0.100×10
		0.1790×10^{-2}	0.000 00

Wideband Noise Variance 0.05

<u>Mean Square Value of added noise</u>	<u>No. of times it occurs in an amplitude inter.</u>	<u>Mean Square Value of coder noise</u>	<u>No. of times it occurs in an amplitude inter.</u>
0.0000 00	0.000 00	0.000 00	0.0000 00
0.1061×10^{-1}	0.1000×10	0.5404×10^{-2}	0.1000×10
0.1079×10^{-1}	0.1000×10	0.5648×10^{-2}	0.0000 00
0.1097×10^{-1}	0.0000 00	0.5891×10^{-2}	0.0000 00
0.1115×10^{-1}	0.1000×10	0.6135×10^{-2}	0.3000×10
0.1133×10^{-1}	0.4000×10	0.6378×10^{-2}	0.4000×10
0.1151×10^{-1}	0.5000×10	0.6622×10^{-2}	0.5000×10
0.1169×10^{-1}	0.1500×10^2	0.6865×10^{-2}	0.9000×10
0.1187×10^{-1}	0.1000×10^2	0.7109×10^{-2}	0.1100×10^2
0.1205×10^{-1}	0.9000×10	0.7352×10^{-2}	0.1200×10^2
0.1223×10^{-1}	0.6000×10	0.7596×10^{-2}	0.1100×10^2
0.1241×10^{-1}	0.1300×10^2	0.7839×10^{-2}	0.1600×10^2
0.1259×10^{-1}	0.9000×10	0.8083×10^{-2}	0.1300×10^2
0.1277×10^{-1}	0.8000×10	0.8327×10^{-2}	0.4000×10
0.1295×10^{-1}	0.4000×10	0.8570×10^{-2}	0.6000×10
0.1313×10^{-1}	0.7000×10	0.8814×10^{-2}	0.3000×10
0.1331×10^{-1}	0.1000×10	0.9057×10^{-2}	0.1000×10
0.1350×10^{-1}	0.3000×10	0.9301×10^{-2}	0.000 00
0.1368×10^{-1}	0.0000 00	0.9544×10^{-2}	0.0000 00
0.1386×10^{-1}	0.2000×10	0.9788×10^{-2}	0.0000 00
0.1404×10^{-1}	0.1000×10	0.1003×10^{-1}	0.0000 00
0.1422×10^{-1}	0.0000 00	0.1027×10^{-1}	0.1000×10

Low Pass Bandlimited Noise Variance 0.05

<u>Mean Square Value of added noise</u>	<u>No. of times it occurs in an amplitude inter.</u>	<u>Mean Square Value of coder noise</u>	<u>No. of times it occurs in an amplitude inter.</u>
0.0000 00	0.000 00	0.0000 00	0.0000 00
0.2312×10^{-2}	0.100×10	0.2734×10^{-2}	0.2000×10
0.2409×10^{-2}	0.000×00	0.2846×10^{-2}	0.3000×10
0.2506×10^{-2}	0.200×10	0.2958×10^{-2}	0.2000×10
0.2603×10^{-2}	0.500×10	0.3069×10^{-2}	0.6000×10
0.2700×10^{-2}	0.500×10	0.3181×10^{-2}	0.7000×10
0.2797×10^{-2}	0.1200×10	0.3293×10^{-2}	0.1100×10^2
0.2894×10^{-2}	0.800×10	0.3404×10^{-2}	0.1100×10^2
0.2991×10^{-2}	0.900×10	0.3516×10^{-2}	0.1500×10^2
0.3088×10^{-2}	0.1300×10^2	0.3628×10^{-2}	0.6000×10
0.3185×10^{-2}	0.1200×10^2	0.3739×10^{-2}	0.9000×10
0.3282×10^{-2}	0.8000×10	0.3851×10^{-2}	0.8000×10
0.3379×10^{-2}	0.900×10	0.3963×10^{-2}	0.9000×10
0.3476×10^{-2}	0.4000×10	0.4074×10^{-2}	0.3000×10
0.3573×10^{-2}	0.4000×10	0.4186×10^{-2}	0.2000×10
0.3670×10^{-2}	0.200×10	0.4298×10^{-2}	0.1000×10
0.3767×10^{-2}	0.1000×10	0.4409×10^{-2}	0.1000×10
0.3864×10^{-2}	0.2000×10	0.4521×10^{-2}	0.0000×00
0.3961×10^{-2}	0.1000×10	0.4633×10^{-2}	0.2000×0
0.4058×10^{-2}	0.1000×10	0.4744×10^{-2}	0.0000×00
0.4156×10^{-2}	0.1000×10	0.4856×10^{-2}	0.2000×00
0.4252×10^{-2}	0.000×00	0.4968×10^{-2}	0.0000×00

APPENDIX I

Analysis of a 102 MHz Crystal Controlled Oscillator Circuit

The crystal controlled oscillator, whereby the crystal oscillates at series resonance at its fifth overtone, is shown in figure 6.7a. The equivalent circuit is shown in figure 6.7(b).

At resonance the output circuit can be represented by a load resistance R_L .

The crystal has a very high Q-factor, hence it offers low series resistance for series resonance. If R is the series impedance at resonance, $Q = \frac{\omega L_1}{R}$

C_1 included the input capacitance for the transistor.

From the equivalent circuit diagram,

$$V_s = -i_s (R_s + j\omega L_1) \quad (1)$$

$$V_s = V_1 + V_E \quad (2)$$

$$V_1 = i_a X_{cl} = i_1 R_{in} \quad (3)$$

$$X_{cl} = \frac{1}{j\omega C_1}$$

Also $V_E = i_E Z_E \quad (4)$

$$Z_E = \frac{R_3}{1 + j\omega C_2 R_3}$$

Substituting the values of V_1 and V_E in (2)

$$V_s = i_a X_{cl} + i_E Z_E \quad (5)$$

$$V_s = i_a X_{cl} + (i_2 + i_s) Z_E \quad (6)$$

Because $I_E = I_2 + I_s$

$$i_a = \frac{R_{in}}{R_{in} + X_{cl}} I_s \quad (7)$$

$$\therefore V_s = I_s \frac{X_{cl} R_{in}}{R_{in} + X_{cl}} + \frac{(I_2 + I_s) R_3}{1 + j\omega c_2 R_3} \quad (8)$$

Putting the value of V_s from (1) in (8)

$$-I_s (R_s + j\omega L_1) = I_s \left[\frac{R_{in}}{1 + R_{in} j\omega c_1} + \frac{R_3}{1 + j\omega c_2 R_3} \right] + \frac{R_3 I_2}{1 + j\omega c_2 R_3} \quad (9)$$

$$I_s = \frac{\frac{-(I_2 R_3)}{(1 + j\omega c_2 R_3)}}{j\omega L_1 + \frac{R_{in}}{1 + j\omega c_1 R_{in}} + \frac{R_3}{1 + j\omega c_2 R_3}} \quad \text{neglecting } R_s \quad (10)$$

$$\text{Also } i_1 = \frac{I_s X_{cl}}{R_{in} + X_{cl}} = \frac{I_s}{1 + j\omega c_1 R_{in}} \quad (11)$$

From the last two equations, i.e. (10) and (11)

$$\frac{i_2}{i_1} = - \frac{\left[j\omega L_1 + \frac{R_{in}}{(1 + j\omega c_1 R_{in})} + \frac{R_3}{(1 + j\omega c_2 R_3)} \right] (1 + j\omega c_1 R_{in})}{R_3 (1 + j\omega c_2 R_3)} \quad (12)$$

But $\frac{i_2}{i_1} = h_{fe}$ is the current amplification factor of the transistor

rearranging the eqn.(12)

$$= - \left[\frac{(1 + j\omega c_1 R_{in}) (1 + j\omega c_2 R_3)}{R_3} \right] \left[j\omega L_1 + \frac{R_{in}}{1 + j\omega c_1 R_{in}} + \frac{R_3}{1 + j\omega c_2 R_3} \right]$$

$$\begin{aligned}
&= \left[1 + j\omega c_1 R_{in} + \frac{R_{in}}{R_3} (1 + j\omega c_2 R_3) \right] + \frac{j\omega L_1}{R_3} \left[1 + j\omega c_1 R_{in} + j\omega c_2 R_3 - \omega^2 c_1 c_2 R_3 R_{in} \right] \\
&= 1 + \frac{R_{in}}{R_3} - \omega^2 L_1 c_1 \frac{R_{in}}{R_3} - \omega^2 L_1 c_2 + j(\omega c_1 R_{in} + \omega c_2 R_{in} + \frac{\omega L_1}{R_3} - \omega^3 L_1 c_1 c_2 R_{in}) \quad (13)
\end{aligned}$$

At resonance there is no reactance

Therefore, equating the imaginary term to zero

$$\omega c_1 R_{in} + \omega c_2 R_{in} + \frac{L_1}{R_3} - \omega^3 L_1 c_1 c_2 R_{in} = 0$$

or
$$\omega^2 L_1 c_1 c_2 R_{in} = (c_1 + c_2) R_{in} + \frac{L_1}{R_3}$$

$$\omega^2 = \frac{c_1 + c_2}{L_1 c_1 c_2} + \frac{1}{c_1 c_2 R_{in} R_3}$$

If
$$\frac{c_1 + c_2}{L_1} \gg \frac{1}{R_{in} R_3}$$

$$\omega^2 = \frac{(c_1 + c_2)}{L_1 c_1 c_2}$$

This gives the frequency of oscillation, and,

$$\frac{i_2}{i_1} = 1 + \frac{R_{in}}{R_3} - \omega^2 L_1 c_1 \frac{R_{in}}{R_3} - \omega^2 L_1 c_2$$

substituting the value of ω^2 into the real part of equation,

$$\begin{aligned}
-\frac{i_2}{i_1} = -h_{fe} &= 1 + \frac{R_{in}}{R_3} - \frac{R_{in}}{R_3} \left[\frac{c_1 + c_2}{c_2} \right] - \left[\frac{c_1 + c_2}{c_1} \right] \\
&= 1 + \frac{R_{in}}{R_3} - \frac{R_{in}}{R_3} \frac{c_1}{c_2} - \frac{R_{in}}{R_3} - 1 - \frac{c_2}{c_1}
\end{aligned}$$

$$= - \left[\frac{c_2}{c_1} + \frac{c_1}{c_2} \frac{R_{in}}{R_3} \right]$$

If $c_1 R_{in} \ll c_2 R_3$

$$\text{then } h_{fe} = \frac{c_2}{c_1}$$

This gives the condition for oscillation.

APPENDIX JCOMPUTER PROGRAMMES

- J₁) Delta modulation system with ECG waveform as an Input
- J₂) Delta sigma modulation system with ECG waveform as an Input
- J₃) Computation of the weighting coefficients of the low pass filter
- J₄) Interpolation of frequency response of the low pass filter
- J₅) Programs for spectrum analysis
- J₆) Cepstrum
- J₇) Time-variant delta modulation and histogram
- J₈) Effect of error pulses at the output.

```

MASTER DEL
DIMENSION X(920), Y(920), T(920), Z(920), H(920), V(920), G(920),
1 CLOCK(920)
CALL UIPOP
S=0.99
AM=1
C=0.2
PI=3.14159
DO 10 I=26,226
10 X(I)=C*SIN(PI*((I-26)/200.))
DO 20 I=276,376
20 X(I)=AM*(I-276)/100
DO 30 I=376,476
30 X(I)=AM*(476-I)/100
C=0.4
DO 40 I=551,851
40 X(I)=C*SIN(PI*((I-551)/300.))
DO 41 I=1,25
41 X(I)=0.0
DO 42 I=227,275
42 X(I)=0.0
DO 43 I=477,550
43 X(I)=0.0
READ(1,21)(H(I),I=1,64)
21 FORMAT(F0.0)
CALL PRO2(H,64,X,851,V,914)
B=0.0
Z(1)=1.0
DO 17 I=2,851
A=V(I)-Z(I-1)
B=(B+A)+A
IF(B=0) 14,14,16
14 Z(I)=1.0
GO TO 17
16 Z(I)=1.0
17 CONTINUE
DO 18 I=2,851
P=0.00
B=0.001
18 G(I)=P*G(I-1)+Z(I)
CALL PRO2(H,64,Z,851,Y,914)
CALL PRO2(H,64,G,851,T,914)
WRITE(2,300)(I,Z(I),V(I),I=1,851)
300 FORMAT(1H,10X,14,10X,E10.4,10X,F10.4)
DO 400 I=1,851
400 CLOCK(I)=I
XMIN=1.0
XMAX=851.0
YMIN=0.05
YMAX=1.0
XINS=15.0
YINS=15.0
CALL UTP4R(XMIN,XMAX,YMIN,YMAX,XINS,YINS)
CALL UTP4R(CLOCK,X,850,2)
CALL UTP4R(CLOCK,V,850,2)
CALL UTP4R(CLOCK,Y,850,2)
CALL UTP4R(CLOCK,T,850,2)
CALL UTPCL
STOP
END

```

```

DIMENSIONX(1100),H(200),V(1100),Y(1100),CLOCK(1100),Z(1100)
COMPLEX COMPY(1024)
CALL UTPOP
READ(1,21)(H(M),M=1,64)
DO 100 ID=1,2
S=0.985
AM=1
DIR=-1.0
N=10
LX=1024
EPS=0.015
KRAND=0.0
EPS2=EPS*2
C=0.2
PI=3.14159
DO 10 I=26,226
10 X(I)=C*SIN(PI*((I-26)/200.))
DO 20 J=276,376
20 X(I)=AM*(I-276)/100
DO 30 I=376,476
30 X(I)=AM*(476-I)/100
C=0.4
DO 40 I=551,851
40 X(I)=C*SIN(PI*((I-551)/300.))
C=0.2
DO 44 I=876,1024
44 X(I)=C*SIN(PI*((I-876)/200.))
DO 41 I=1,25
41 X(I)=0.0
DO 42 I=227,275
42 X(I)=0.0
DO 43 I=477,550
43 X(I)=0.0
DO 45 I=852,875
45 X(I)=0.0
21 FORMAT(F0.0)
CALL PRO2(H,64,X,1024,V,1087)
IF(ID.EQ.1)GO TO 11
DO 22 I=1,1024
22 V(I)=V(I)+UTR1(1,1,KRAND)*EPS2-EPS
11 B=0.0
Z(1)=1.0
DO 17 I=2,1024
A=V(I)-Z(I-1)
B=(S*B)+A
IF(B=0) 14,14,16
14 Z(I)=-1.0
GO TO 17
16 Z(I)=1.0
17 CONTINUE
CALL PRO2(H,64,Z,1024,Y,1087)
DO 400 I=1,1024
400 CLOCK(I)=I
XMIN=1.0
XMAX=1024
YMIN=-0.1
YMAX=1.0
XINS=10.0
YINS=12.0
CALL UTP4D(XMIN,XMAX,YMIN,YMAX,XINS,YINS)
CALL UTP4B(CLOCK,X,1024,2)

```

CALL UTP4B(CLOCK,V,1024,2)
CALL UTP4B(CLOCK,Y,1024,2)
100 CONTINUE
CALL UTPCL
STOP
END

313

SEGMENT, LENGTH 516, NAME DELSIN

```
      SUBROUTINE PRO2 (A,LA,B,LB,C,LC)
C
C   CONVOLVES ARRAYS A(LA) AND B(LB), LEAVING RESULT IN C(LC)
C   LC MUST NOT BE LESS THAN LA+LB-1.      J.S.S NOV 1970
C
      DIMENSION A(LA),B(LB),C(LC)
      DO 1 I=1,LC
1     C(I)=0.0
      DO 2 I=1,LA
      DO 2 J=1,LB
      K=I+J-1
2     C(K)=C(K)+A(I)*B(J)
      RETURN
      END
```

SEGMENT, LENGTH 117, NAME PRO2

```

0016         MASTER FFT
0017         COMPLEX X(64)
0018         DIMENSION A(128)
0019         EQUIVALENCE(A(1),X(1))
0020         LX=64
0021         N=6
0022         READ(1,10) (A(I), I=1,128,2)
0023     10  FORMAT(F0.0)
0024         WRITE(2,21) (A(I), I=1,128,2)
0025         DIR=1.0
0026         CALL NLOGN(1,X,LX,DIR)
0027         WRITE(2,21) (X(I), I=1,64)
0028         WRITE(3,21) (X(I), I=1,64)
0029     21  FORMAT(1H,10X,E10.4,10X,E10.4)
0030         STOP
0031         END

```

END OF SEGMENT, LENGTH 81, NAME FFT

J4. INTERPOLATION OF FREQUENCY RESPONSE OF THE LOW PASS FILTER

```

MASTER BEAMFORM
DIMENSION Y(1024),CLOCK(1024),XAXIS(1024)
COMPLEX X,LX,DIR,0,B(1024)
READ(1,1) (B(I), I=1,31)
1  FORMAT(62F0.0)
DO 9 I=32,991
B(I)=(0.0,0.0)
9  CONTINUE
READ(1,7) (B(I), I=992,1024)
7  FORMAT(66F0.0)
CALL NLOGN(10,B,1024,-1.0)
DO 3 I=1,1024
3  Y(I)=REAL(B(I))
DO 5 I=1,1024
5  Y(I)=(Y(I))**2
WRITE(2,99) (Y(I), I=1,1024)
99  FORMAT(5F10.11)
STOP
END

```

```

MASTER
DIMENSION X(1024), H(140), V(1089), Y(1089), FREQ(1089), AVP(1089),
12(1024)
COMPLEX COPY(1024)
CALL UTRPOP
READ(1,21)(H(1),N=1,64)
DO 300 I=1,2
S=0.985
AM=1
DIR=1.0
N=10
LX=1024
EPS=0.0101
K=0.0
EPS2=EPS*2
C=0.2
PI=3.14159
DO 10 I=26,226
10 X(I)=C*SIN(PI*((I-26)/200.))
DO 20 I=276,376
20 X(I)=AM*(I-276)/100
DO 30 I=376,476
30 X(I)=AM*(476-I)/100
C=0.4
DO 40 I=551,851
40 X(I)=C*SIN(PI*((I-551)/300.))
C=0.2
DO 44 I=876,1024
44 X(I)=C*SIN(PI*((I-876)/200.))
DO 41 I=1,25
41 X(I)=0.0
DO 42 I=227,275
42 X(I)=0.0
DO 43 I=477,550
43 X(I)=0.0
DO 45 I=852,875
45 X(I)=0.0
21 FORMAT(20.0)
CALL PR2(H,64,N,1024,V,1089)
IF(10,20,1) GO TO 11
DO 22 I=1,1024
22 V(I)=V(I)+UTR1(1,3,IRAND)*EPS2-CPS
11 B=0.0
Z(I)=1.0
DO 17 I=2,1024
AM=V(I)-Z(I-1)
B=(S+B)*A
IF(B=0) 14,14,16
14 Z(I)=1.0
GO TO 17
16 Z(I)=1.0
17 CONTINUE
CALL PR2(H,64,N,1024,Y,1089)
DO 27 I=1,1024
27 COPY(I)=COMPLX(Y(I),0.0)
CALL BLOGN(N,COPY,LX,DIR)
FUND=4000./1024
FREQ(1)=0.0
DO 24 I=2,LX/2
24 FREQ(I)=I*FUND
DO 29 I=1,LX/2
COPY(I)=COPY(I)/1024

```



```

8      20  AVP(I)=2.*(CA99(CORPY(I)**2))
9      WRITE(27600)(I,FREQ(I),AVP(I),I=1,512)
0      400  FORMAT(1H ,10X,14,10X,E10,4,10X,E10,4)
1      YMAX=0.0000E+01
2      YMIN=0.1500E+07
3      XMAX=5000*FLOAT(LX)/8
4      XMIN=0.0
5      XINC=12.0
6      YINC=15.0
7      CALL UTPRA(XMIN,XMAX,YMIN,YMAX,XINS,YINS,XTITLE,0,YTITLE,0)
8      CALL UTPRA(FREQ,AVP,512,2)
9      100  CONTINUE
0      CALL UTPCL
1      STOP
2      END

```

OF SEGMENT, LENGTH 640, NAME DELSIM

```

MASTER CEPS
COMPLEX T(1024),S
DIMENSIONX(1024),Y(1088),P(1024),R(1024),S(1024),H(100),
1U(1024),CLOCK(8>1),V(1089),A(1024),B(1024)
EQUIVALENCE(S(1),T(1)),(X(1),B(1))
CALL UTPOP
READ (1,21) (H(M), M=1,64)
21 FORMAT (F0.0)
C=0.2
PI=3.14159
DO 10 I=26,226
10 X(I)=C*SIN(PI*((I-26)/200.))
AM=0.1
DO 51 I=256,266
51 X(I)=- (AM*(I-256)/10.)
DO 52 I=266,276
52 X(I)=- (AM*(276-I)/10.)
AM=1
DO 20 I=276,376
20 X(I)=AM*(I-276)/100
DO 30 I=376,476
30 X(I)=AM*(476-I)/100
AM=0.1
DO 53 I=476,491
53 X(I)=- (AM*(I-476)/15.)
DO 54 I=491,506
54 X(I)=- (AM*(506-I)/15.)
C=0.4
DO 40 I=551,851
40 X(I)=C*SIN(PI*((I-551)/300.))
C=0.2
DO 44 I=876,1024
44 X(I)=C*SIN(PI*((I-876)/200.))
DO 41 I=1,25
41 X(I)=0.0
DO 42 I=227,275
42 X(I)=0.0
DO 43 I=477,550
43 X(I)=0.0
DO 45 I=852,875
45 X(I)=0.0
CALL PRO2(H,64,X,1024,V,1087)
Q=0.985
A(1)=0.001
DO 50 I=1,1024
B(I)=V(I)-A(I)
15 IF(B(I)-0) 17,17,18
17 A(I+1)=Q*A(I)-0.02
GO TO 50
18 A(I+1)=Q*A(I)+0.02
50 CONTINUE
CALL PRO2(H,64,A,1024,Y,1087)
DO 2 I=1,1024
T(I)=CMPLX(Y(I),0.0)
2 CONTINUE
CALL NLOGN(10,T,1024,-1.0)
DO 3 I=1,1024
3 R(I)=CABS(T(I))
DO 7 I=1,1024
IF(R(I).EQ.0.) GO TO 7
U(I)=ALOG(R(I))
7 CONTINUE

```

```
DO 5 I=1,1024
5 S(I)=CMPLX(U(I),0.0)
CALL NLOGN(10,S,1024,+1.0)
DO 6 I=1,1024
6 P(I)=CABS(S(I))
DO 400 I=1,851
400 CLOCK(I)=I
XMIN=1.0
XMAX=512
YMIN=-2.0
YMAX=4.0
XINS=6.0
YINS=5.0
CALL UTP4D(XMIN,XMAX,YMIN,YMAX,XINS,YINS)
CALL UTP4B(CLOCK,R,512,2)
CALL UTP4D(XMIN,XMAX,YMIN,YMAX,XINS,YINS)
CALL UTP4B(CLOCK,U,512,2)
YMIN=-0.01
YMAX=0.1
CALL UTP4D(XMIN,XMAX,YMIN,YMAX,XINS,YINS)
CALL UTP4B(CLOCK,P,512,2)
XMIN=1.0
XMAX=851
YMIN=-0.05
YMAX=1.0
CALL UTP4D(XMIN,XMAX,YMIN,YMAX,XINS,YINS)
CALL UTP4B(CLOCK,Y,851,2)
CALL UTPCL
STOP
END
```

SEGMENT, LENGTH 546, NAME CEPS

```

MASTER HIST
DIMENSIONX(852),H(150),V(915),Y(947),CSUM(110),PROB(110),
1A(852),B(852),U(852),W(916)
CALL UTRPOP
S=0.285
AM=1
DIR=-1.0
N=10
LX=1024
EPS=0.015
KRAND=0.0
EPS2=EPS*2
READ(1,21)(H(M),M=1,64)
PI=3.14159265358979
C=0.2
21 FORMAT(F0.0)
DO 10 I=26,226
10 X(I)=C*SIN(PI*((I-26)/200.))
AM=0.1
DO 51 I=256,266
51 X(I)=- (AM*(I-256)/10.)
DO 52 I=266,276
52 X(I)=- (AM*(276-I)/10.)
AM=1
DO 20 I=276,376
20 X(I)=AM*(I-276)/100
DO 30 I=376,476
30 X(I)=AM*(476-I)/100
AM=0.1
DO 53 I=476,491
53 X(I)=- (AM*(I-476)/15.)
DO 54 I=491,506
54 X(I)=- (AM*(506-I)/15.)
C=0.4
DO 40 I=551,851
40 X(I)=C*SIN(PI*((I-551)/300.))
C=0.2
DO 41 I=1,25
41 X(I)=0.0
DO 42 I=227,256
42 Y(I)=0.0
DO 43 I=506,550
43 X(I)=0.0
DO 100 M=1,100
DO 22 I=1,851
22 U(I)=X(I)+UTR1(1,1,KRAND)*EPS2-EPS
CALL PROB(H,64,U,851,V,914)
DO 50 I=2,851
A(I)=0.001
P(I)=V(I)-A(I)
15 IF(S(I)-0) 17,17,18
17 A(I+1)=S*A(I)-0.02
GO TO 50
18 A(I+1)=S*A(I)+0.02
50 CONTINUE
CALL PROB(H,64,A,851,Y,914)
ASUM=0.0
DO 7 I=1,851
ASUM=ASUM+(Y(I+63)-X(I))*(Y(I+63)-X(I))/851.
7 CONTINUE
CSUM(M)=ASUM
R=UTR1(1,1,KRAND)*EPS2-EPS

```

```

0076 WRITE(2,500)R
0077 500 FORMAT(E10.4)
0078 100 CONTINUE
0079 WRITE(2,300)((I,CSUM(I)),I=1,100)
0080 CALL UTS5(100,CSUM(1))
0081 WRITE(2,300)((I,CSUM(I)),I=1,100)
0082 300 FORMAT(1H ,10X,14,10X,E10.4)
0083 K=2
0084 XJ=(CSUM(100)-CSUM(1))/20.
0085 CLASS=CSUM(1)+XJ
0086 DO 200 I=1,100
0087 5 IF(CSUM(I).LT.CLASS) GO TO 11
0088 K=K+1
0089 CLASS=CLASS+XJ
0090 GO TO 5
0091 11 PROB(K)=PROB(K)+1
0092 200 CONTINUE
0093 DO 4 I=2,25
0094 4 CSUM(I)=(I-1)*XJ+CSUM(1)
0095 PROB(1)=0.0
0096 CSUM(1)=0.0
0097 PROB(K+1)=0.0
0098 YINS=8.0
0099 XINS=6.0
0100 WRITE(2,400)(CSUM(I),PROB(I),I=1,K+1)
0101 400 FORMAT(2(10X,E10.4))
0102 CALL UTP5(CSUM,PROB,K+1,XINS,YINS)
0103 CALL UTPCL
0104 STOP
0105 END

```

ND OF SEGMENT, LENGTH 566, NAME HIST

J8. EFFECT OF ERROR PULSES AT THE OUTPUT

```

5     MASTER
6     DIMENSION X(1025), V(1025), A(1025), B(1025), Z(1025),
7     TAMP(1025), FREQ(1024)
8     COMPLEX COMPZ(1024)
9     EQUIVALENCE (X(1), A(1))
0     CALL UTPOP
1     S=0.285
2     AM=1
3     DIR=-1.0
4     N=10
5     LX=1024
6     KRAND=0.0
7     FUND=1.0
8     EPS=0.4
9     C=0.2
0     PI=3.14159
1     DO 10 I=26,226
2     10 X(I)=C*SIN(PI*((I-26)/200.))
3     AM=0.1
4     DO 51 I=256,266
5     51 Y(I)=- (AM*(I-256)/10.)
6     DO 52 I=266,276
7     52 Y(I)=- (AM*(276-I)/10.)
8     AM=1
9     DO 20 I=276,376
0     20 Y(I)=AM*(I-276)/100
1     DO 30 I=376,476
2     30 X(I)=AM*(476-I)/100
3     AM=0.1
4     DO 53 I=476,491
5     53 Y(I)=- (AM*(I-476)/15.)
6     DO 54 I=491,506
7     54 X(I)=- (AM*(506-I)/15.)
8     C=0.4
9     DO 40 I=551,851
0     40 X(I)=C*SIN(PI*((I-551)/300.))
1     C=0.2
2     DO 44 I=876,1024
3     44 Y(I)=C*SIN(PI*((I-876)/200.))
4     DO 41 I=1,25
5     41 Y(I)=0.0
6     DO 42 I=227,275
7     42 Y(I)=0.0
8     DO 43 I=477,550
9     43 X(I)=0.0
0     DO 45 I=852,875
1     45 X(I)=0.0
2     S=0.285
3     A(I)=0.001
4     DO 50 I=1,1024
5     B(I)=X(I)-A(I)
6     15 IF (B(I)=0) 17,17,18
7     17 A(I+1)=4*A(I)-0.02
8     Z(I)=1.0
9     DO 50 I=1,1024
0     18 A(I+1)=4*A(I)+0.02
1     Z(I)=1.0
2     50 CONTINUE
3     DO 22 I=1,1024
4     22 V(I)=Z(I)+UTRI(17,1,KRAND)*EPS
5     DO 24 I=1,1024
6     IF (V(I)=0) 23,23,24

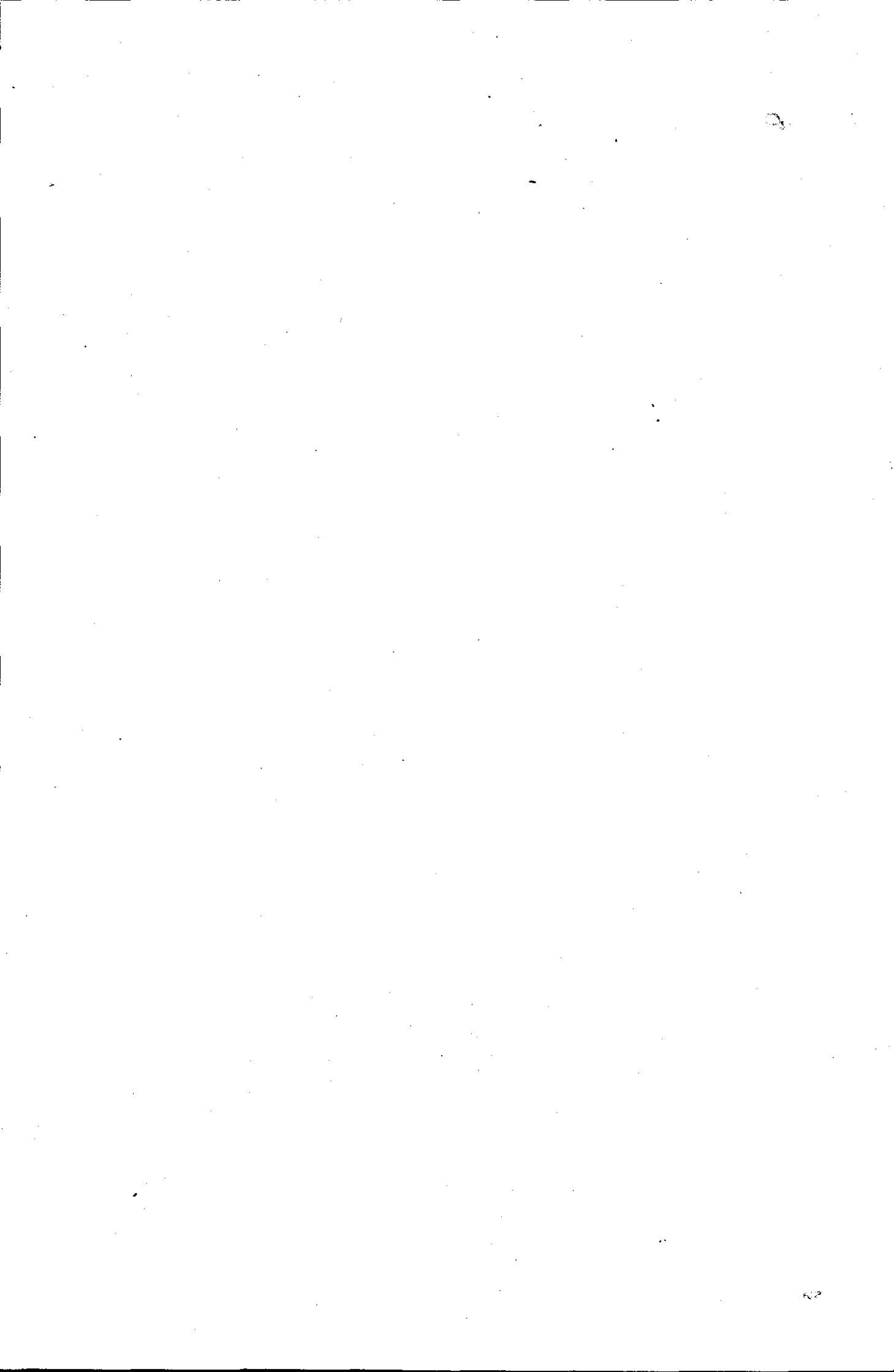
```

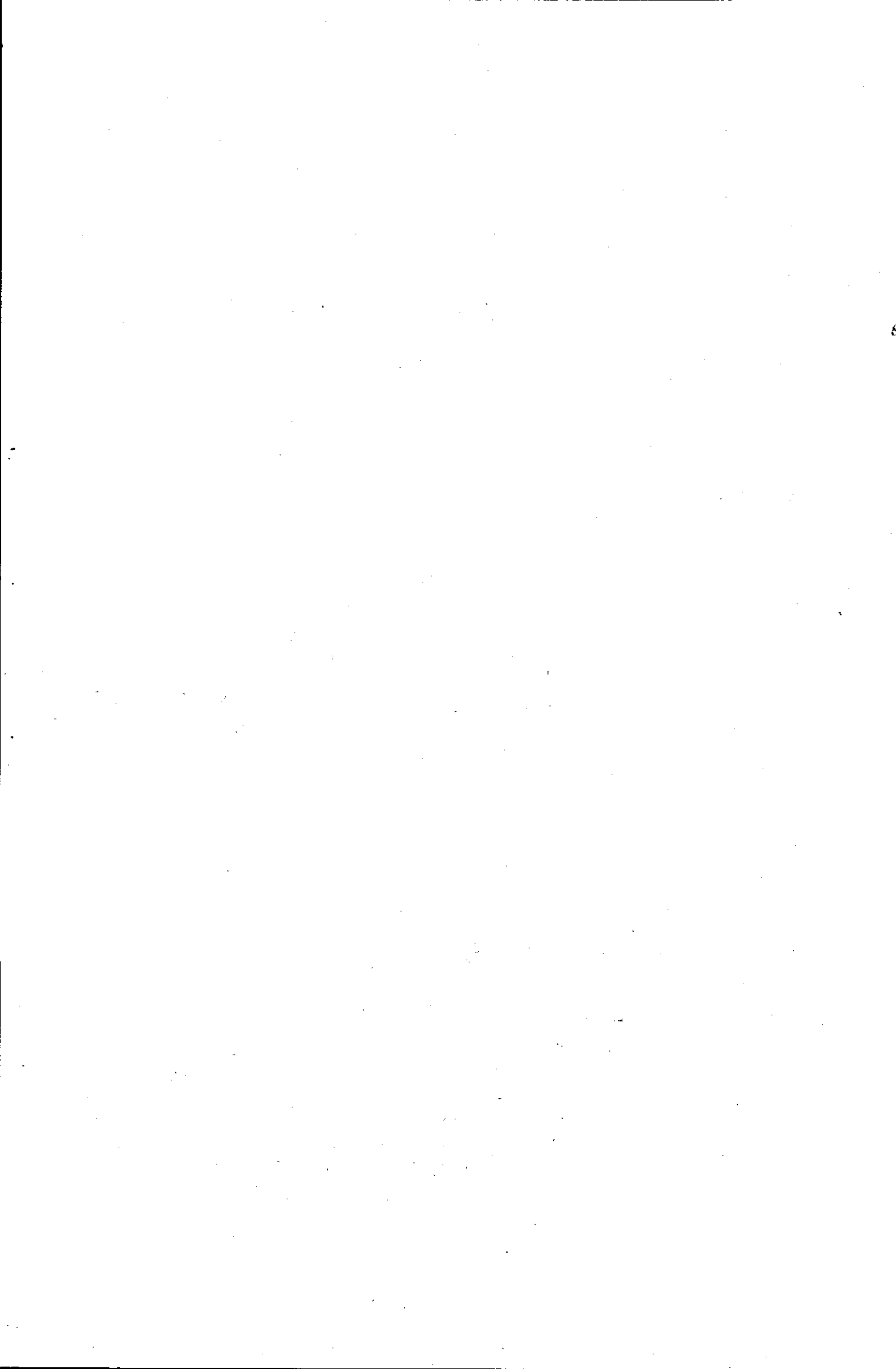
```

23 Z(I)=Z(I)-(-1.0)
   GO TO 26
24 Z(I)=Z(I)-(+1.0)
26 CONTINUE
   DO 33 I=1,1024
33 COMPZ(I)=COMPLEX(Z(I),0.0)
   CALL WLOG8(N,COMPZ,LX,-1.0)
   DO 34 J=1,1024
34 FREQ(J)=I*FUND
   DO 30 I=1,1024
30 AVP(I)=CABS(COMPZ(I))
   WRITE(2,200) (FREQ(I),AVP(I),Z(I),I=1,1024)
400 FORMAT(57F10X,5D,4I)
   VMAX=UTS2(512,AVP(I))
   VMIN=UTS3(512,AVP(I))
   XMIN=1.0
   XMAX=512
   YINS=5.0
   YINS=5.0
   CALL UTPLD(XMIN,XMAX,VMIN,VMAX,XINS,YINS)
   CALL UTPLB(FREQ,AVP,512,2)
   CALL UTPLA(XMIN,XMAX,VMIN,VMAX,XINS,YINS,XTITLE,0,YTITLE,0)
   CALL UTPLC(FREQ,AVP,512,2)
   CALL UTPLB(XMIN,XMAX,VMIN,VMAX,XINS,YINS,XTITLE,0,YTITLE,0)
   CALL UTPLD(FREQ,AVP,512,2)
   CALL UTPLC
   STOP
   END

```

SEGMENT, LENGTH 526, NAME SPEC





A TIME-DIVISION MULTIPLEXED TELEMETRY SYSTEM USING DELTA-MODULATION

J. M. IVISON, D. W. HOARE and S. QAZI*

Abstract

The paper discusses the principles of multichannel time-division multiplexed telemetry systems using digital techniques and suitable for the transmission of biomedical signals. The operation of a system of modulation, known as delta modulation, used for encoding the analogue signals from the transducers is described and its advantages and limitations mentioned.

Reference is made to a four-channel system using a radio link, and a system using a single-wire link is discussed in more detail.

1. Introduction

The use of digital techniques for the transmission of data has a number of attractive features, including the more economical realization of time division multiplexing and less severe requirements with respect to signal-to-noise ratio. The most efficient digital modulation system is probably Pulse Code Modulation (PCM), but the circuits used for modulation and demodulation are quite complex; an alternative digital modulation system, requiring greater bandwidth than PCM but using much simpler circuits, is known as Delta Modulation (DM). Using integrated circuits it is possible to design and construct very simple delta modulators that are capable of handling biomedical signals.

2. The principles of delta modulation

Delta modulation, like PCM, is a code-modulation system, using a 1-digit code (de Jager 1952, Panter 1965). Instead of the absolute amplitude of the signal being transmitted at each instant of sampling, as in PCM, only the changes in amplitude between one sampling instant and the next are transmitted. The principle of operation may be described with reference to Figure 1.

The delta modulator is essentially a closed-loop sampled data system, the digital output $f(t)$ being fed back in a modified form $c(t)$ which is similar to the analogue input $b(t)$ and is subtracted from the latter to

* Department of Electronic and Electrical Engineering, Loughborough University of Technology, Loughborough, England

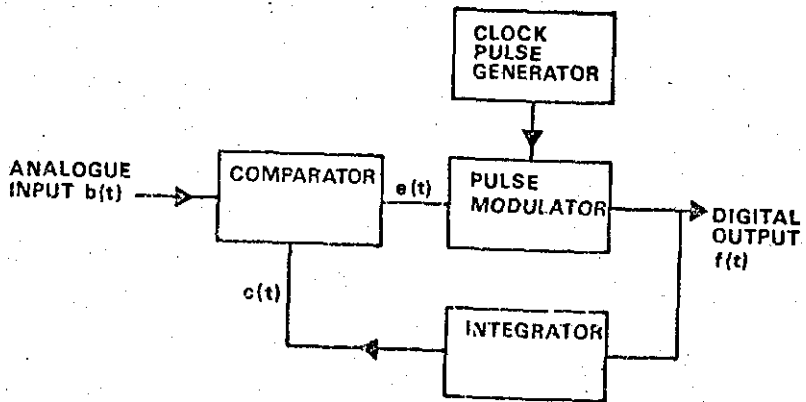


Figure 1. Basic delta modulator

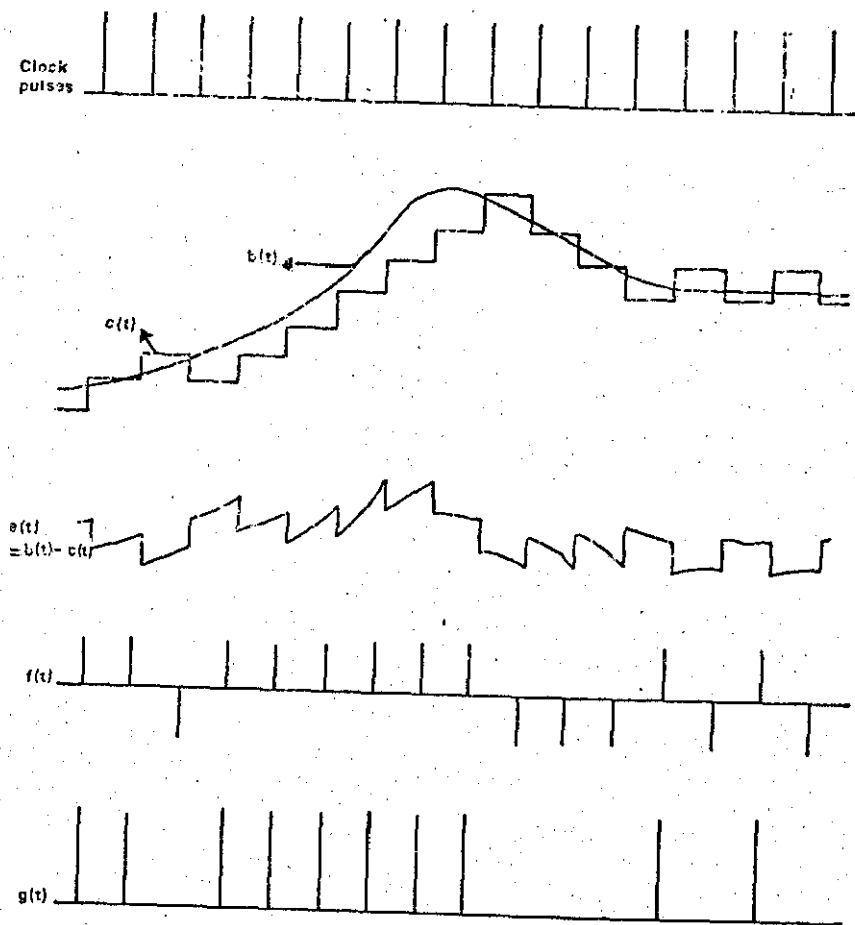


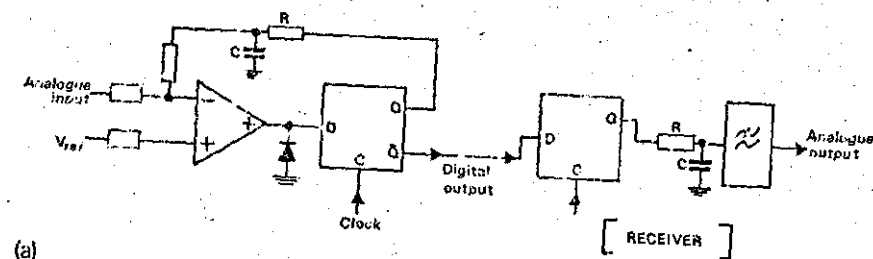
Figure 2. Typical waveforms for delta modulator

produce an error signal $e(t) = b(t) - c(t)$. If the error is positive the digital output at the next sampling instant will increase to reduce the error. Conversely if the error is negative the digital output will decrease to reduce the error. The operation is shown by the waveforms of Figure 2. In practice the negative pulses may be omitted and the waveform $g(t)$ transmitted.

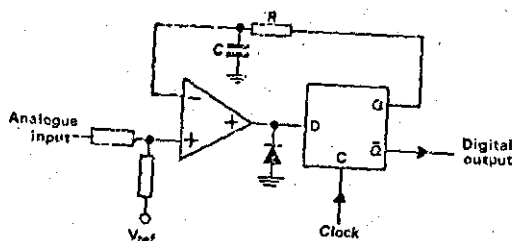
It should be noted that when the gradient of $b(t)$ is increasing rapidly in the positive direction $f(t)$ has many more positive pulses than negative ones, for a gradual increase in gradient the difference between the number of positive pulses and the number of negative pulses is smaller. The circuit required to decode the DM signal is quite simple and consists essentially of an integrator and a low pass filter. The transmitted signal is $f(t)$ of Figure 2; when this is integrated $c(t)$ results and this, when smoothed by means of the low pass filter, closely approximates to the original analogue signal $b(t)$.

3. The practical delta modulator

The delta modulators in the four-channel biomedical radio telemetry system and the single-wire system described later in this paper use integrated circuit packages in a modified circuit. The salient features of the circuit, shown in Figure 3(a), are:- an operational amplifier with a reference supply is used as the comparator and a D flip flop (bistable element) is employed to provide the digital output '1' or '0'. The perfect



(a)



(b)

Figure 3. Practical delta modulator circuits

integrator in the feedback loop is replaced by an RC circuit and the clock pulses are applied to the bistable element. Using the operational amplifier as shown it is more convenient to use an adder than a subtractor so that the '0' state of the bistable is fed back. An alternative circuit arrangement is shown in Figure 3(b).

It is possible to obtain two operational amplifiers or two D flip flops in each dual in-line package, so that two delta modulators can be constructed from two such packages with the addition of a few resistors and capacitors.

4. Some limitations of the delta modulator

In a DM system the information contained in the output corresponds to changes in the amplitude of the input signal and not to the absolute value of the amplitude; because the signal $c(t)$ can change by only one level per clock pulse, overloading occurs when the slope of the input signal is too great. When the amplitude of the input signal is increasing the output from the delta modulator consists of a series of positive pulses and $c(t)$ is a staircase waveform as shown in Figure 4; the average rate of rise of this waveform is V/T v/s. If $b(t) = V_s \sin \omega t$, the delta modulator will overload when $\left[\frac{db(t)}{dt} \right]_{\text{max}} = V_s \omega > V/T$; thus the signal handling capacity is inversely proportional to the signal frequency. It should be noted that in this respect it is advantageous to increase the clock frequency (that is, decrease T) and increase the quantization level. In general, biomedical signals do not have a large high frequency content so that the delta modulation is capable of handling them.

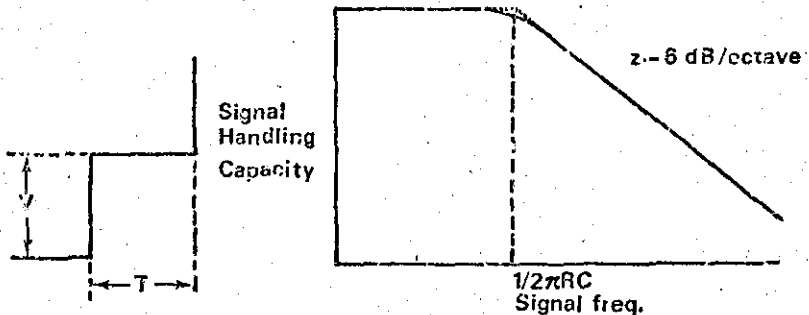


Figure 4: Overload characteristics of delta modulator

The method of quantization is coarse and results in quantization noise which increases with the bandwidth of the filter in the receiver and the quantization level V , and decreases as the clock frequency is increased. In the systems to be described quantization noise has not proved to be serious.

5. Telemetry systems using delta modulation

A four-channel biomedical telemetry system using delta-modulation has been described previously by the authors (Hoare, Ivison and Qazi, 1969); this uses a radio link operating at 102 MHz and is capable of having the number of channels increased without extensive modifications. A block diagram of the system is shown in Figure 5.

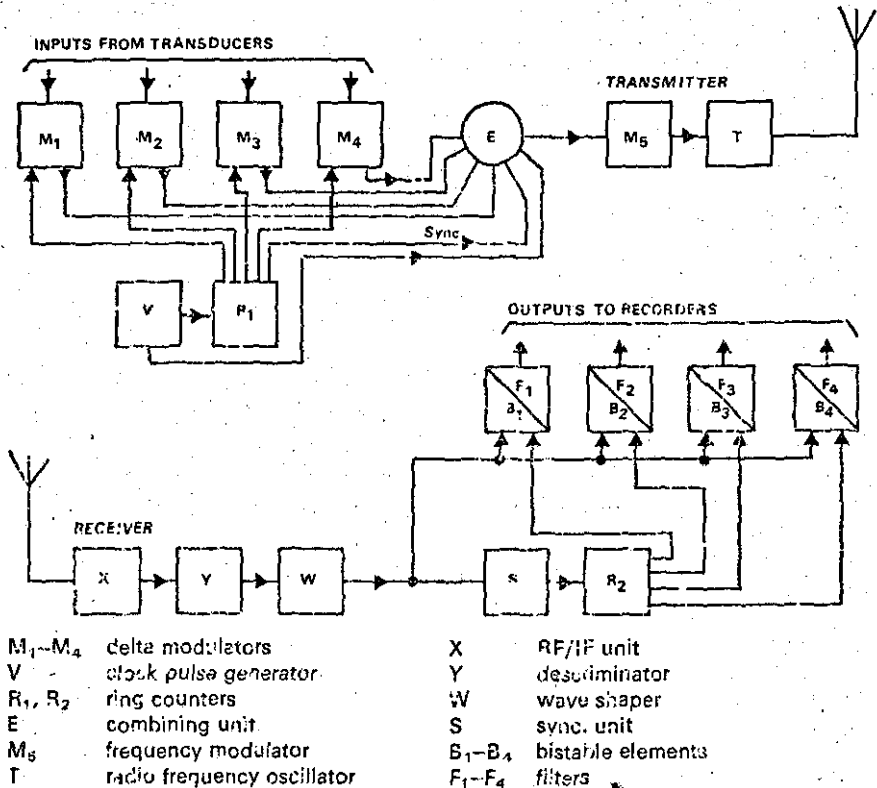


Figure 5. Multichannel biomedical telemetry system using delta modulation

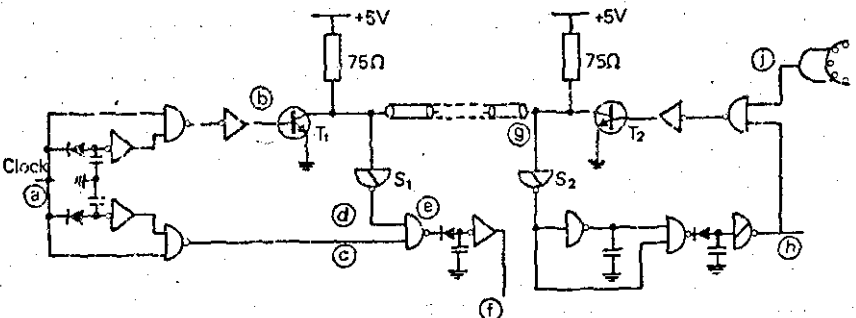


Figure 6. Cable and control circuits for single-wire telemetry system

A time-division multiplexed system has recently been developed in which a number of signals, encoded by delta modulators, are transmitted to a remote point by means of a single coaxial cable. In physical situations where this system can be used the requirements for the clock pulse generator are less stringent than with the radio system.

The cable and control circuits are shown in Figure 6; Figure 7 shows typical waveforms. Each time the clock pulse (a) goes positive, a pulse (b) of approximately 200 ns duration is generated; this pulse causes the transistor T1 to conduct and a pulse is transmitted along the line. At the same time a pulse (c), derived from the clock pulse, is used to suppress the output (d) from the Schmitt trigger ST 1. The pulse travels along the line with a velocity of approximately 5 ns/m until it reaches the far end of the line where it is detected by the Schmitt trigger ST 2 (g); from the negative going edge, a positive going pulse (h) is produced. The information currently being stored in the form of a DC level (j). If a '0' is being stored the pulse (h) will not pass through the gate and transistor T2 will remain non-conducting; hence the line remains terminated by 75Ω and the pulse is absorbed without reflection. If a '1' is being

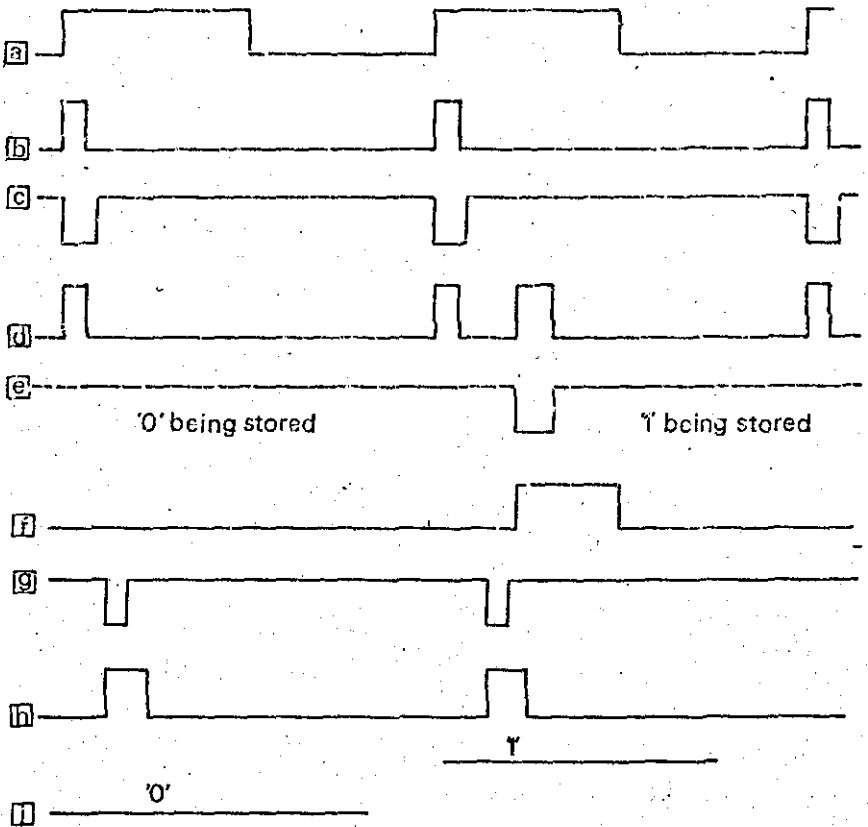


Figure 7. Waveforms for single-wire telemetry system

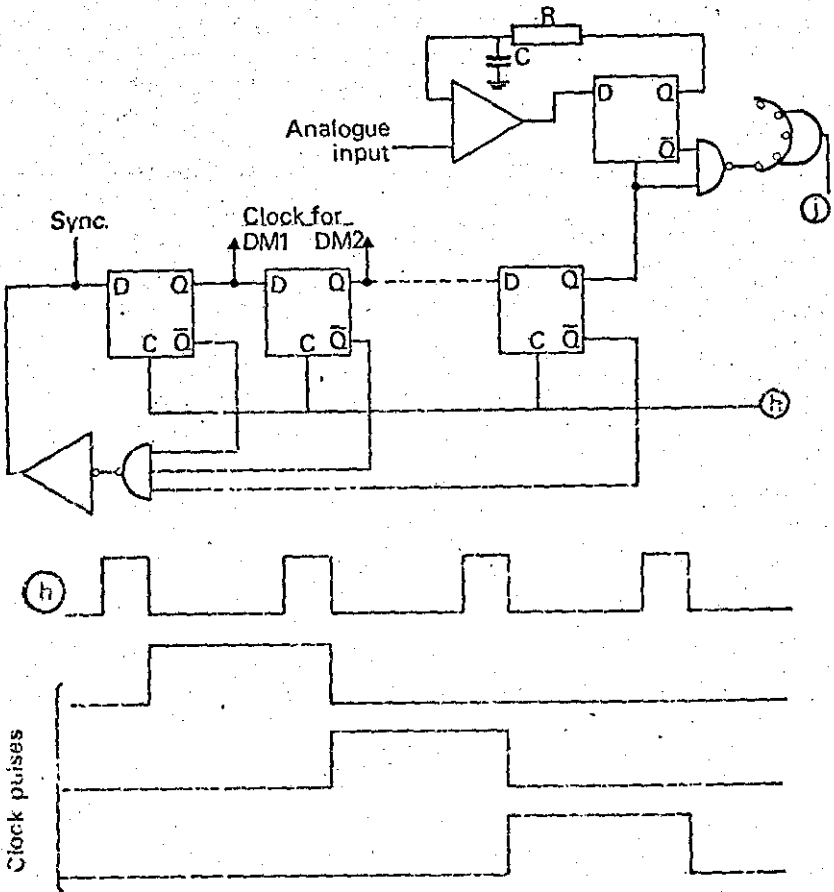


Figure 8. Transmitter circuits for single-wire telemetry system

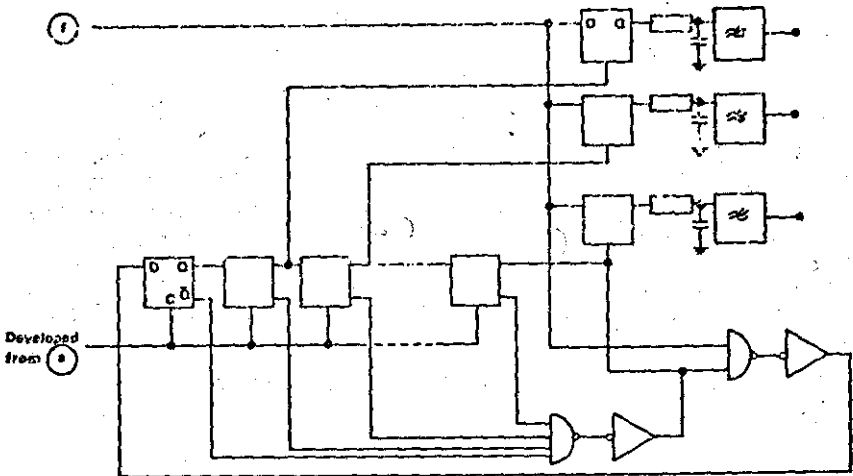


Figure 9. Receiver circuits for single-wire telemetry system

stored, pulse (h) causes the transistor T2 to conduct and a pulse is transmitted back along the line and holds the output of ST 2 for the duration of the pulse. The pulse travels back along the line where the output from ST 1 now produces an output (e). This pulse is then stretched to ensure that the length of the line is not critical (f).

The delta modulators are sequenced by the received pulse (h) which drives a ring counter as shown in Figure 8. Each cycle of the ring counter clocks each delta modulator once. When each delta modulator is clocked the output is logically 'ANDED' with the clocking signal and, via a logical 'OR' gate, all the outputs form signal (j). On each cycle of the ring counter a '1' is always present at (j) in the sync position. Normal data will cause '0's and '1's but continuous '1's occur only in the event of an overload and then only for a short period.

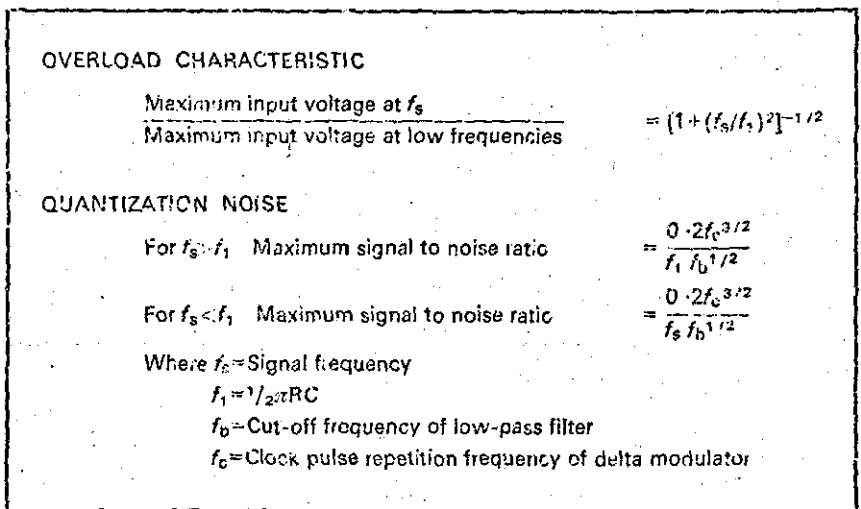
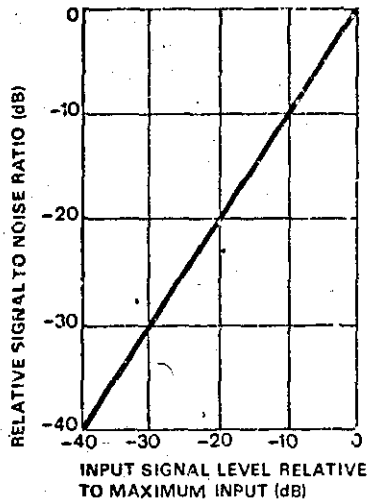
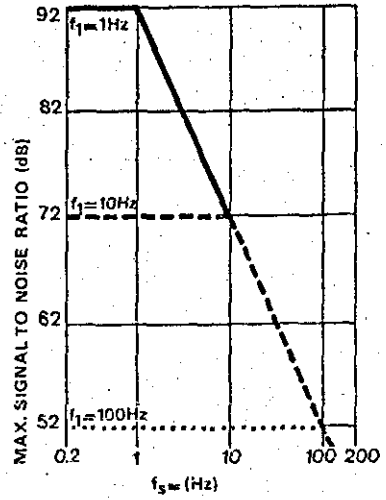
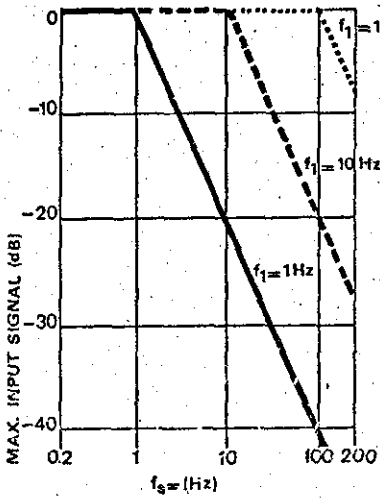


Figure 10. Summary of delta modulator performance

The received data is decoded by using the pulses from the clock to drive another ring counter and using the outputs from this ring counter to strobe the pulses from (f) into flip flops (as shown in Figure 9). Synchronisation is achieved by allowing the ring counter to proceed only at the end of a cycle providing a '1' is present on the line (f). Hence on switching on, the ring counter may proceed for a few cycles out of synchronism because of the '1's in the data. However, it will take only a few cycles for it to be locked to the synchronising pulses. The data on the flip flops is passed through an RC network followed by a low pass filter to recover the original signal.

Typical performance characteristics of the system are shown in Figures 10 and 11, and a possible application of the system is shown in Figure 12.



$f_c = 20$ kHz, $f_b = 200$ Hz, number of channels = 24

Figure 11. Typical system performance characteristics

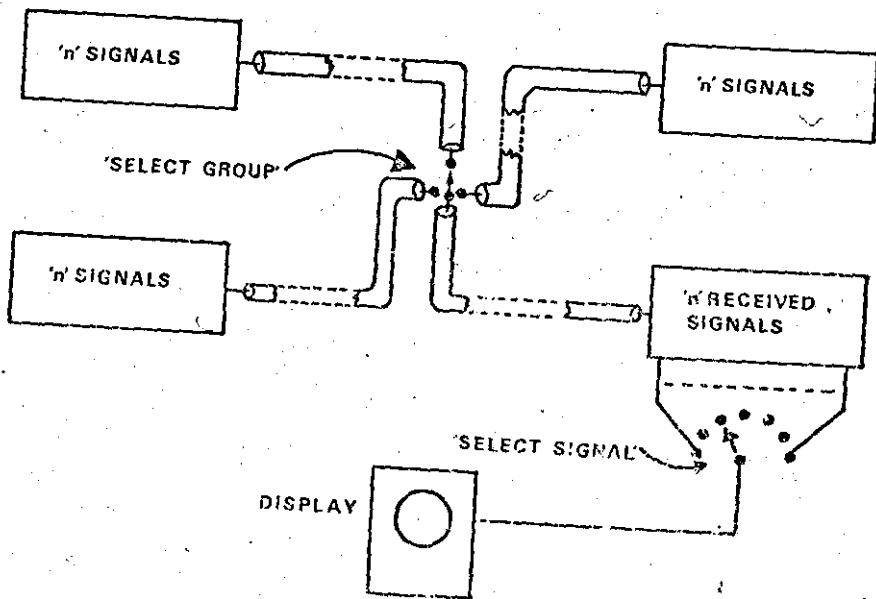


Figure 12. Application of single wire telemetry system

References

- De Jager, F.: *Delta modulation: a Method of PCM Transmission Using 1-unit Code*, Philips Res. Dept. 7, pp. 442-466, 1952.
- Panter, P. F.: *Modulation, Noise and Spectral Analysis*, McGraw-Hill 1965, pp. 679-699.
- Hoare, D.W., Ivison, J. M. and Gazi, S.: *A Multichannel Biomedical Telemetry System using Delta Modulation*. Proc. 8th International Conference on Medical and Biological Engineering, July 1969, Session 30-8.

A MULTICHANNEL BIOMEDICAL TELEMETRY SYSTEM USING DELTA MODULATION.

DAVID W. HOARE, JOHN M. IVISON and SALAHUDDIN QAZI, The University of Technology, Loughborough, Leicestershire, England.

Radio telemetry is frequently used to obtain physiological data from unrestrained active subjects. It is desirable that a telemetry system designed for this purpose is simple to operate, easily reproduced and capable of having the number of channels readily increased. The paper describes a multichannel system having these features, which uses digital techniques for modulation and is based on microelectronic circuits.

The equipment developed is a four-channel, time-division multiplex system (TDM) using modified delta modulators^{1,2} to encode the analogue signals from the transducers; a block diagram is shown in figure 1.

The analogue inputs from the transducers are applied to the delta modulators M1-4, which are also supplied with clock pulses generated by an astable flip-flop V and sequenced by a ring counter R1. The digital outputs from the delta modulators are applied to the combining unit E together with a synchronizing signal from R1. The TDM signal from E feeds the frequency modulator M5 which modulates the radio frequency transmitter T.

The receiver is an RF/IF unit X used in conjunction with a discriminator Y, a waveshaping unit W and a decoder. The TDM signal from W is applied to the bistable flip-flops B1-4, together with a decoding signal from the ring counter R2 which is correctly synchronized by the unit S. Filters F1-4 convert the digital outputs from the bistable elements to analogue form.

The modified delta modulator consists of an operational amplifier A, used as a comparator, a D type flip-flop D and a small number of resistors and capacitors as shown in figure 2a. As there are two operational amplifiers and two D flip-flops in each dual in line package (DIP), two delta modulators can be made from two DIPs. This modulator may be considered as a closed loop system; the output from the flip-flop D is 'integrated' by the CR circuit to form u_t which is then 'subtracted' from the analogue input signal u_a . Depending on whether the resultant is greater or less than the d.c. reference voltage V_r , the output from the comparator A is either state '1' or '0'. When the flip-flop receives its next clock pulse it takes the state of the comparator as shown in figure 2(b). Hence the output from the flip-flop provides information (in quantized form) on the slope of the analogue input signal to the modulator. Integration of the output from D using a similar CR circuit would recover the analogue signal - in practice a further low pass filter is necessary to remove the clock frequency components. The clock pulses are generated as shown in figure 2 using an astable flip-flop, having a pulse repetition frequency of 20 kHz, to drive a ring counter consisting of D type flip-flops. Synchronization is achieved by transmitting a pulse on each cycle of the ring counter.

The combining unit E (figure 1) consists of microelectronic NAND gates; the output from E is applied to a diode which frequency modulates a 102 MHz crystal-controlled oscillator. Solid-state 460 MHz oscillators are available and may also be used.

The characteristics of delta modulation are that the signal is slope limited and the signal handling capacity falls by 6dB per octave^{1,2}; these limitations are not serious in the telemetering of biomedical data.

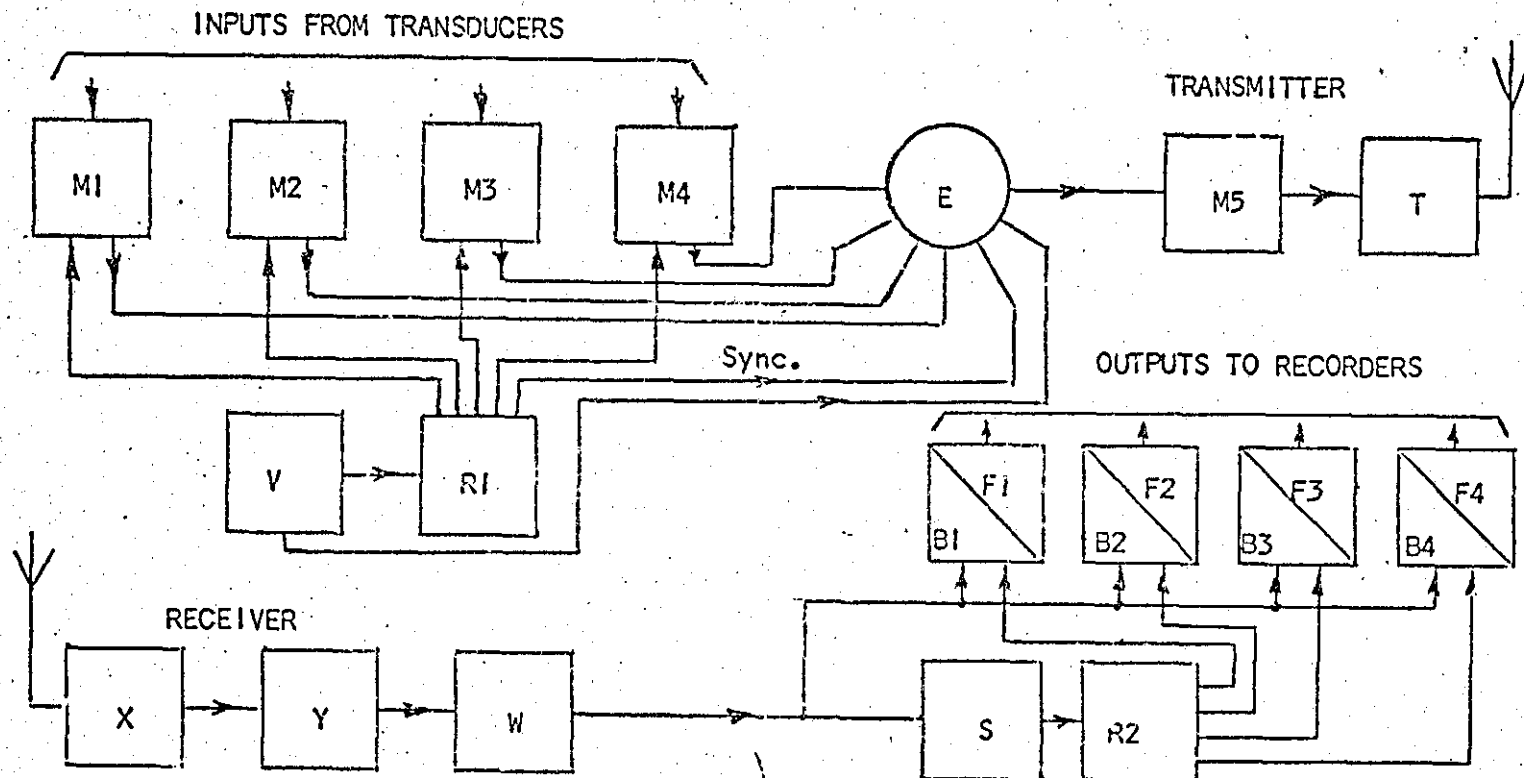
Using a modified delta modulator, d.c. signals may be transmitted by omitting the input coupling capacitor. The drift in the level depends upon the drifts of the common reference voltage V_r and the operational amplifiers in the delta modulators. Delta-sigma modulation³ overcomes this drift problem and a modulator using the same basic components as in the system described has been successfully tested by the author. The digital section of the four-channel transmitter described requires only ten DIPs.

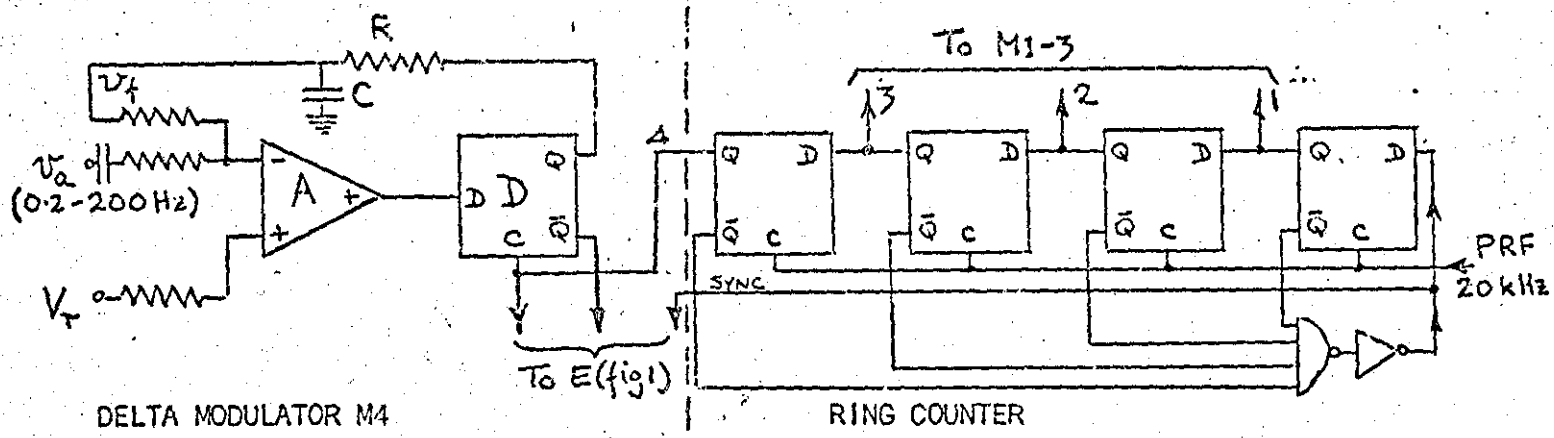
An extension of the number of channels may be achieved by (a) using additional delta modulators (b) using additional D type flip-flops in the ring counter and (c) a linear increase in the pulse repetition frequency of the astable flip-flop driving the ring counter.

It is concluded that the digital encoding method described is flexible and should be reliable in operation because of its basic simplicity and use of microelectronics.

References.

1. Maschhoff, R.H. Delta Modulation, Electro-Technology, January 1964.
2. Steele, R. and Thomas, M.W.S. A Two Transistor Delta Modulator, Electronic Engineering, Sept. 1968.
3. Inose, H.; Yasuda, Y. and Murakami, J. A Telemetering System by Code Modulation - Δ - Σ Modulation. I.R.E. Trans. on Space Electronics and Telemetry. Sept. 1962.

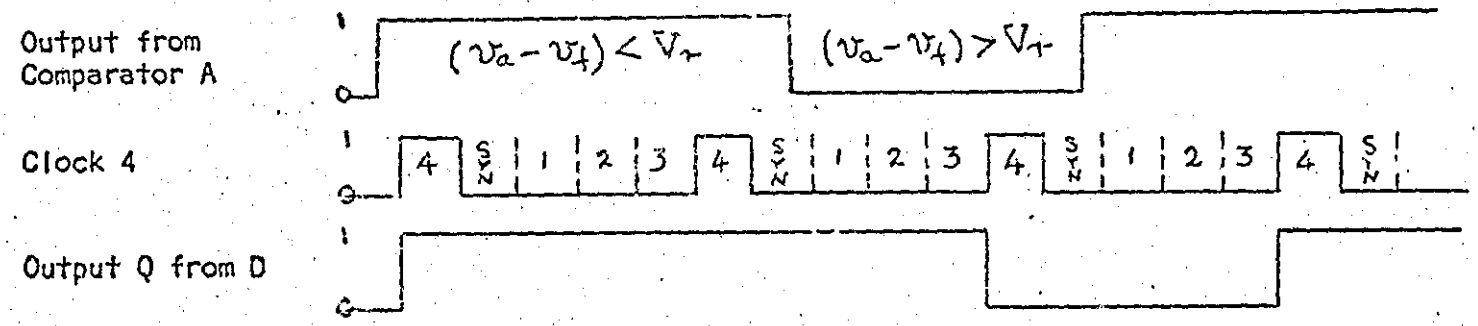




DELTA MODULATOR M4

RING COUNTER

(a) Schematic Diagram of Delta Modulator



(b) Typical Waveforms for Delta Modulator